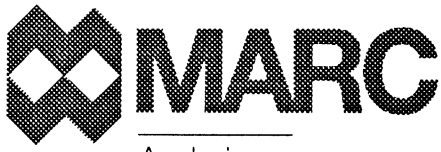

Analysis
Research
Corporation

VOLUME E
DEMONSTRATION PROBLEMS

Part III

- *Heat Transfer*
- *Dynamics*

Disclaimer of Warranties and Limitation of Liabilities

The authors have taken due care in preparing this manual and the examples in it, including the research, development, and testing to ascertain their effectiveness. In no event shall MARC Analysis Research Corporation be liable for incidental or consequential damages in connection with or arising out of the furnishing, performance, or use of any of the examples.

MARC Analysis Research Corporation:

North America

Corporate Headquarters
MARC Analysis Research Corporation
260 Sheridan Avenue, Suite 309
Palo Alto, CA 94306, USA
Telephone: (415) 329-6800
FAX: (415) 323-5892

National Sales Office
MARC Analysis Research Corporation
#6 Venture, Suite 202
Irvine, CA 92718, USA
Telephone: (714) 453-0840
FAX: (714) 453-0141

Europe

European Headquarters
MARC-Europe
Bredewater 26
2715 CA Zoetermeer, The Netherlands
Telephone: 31-79-510411
FAX: 31-79-517560

German Office
MARC Software Deutschland GmbH
Ismaninger Strasse 9
85609 Aschheim, Germany
Telephone: 49-89-904-5033
FAX: 49-89-903-0676

Italian Office
Espri-MARC
Piazza Rossetti 5/16A
16129 Genova, Italy
Telephone: 39-10-585949
FAX: 39-10-585949

Pacific Rim

Far East Headquarters
Nippon MARC Co., Ltd.
P.O. Box 5056
Shinjuku Daiichi Seimei Bldg.
2-7-1 Nishi-Shinjuku
Shinjuku-ku, Tokyo 163, Japan
Telephone: 81-3-3345-0181
FAX: 81-3-3345-1529

Osaka Office
Nippon MARC Co., Ltd.
Dai 2 Kimi Bldg., 4F
2-11 Toyotsu-cho
Suita-city, Osaka 564, Japan
Telephone: 81-6-385-1101
FAX: 81-6-385-4343

Contents Volume E Demonstration Problems

PART III

VOLUME E
DEMONSTRATION
PROBLEMS

Chapter 5
Heat Transfer

Contents Chapter 5 Heat Transfer

Tables Chapter 5 Heat Transfer

Table E 5.0-1 Heat Transfer Analysis Demonstration Problems

Problem Number (E)	Element Type	Parameter Options	Model Definition	Load Incrementation	User Subroutines	Problem Description
5.1	36	HEAT	—	TRANSIENT NON AUTO	—	One-dimensional steady-state heat conduction, constant properties, prescribed temperature boundary conditions, 2-node link element.
5.2	65	HEAT FORCDT	FORCDT INITIAL TEMP	TRANSIENT NON AUTO	FORCDT	One-dimensional transient heat conduction, constant properties, prescribed temperature boundary conditions, 3-node link element.
5.3	41 69 39 37 121 131	HEAT FILMS ALIAS	INITIAL TEMP FILMS CONTROL OPTIMIZE	TRANSIENT NON AUTO	—	Two-dimensional transient heat conduction, constant properties, prescribed temperature and convective boundary conditions, 3-, 4-, and 8-node reduced integration planar elements.
5.4	43 44 71 123	HEAT	INITIAL TEMP CONTROL PRINT CHOICE UDUMP	TRANSIENT NON AUTO	—	Three-dimensional transient heat conduction, constant properties, prescribed temperature and insulated boundary conditions, 8-, 20-node and reduced integration elements.
5.5	42 70	HEAT FILMS ALIAS	INITIAL TEMP CONTROL FILMS	TRANSIENT	FILM	Axisymmetric transient heat conduction, constant properties, convective boundary conditions, 8-node axisymmetric and reduced integration elements.
5.6	41	HEAT FILMS	INITIAL TEMP CONTROL FILMS	TRANSIENT	FILM	Same as problem 5.5, except using 8-node planar element.

Table E 5.0-1 Heat Transfer Analysis Demonstration Problems (Continued)

Problem Number (E)	Element Type	Parameter Options	Model Definition	Load Incrementation	User Subroutines	Problem Description
5.7	39	HEAT	ANISOTROPIC	TRANSIENT NON AUTO	ANKOND	Two-dimensional heat conduction, constant properties, anisotropic conductivity, prescribed conditions, 4-node planar element.
5.8	41	HEAT MESH PLOT	FILMS FLUXES INITIAL TEMP CONTROL TEMP EFFECTS RESTART OPTIMIZE	TRANSIENT	FILM FLUX	Nonlinear heat conduction, temperature dependent properties, prescribed temperature, convective, and radiative boundary conditions, 8-node planar element.
5.9	40 122 132	HEAT	TEMP EFFECTS INITIAL TEMP CONTROL FILMS PRINT CHOICE UDUMP	TRANSIENT NON AUTO	—	Latent heat effect, temperature dependent properties, convective boundary condition 4-node axisymmetric element.
5.10	40	HEAT JOULE	JOULE DIST CURRENT VOLTAGE FILMS	TRANSIENT NON AUTO	—	Evaluate temperatures in a wire due to current.
5.11	42 28	HEAT MARC.PLOT THERMAL T-T-T	TEMP EFFECTS FILMS TIME-TEMP CHANGE STATE INITIAL TEMP	TRANSIENT AUTO THERM CHANGE STATE	—	Evaluate transient temperature response due quenching process. Evaluate thermally-induced stresses.
5.12	39	ALIAS JOULE HEAT	VOLTAGE POST JOULE	TRANSIENT	—	Electro static planar analysis.

Table E 5.0-1 Heat Transfer Analysis Demonstration Problems (Continued)

Problem Number (E)	Element Type	Parameter Options	Model Definition	Load Incrementation	User Subroutines	Problem Description
5.13	85 86 87 88	HEAT SHELL SECT	INITIAL TEMP FILMS POST	TRANSIENT	FILM	Thermal ratchetting using shell elements.
5.14	39	HEAT PRINT, 7	DEFINE TEMP EFFECTS CONRAD GAP CHANNEL FILMS	TRANSIENT	FILM FLOW	Steady state temperature distribution of a fuel nozzle.
5.15	42	HEAT RADIATION	RADIATING CAVITY TEMP EFFECTS FIXED TEMP	STEADY STATE	—	Radiating concentrical spherical bodies.
5.16	123 133	HEAT LUMP	INITIAL TEMP	TRANSIENT	—	Thermal shock.

E 5.1 One-Dimensional Steady State Heat Conduction

A bar has an initial temperature of 0°F. One end is subsequently subjected to 100°F; the other to 200°F. The temperature distribution along the bar is calculated for subsequent times.

Model/Element

This one-dimensional steady-state heat conduction problem is analyzed by using MARC element type 36 (three-dimensional link). The model consists of six nodes and five elements, which allows a linear variation of temperature along its length. The dimensions of the model and a finite element mesh are shown in Figure E 5.1-1.

Material Properties

The conductivity is 0.000213 Btu/sec-in.-°F. The specific heat is 0.105 BTU/lb-°F. The mass density is 0.283 lb/cu/in.

Geometry

The default value of 1.0 sq.in. is used for the cross-sectional area of the link. No geometry input data is required.

Boundary Conditions

Constant nodal temperatures of 100°F and 200°F are prescribed at nodes 1 and 6, respectively.

Transient (Ref. 5.5-2)

A very large time step (Δt = 100,000 sec) is chosen for obtaining the steady-state solution and the total transient time is also assumed to be 100,000 seconds. Consequently, the steady state solution is reached in one time step. The non-automatic time stepping option in MARC is invoked in the analysis. As an alternative, the STEADY STATE option could be used.

Results

A linear distribution of steady state temperatures is obtained, as expected. The nodal temperatures are:

Node Number	Temperature °F
1	100
2	120
3	140
4	160
5	180
6	200

Summary of Options Used

Listed below are the options used in example e5x1.dat:

Parameter Options

ELEMENT
END
HEAT
SIZING
TITLE

Model Definition Options

CONNECTIVITY
COORDINATE
END OPTION
FIXED TEMPERATURE
ISOTROPIC

Load Incrementation Options

CONTINUE
TRANSIENT

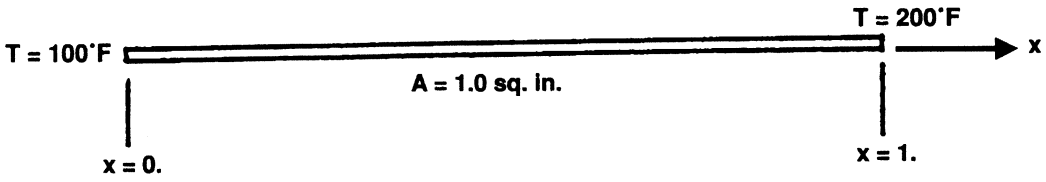

MARC

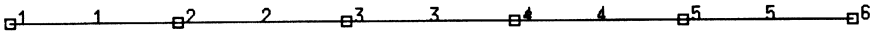

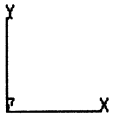

Figure E 5.1-1 One-Dimensional Link and Mesh

E 5.2 One-Dimensional Transient Heat Conduction

A bar has an initial temperature of 0°F. One end is subsequently subjected to 100°F, the other to 200°F. The temperature distribution along the bar is calculated for subsequent times.

Model

This one-dimensional transient heat conduction problem is analyzed by using MARC element type 65 (3-node truss). The model consists of eleven nodes and five elements. The element type 65 allows a quadratic variation of temperature along its length. The dimension of the model and a finite element mesh are shown in Figure E 5.2-1.

Material Properties

Material properties of the model are:

Conductivity is 0.000213 Btu/sec-in.-°F
Specific heat is 0.105 Btu/lb-°F
Mass density is 0.283 lb/cu.in.

Geometry

The default value of 1.0 sq.in. is used for the cross-section area of the link. No geometry input data is required.

Boundary Conditions

Constant nodal temperatures of 100°F and 200°F are prescribed at nodes 1 and 11, respectively. This problem is evaluated twice: In the first input, the boundary temperature is specified using the FIXED TEMP option; in the second, case subroutine FORCDT is used to specify the temperatures.

Initial Condition

Initial nodal temperatures are assumed to be 0°F.

Transient

The transient time is assumed to be 20 sec. and a constant time step of 1.0 sec. selected for the analysis. The total number of time steps in the analysis is 20. The time step is kept constant by using the nonautomatic time stepping option in the program.

Results

Temperature distributions are tabulated in Table E 5.2-1 and plotted in Figure E 5.2-2, Figure E 5.2-3 and Figure E 5.2-4. At the end of 20 sec., the steady-state conditions have not yet been achieved.

Because there are no temperature-dependent material properties and the time increment is fixed, the analysis is performed through a series of back substitutions. In increment 3, the total temperature change was greater than that given in the CONTROL option. In increment 4, the program resassembled. This was not necessary for the accuracy of this particular problem.

Table E 5.2-1 Nodal Temperatures

Time Sec.	Node 1	Node 2	Node 3	Node 4	Node 5	Node 6	Node 7	Node 8	Node 9	Node 10	Node 11
2.	100	49.0	20.3	8.3	3.9	3.3	6.5	16.2	40.4	98.0	200
4.	100	64.9	37.8	21.0	13.2	13.0	20.7	39.5	74.5	129.5	200
6.	100	72.4	49.3	33.2	25.4	26.5	37.3	59.8	95.5	143.7	200
8.	100	77.4	58.0	44.3	38.1	40.6	53.0	76.1	109.7	152.3	200
10.	100	81.4	65.4	54.3	50.1	54.0	67.0	89.4	120.4	158.3	200
S.S	100	110	120	130	140	150	160	170	180	190	200

Summary of Options Used

Listed below are the options used in example e5x2a.dat:

Parameter Options

ELEMENT
END
HEAT
SIZING
TITLE

Model Definition Options

CONNECTIVITY
CONTROL
COORDINATE
END OPTION
FIXED TEMPERATURE
INITIAL TEMPERATURE
ISOTROPIC

Load Incrementation Options

CONTINUE
TRANSIENT

Listed below is the user subroutine found in u5x2.f:

FORCDT

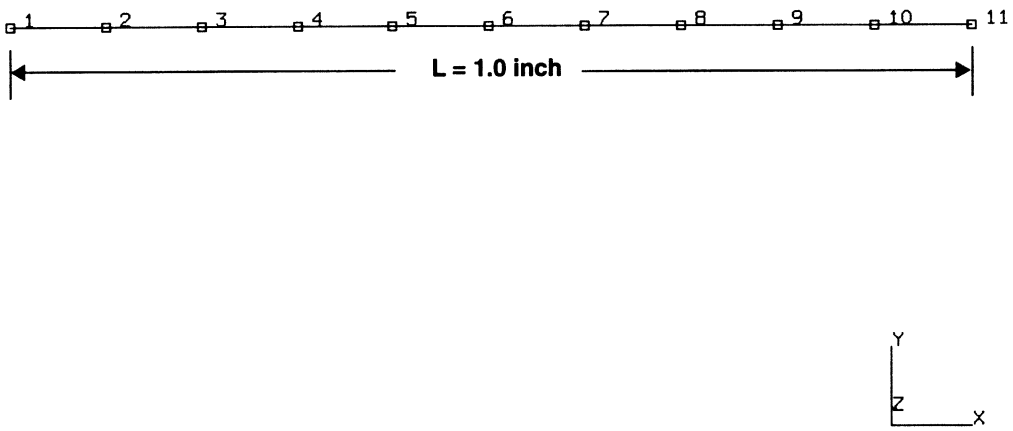

Figure E 5.2-1 One Dimensional Link and Mesh

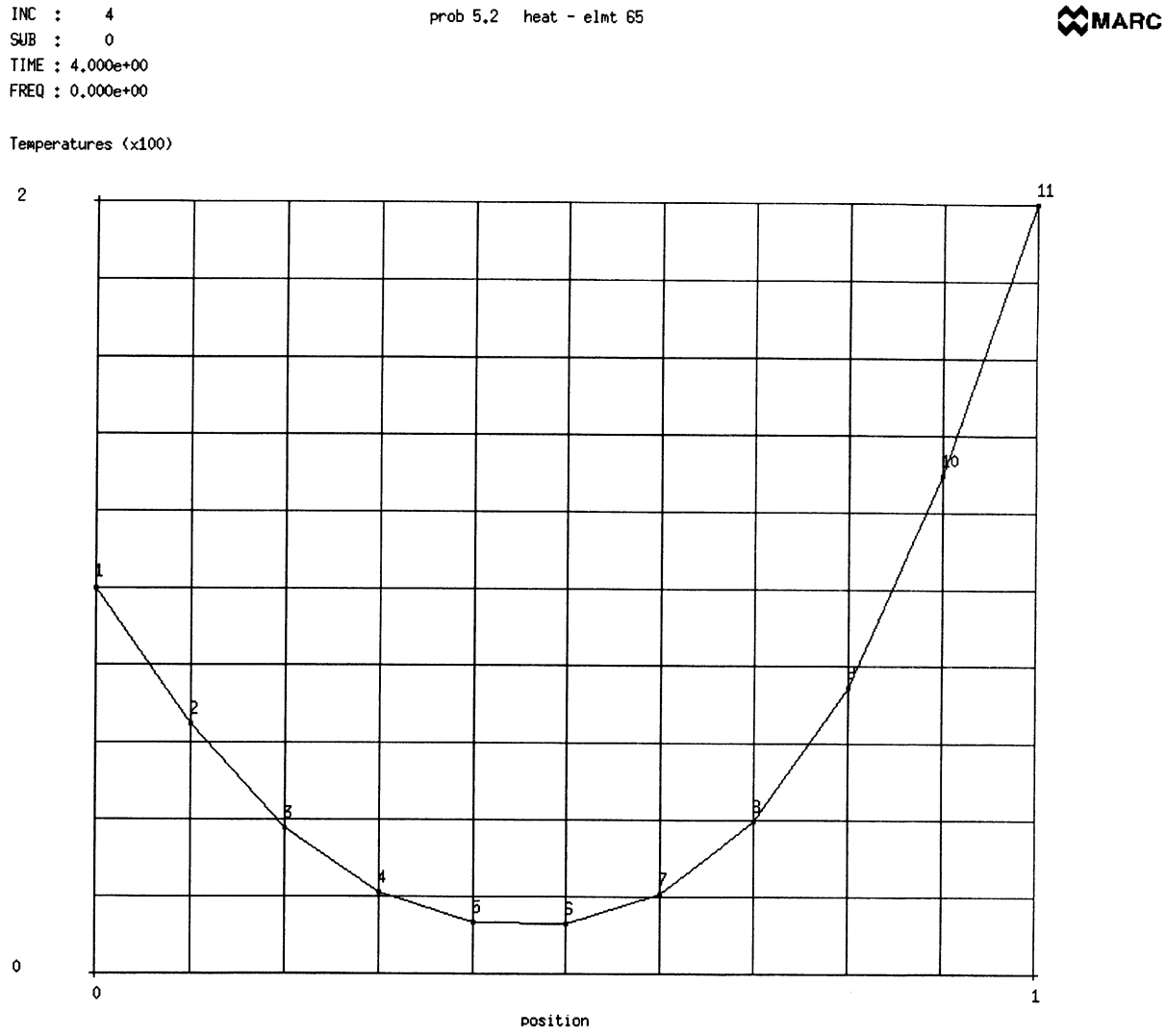

Figure E 5.2-2 Temperature Distributions, t = 4 seconds

Figure E 5.2-3 Temperature Distributions, t = 10 seconds

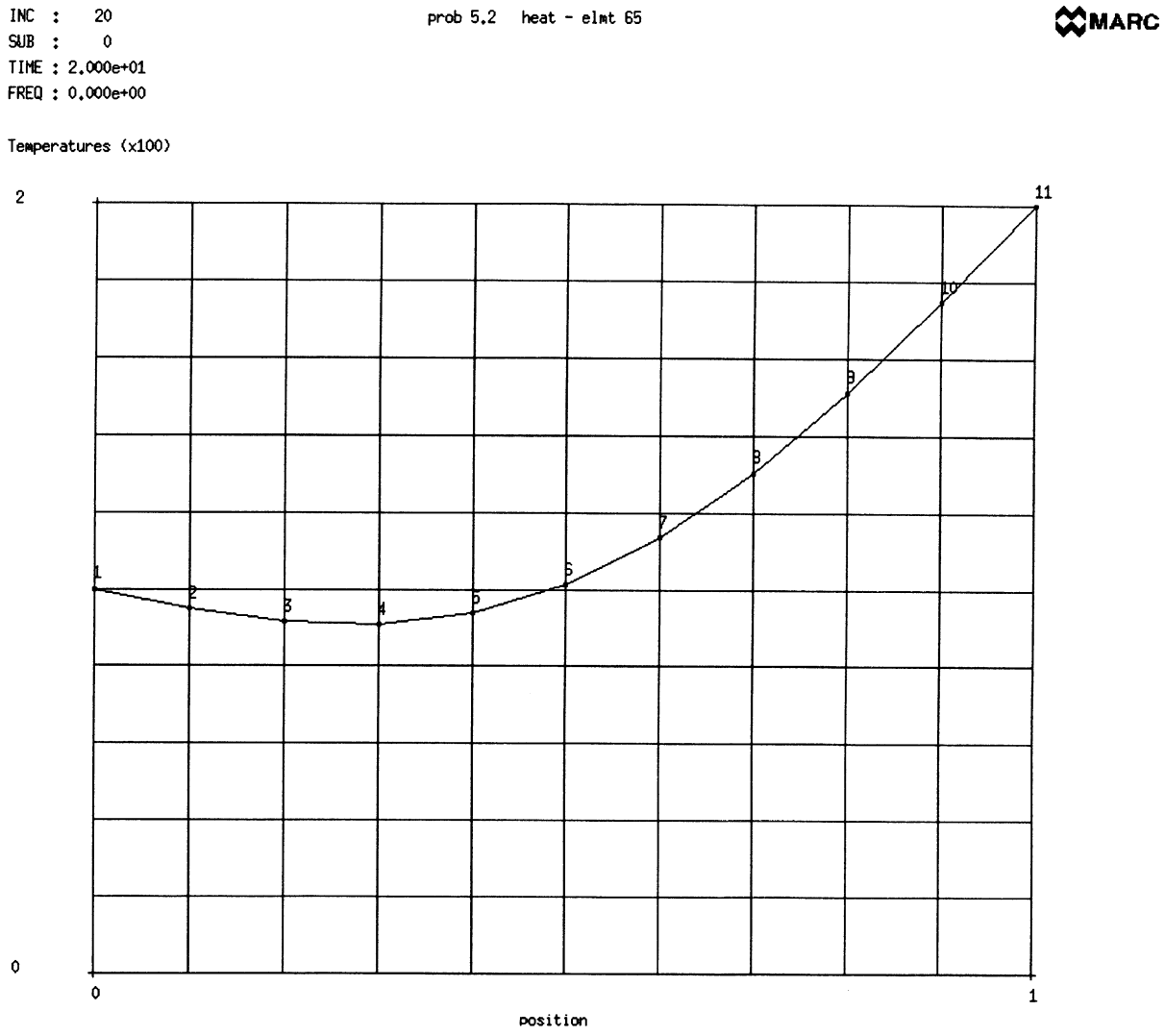

Figure E 5.2-4 Temperature Distribution, t = 20 seconds

E 5.3 Plate With A Fluid Passing Through A Circular Hole

A two-dimensional transient heat conduction problem of a plate with a circular hole is analyzed by using several MARC elements. The hole is filled with a fluid at a temperature 1000°F and the exterior square edges are at a fixed temperature of 500°F. The plate is initially at 500°F and is allowed to heat up for 5 seconds.

Element

MARC element types 37, 39, 41, 69, 121 and 131 (3-, 4-, 8-, 8-, 4-, and 6-node planar elements). Type 69 is an 8-node quadrilateral element with reduced integration. Type 121 is a 4-node quadrilateral element with reduced integration with hourglass control. Type 131 is a 6-node triangular element.

Model

This problem demonstrates the use of a variety of elements and the FILM option for prescribing convective boundary conditions. A rectangular plate 20 inches by 29 inches with a hole of radius 5 inches placed in the center is modeled.

Due to symmetry only a quarter of the plate is modeled for the analysis as shown in Figure E 5.3-1 through Figure E 5.3-4.

Thermal Property

One set of thermal properties is specified in the PROPERTY block: the isotropic thermal conductivity value of 0.42117 E5 Btu/sec-in.-°F; the specific heat is 0.3523 E-3 Btu/lb-°F; and the mass density is 0.7254 E-3 lb/cu.in.

Geometry

The thickness of the plate is 0.1 in.

Thermal Boundary Conditions

The initial temperature distribution is that all nodes have a temperature of 500.0°F. The lines of symmetry (x = 0 and y = 0) are adiabatic and require no data input. A time, t = 0, the fluid is exposed to the circular hole with a sink temperature of 1000°F, and a film coefficient of 0.4678E-5 Btu/sec-sq.in.-°F. The outer edges (x = y = 12 inches) are held at a fixed temperature of 500°F.

Load History

The maximum number of time points are fixed at 10 with a final time of 5 seconds. Nonautomatic time stepping is used with a constant time step of 0.5 seconds/increment.

Results

The temperature history at the center point between the radius of the hole and the corner of the plate (nodes 11, 23, 9, 9, 23, 9 for mesh composed of element type 37, 39, 41, 69, 121 and 131) is shown in Figure E 5.3-4.

Summary of Options Used

Listed below are the options used in example e5x3a.dat:

Parameter Options

ELEMENT
END
HEAT
SIZING
TITLE

Model Definition Options

CONNECTIVITY
CONTROL
COORDINATE
END OPTION
FILMS
FIXED TEMPERATURE
GEOMETRY
INITIAL TEMPERATURE
ISOTROPIC
POST
UDUMP

Load Incrementation Options

CONTINUE
STEADY STATE
TRANSIENT

Listed below are the options used in example e5x3b.dat:

Parameter Options

ELEMENT
END
HEAT
SIZING
TITLE

Model Definition Options

CONNECTIVITY
CONTROL
COORDINATE
END OPTION
FILMS
FIXED TEMPERATURE
GEOMETRY
INITIAL TEMPERATURE
ISOTROPIC
POST

Load Incrementation Options

CONTINUE
TRANSIENT

Listed below are the options used in example e5x3c.dat:

Parameter Options

ELEMENT
END
HEAT
SIZING
TITLE

Model Definition Options

CONNECTIVITY
CONTROL
COORDINATE
END OPTION
EXIT
FILMS
FIXED TEMPERATURE
GEOMETRY
INITIAL TEMPERATURE
ISOTROPIC
POST

Load Incrementation Options

CONTINUE
TRANSIENT

Listed below are the options used in example e5x3d.dat:

Parameter Options

ELEMENT
END
HEAT
SIZING
TITLE

Model Definition Options

CONNECTIVITY
CONTROL
COORDINATE
END OPTION
EXIT
FILMS
FIXED TEMPERATURE
GEOMETRY
INITIAL TEMPERATURE
ISOTROPIC
POST

Load Incrementation Options

CONTINUE
TRANSIENT

Listed below are the options used in example e5x3e.dat:

Parameter Options

ALIAS
ELEMENT
END
HEAT
SIZING
TITLE

Model Definition Options

CONNECTIVITY
CONTROL
COORDINATE
END OPTION
FILMS
FIXED TEMPERATURE
GEOMETRY
INITIAL TEMPERATURE
ISOTROPIC
POST

Load Incrementation Options

CONTINUE
TRANSIENT

Listed below are the options used in example e5x3f.dat:

Parameter Options

ALL POINTS
ELEMENT
END
HEAT
SIZING
TITLE

Model Definition Options

CONNECTIVITY
CONTROL
COORDINATE
END OPTION
FILMS
FIXED TEMPERATURE
GEOMETRY
INITIAL TEMPERATURE
ISOTROPIC
POST

Load Incrementation Options

CONTINUE
TRANSIENT

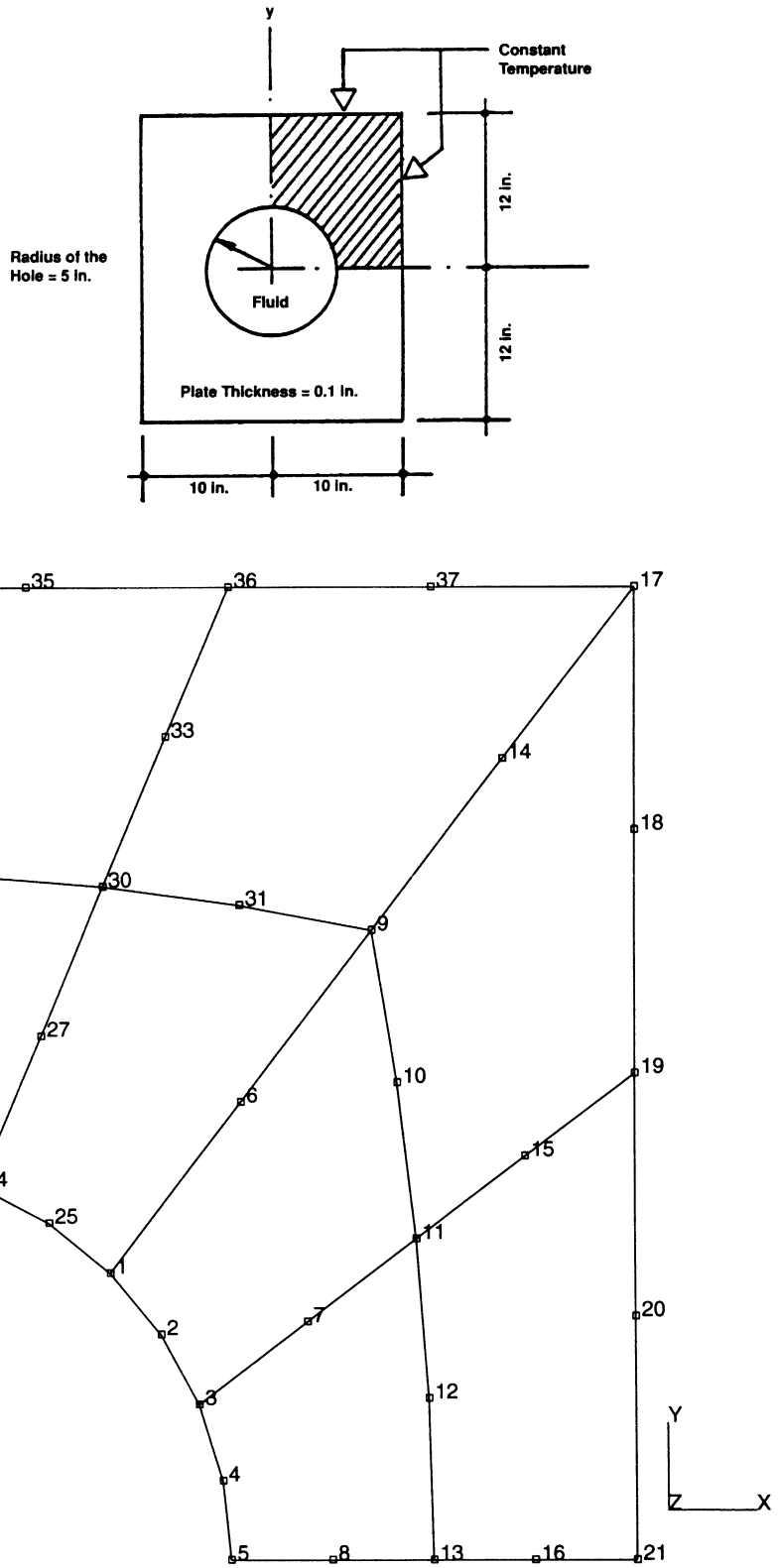

Figure E 5.3-1 Mesh for Element Type 41

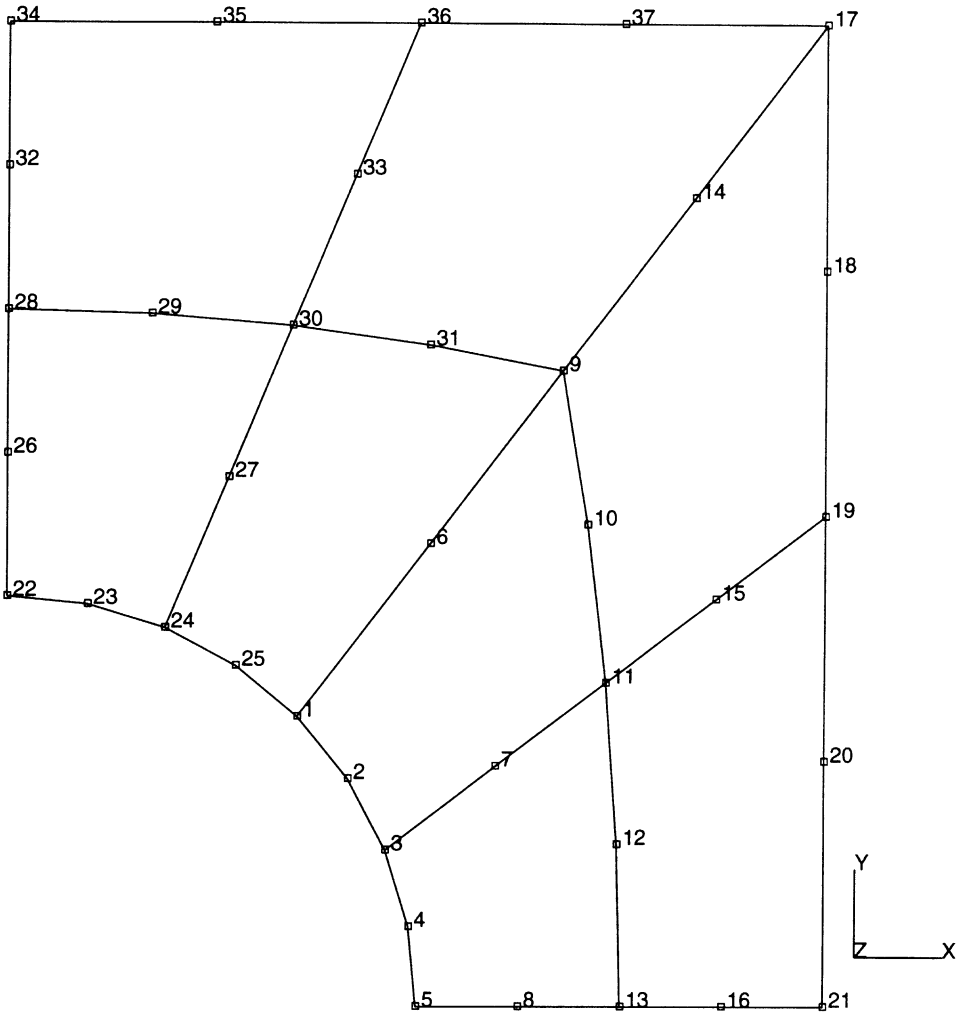

Figure E 5.3-2 Mesh for Element Type 69

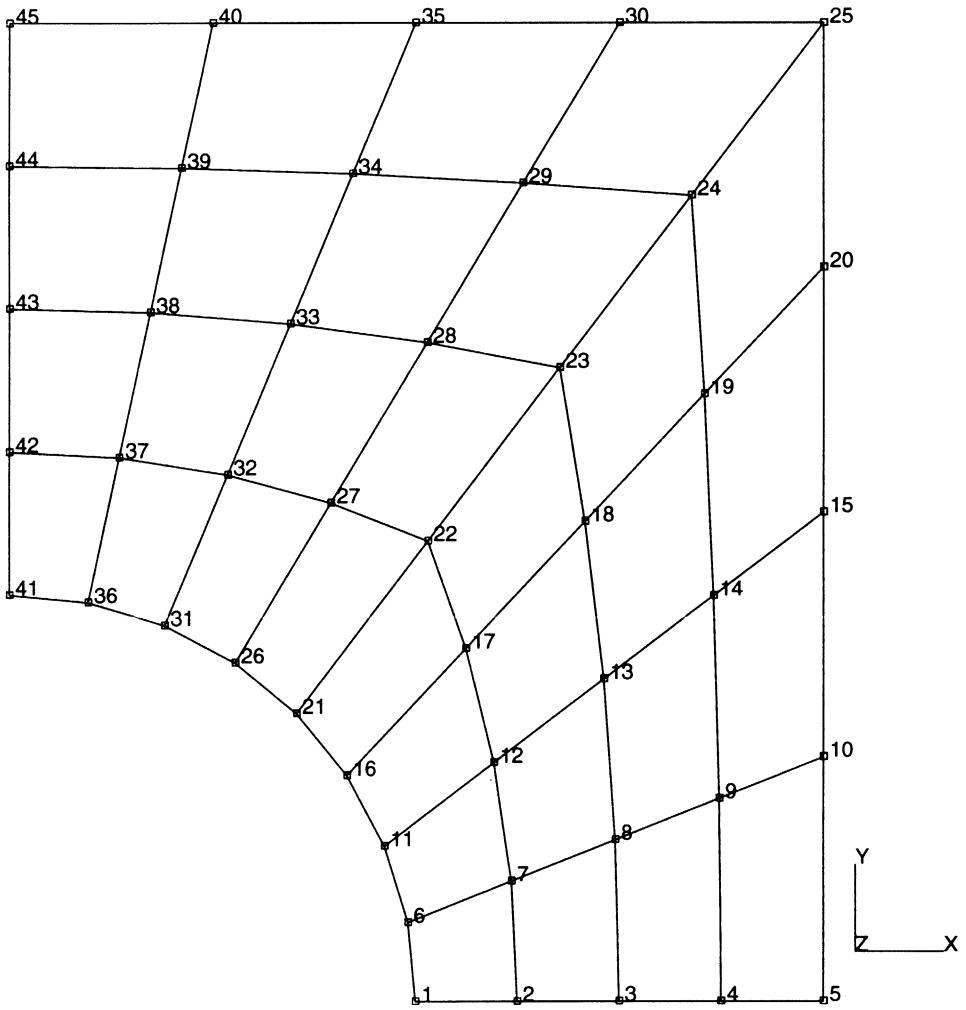

Figure E 5.3-3 Mesh for Element Type 39

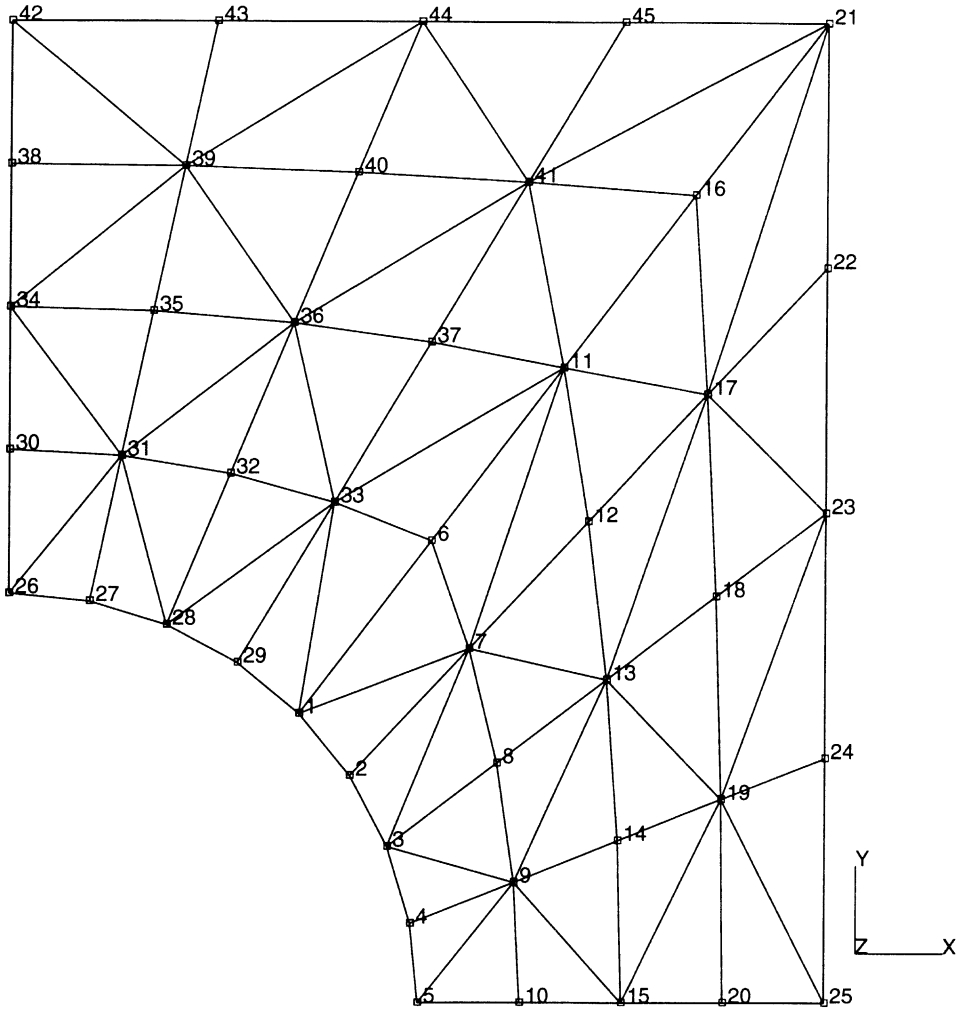

Figure E 5.3-4 Mesh for Element Type 37

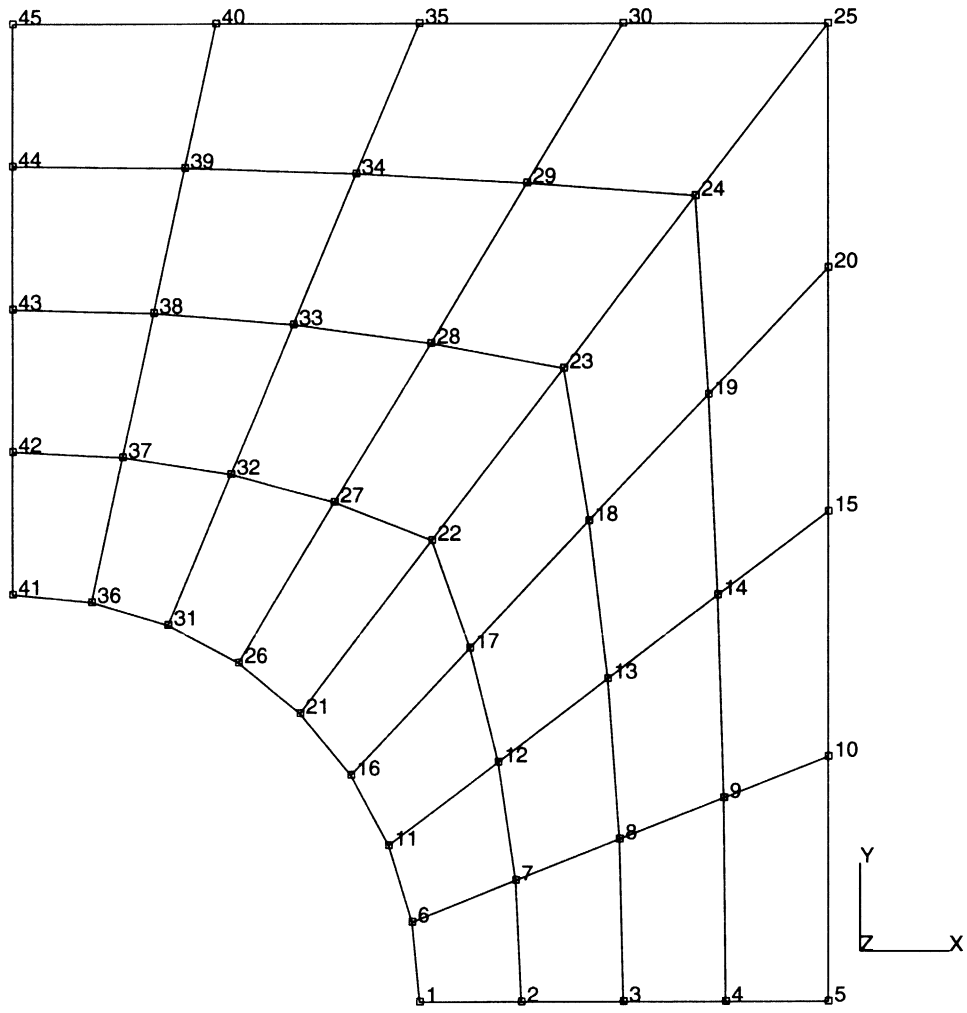

Figure E 5.3-5 Mesh for Element Type 121

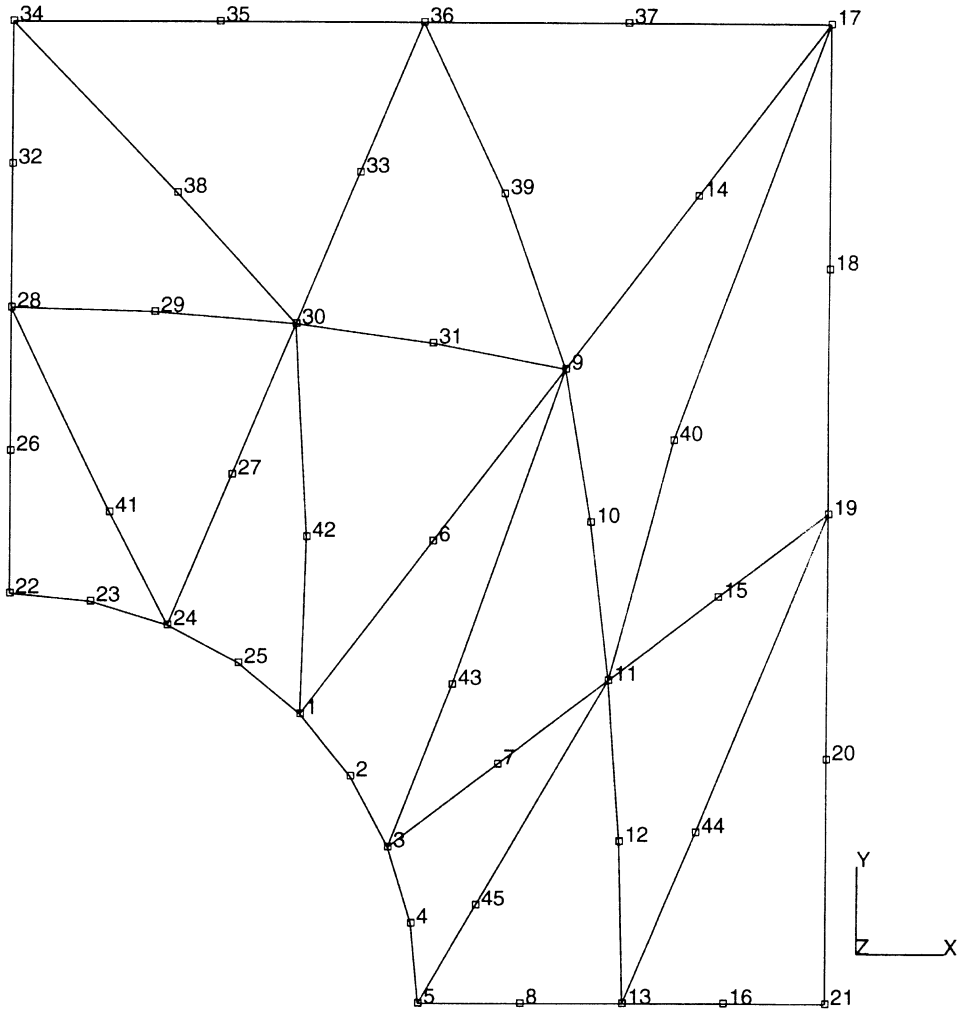

Figure E 5.3-6 Mesh for Element Type 131

Time Sec	Temperatures (element type, node number)					
	41, n9	69, n9	39, n23	37, n11	121, n23	131, n9
.50	535.403	534.993	529.728	526.038	529.731	528.283
1.0	561.951	561.689	558.964	555.728	558.690	556.195
1.5	577.971	577.786	575.893	573.122	575.814	573.194
2.0	585.914	585.783	584.044	581.475	584.040	581.393
2.5	589.609	589.509	587.735	585.241	589.839	585.109
3.0	591.287	591.206	589.369	586.900	591.577	586.756
3.5	592.042	591.970	590.086	587.624	592.278	587.481
4.0	592.381	592.314	590.400	587.939	592.577	587.799
4.5	592.533	592.468	590.537	588.076	592.707	587.938
5.0	592.601	592.538	590.597	588.136	592.763	587.999

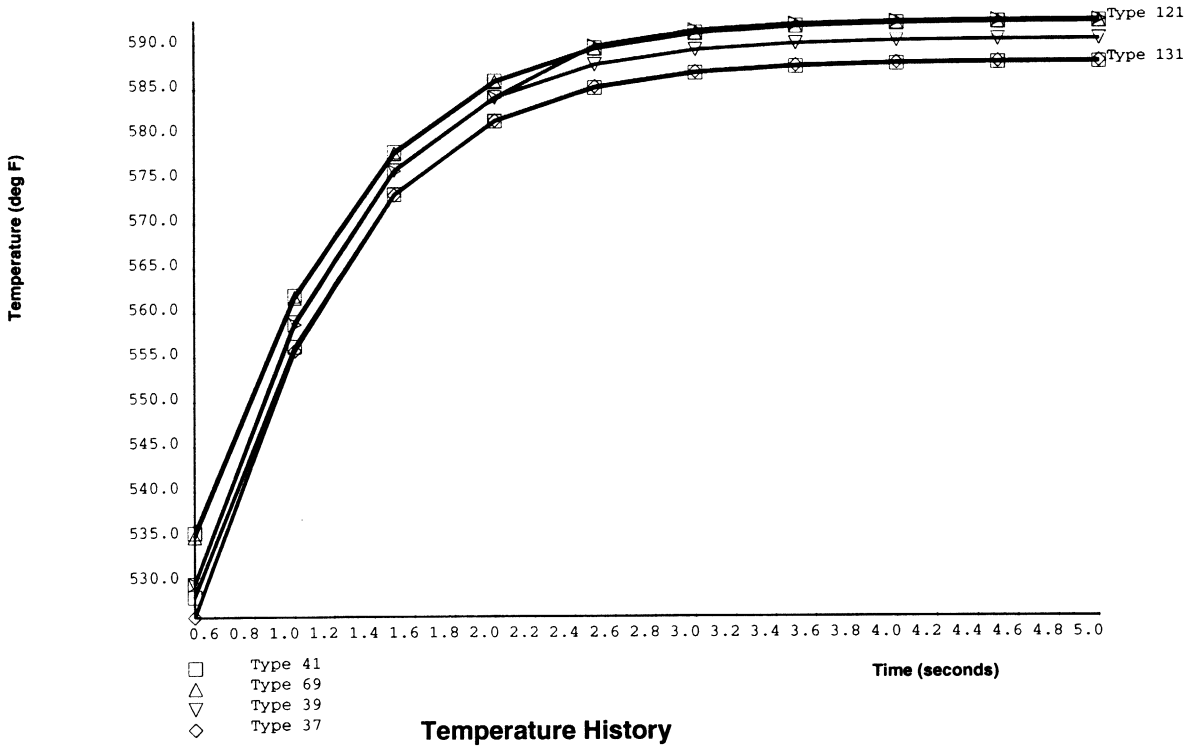

Figure E 5.3-7 Temperature History for Elements Types: 37, 39, 41, 69, 121 and 131

E 5.4 Three-Dimensional Transient Heat Conduction

A unit cube is initially at a temperature of 100°F throughout. Two faces of the cube have a temperature of 0°F. The other faces are insulated. The temperature at the center of the cube is calculated for subsequent times (0 to 10 secs.).

Element (Ref. B43.1, B44.1, B71.1 and B123.1)

MARC element types 43 and 123 are 8-node linear brick elements where type 123 has reduced integration with hourglass control. Types 44 and 71 are 20-node parabolic brick elements where type 71 uses reduced integration. The cube has equal dimensions of 1 inch where x,y and z range from 0 to 1 inch. The cube is modeled with 8 brick elements as shown in Figure E 5.4-2 and Figure E 5.4-3 for the linear and parabolic meshes.

Thermal Properties

One set of thermal properties is specified in the ISOTROPIC block: the isotropic thermal conductivity value is 1.0 Btu/sec-in-°F; the specific heat is 1.0 Btu/lb-°F; and the mass density is 1.0 lb/cu.in.

Thermal Boundary Conditions

The initial temperature distribution is that all nodes have a temperature of 100.0°F. At time t = 0, x = 0 and z = 1 surfaces have a prescribed temperature of 0°F; all other surfaces are adiabatic and require no data input. A transient solution is performed with 10 uniform time steps of 0.1 seconds each for a total time of 1 second.

Results

The temperature at the center of the unit cube is plotted versus time for the various element types and is shown in Figure E 5.4-3. The cube has almost cooled down completely after 1 second. The linear elements (types 43 and 123) initially cool down slower than the parabolic elements (types 44 and 71).

Summary of Options Used

Listed below are the options used in example e5x4a.dat:

Parameter Options

ELEMENT
END
HEAT
SIZING
TITLE

Model Definition Options

CONNECTIVITY
CONTROL
COORDINATE
END OPTION
FIXED TEMPERATURE

INITIAL TEMPERATURE
ISOTROPIC
POST
PRINT CHOICE
UDUMP

Load Incrementation Options

CONTINUE
TRANSIENT

Listed below are the options used in example e5x4b.dat:

Parameter Options

ELEMENT
END
HEAT
SIZING
TITLE

Model Definition Options

CONNECTIVITY
CONTROL
COORDINATE
END OPTION
FIXED TEMPERATURE
INITIAL TEMPERATURE
ISOTROPIC
POST
PRINT CHOICE

Load Incrementation Options

CONTINUE
TRANSIENT

Listed below are the options used in example e5x4c.dat:

Parameter Options

ELEMENT
END
HEAT
SIZING
TITLE

Model Definition Options

CONNECTIVITY
CONTROL
COORDINATE
END OPTION
FIXED TEMPERATURE
INITIAL TEMPERATURE
ISOTROPIC
POST
PRINT CHOICE

Load Incrementation Options

CONTINUE
TRANSIENT

Listed below are the options used in example e5x4d.dat:

Parameter Options

ALIAS
ELEMENT
END
HEAT
SIZING
TITLE

Model Definition Options

CONNECTIVITY
CONTROL
COORDINATE
END OPTION
FIXED TEMPERATURE
INITIAL TEMPERATURE
ISOTROPIC
POST
PRINT CHOICE

Load Incrementation Options

CONTINUE
TRANSIENT

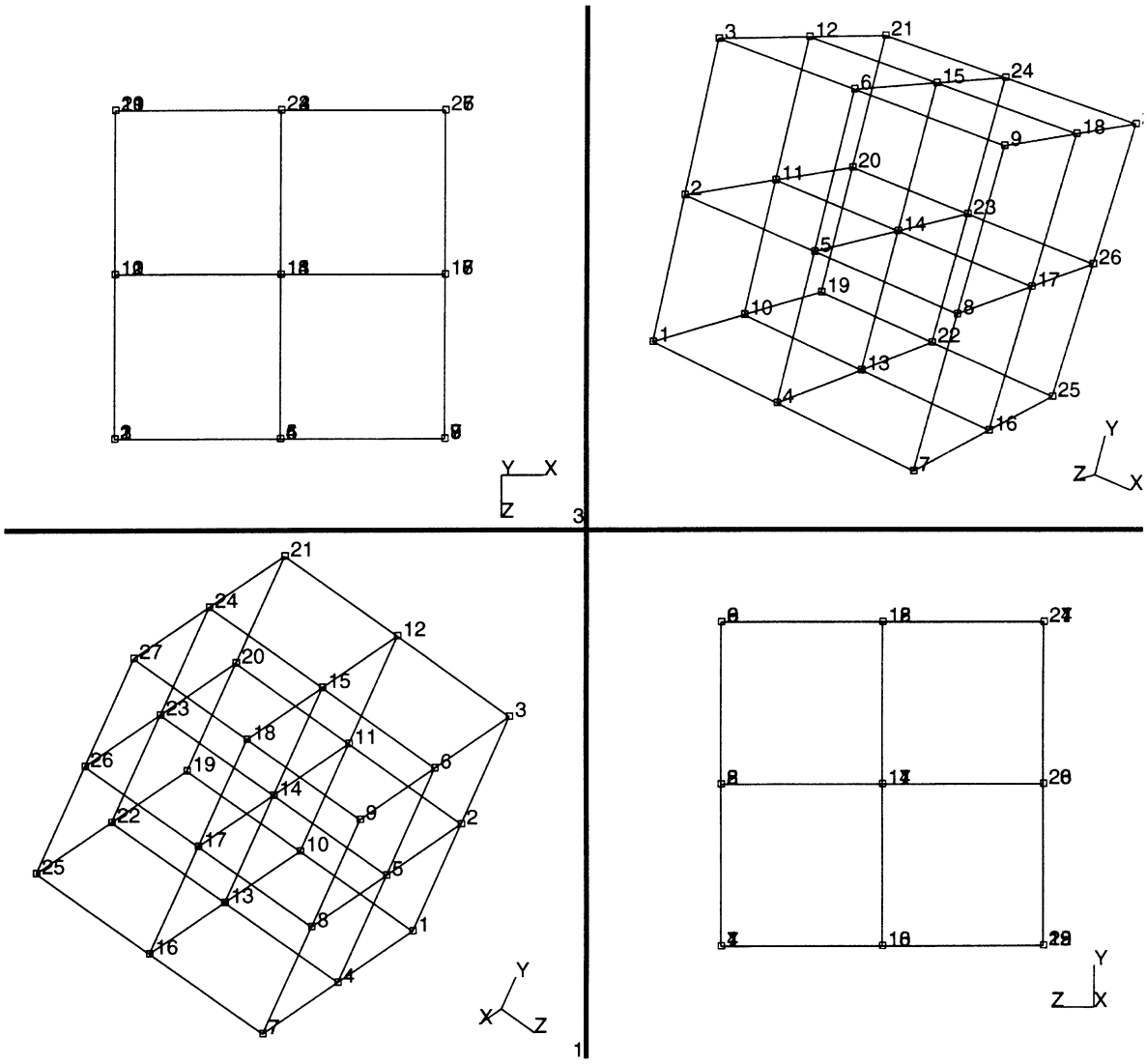

Figure E 5.4-1 Mesh for the Unit Cube Linear Elements

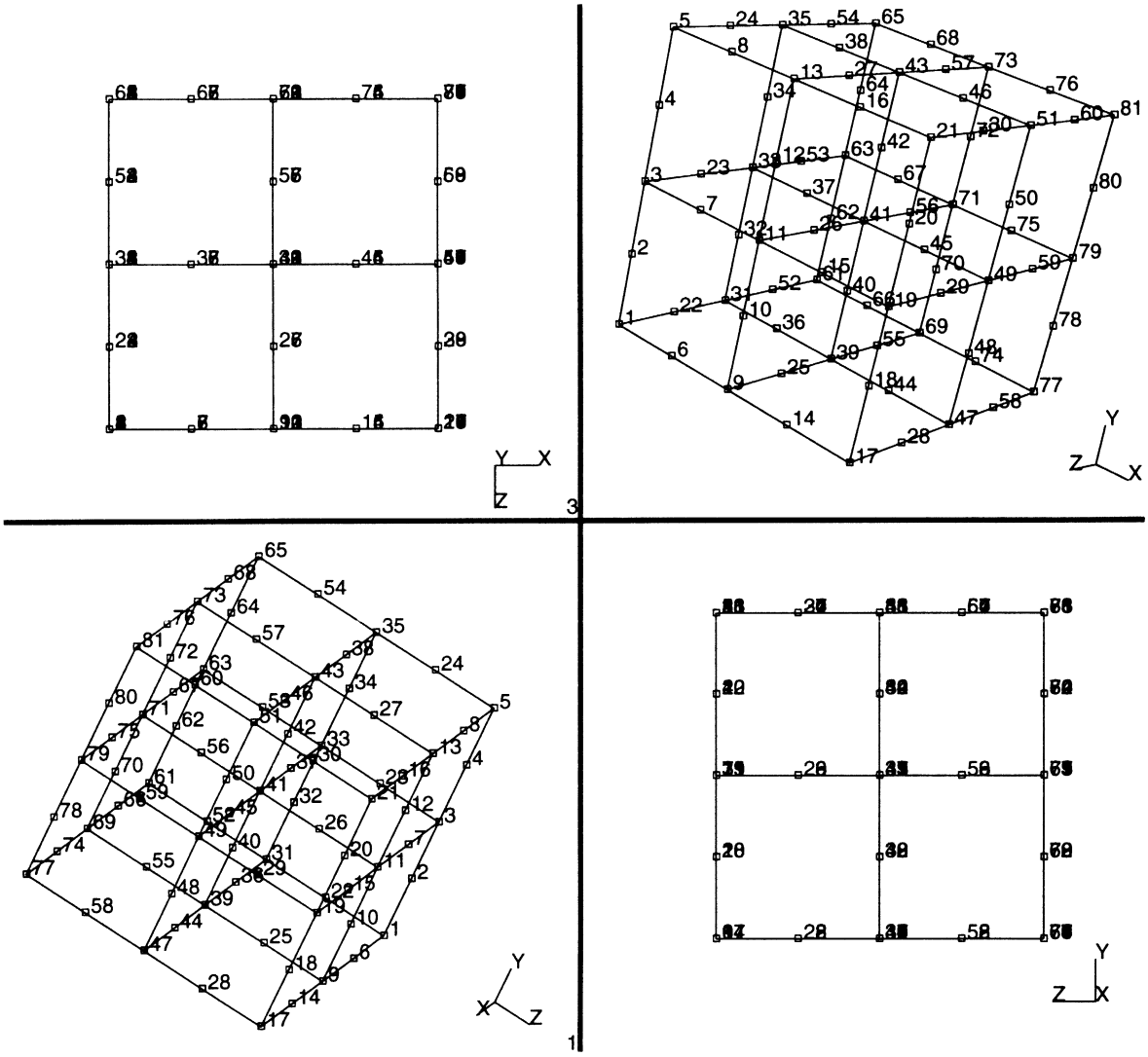

Figure E 5.4-2 Mesh for the Unit Cube Parabolic Elements

Time (Seconds)	Temperatures (element type, node number)			
	Type 43, n14	Type 44, n41	Type 71, n41	Type 123, n41
0.0	1.00000E+02	1.00000E+02	1.00000E+02	1.00000E+02
1.00000E-01	7.49796E+01	6.36616E+01	6.33202E+01	7.49796E+01
2.00000E-01	4.22526E+01	4.03147E+01	4.02325E+01	4.22526E+01
3.00000E-01	2.62808E+01	2.55396E+01	2.55179E+01	2.62808E+01
4.00000E-01	1.69623E+01	1.66272E+01	1.66202E+01	1.69623E+01
5.00000E-01	1.10900E+01	1.09937E+01	1.09915E+01	1.10900E+01
6.00000E-01	7.28266E+00	7.32065E+00	7.32054E+00	7.28266E+00
7.00000E-01	4.78960E+00	4.88981E+00	4.89058E+00	4.78960E+00
8.00000E-01	3.15160E+00	3.27040E+00	3.27148E+00	3.15160E+00
9.00000E-01	2.07415E+00	2.18852E+00	2.18962E+00	2.07415E+00
1.00001E+00	1.36513E+00	1.46487E+00	1.46587E+00	1.36513E+00

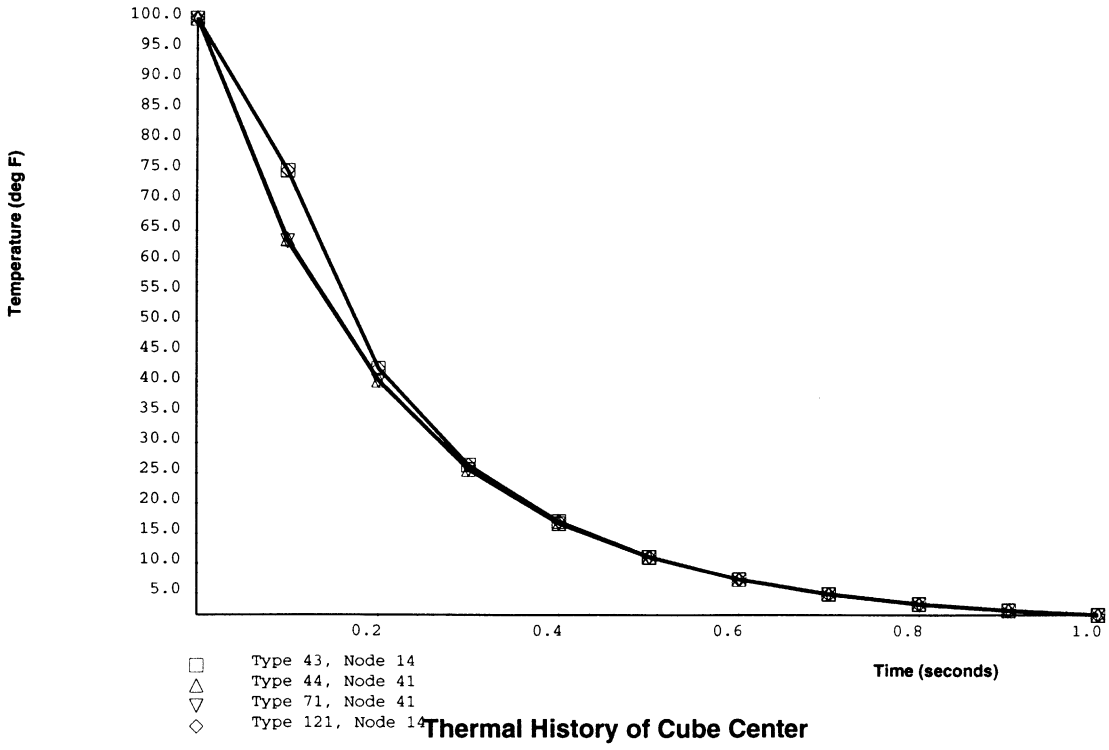

Figure E 5.4-3 Cube Center Temperature History for Element Types: 43, 44, 71 and 123

E 5.5 Pressure Vessel Subjected To Thermal Downshock

A realistic design problem, such as thermal ratcheting analysis, involves a working knowledge of a significant number of program features. This example illustrates how these features are used to analyze a simplified form of a pressure vessel component which is subjected to a thermal downshock. This problem is typical of reactor component analysis. The general temperature-time history which will be used is shown in Figure E 5.5-1.

An analysis of this type requires heat transfer analysis to determine the transient temperature distribution. This distribution is calculated for the wall of a cylindrical pressure vessel under cool-down conditions. The resulting data must be saved for use in the stress analysis.

Element (Ref. B42.1, B70.1)

The 8-node axisymmetric, quadrilateral elements are used in this example. The heat transfer elements 42 and 70, are used in the determination of the transient temperature distributions.

Model

The geometry and mesh for this example are shown in Figure E 5.5-2. A cylindrical wall segment is evenly divided in six axisymmetric quadrilateral elements with a total of 33 nodes. The mesh data is entered as element type 28. The ALIAS parameter option allows the user to generate his connectivity data with the stress analysis element and then to replace this element with the corresponding heat transfer element type.

Heat Transfer Properties

It is assumed here that the material properties do not depend on temperature; no slope-breakpoint data are input. The uniform properties used here are:

specific heat (c) = 0.116 Btu/lb-°F
thermal conductivity (k) = 4.85 (10^{-4}) Btu/in-sec-°F
density (ρ) = 0.283 lb/cu.in.

Heat Transfer Boundary Conditions

The initial temperature across the wall and ambient temperature are 1100°F as specified in the initial conditions block. The outer ambient temperature is held constant at 1100°F while the inner ambient temperature decreases from 1100°F to 800°F in 10 secs and remains constant thereafter.

The FILMS option is used to input the film coefficients and associated sink temperatures for the inner and outer surface. A uniform film coefficient for the outside surface is specified for element 6 as 1.93 x 10^{-6} Btu/sq.in-sec-°F in order to provide a nearly insulated wall condition. The inner surface has a film coefficient of 38.56 x 10^{-5} Btu/sq.in-sec-°F to simulate forced convection. The temperature down-ramp of 300°F for this inner wall is specified here as a nonuniform sink temperature and is applied using user subroutine FILM.

Subroutine FILM linearly interpolates the 300°F decrease in ambient temperature over 10 secs and holds the inner wall temperature constant at 800°F. It is called at each time step for each integration point on each element surface given in the FILMS option. Thus, this subroutine does nothing if it is called for element 6 to keep the outer surface at 1100°F. It applies the necessary ratio to reduce the inner wall temperature.

The TRANSIENT option controls the heat transfer analysis. The program automatically calculates the time steps to be used based on the maximum nodal temperature change allowed as input in the CONTROL option. The solution begins with the suggested initial time step of one-half second input and ends according to the time period of 250 secs specified. It will not exceed the maximum number of steps input as 120 in this option.

The CONTROL option requires that the maximum temperature change per increment is 15°F. If this is exceeded, the program automatically scales down the time step. The second tolerance on the CONTROL option requires that the program reassembles the operator matrix if the temperature has changed by 1000°F since the last reassembly.

Finally, note in the heat transfer run the use of the POST option. This allows the creation of a post-processor tape containing element temperatures at each integration point and nodal point temperatures. The tape is used later as input to the stress analysis run.

Heat Transfer Results

The transient thermal analysis is linear in that material properties do not depend on temperature and the boundary conditions depend on the surface temperature linearly. The analysis has been completed using the automatic time step feature in the TRANSIENT option.

The TRANSIENT run reached completion in 33 increments with a specified starting time step of 0.5 sec. A 15°F temperature change tolerance was input in the CONTROL option and controlled the auto time stepping scheme. The reduction to approximately 800°F throughout the wall was reached in increment 33 at a total time of 250 secs.

The temperature-time histories of elements 1 (inner wall) and 6 (outer wall) for auto time stepping is shown in Figure E 5.5-3.

The temperature distribution across the wall at various solution times is shown in Figure E 5.5-4. Convergence to steady state is apparent here as is the thermal gradient characteristic of the downshock.

Summary of Options Used

Listed below are the options used in example e5x5a.dat:

Parameter Options

ALIAS
ELEMENT
END
HEAT
SIZING
TITLE

Model Definition Options

CONNECTIVITY
CONTROL
COORDINATE
END OPTION
FILMS
INITIAL TEMPERATURE
ISOTROPIC
POST

Load Incrementation Options

CONTINUE
TRANSIENT

Listed below is the user subroutine found in u5x5.f:

FILM

Listed below are the options used in example e5x5b.dat:

Parameter Options

ELEMENT
END
HEAT
SIZING
TITLE

Model Definition Options

CONNECTIVITY
CONTROL
COORDINATE
END OPTION
FILMS
INITIAL TEMPERATURE
ISOTROPIC
POST

Load Incrementation Options

CONTINUE
TRANSIENT

Listed below is the user subroutine found in u5x5.f:

FILM

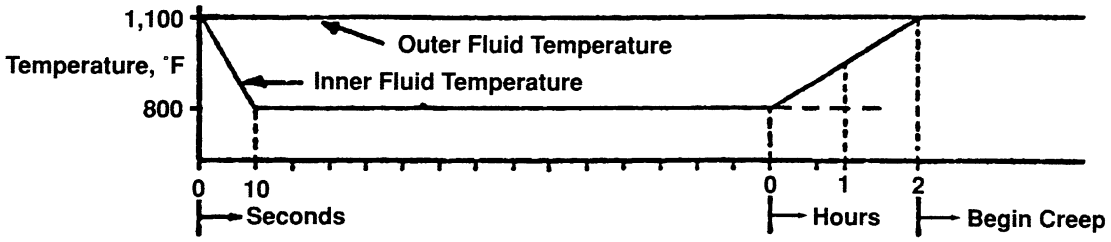

Figure E 5.5-1 Temperature Time History

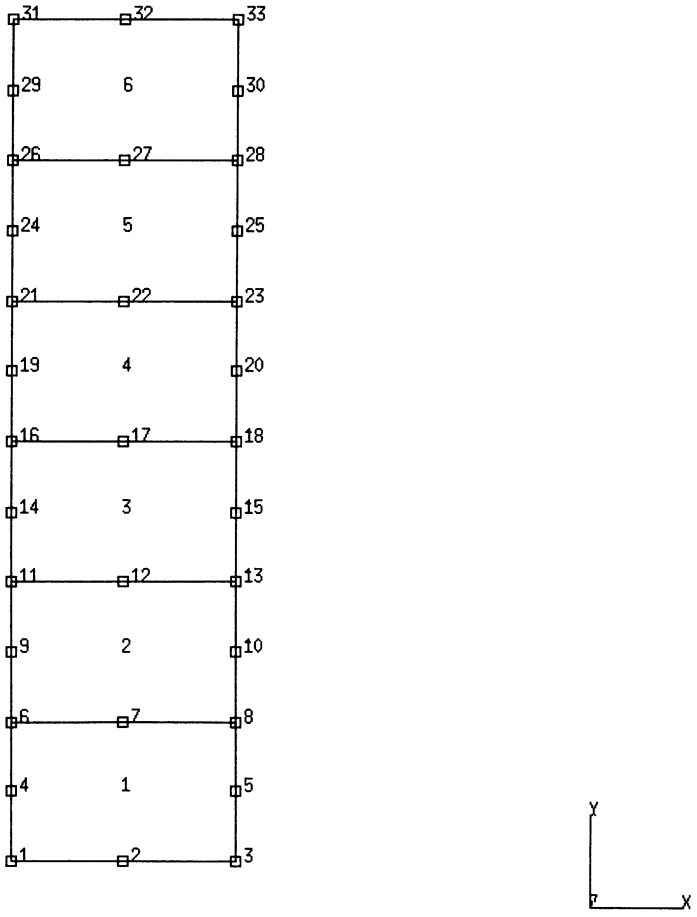

Figure E 5.5-2 Geometry and Mesh

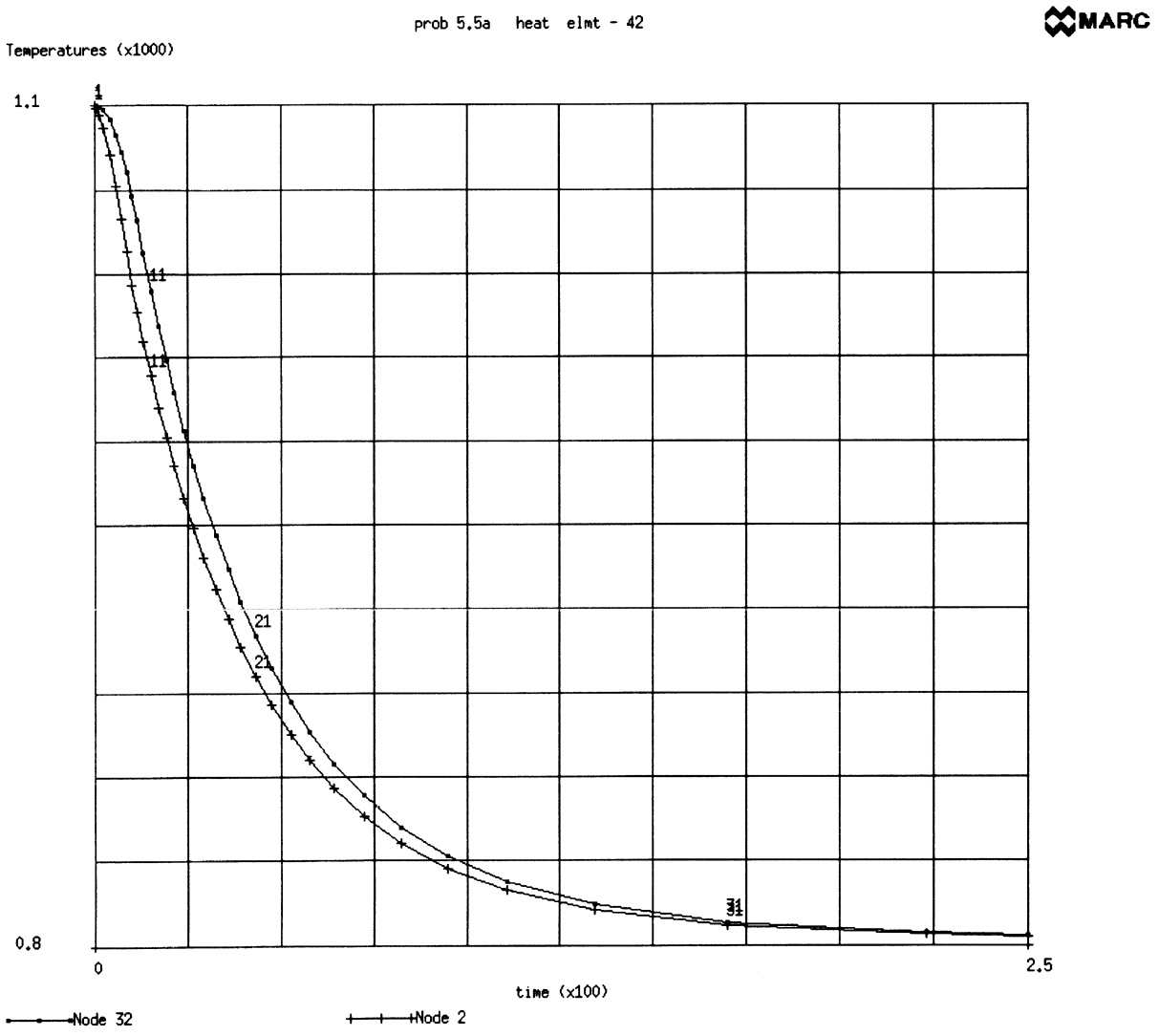

Figure E 5.5-3 Transient Temperature Time History (Auto Time Step)

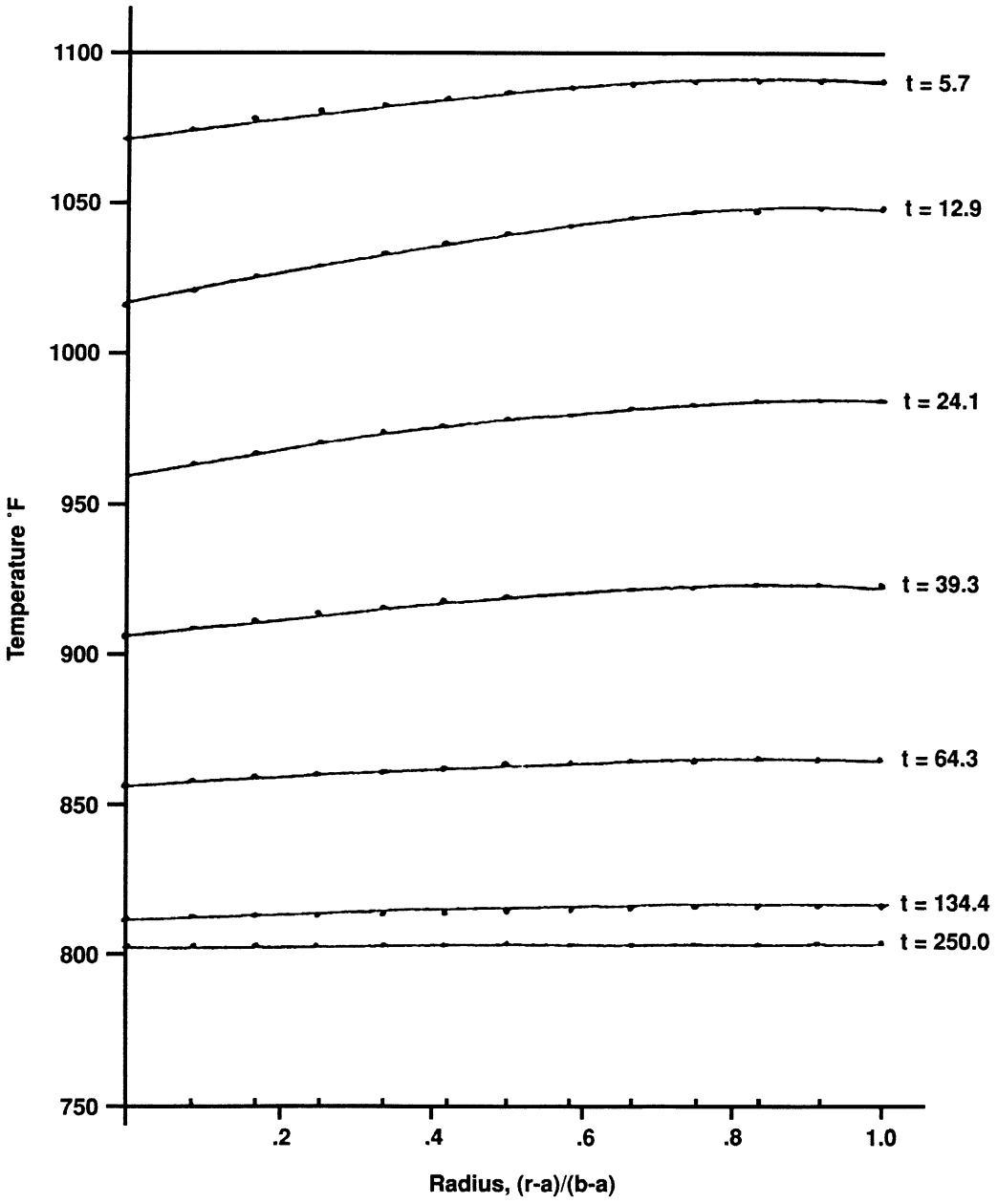

Figure E 5.5-4 Temperature Distribution in Cylinder Wall

E 5.6 Axisymmetric Transient Heat Conduction Simulated By Planar Elements

The transient heat conduction of a thick cylinder, subjected to a thermal downshock, is analyzed by using MARC planar heat transfer element. This is the same problem as E 5.5. The model and input data of the problem are:

Model/Element (Ref. B41.1)

A 45-degree sector of the cylinder is modeled in the x-y plane as shown in Figure E 5.6-1. The MARC heat transfer element type 41 (8-node planar quadrilateral) is selected for the analysis.

Material Properties

The conductivity is 4.85 x 10^{-4} Btu/sec-in- F. The specific heat is 0.116 Btu/lb-°F. The mass density is 0.283 lb/cu.in.

Initial Condition

Initial nodal temperatures are assumed to be homogeneous at 1100°F.

Boundary Conditions

No input data is required for insulated boundary conditions along symmetry lines at y = 0 and y = x. Fluid temperatures and film coefficients for both inner and outer surfaces of the cylinder are:

Inner surface: H_i = 38.56 x 10^{-5} Btu/sec-sq.in-°F
T_i = 1100°F at t = 0. sec
800°F at t = 10. sec

Outer surface: H_0 = 1.93 x 10^{6} Btu/sec-sq.in-°F
(low value to simulate insulated boundary condition).
T_0 = 1100°F

The FILMS option is used to input the film coefficients and associated fluid temperatures for the inner and outer surfaces. Subroutine FILM linearly interpolates the 300°F decrease in ambient temperature over 10 secs and holds the inner wall temperature constant at 800°F. It is called at each time step for each integration point on each element surface given in the FILMS option.

POST

In the heat transfer run, the use of the POST option allows the creation of a postprocessor tape containing element temperatures at each integration point and nodal point temperatures. The tape can be used later as input to the stress analysis run.

TRANSIENT

The TRANSIENT option controls the heat transfer analysis. The program automatically calculates the time steps to be used based on the maximum nodal temperature change allowed as input in the CONTROL option. The solution begins with the suggested initial time step input of 0.5 sec and ends according to the time period specified of 250 secs. It will not exceed the maximum number of steps input in this option.

Results

A comparison of nodal temperatures with the results of an axisymmetric model (problem number E 5.5) are shown in Table E 5.6-1.

Table E 5.6-1 Comparison of Nodal Temperatures

Increment No.	Time (Seconds)	Nodal Temperature (°F)	
		Problem 5.5	Problem 5.6
2	1.25	1099.3	1099.3
4	4.06	1092.6	1092.6
6	7.22	1078.1	1078.1
8	9.94	1068.4	1060.4
10	12.96	1039.8	1039.8
12	17.21	1014.0	1014.0
14	21.44	990.8	990.8
16	26.72	965.7	965.7
18	32.65	941.7	941.5
20	39.2	919.0	918.8

Summary of Options Used

Listed below are the options used in example e5x6.dat:

Parameter Options

ELEMENT
END
HEAT
SIZING
TITLE

Model Definition Options

CONNECTIVITY
CONTROL
COORDINATE
END OPTION
FILMS
INITIAL TEMPERATURE
ISOTROPIC
POST

Load Incrementation Options

CONTINUE
TRANSIENT

Listed below is the user subroutine found in u5x6.f:

FILM

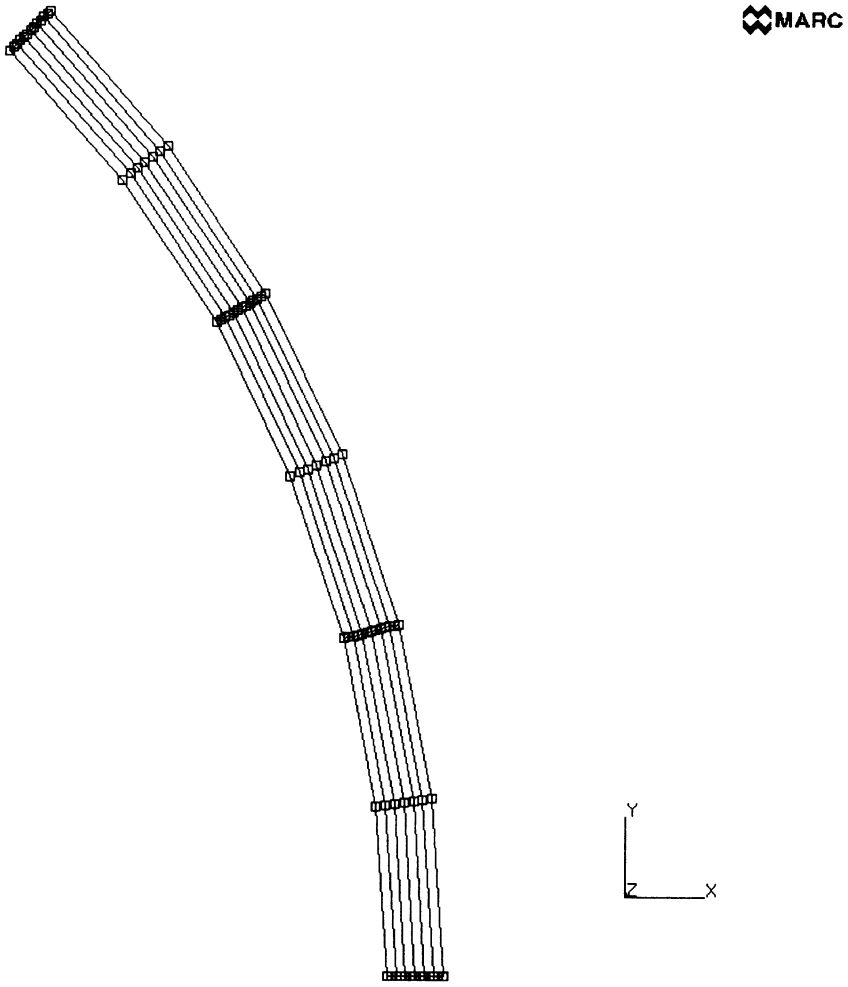

Figure E 5.6-1 Cylinder and Mesh

E 5.7 Steady State Analysis Of An Anisotropic Plate

Two plates are subjected to similar temperature conditions. One plate has thermally isotropic properties; the other is anisotropic. The temperatures of the plate centers are calculated. In the problem, the thermal conductivity of the material is assumed to be anisotropic.

Model/Element (Ref. B39.1)

This two-dimensional steady state heat conduction problem is analyzed using MARC heat transfer element type 39 (4-node planar quadrilateral). A plate is modeled by using four MARC planar heat transfer elements; the number of nodes in the mesh is nine. The size of the plate is 2.0 x 2.0 sq.in. for the anisotropic material and 0.2 x 2.0 sq.in. for the isotropic material.The plate and meshes are shown in Figure E 5.7-1.

Material Properties

The conductivity is 1.0 Btu/sec-in-°F for the isotropic material. k_x is 100.0 and k_y is 1.0 for the anisotropic material. The specific heat is 1.0 Btu/lb.-°F for both plates. The mass density of 1.0 lb/cu.in. is the same for both cases.

Boundary Conditions

A constant temperature of 100°F is prescribed at nodes 1, 2, 3, 4, 6 and of 0°F at nodes 7, 8 and 9.

Transient

A transient time of 1000 secs is assumed for the analysis and the selected time step is 250 secs. Non-automatic time-stepping option is also invoked.

User Subroutine ANKOND

The COND array in the subroutine ANKOND is used for the modification of conductivity due to anisotropic behavior of the material.

Results

Node temperatures at node 5 are identical (25.743°F) for both plates. This is to be expected as the length of the anisotropic plate was adjusted so that the same behavior would be obtained.

Summary of Options Used

Listed below are the options used in example e5x7a.dat:

Parameter Options

ELEMENT
END
HEAT
SIZING
TITLE

Model Definition Options

ANISOTROPIC
CONNECTIVITY
COORDINATE
END OPTION
FIXED TEMPERATURE

Load Incrementation Options

CONTINUE
TRANSIENT

Listed below is the user subroutine found in u5x7a.f:

ANKOND

Listed below are the options used in example e5x7b.dat:

Parameter Options

ELEMENT
END
HEAT
SIZING
TITLE

Model Definition Options

CONNECTIVITY
COORDINATE
END OPTION
FIXED TEMPERATURE
ISOTROPIC

Load Incrementation Options

CONTINUE
TRANSIENT

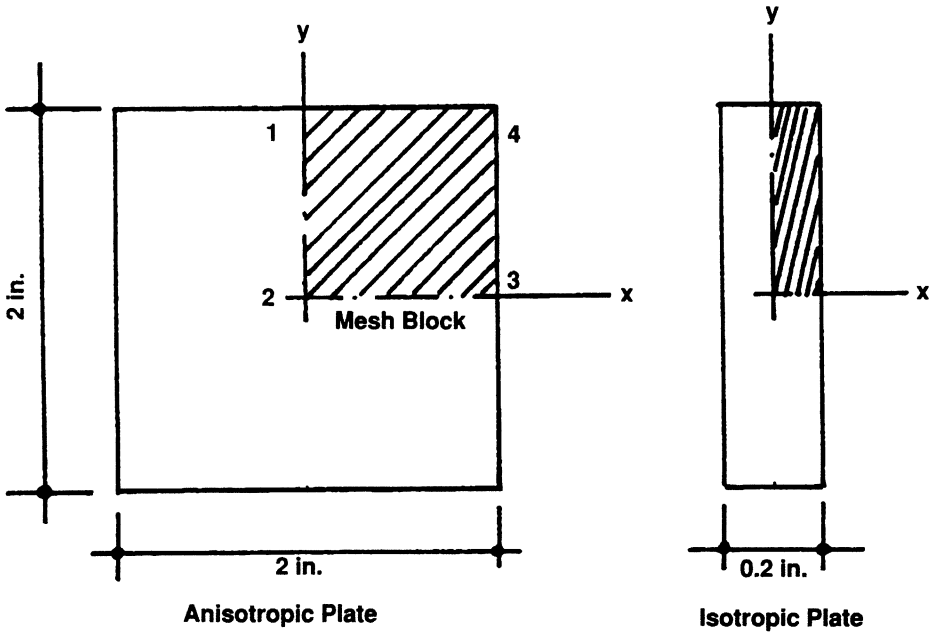

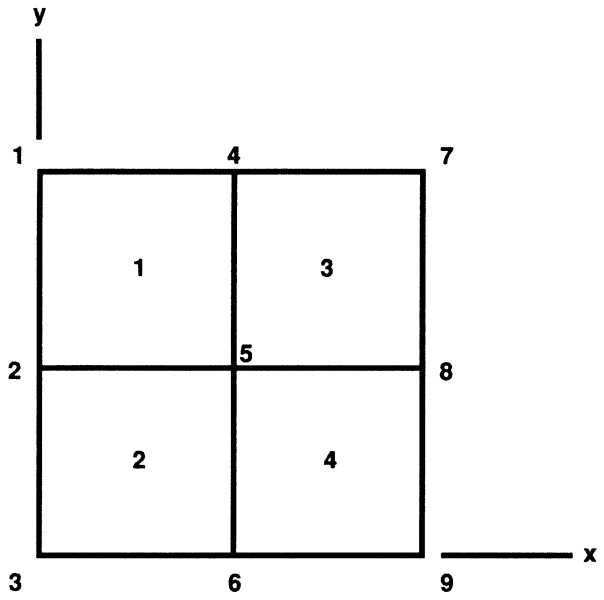

Figure E 5.7-1 Plate and Mesh

E 5.8 Nonlinear Heat Conduction Of A Channel

Many important problems in heat transfer involve the interaction between transient heat conduction in a solid body and convection and radiative heat transfer in surrounding media. These problems are inherently nonlinear (although a linearized model is often sufficient) due to the complex nature of this interaction. For instance, radiative heat transfer rates depend on the surface temperature raised to the fourth power and the emissivity, ε, of a gray body may be a strong function of surface temperature, as well. Convective heat transfer rates depend linearly on the surface temperature explicitly, but the convective coefficients themselves may depend on the surface temperature (e.g., in evaluating mean film properties), giving rise to an implicit nonlinear dependence.

This example illustrates the ability of MARC to treat this class of nonlinear problems, provided that some care is taken in modeling. A user-supplied subroutine is exhibited which, in this case, computes the radiation and convection effects for the surface of the solid by using estimates of the surface temperatures, iterating if necessary.

The user should understand that the mesh used and tolerances set in this example are intended for demonstration purposes only – an accurate solution would require a more detailed mesh as well as tighter tolerances.

Element (Ref. B41.1)

The element used here is the 8-node planar heat transfer element, element type 41. (See Volume B for details of this element.)

Model

The geometry for the heat transfer problem is shown in Figure E 5.8-1. A liquid flows down a U-shaped channel at 10 in/sec. The liquid temperature increases steadily from 70°F to 400°F and remains at 400°F for the rest of the analysis. A uniform heat flux of 10^{-4} Btu/sq.in-sec is being steadily applied along the extremities of the channel legs; free convective transfer and radiative transfer are specified on the inside and outside faces of the channel legs, respectively; and a uniform temperature of 70°F is maintained on the base of the channel. The problem is not intended to represent any physical situation – it simply serves as an illustration of the modeling techniques used with heat transfer analysis.

The mesh is shown in Figure E 5.8-2. For a more accurate geometric modeling more blocks should be used at the corner.

Boundary Conditions

The boundary conditions for the analysis are shown in Figure E 5.8-1. The simpler conditions (fixed temperature, flux) are input directly. The more complex radiation and convection conditions are input through subroutine FILM.

The FILMS Model Definition block causes the routine to be called at each surface integration point of each element listed in that model definition set. Then, based on the element number (which is passed in to the routine) the following sections are provided:

a. Forced, liquid metal convection on all elements adjacent to the metal stream. Here the routine calculates a film coefficient as follows:

The liquid metal properties – conductivity, Prandtl number, and kinematic viscosity – are assumed to be functions of the average boundary layer temperature (the average temperature is based on the mean of the free stream temperature and the estimated surface temperature). Then, the hydraulic diameter is computed from the formula:

$$D_H = \frac{4\ (\text{flow cross-sectional area})}{(\text{wetted perimeter})}$$

For this example, D_H = 10 in. approximately. The Reynolds number is given by the relation:

$$Re_D = \frac{D_H V}{\nu}$$

where:

V is the velocity of the flow
ν is the kinematic velocity

The Peclet number, Pe, is given by the product of the Reynolds and Prandtl (Pr) numbers. Then the average Nusselt number, Nu, is found from the experimentally verified formula for fully developed turbulent flow of liquid metals (see Lubarsky, B, and Kaufman, S. J., "Review of Experimental Investigations of Liquid-Metal Heat Transfer", NACA TN 3336, 1955.):

$$\bar{N}u = 0.625\ (Pe)^{0.4}$$

The final step is to find the average heat transfer coefficient from:

$$\bar{h}_e = \frac{k\ \bar{N}u}{D_H}$$

where k is the thermal conductivity of the liquid metal. The bulk fluid temperature increases linearly with time from 70°F to 400°F, then remains constant at 400 F for the rest of the analysis. These values of $\bar{h}_e$ and the bulk fluid temperature are passed back from FILM in H and TINF, respectively. Note that the film coefficient is so high that the surface nodes effectively take on the bulk fluid temperature directly as a prescribed surface temperature boundary condition.

b. Free Convection:

Here the constant film coefficient and bulk temperature are entered directly in H and TINF.

c. Radiation:

The radiation law is: $q = \varepsilon\sigma (T^4 - T_\infty^4)$

where ε is the emissivity of the surface (here assumed to be 0.6), σ is the Stefan-Boltzmann constant, and temperatures are in absolute units. In this case, T_∞ is 460 + 70 = 530°R. In order to perform a linear time stepping scheme, the above equation is rewritten as:

$$q = \varepsilon\sigma (T^3 + T^2T_\infty + T\ T_\infty^2)\ (T - T_\infty)$$

and a temperature dependent film coefficient:

$$h = \varepsilon\sigma (T^3 + T^2T_\infty + T\ T_\infty^2 + T_\infty^3)$$

is calculated in the subroutine.

Subroutine FILM defines relative values, i.e. multipliers of the data values for H and TINF entered on the FILMS model definition set. In this case, it is more convenient to program absolute values in FILM; therefore, values of 1. are entered in the Model Definition set.

Time Stepping

In this case, the automatic time stepping scheme is chosen, based on a maximum temperature change per increment of 50°F. The program adjusts time steps to conform to this criterion according to the scheme defined in Volume F. Tolerances are also placed on the maximum temperature change before the program recalculates nonlinear effects; i.e. temperature-dependent material properties and temperature-dependent boundary conditions, both of which are present in this example, and on the maximum temperature variation between that temperature used to evaluate properties and the resulting solution, to allow iteration as necessary. It should be emphasized that for an accurate solution as well as a finer mesh, a tighter tolerance on temperature change per step should be provided.

Results

Isotherm plots are shown in Figure E 5.8-3, Figure E 5.8-4 and Figure E 5.8-5 showing the temperature field after 100, 400 and 10,000 secs. They illustrate the progress toward steady state conditions. At 10,000 secs., the solution is not yet at steady state. The last step of about 1000 secs. shows a maximum nodal temperature change of 11°F. Therefore, steady state would be reached in a smaller number of additional steps. The program used 18 steps to produce this solution (based on the 50°F per step maximum temperature change tolerance) with an initial step of 100 sec. and a final step size of about 2000 sec. This is a typical illustration of the effectiveness of the automatic stepping scheme. The transient temperature for selected nodes is shown in Figure E 5.8-6.

Summary of Options Used

Listed below are the options used in example e5x8a.dat:

Parameter Options

ELEMENT
END
HEAT
MESH PLOT
SIZING
TITLE

Model Definition Options

CONNECTIVITY
CONTROL
COORDINATE
DIST FLUXES
END OPTION
FILMS
FIXED TEMPERATURE
INITIAL TEMPERATURE
ISOTROPIC
OPTIMIZE
POST
RESTART
TEMPERATURE EFFECTS

Load Incrementation Options

CONTINUE
TRANSIENT

Listed below is the user subroutine found in u5x8.f:

FILM
FLUX

Listed below are the options used in example e5x8b.dat:

Parameter Options

ELEMENT
END
HEAT
MESH PLOT
SIZING
TITLE

Model Definition Options

END OPTION
RESTART

Load Incrementation Options

CONTINUE

Listed below are the options used in example e5x8c.dat:

Parameter Options

ELEMENT
END
HEAT
SIZING
TITLE

Model Definition Options

CONNECTIVITY
CONTROL
COORDINATE
DIST FLUXES
END OPTION
FILMS
FIXED TEMPERATURE
INITIAL TEMPERATURE
ISOTROPIC
OPTIMIZE
POST
RESTART
TEMPERATURE EFFECTS

Load Incrementation Options

CONTINUE
TRANSIENT

Listed below are the options used in example e5x8d.dat:

Parameter Options

ELEMENT
END
HEAT
SIZING
TITLE

Model Definition Options

CONNECTIVITY
CONTROL
COORDINATE
DIST FLUXES
END OPTION
FILMS
FIXED TEMPERATURE
INITIAL TEMPERATURE
ISOTROPIC
OPTIMIZE
POST
RESTART
TEMPERATURE EFFECTS

Load Incrementation Options

CONTINUE
TRANSIENT

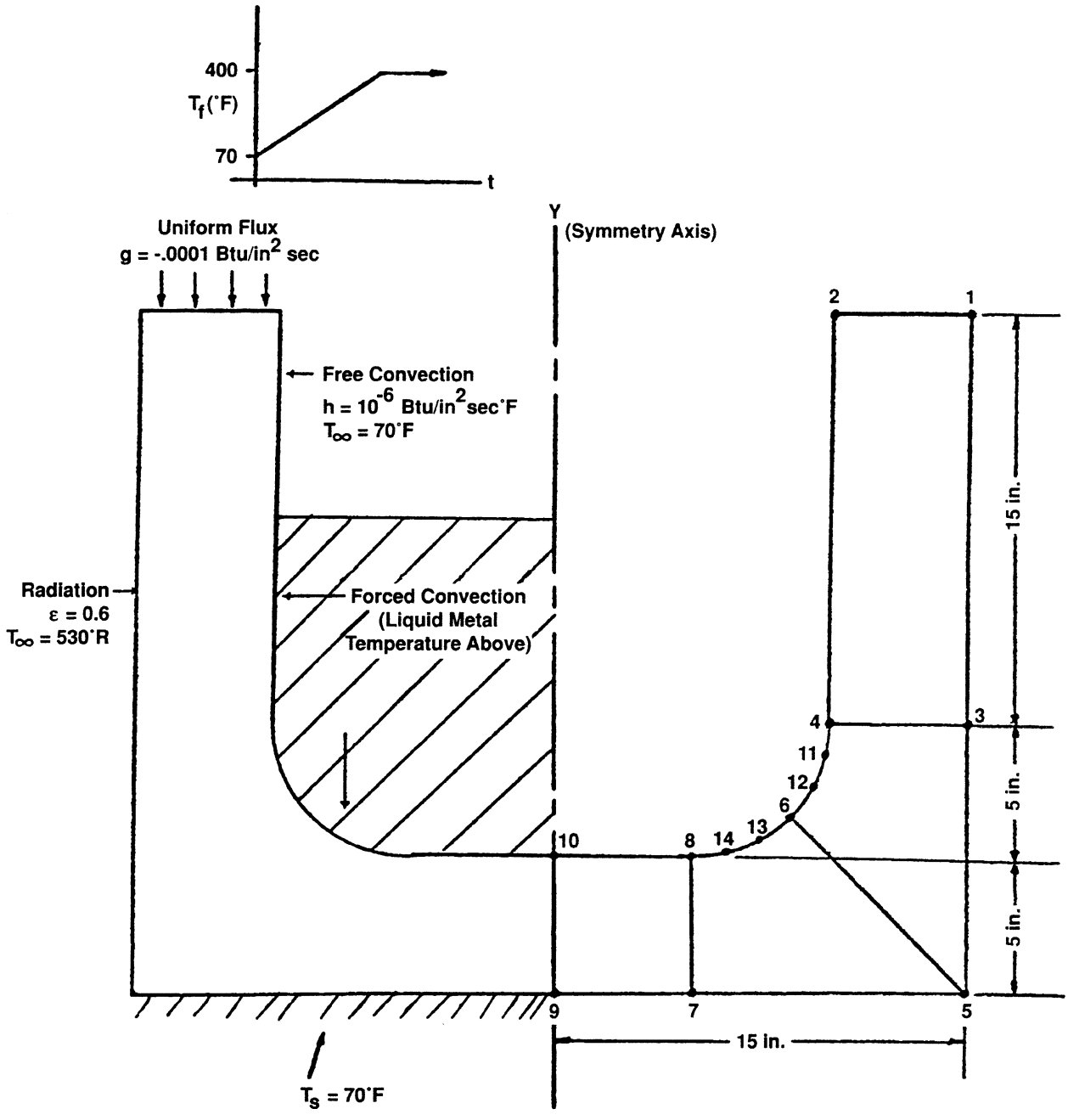

Figure E 5.8-1 Geometry for Nonlinear Heat Conduction

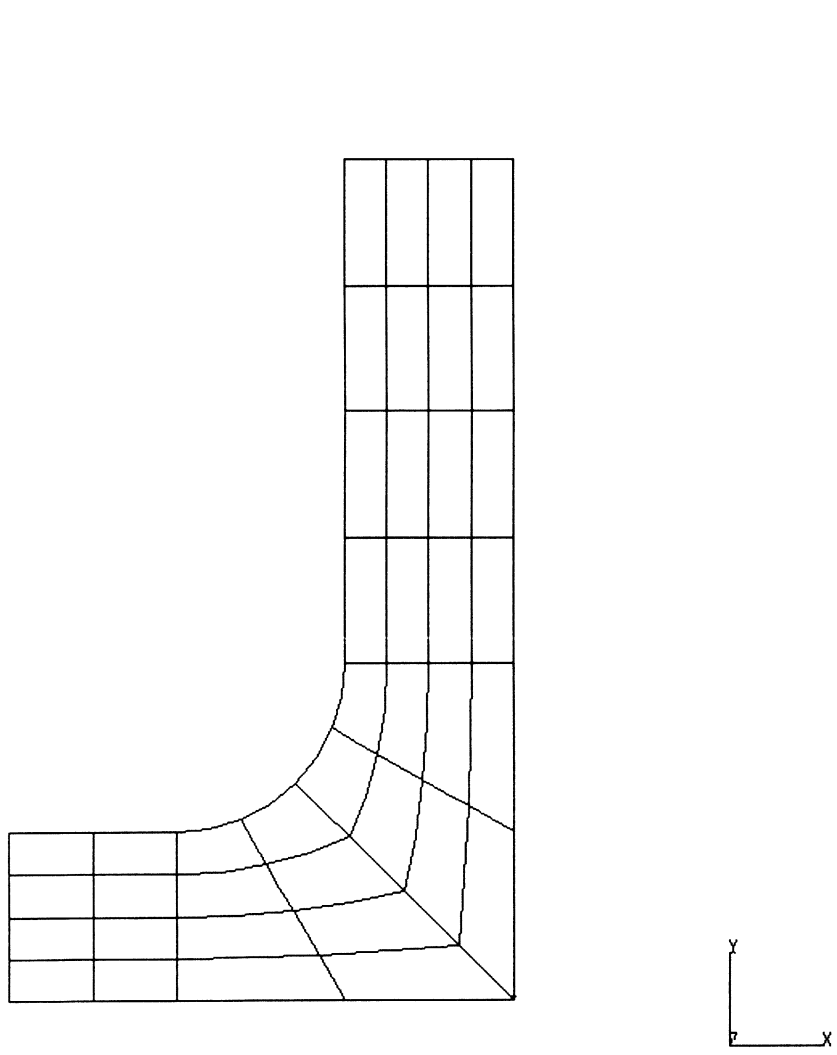

Figure E 5.8-2 Heat Transfer Example Mesh

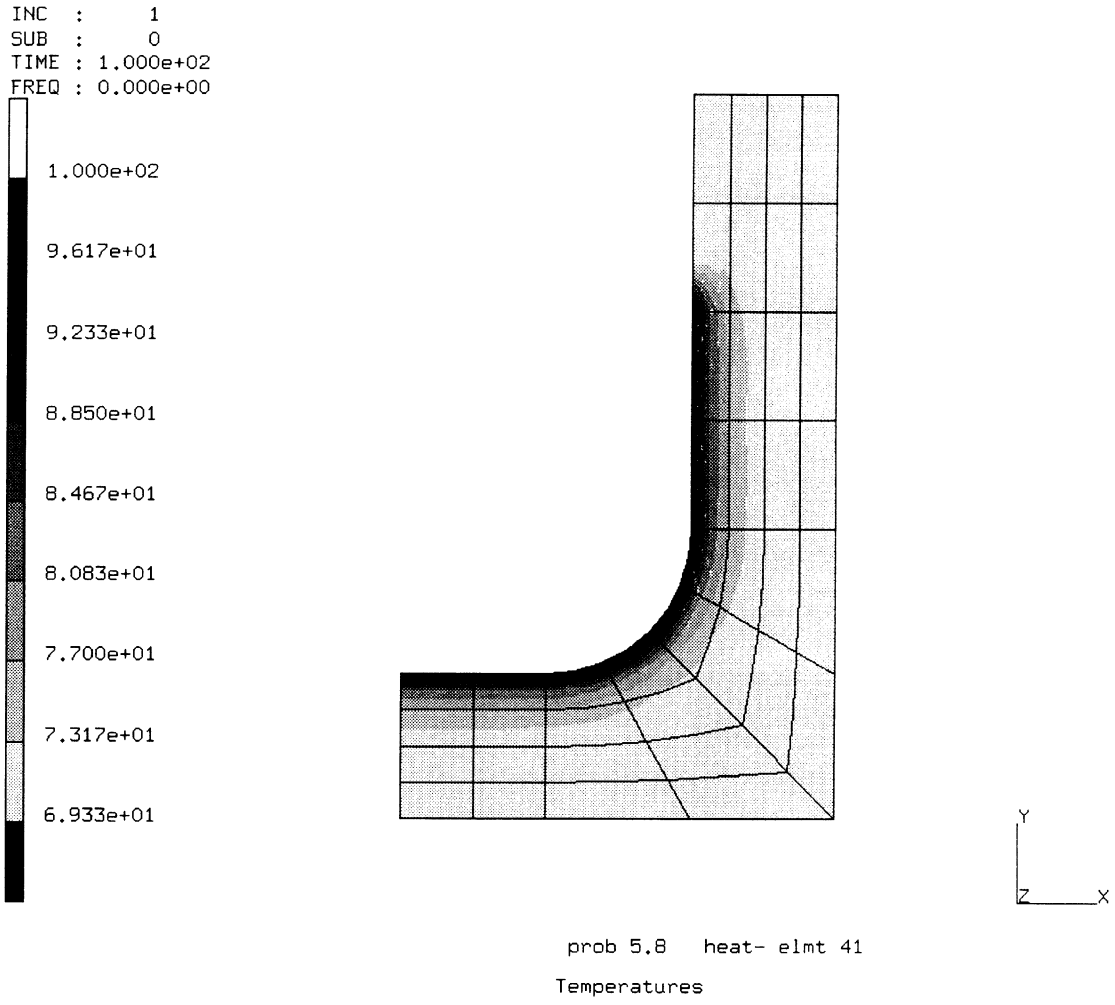

Figure E 5.8-3 Isotherms at 100 Secs.

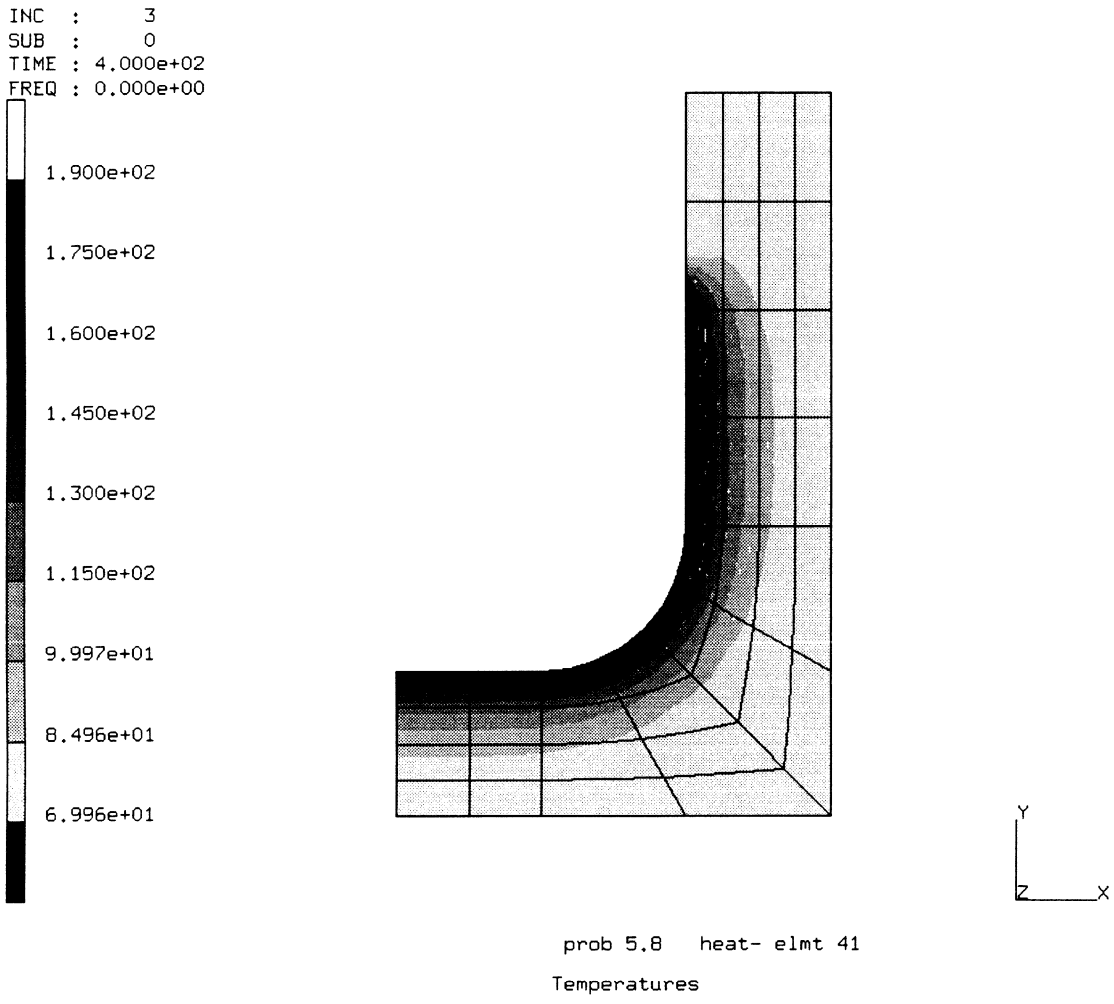

Figure E 5.8-4 Isotherms at 400 Secs.

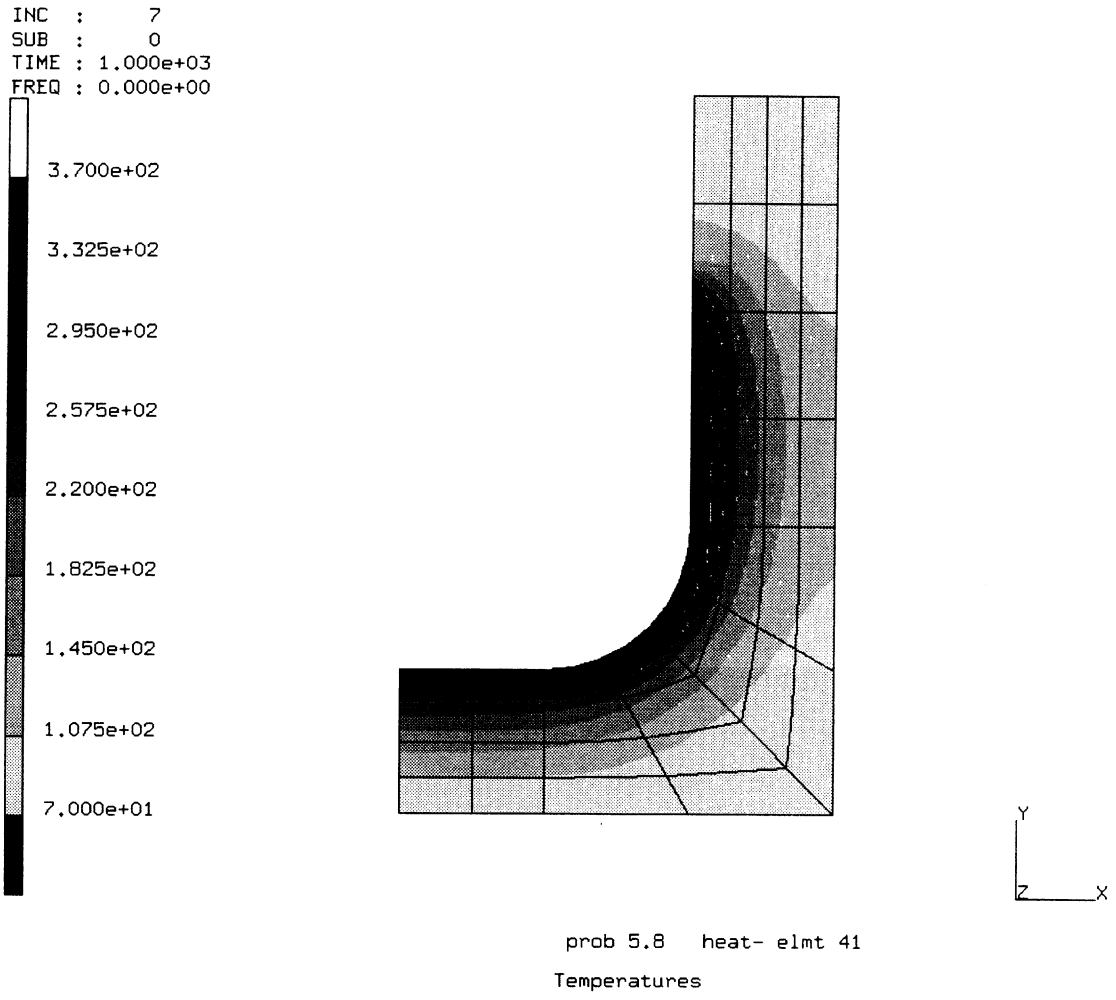

Figure E 5.8-5 Isotherms at 1000 Seconds

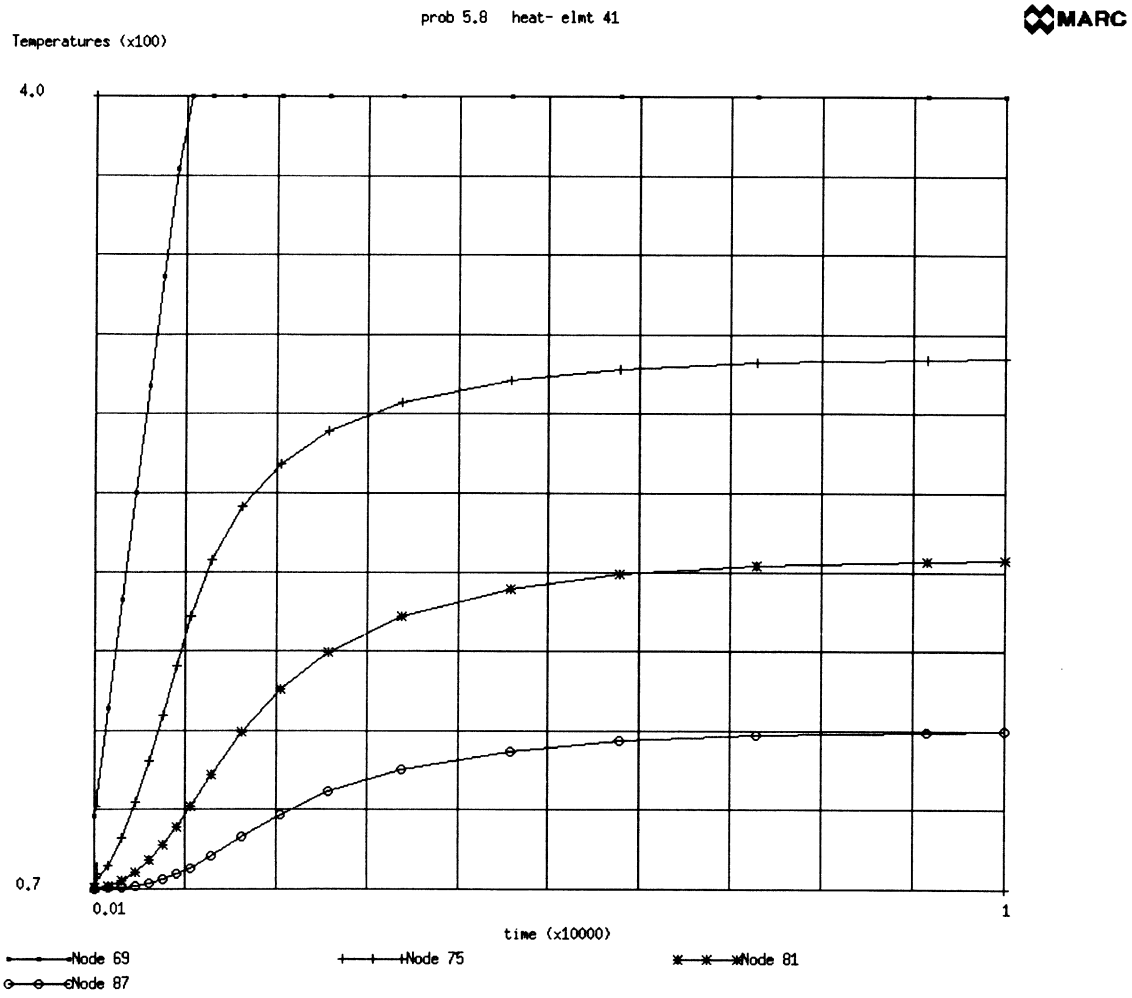

Figure E 5.8-6 Temperature History

E 5.9 Latent Heat Effect

In heat conduction analysis, the material may exhibit phase change at certain temperature levels. This change of phase can be characterized by a sharp change in temperature dependent specific heat of the material or a latent heat associated with a given temperature range. A solid cylinder subjected to convective boundary condition and the effect of latent heat on the thermal response is studied.

Model

MARC element types 40 and 122 are 4-node axisymmetric quadrilateral elements where type 122 has reduced integration with hourglass control. Type 132 is a 6-node axisymmetric triangular element. The cylinder of radius 0.594 inches is modeled with 10 quadrilateral elements that span 0.1 inches of its length. The 10 quadrilateral elements are triangulated into 20 type 132 elements as shown in Figure E 5.9-1.

Thermal Properties

Material properties are as follows: isotropic thermal conductivity is 0.5712E-04 Btu/sec-in°F; specific heat is 0.11199 Btu/lb-°F; mass density is 0.281 lb/cu.in.; latent heat is 76.51 Btu/lb with a solidus temperature of 423°F and a liquidus temperature of 757°F.

The properties as a function of temperature are shown in Figure E 5.9-2. A second temperature dependent specific heat curve with a latent heat is also shown in the same figure. TEMPERATURE EFFECTS option of the program is used to input these functions.

Thermal Boundary Conditions

The initial temperature distribution is that all nodes have a temperature of 1550.0°F. At time t = 0, the outer surface begins to convect to the surroundings with a sink temperature of 100°F and a film coefficient of 0.009412 Btu/sec.-sq.-in.-°F. Nonautomatic time-stepping is invoked where the total transient time is 100 seconds using eight different time steps. The time steps are:

Time Step (seconds)	Number of Steps	Transient Time (seconds)
0.001	10	0.01
0.005	8	0.04
0.01	15	0.15
0.05	16	0.80
0.1	20	2.00
0.5	44	22.00
1.0	15	15.00
5.0	12	60.00
Total =	140	100.0

Results

The thermal response is summarized by plotting the temperature history of the center and outer surface of the cylinder shown in Figure E 5.9-3. Notice how the temperature at the center of the cylinder drops as the material solidifies.

Summary of Options Used

Listed below are the options used in example e5x9a.dat:

Parameter Options

ELEMENT
END
HEAT
SIZING
TITLE

Model Definition Options

CONNECTIVITY
CONTROL
COORDINATE
END OPTION
FILMS
INITIAL TEMPERATURE
ISOTROPIC
POST
TEMPERATURE EFFECTS
UDUMP

Load Incrementation Options

CONTINUE
TRANSIENT

Listed below are the options used in examplee5x9b.dat:

Parameter Options

END
SIZING
TITLE

Model Definition Options

CONNECTIVITY
CONTROL
COORDINATE
END OPTION
FILMS
INITIAL TEMPERATURE
ISOTROPIC
POST
PRINT CHOICE
TEMPERATURE EFFECTS

Load Incrementation Options

CONTINUE
TRANSIENT

Example e5.9c used MARC-PLOT.

Listed below are the options used in example e5x9d.dat:

Parameter Options

ELEMENT
END
HEAT
SIZING
TITLE

Model Definition Options

CONNECTIVITY
CONTROL
COORDINATE
END OPTION
FILMS
INITIAL TEMPERATURE
ISOTROPIC
POST
TEMPERATURE EFFECTS

Load Incrementation Options

CONTINUE
TRANSIENT

Listed below are the options used in example e5x9e.dat:

Parameter Options

ELEMENT
END
HEAT
SIZING
TITLE

Model Definition Options

CONNECTIVITY
CONTROL
COORDINATE
DEFINE
END OPTION
FILMS
INITIAL TEMPERATURE
ISOTROPIC
POST
TEMPERATURE EFFECTS

Load Incrementation Options

CONTINUE
TRANSIENT

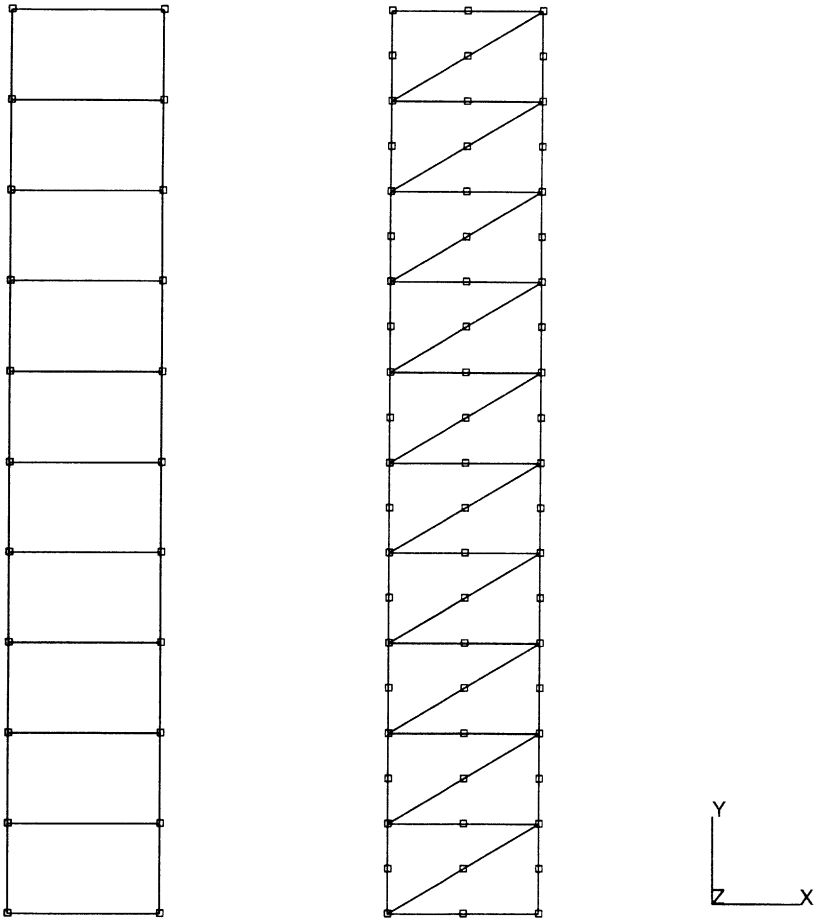

Mesh used for element types 40 and 122 **Mesh used for element type 132**

Figure E 5.9-1 Cylinder Meshes

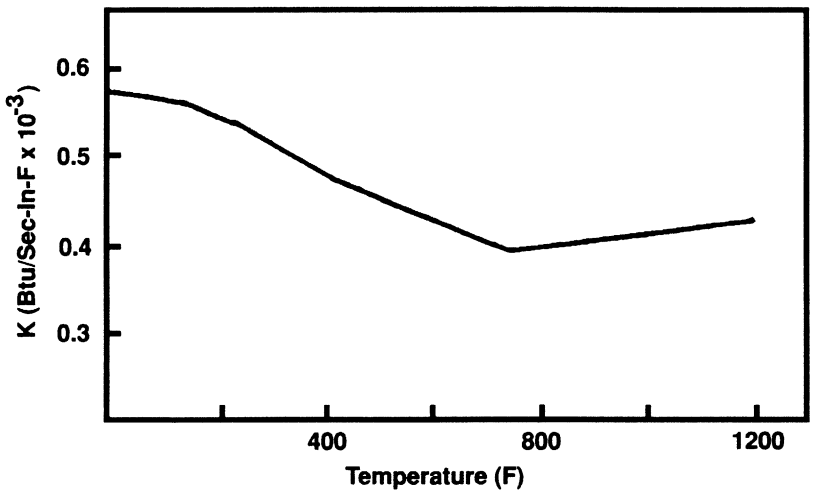

Specific heat as a function of temperature used in problem 5.9A

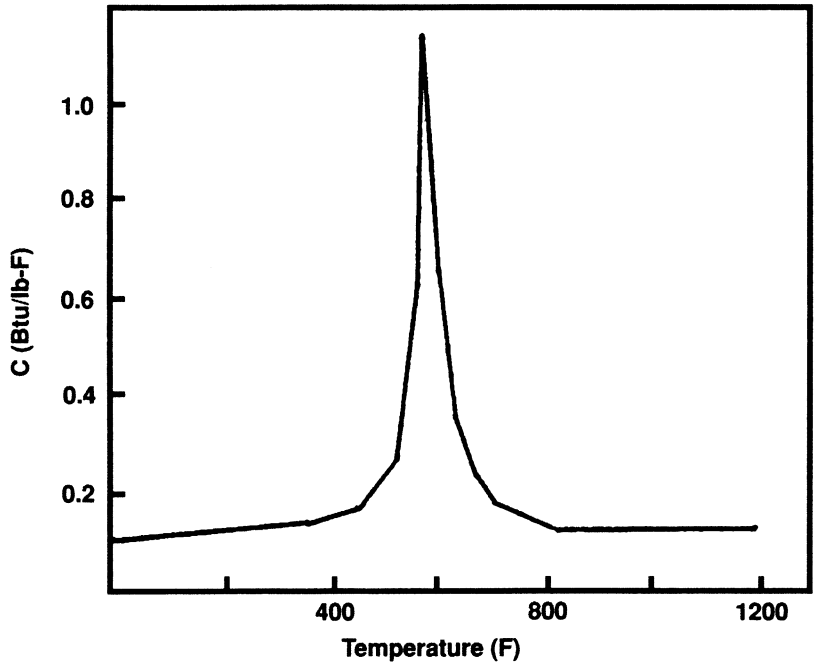

Specific heat as a function of temperature used in problem 5.9B

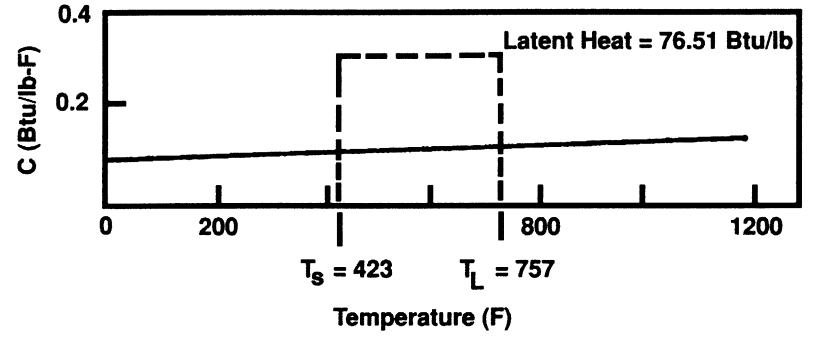

Figure E 5.9-2 Temperature Dependent Thermal Properties

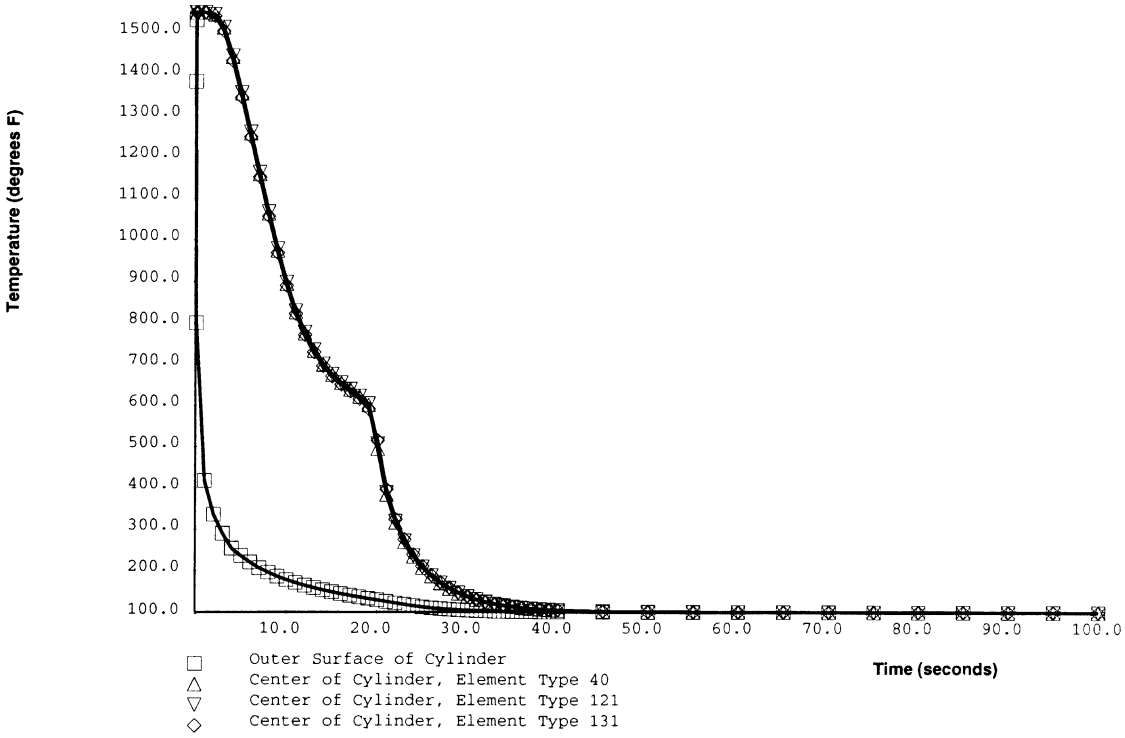

Figure E 5.9-3 Temperature History for Center and Outer Surface of Cylinder

E 5.10 Centerline Temperature Of A Bare Steel Wire

The problem is to determine the centerline temperature of a bare steel wire of constant diameter, carrying a constant current. This wire is 0.75 in. (0.0625 ft.) in diameter with conductivity of 13 Btu/hr-ft-°F. A current of 0.325946×10^6 amps is continuously run through the wire. The surface film coefficient is 5.0 Btu/hr-sq.ft-°F for the outer wire surface.The ambient air temperature is 70°F. The electric resistance of the wire is 30.68×10^{-8} ohm/ft. A centerline temperature of 420°F and a surface temperature of 418°F were predicted by Rohsenow and Choi [1]. This same problem is analyzed by using the Joule heating capability developed in the MARC program.

Model

A finite element model of five 4-node axisymmetric elements (MARC element type 40) and 12 nodal points was selected for this problem. Dimensions of the model and the mesh are depicted in Figure E 5.10-1.

Material Properties

The electrical resistivity is given as 30.68×10^{-8} ohm-ft. The thermal conductivity is 13 Btu/hr-ft-°F.

Current

A distributed current of 0.325946×10^6 amps/sq.ft. is applied to the entire surface of the wire at z = 0.

Joule

A conversion factor of 3.4129 is chosen for the electricity-to-heat unit conversion (from Watts/ft to Btu/hr-ft). The model definition card JOULE is used for the input of this data.

Films

In the thermal analysis, a convective boundary condition is assumed to exist at the outer surface of the wire (element No. 1). The film coefficient and the ambient temperature are 5.0 Btu/hr-sq.ft-°F and 70°F, respectively.

Transient

In order to obtain a steady-state solution of the problem, a large time step (10,000 hrs) is used for a time period of 10,000 hours.

Results

Both the nodal voltages and the nodal temperatures are tabulated as shown in Table E 5.10-1. The agreement between finite element and calculated results is excellent.

Table E 5.10-1 Nodal Voltages and Temperatures

Node No.	Voltages	Temperatures
1	0.1	417.63
2	0.1	418.39
3	0.1	418.98
4	0.1	419.40
5	0.1	419.66
6	0.1	419.77
7	0.0	417.63
8	0.0	418.39
9	0.0	418.98
10	0.0	419.40
11	0.0	419.66
12	0.0	419.77

Reference

Rohsenow, W. M. and Choi, H. Y., *Heat, Mass and Momentum Transfer*, Prentice-Hall, Inc., 1961, p. 106.

Summary of Options Used

Listed below are the options used in example e5x10.dat:

Parameter Options

END
HEAT
JOULE
SIZING
TITLE

Model Definition Options

CONNECTIVITY
COORDINATE
DIST CURRENT
END OPTION
FILMS
ISOTROPIC
JOULE
VOLTAGE

Load Incrementation Options

CONTINUE
TRANSIENT

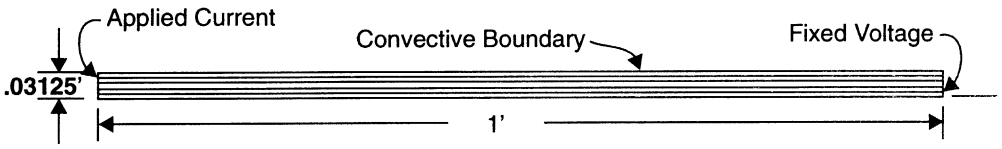

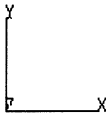

Figure E 5.10-1 Mesh of Steel Wire

E 5.11 Heat Transfer And Stress Analysis Of A Jominy End Quench Test Specimen

This example considers the transient heat transfer and thermal stress analyses of the Jominy End Quench Test. A right circular cylindrical bar of 1-in. diameter and 3-in. length, initially at a uniform temperature of 1550°F, is quenched to steady-state temperature. The quenching process consists of water impinging on one of the circular faces of the cylinder. The quench water temperature is 71°F. The bar is made from AISI 4140 steel. Its thermal (i.e., heat transfer) properties are a function of temperature only. The thermal conductivity data is listed in Table E 5.11-1 and plotted in Figure E 5.11-1. The specific heat data is listed in Table E 5.11-2 and plotted in Figure E 5.11-2.

Cooling occurs by forced convection along the quench end and by free convection along the cylindrical surface. It is assumed that the cylindrical face opposite the quench end is fully insulated. The "forced" heat transfer coefficient for cooling of the material in water is 9.412 x 10^{-3} Btu/sec-°F-sq.in. The "free" heat transfer coefficient for cooling in air is 5.5941 x 10^{-6} Btu/sec-°F-sq.in.

Element

Element type 42 is used for the heat-transfer analysis of the specimen. This is an axisymmetric 8-node biquadratic element, with one degree of freedom (temperature). Element type 28 is used for the stress analysis portion of this example. This element is an 8-node distorted quadrilateral, with two degrees of freedom at each node.

Model

The nonuniform transient temperature field was computed in a preliminary heat transfer analysis.The finite element model is illustrated in Figure E 5.11-3 and Figure E 5.11-4. Due to symmetry, only one-half of the bar is modeled. This same model is used in the subsequent transient thermal stress analysis.

Geometry

No values need be given in this option.

Material Properties

The mechanical properties of AISI 4140 are a function of both time and temperature. The data pertaining to Young's modulus, Poisson's ratio, yield stress, and the work-hardening rate are given in Figure E 5.11-5, Figure E 5.11-6, and Figure E 5.11-7. The data is presented in the form of property values as a function of both temperature and the previously described fixed cooling rates. Data is provided for two rates. The durations of these two "Newton Cooling" processes (see Figure E 5.11-3) are 6 and 20 secs. The mass density of the material is 0.281 lb/cu.in.

The thermal conductivity vs. temperature curve (Figure E 5.11-7) was approximated by three straight-line segments. The corresponding slope-breakpoint data was entered in the TEMPERATURE EFFECTS block. The data for the specific heat (Figure E 5.11-2) was reexpressed in slope-breakpoint form and also entered in this block.

The thermal coefficient of expansion is also a function of time and temperature. In this instance, this property is derived from thermal strain data which is described in terms of fourth order polynomial expansions about different temperature levels. This is done for the above two mentioned cooling rates. The coefficients for each of the polynomials are listed in Table E 5.11-3 along with the corresponding temperature levels.

Results

Thermal Analysis

It will be noted that a variable time step was used in the analysis and that 61 increments were required. The program automatically recomputed the time step at each increment such that the maximum incremental change in temperature never exceeded 100°F. Also, the temperature-dependent heat transfer properties were recomputed whenever a maximum change of 100°F occurred anywhere within the model.

The quenching process was found to take approximately 1600 secs. The temperatures at selective points along the axis are plotted as a function of time in Figure E 5.11-8. Stress contours and deformed structure plots will be presented for the same four stages of the thermal stress analysis. The temperature history for each integration point in the model was stored on a POST tape for subsequent use in the stress run.

Stress Analysis

It will be noted that the time-temperature dependent material property data is described in the TIME-TEMP model definition block. The thermal loading is read from the heat transfer POST tape via the CHANGE STATE option. The program controls were such that the maximum allowable temperature change in any increment did not exceed 100°F. In view of the controls which were set for the heat transfer analysis, this caused two or more heat increments to be merged into a single stress increment at occasional stages in the analysis. Eighty increments were required for this analysis. The resultant temperature, as a function of increment, is given in Figure E 5.11-9.

It is interesting to note that in the early stages of cooling; i.e., within approximately the first 50 secs, the Jominy bar actually increases in volume. As the nominal steady-state room temperature is approached, the bar then shrinks to less than its initial dimensions. The initial increase in volume can be attributed to phase changes which occur at the higher temperatures. These are accounted for via the piecewise polynominal description of the thermal coefficient of expansion. (See Table E 5.11-3.)

The effective, or von Mises, equivalent stress, the axial, radial and hoop components of stress are plotted against the increment number in Figure E 5.11-10 to Figure E 5.11-13. The most severely stressed region occurs at the intersection between the quench end face and the center cylindrical surface. It is interesting to note from the equivalent stress plots that the stress intensity in this region grows from a level of 32,930 psi at stage 1 to a final level of 130,400 psi. Nevertheless, throughout the cooling process the maximum intensity never exceeded the corresponding instantaneous yield stress level; i.e., no plastic deformation was found to occur.

Despite this fact, it will be observed from the stress contour plots that there is still a significant nonuniform and appreciable distribution of stress in the bar. However, it should be noted that the analysis was terminated before a uniform steady-state temperature was reached. At the final increment of the analysis, a temperature gradient still exists which ranges from 73°F at the quench end to approximately 90°F at the opposite end. It is believed that a portion of the

essentially residual stress state is not due simply to thermal gradients, but rather to nonuniform volumetric changes which occurred in the early stages of cooling. The temperature at elements 1, 10, 13, and 16 are plotted against increment and temperature, respectively, in Figure E 5.11-12 and Figure E 5.11-13.

Coefficients for a polynomial fit of thermal strain, e(T), where:

$$e(T) = A_1 + A_2T + A_3T^2 + A_4T^3 + A_5T^4$$

Summary of Options Used

Listed below are the options used in example e5x11a.dat:

Parameter Options

END
HEAT
MATERIAL
SIZING
THERMAL
TITLE

Model Definition Options

CONNECTIVITY
CONTROL
COORDINATE
END OPTION
FILMS
INITIAL TEMPERATURE
ISOTROPIC
POST
PRINT CHOICE
TEMPERATURE EFFECTS

Load Incrementation Options

CONTINUE
TRANSIENT

Listed below are the options used in example e5x11b.dat:

Parameter Options

ELEMENT
END
TITLE

Listed below are the options used in example e5x11c.dat:

Parameter Options

END
SIZING
T-T-T
THERMAL
TITLE

Model Definition Options

CHANGE STATE
CONNECTIVITY
CONTROL
COORDINATE
END OPTION
FIXED DISP
POST
PRINT CHOICE
RESTART
TIME-TEMP

Load Incrementation Options

AUTO THERM
CHANGE STATE
CONTINUE

Listed below are the options used in example e5x11d.dat:

Parameter Options

ELEMENT
END
TITLE

Table E 5.11-1 Thermal Conductivity vs. Temperature (AISI 4140 Steel)

Temperature (°C)	Conductivity (cal/cm-sec)	Temperature (°C)	Conductivity (cal/cm-sec)
0	.102	500	.052
19	.102	550	.054
39	.101	600	.055
58	.099	650	.056
78	.098	700	.058
97	.095	750	.059
116	.093	800	.060
136	.092	850	.062
155	.088	900	.063
174	.084	950	.064
193	.080	1000	.065
213	.073	1050	.067
233	.068	1100	.068
252	.063	1150	.069
271	.057	1200	.071
291	.051	1250	.072
310	.047	1300	.074
350	.048	1350	.075
400	.050	1400	.076

Table E 5.11-2 Specific Heat vs. Temperature (AISI 4140)

Temperature (°C)	Specific Heat (cal/cm-sec)
50	.112
110	.117
120	.118
130	.121
140	.126
150	.132
160	.141
170	.153
180	.167
190	.184
200	.205
210	.238
220	.289
230	.615
240	1.482
250	.824
260	.530
270	.357
280	.290
290	.247
300	.214
310	.189
320	.168
330	.150
340	.136
350	.121
450	.122
550	.126
650	.131

Table E 5.11-3 Coefficient of Thermal Expansion (AISI 4140)

A_1	A_2	A_3	A_4	A_5	T	Cooling Rate (sec)
0.3439E-02	0.1063E-04	0.2847E-07	0.4245E-10	-0.2345E-13	32	6
0.1603E-01	0.3600E-04	0.2147E-07	0.0	0.0	753	
0.5852E-02	0.2047E-05	0.5401E-09	0.0	0.0	1148	
0.2204E-01	0.5857E-04	-0.5401E-09	0.4211E-09	-0.2792E-12	32	20
0.7145E-01	0.7366E-04	-0.5966E-07	-0.3517E-10	0.3747E-13	545	
0.2193-01	-0.7130E-06	0.5190E-08	-0.1872E-11	0.2479E-15	896	

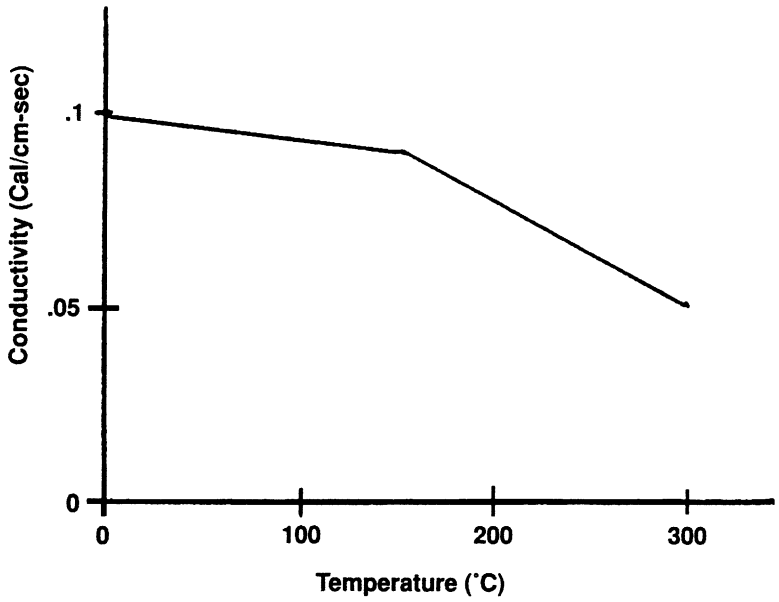

Figure E 5.11-1 Thermal Conductivity vs. Temperature

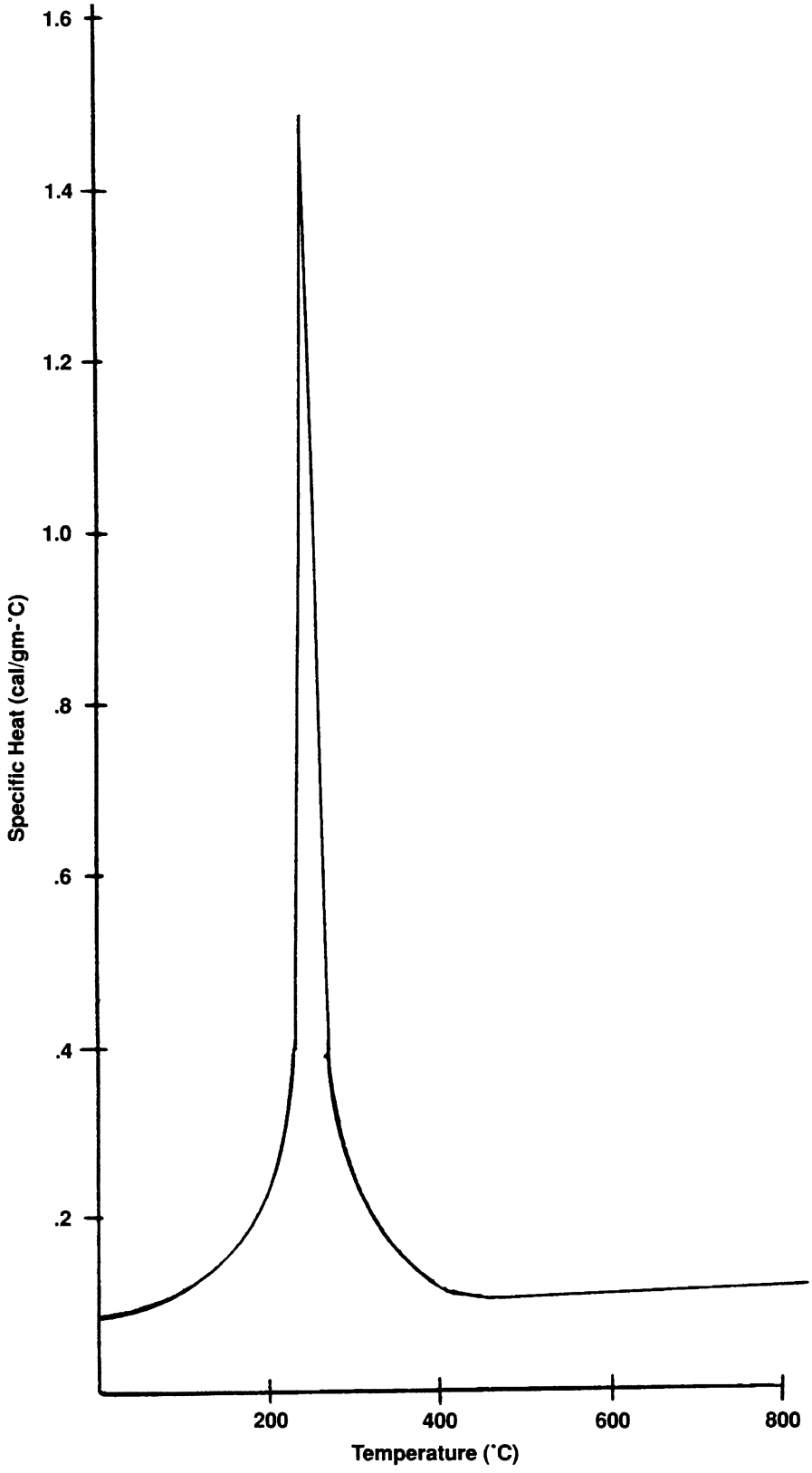

Figure E 5.11-2 Specific Heat vs. Temperature

MARC

1	2	3	10	11	12	13	14	15	16
4	6	8	17	19	21	23	25	27	29
5	7	9	18	20	22	24	26	28	30

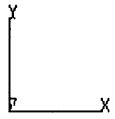

Figure E 5.11-3 Jominy Bar – Axisymmetric Finite Element Model (Elements)

MARC

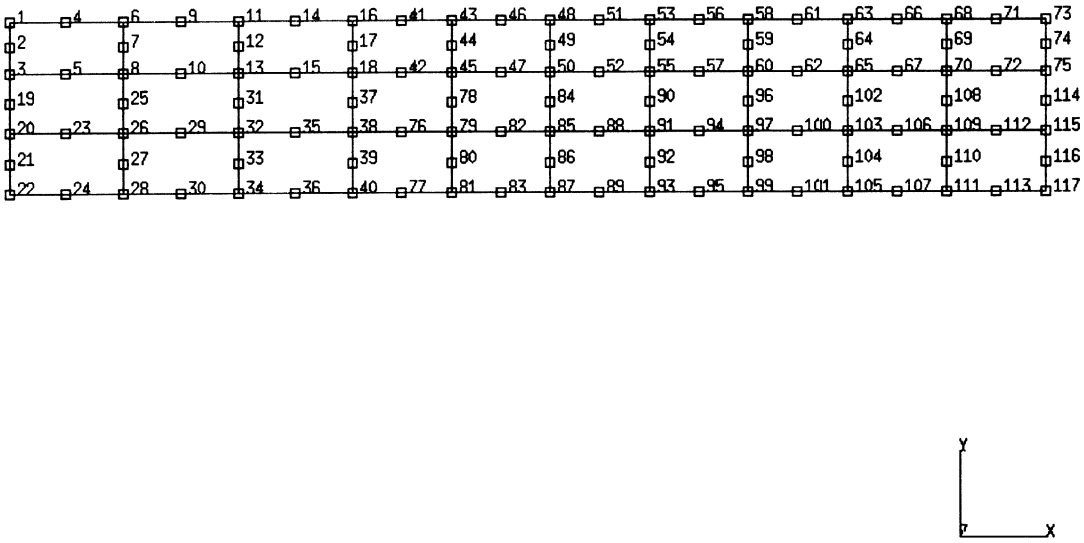

Figure E 5.11-4 Jominy Bar – Axisymmetric Finite Element Model (Nodes)

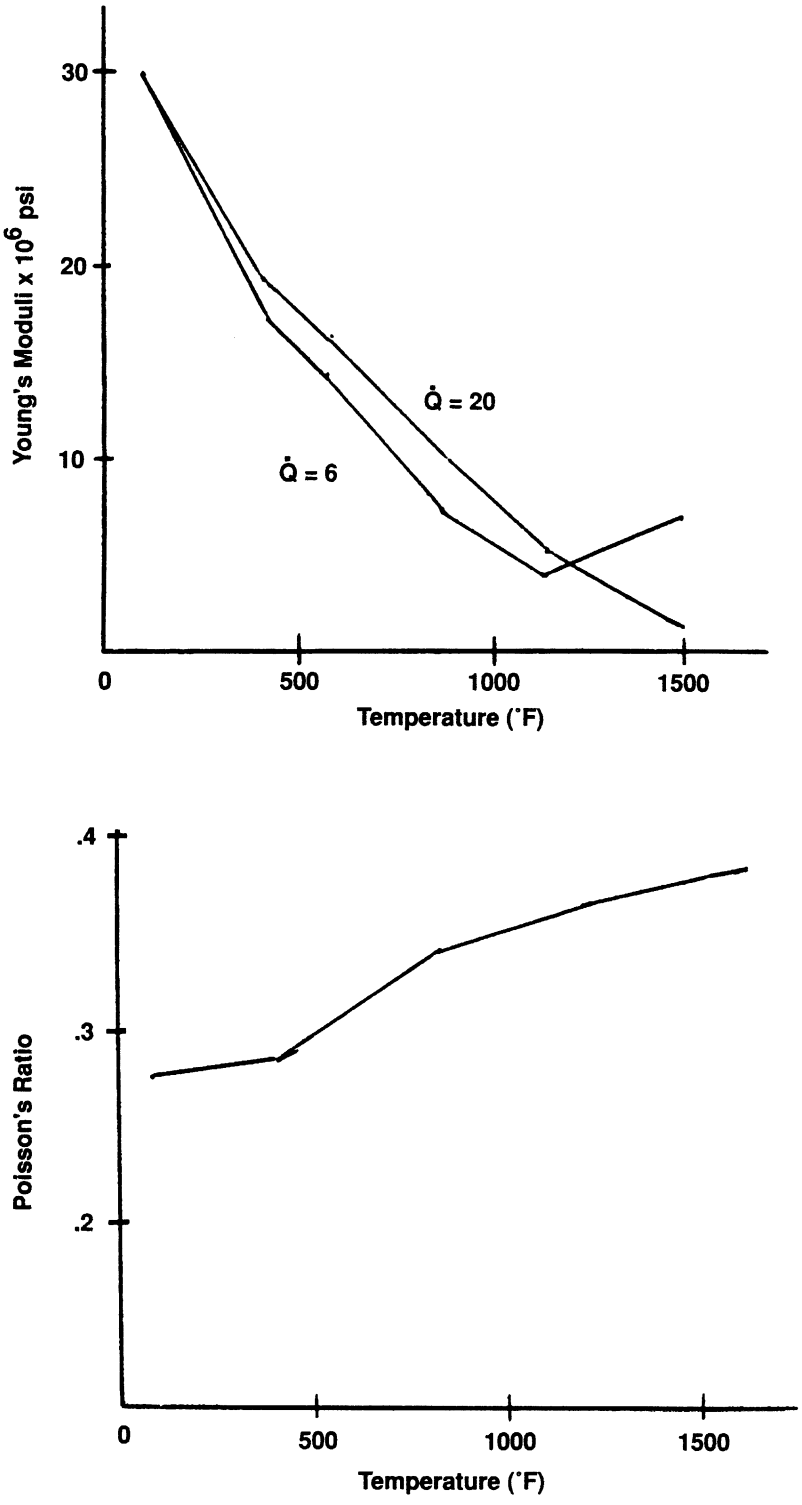

Figure E 5.11-5 Material Properties vs. Temperature

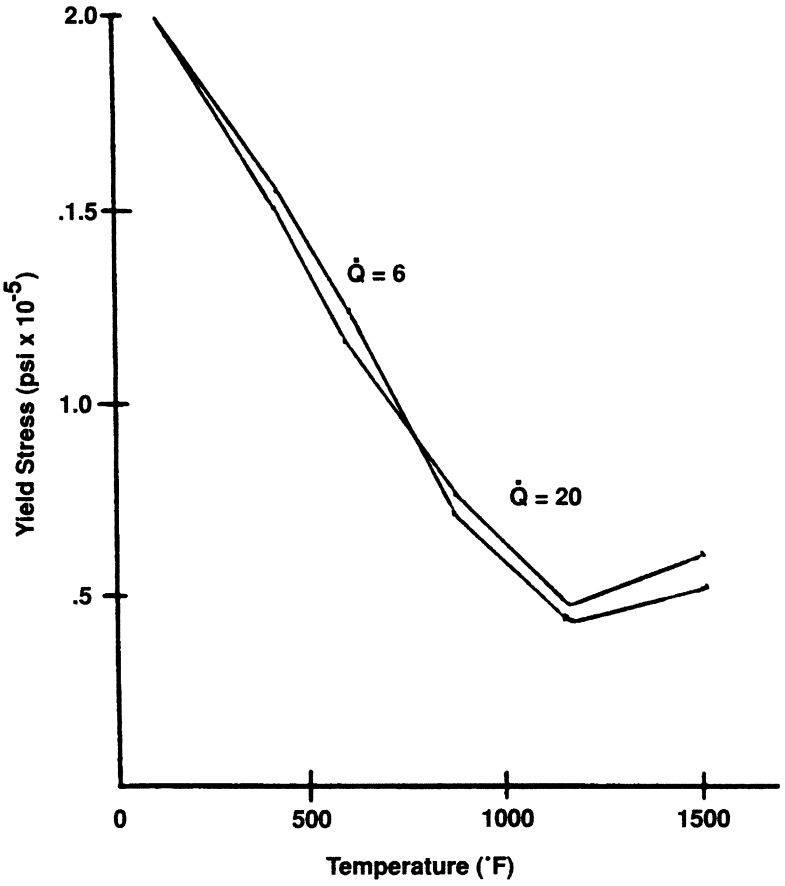

Figure E 5.11-6 Yield Stress vs. Temperature

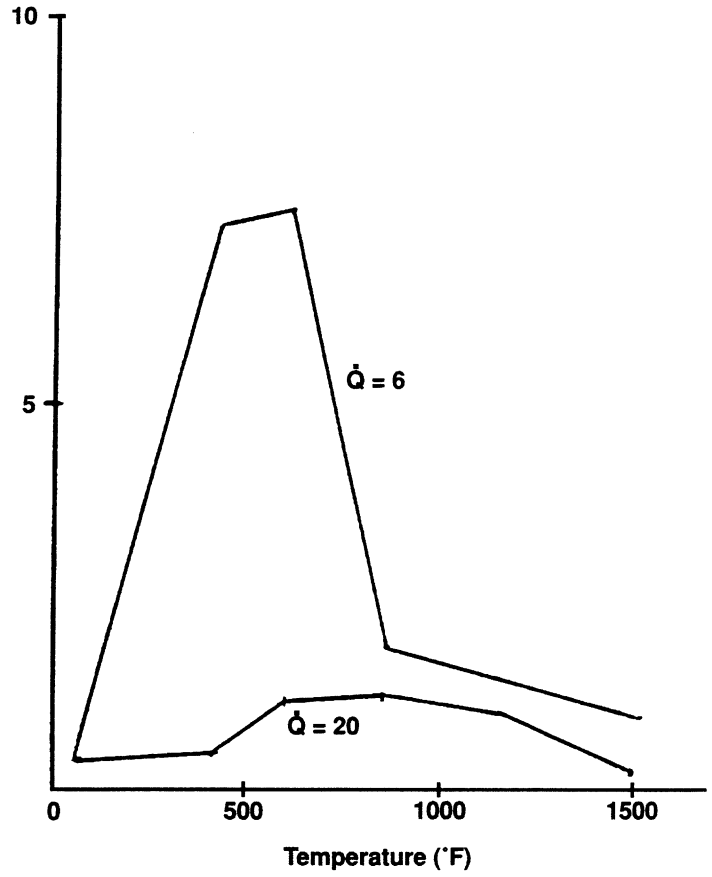

Figure E 5.11-7 Work-Hardening vs. Temperature

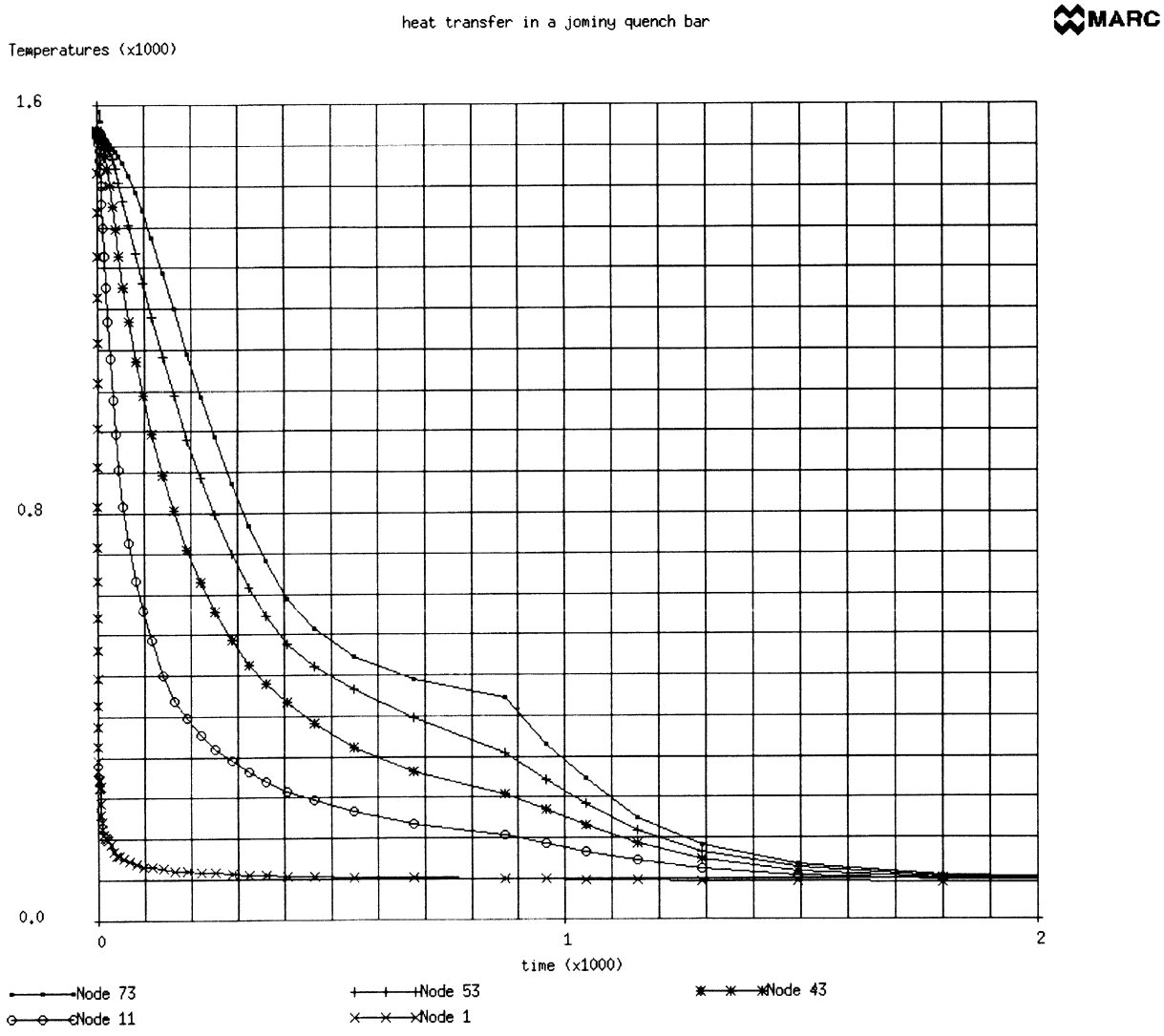

Figure E 5.11-8 Jominy End Quench Test – Temperature vs. Time

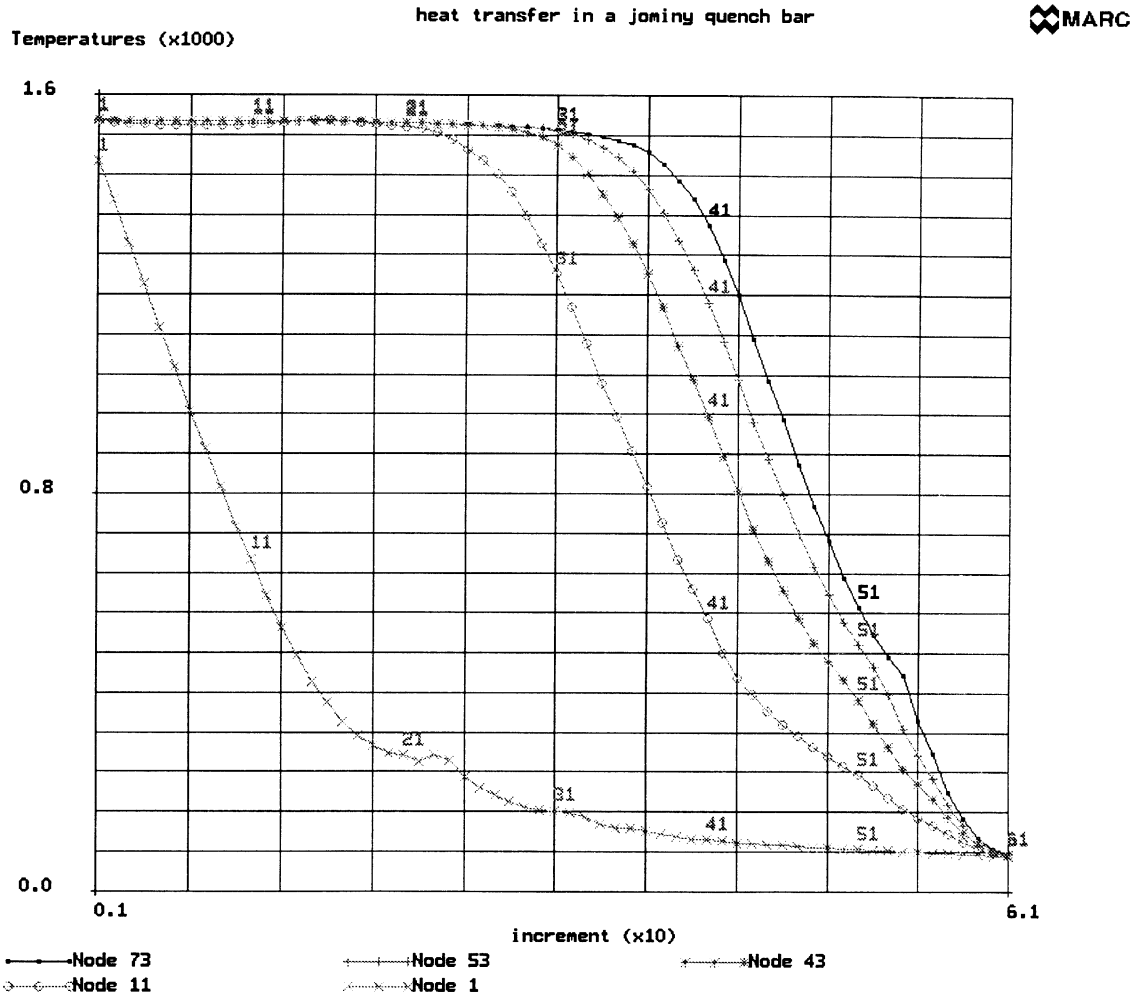

Figure E 5.11-9 Jominy End Quench Test – Temperature vs. Increment

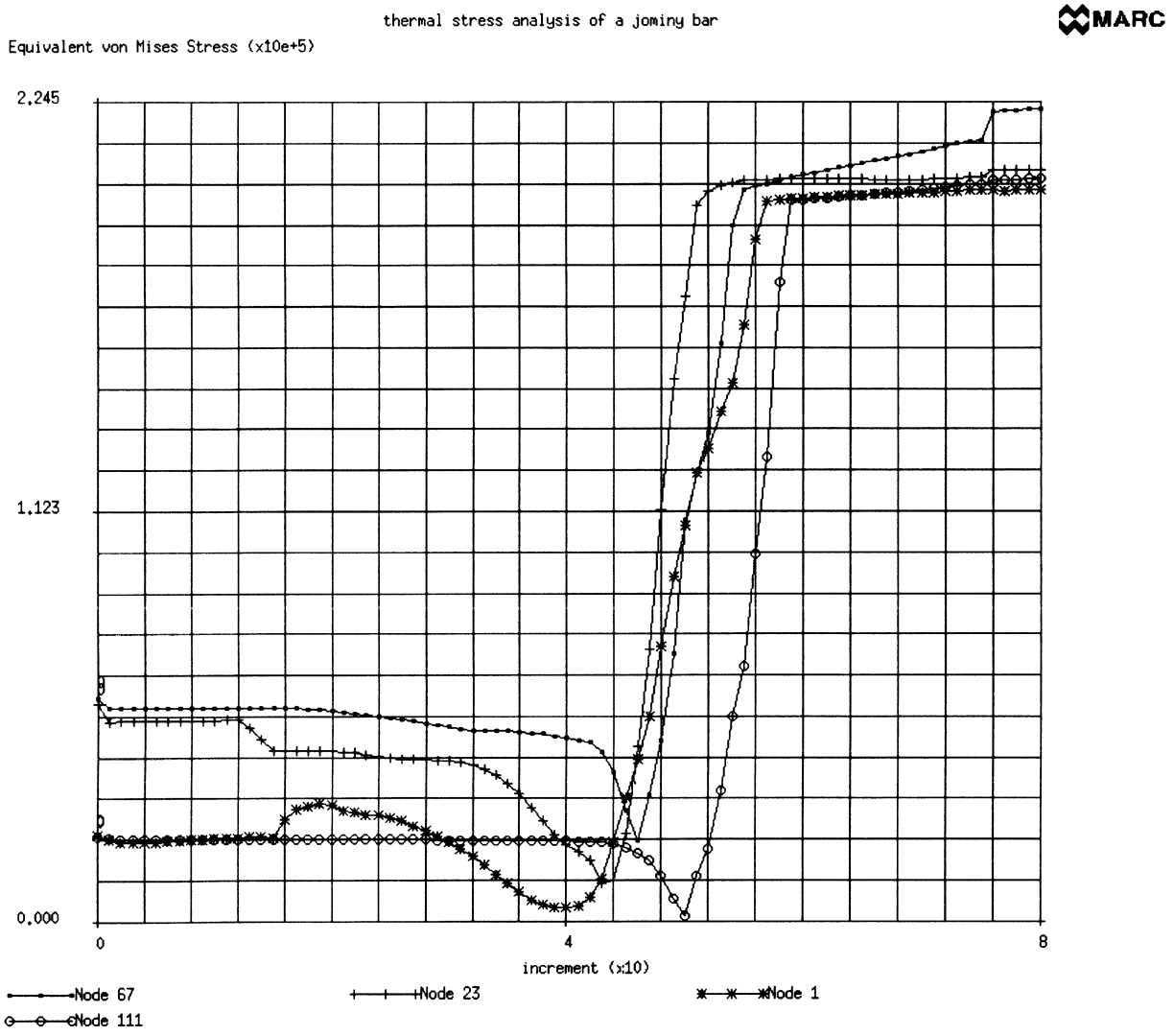

Figure E 5.11-10 Jominy End Quench Test – Equivalent Stress vs. Increment

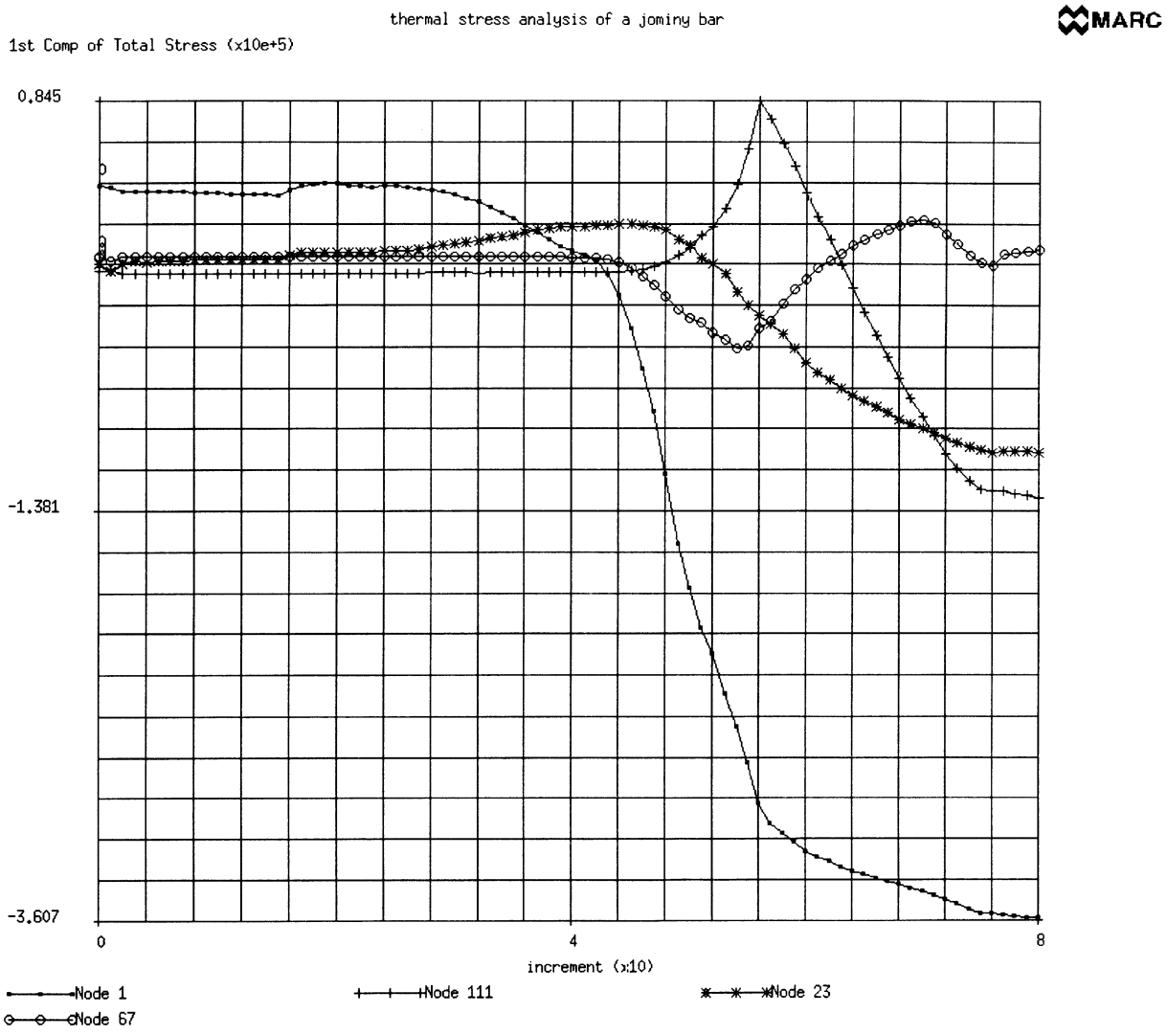

Figure E 5.11-11 Jominy End Quench Test – Axial Stress vs. Increment

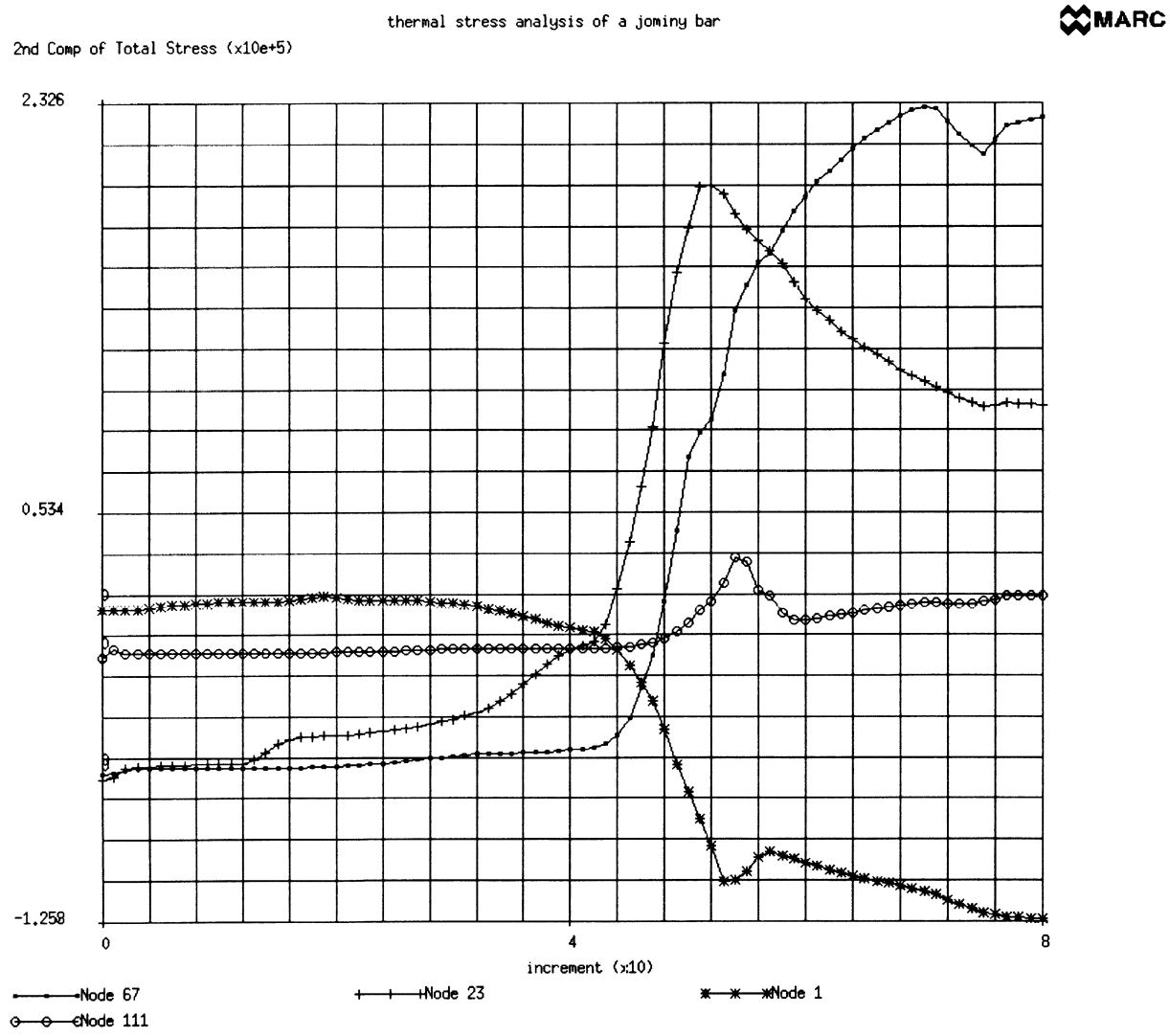

Figure E 5.11-12 Jominy End Quench Test – Radial Stress vs. Increment

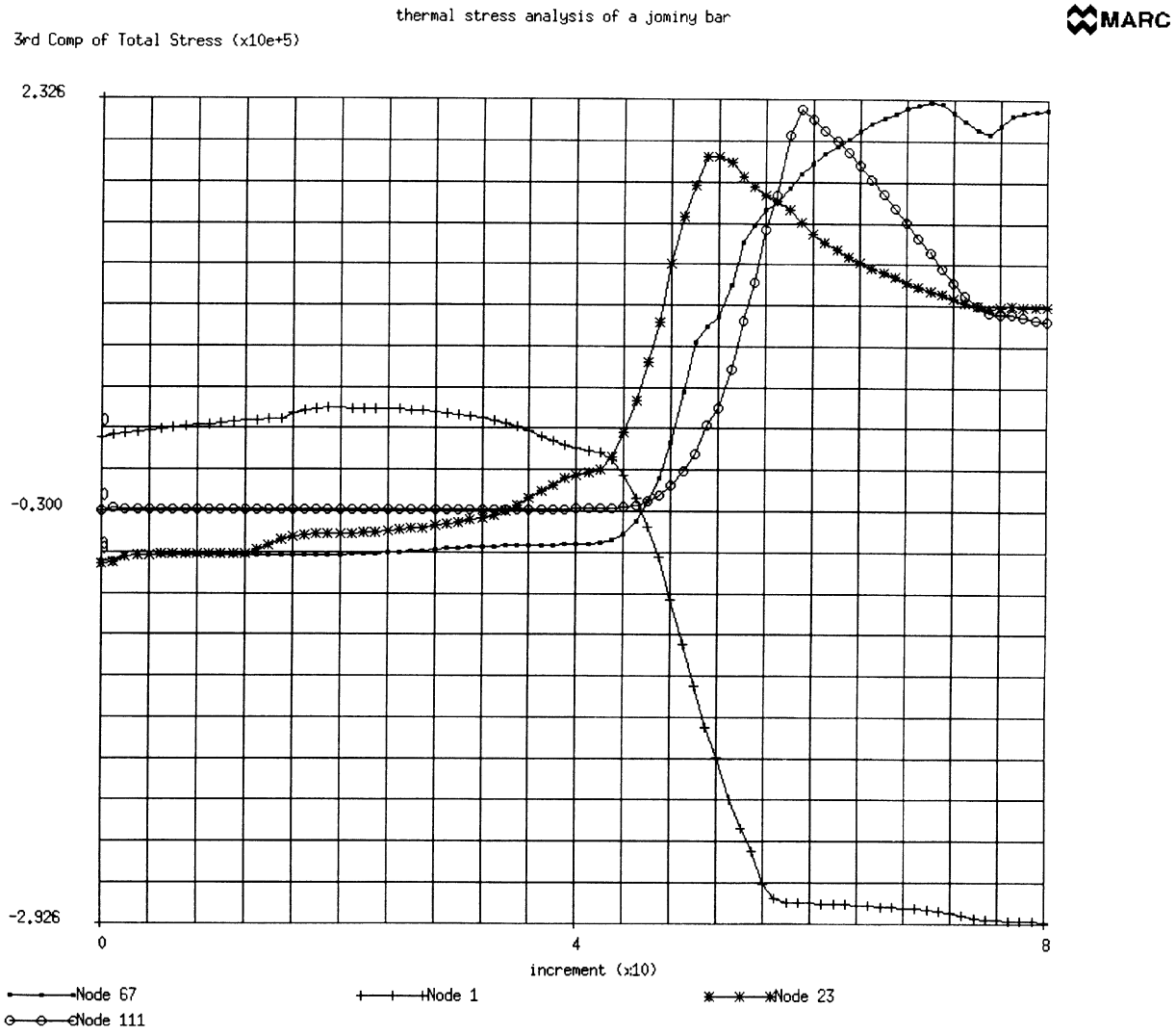

Figure E 5.11-13 Jominy End Quench Text – Hoop Stress vs. Increment

E 5.12 Cylinder-Plane Electrode

A cylinder-plane electrode has been analyzed using a coupled thermo-electric model. MARC element type 39 (4-node isoparametric quadrilateral element) has been used. Two electrodes are applied to the two faces shown in Figure E 5.12-1, producing a uniform difference of electric potential between the upper and the lower face.

Model

This problem demonstrates the use of the JOULE option for Joule heating problems. (See A2.36-1 for a general discussion of the problem).

Material Properties

The specific heat and density of the material are 0.26 cal/gm-°C and 3.4 gm/cm^3, respectively. The surface film coefficient is 0.677-3 cal/sec-cm^2-°C. The temperature dependent thermal conductivity and resistivity are shown in Figure E 5.12-2.

Initial Conditions

The initial nodal temperatures are 20°C throughout.

Boundary Conditions

The upper face has 1 V; V = 0 at the lower face. Convective boundary conditions are assumed to exist at the lower face.

Transient

Nonautomatic time stepping is used setting the initial step at 100 sec. The transient solution lasts for 100 sec.

Results

Voltage, current and temperature distributions are shown in Figure E 5.12-4 through Figure E 5.12-6.

Summary of Options Used

Listed below are the options used in example e5x12.dat:

Parameter Options

ALIAS
END
HEAT
JOULE
SIZING
TITLE

Model Definition Options

CONNECTIVITY
COORDINATE
END OPTION
FIXED TEMPERATURE
ISOTROPIC
JOULE
POST
VOLTAGE

Load Incrementation Options

CONTINUE
TRANSIENT

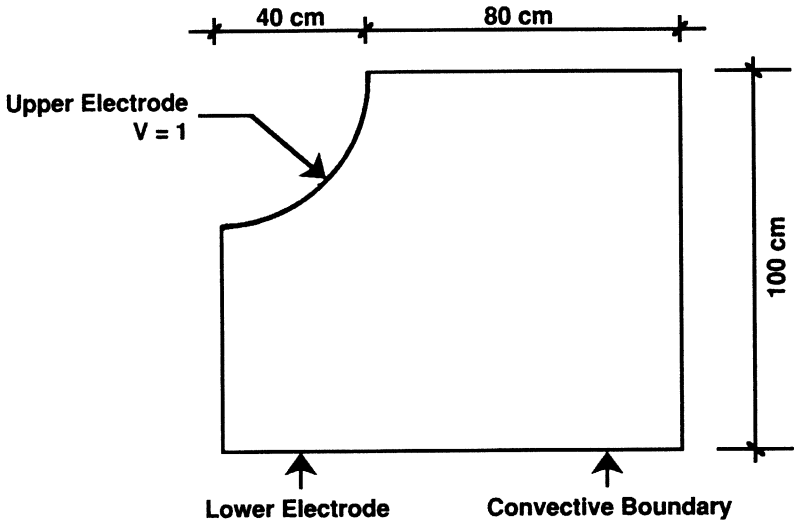

Figure E 5.12-1 Geometry of the Problem

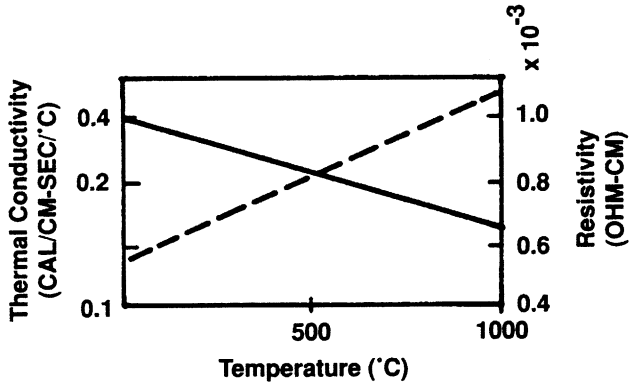

Figure E 5.12-2 Temperature Dependent Properties

MARC

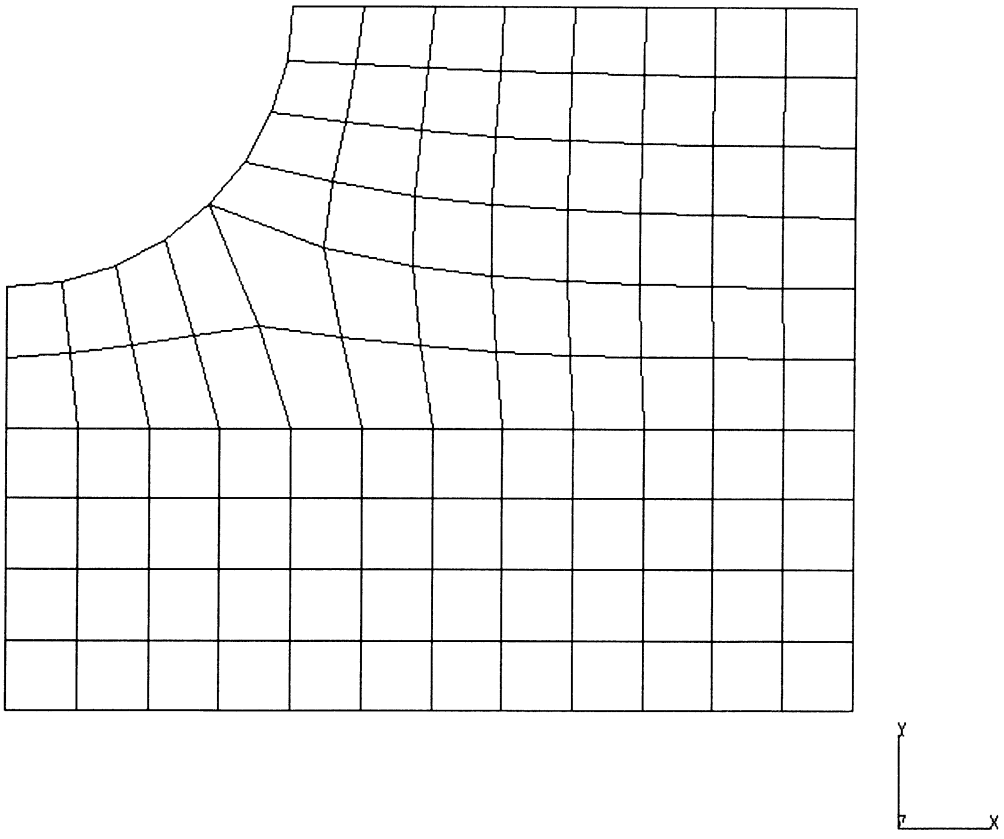

Figure E 5.12-3 Mesh

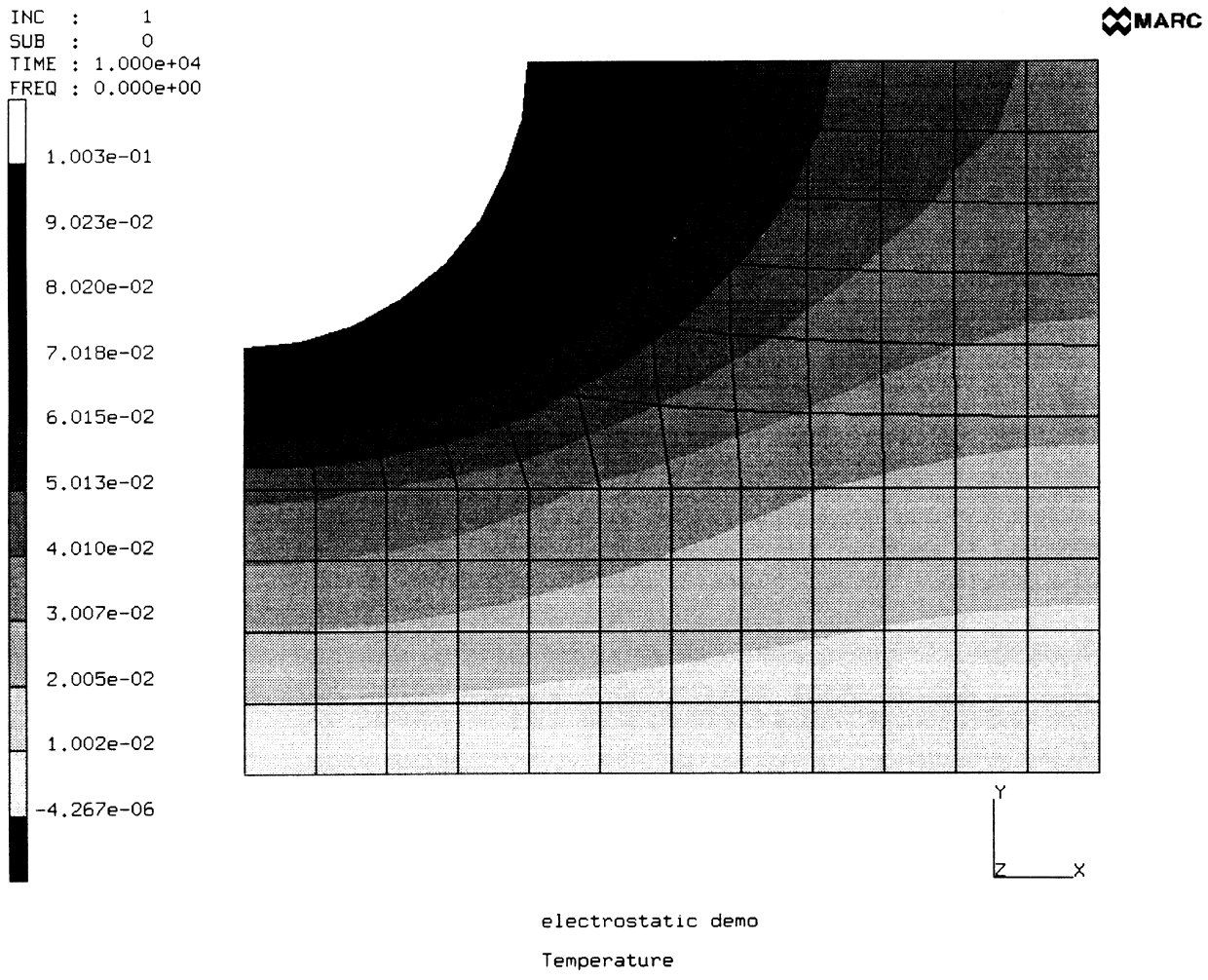

Figure E 5.12-4 Temperature Distribution

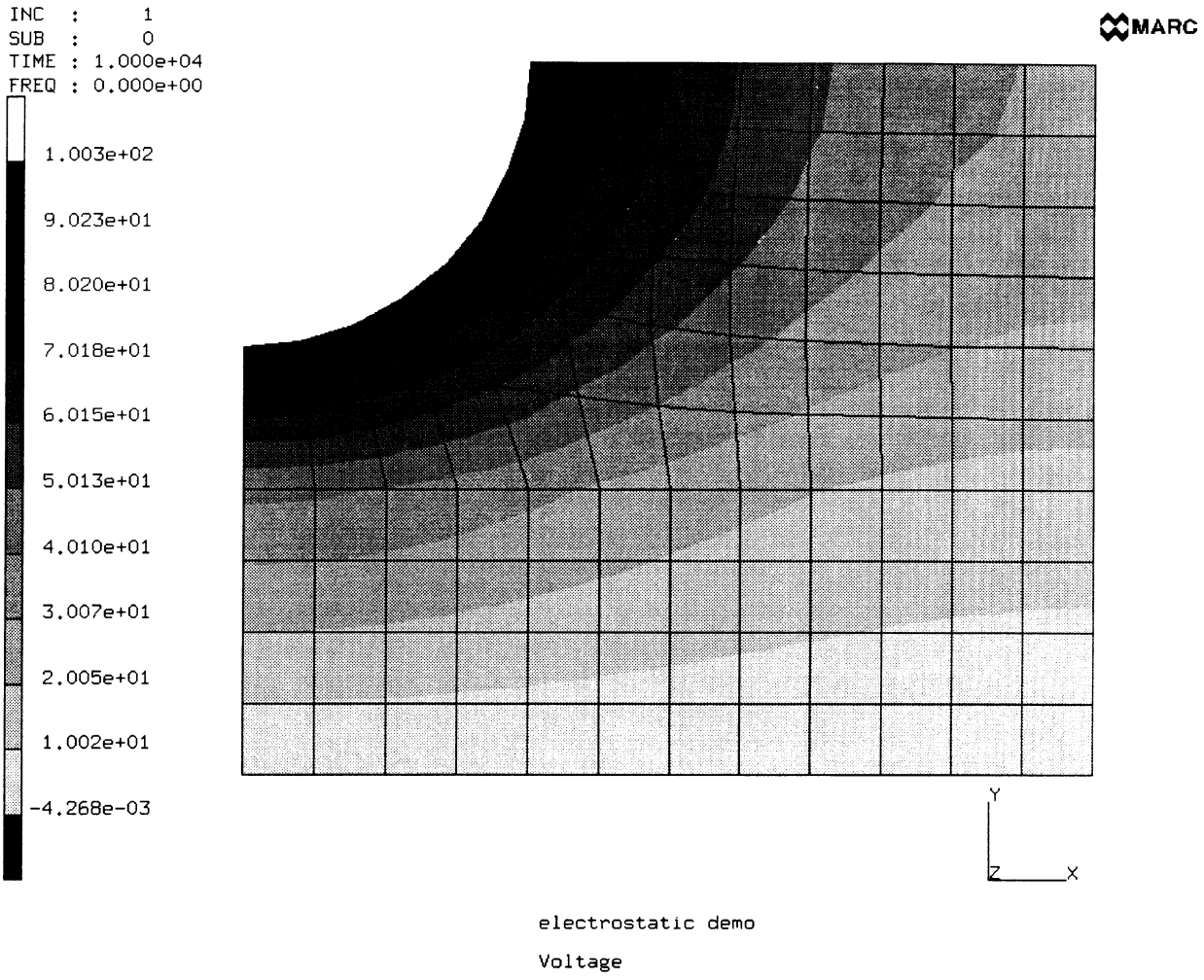

Figure E 5.12-5 Voltage Distribution

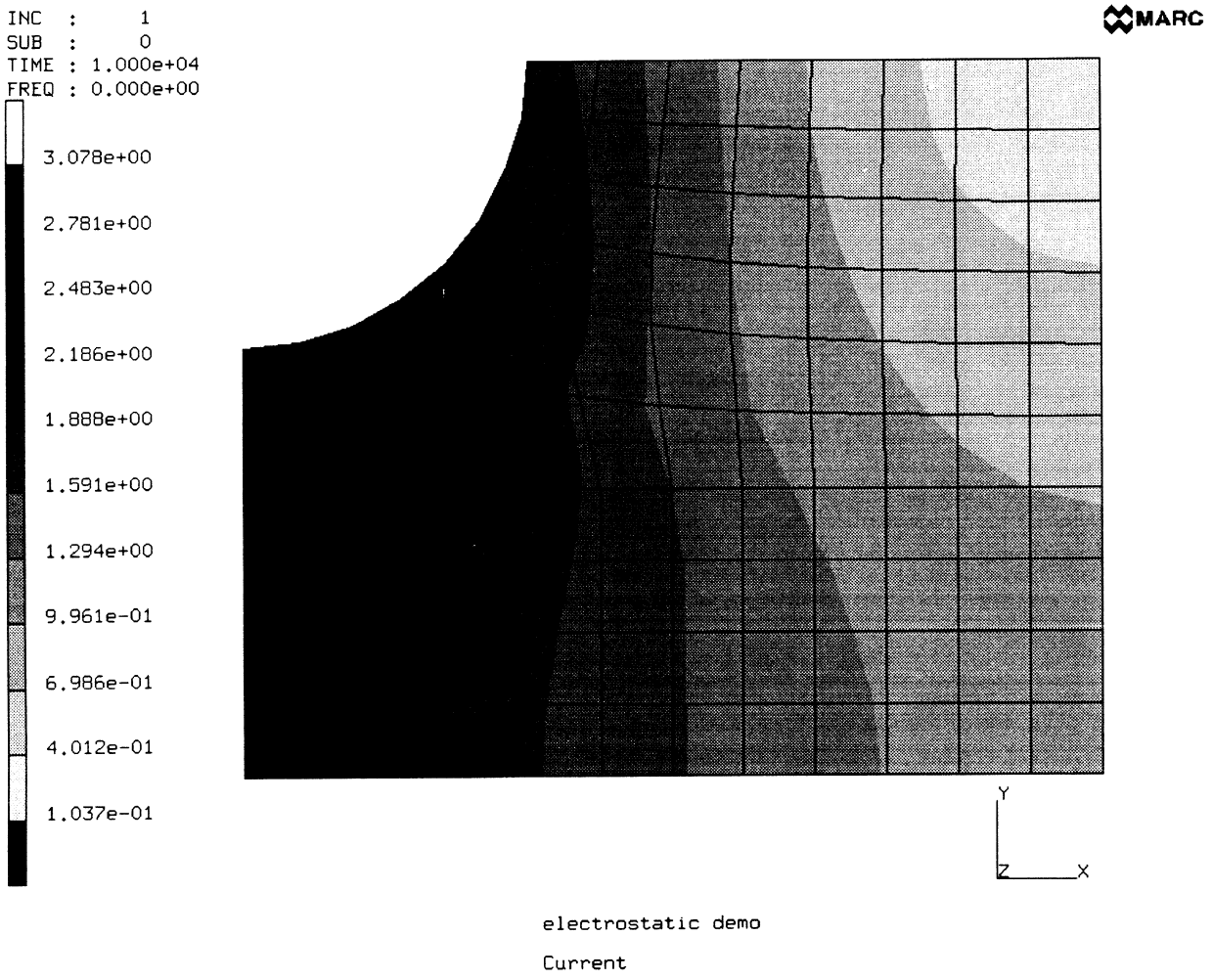

Figure E 5.12-6 Current Distribution

E 5.13 Axisymmetric Transient Heat Conduction Simulated By Heat Transfer Shell Elements

The transient heat conduction of a cylinder, subjected to a thermal downshock, is analyzed by using MARC heat transfer shell elements. This is the same problem as E 5.5. The model and input data of the problem are:

Model/Element (Ref. B85.1, B86.1, B87.1, B88.1)

The MARC heat transfer shell elements consist of Element 85 (4-node), Element 86 (8-node), Element 87 (3-node axisymmetric) and Element 88 (2-node axisymmetric). Element temperatures are either linearly (Elements 85 and 88) or quadratically interpolated in the plane of the shell and assumed to have a linear/quadratic distribution in the thickness direction of the shell. The nodal degrees-of-freedom is two if a linear distribution of temperatures is assumed in the shell thickness direction, and three if a quadratic distribution of temperatures is assumed in the thickness direction of the shell. This is set by the user on the HEAT parameter option. These heat transfer shell elements are compatible with stress shell elements (see below) for thermal stress analysis.

Heat Transfer Shell Elements	Stress Shell Elements
85	72, 75
86	22
87	89
88	1

Models

As shown in Figure E 5.13-1, the cylinder has an inner radius of 8.625 inches and a wall thickness of 0.375 inches. It is subjected to a constant initial condition and different convective boundary conditions on the inner and outer surfaces of the cylinder. Finite meshes for heat transfer shell elements 85, 86, 87, and 88 and shown in Figure E 5.13-2 through Figure E 5.13-5, respectively. The number of elements and number of nodes in each mesh are:

Mesh	Element	No. of Elements	No. of Nodes
A	85	6	12
B	86	6	29
C	87	2	5
D	88	2	3

SHELL SECT

This option allows the user to specify the number of points to be used for numerical integration in the thickness direction of the shell. The number of integration points in the thickness direction of the shell is chosen to be seven in this example.

Geometry

The shell thickness of 0.375 inches is entered as EGEOM1 in the GEOMETRY block and a positive (non-zero) number is entered as EGEOM2 for the selection of a quadratic distribution of temperatures in the thickness direction.

Material Properties

The conductivity is 4.85E-4 BTU/second-inch-°F. The specific heat is 0.116 BTU/pound-°F. The mass density is 0.283 pound/cubic inch.

Initial Condition

Initial nodal temperatures are assumed to be homogeneus at 1100°F.

Boundary Conditions

No input data is required for insulated boundary conditions at z = 0 and z = 2.0. Fluid temperatures and film coefficients for both inner and outer surfaces of the cylinder are:

Inner surface:

H_i = 38.56E-5 BTU/second-square inch-°F
T_i = 1100°F at t = 0. second
800°F at t = 10. seconds

Outer surface:

H_0 = 1.93E-6 BTU/second-square inch-°F (low value to simulate insulated boundary condition).
T_0 = 1100°F

The low value of H_0 simulates an insulated boundary.

The FILMS option is used to input the film coefficients and associated fluid temperatures for the inner and outer surfaces. Subroutine FILM linearly interpolates the 300°F decrease in ambient temperature over 10 seconds and then holds the inner wall temperature constant at 800°F. It is called at each time step for each integration point on each element surface given in the FILMS option.

POST

In a heat transfer run the use of the POST option allows the creation of a post tape containing element temperatures at each integration point and nodal point temperatures. The tape can be used later as input to the stress analysis run. The code number for element temperatures of heat transfer elements is 9 followed by a layer number (i.e., 9,1, and 9,2, etc.). These code numbers must be entered sequentially.

Transient

The TRANSIENT option controls time steps in a transient heat transfer analysis. The program automatically calculates the time steps to be used based on the maximum nodal temperature change allowed as input in the CONTROL option. The solution begins with the suggested initial time step input and ends according to the time period specified. It will not exceed the maximum number of steps input in this option.

Results

A comparison of nodal temperatures with the results of an axisymmetric model (problem E 5.5) is shown in Table E 5.13-1.

Table E 5.13-1 Comparison of Nodal Temperatures

Time (Sec.)	Nodal Temperature (°F) (Node 17)	Element Temperatures (°F) – 4th Layer			
		Element 85	Element 86	Element 87	Element 88
	E5.5	(Model A)	(Model B)	(Model C)	(Model D)
1.25	1099.3	1099.3	1099.3	1099.3	1099.3
4.06	1092.6	1092.4	1092.4	1092.4	1092.4
7.18	1078.3	1077.9	1077.9	1077.9	1077.9
9,.84	1061.2	1060.3	1060.3	1060.3	1060.3
12.79	1041.1	1039.7	1039.7	1039.7	1039.7
16.90	1015.7	1013.8	1013.8	1013.8	1013.8
21.00	993.1	990.7	990.7	990.7	990.7
26.13	968.3	965.5	965.5	965.5	965.5
31.90	944.3	941.3	941.3	941.3	941.3
38.31	921.8	918.5	918.5	918.5	918.5

Summary of Options Used

Listed below are the options used in example e5x13a.dat:

Parameter Options

ELEMENT
END
SHELL SECT
SIZING
TITLE

Model Definition Options

CONNECTIVITY
CONTROL
COORDINATE
END OPTION
FILMS
GEOMETRY
INITIAL TEMPERATURE
ISOTROPIC
POST
PRINT CHOICE

Load Incrementation Options

CONTINUE
TRANSIENT

Listed below is the user subroutine found in u5x13.f:

FILM

Listed below are the options used in example e5x13b.dat:

Parameter Options

ELEMENT
END
SHELL SECT
SIZING
TITLE

Model Definition Options

CONNECTIVITY
CONTROL
COORDINATE
END OPTION
FILMS
GEOMETRY
INITIAL TEMPERATURE
ISOTROPIC
POST
PRINT CHOICE

Load Incrementation Options

CONTINUE
TRANSIENT

Listed below is the user subroutine found in u5x13.f:

FILM

Listed below are the options used in example e5x13c.dat:

Parameter Options

ELEMENT
END
SHELL SECT
SIZING
TITLE

Model Definition Options

CONNECTIVITY
CONTROL
COORDINATE
END OPTION
FILMS
GEOMETRY
INITIAL TEMPERATURE
ISOTROPIC
POST
PRINT CHOICE

Load Incrementation Options

CONTINUE
TRANSIENT

Listed below is the user subroutine found in u5x13.f:

FILM

Listed below are the options used in example e5x13d.dat:

Parameter Options

ELEMENT
END
SHELL SECT
SIZING
TITLE

Model Definition Options

CONNECTIVITY
CONTROL
COORDINATE
END OPTION
FILMS
GEOMETRY
INITIAL TEMPERATURE

ISOTROPIC
POST
PRINT CHOICE

Load Incrementation Options

CONTINUE
TRANSIENT

Listed below is the user subroutine found in u5x13.f:

FILM

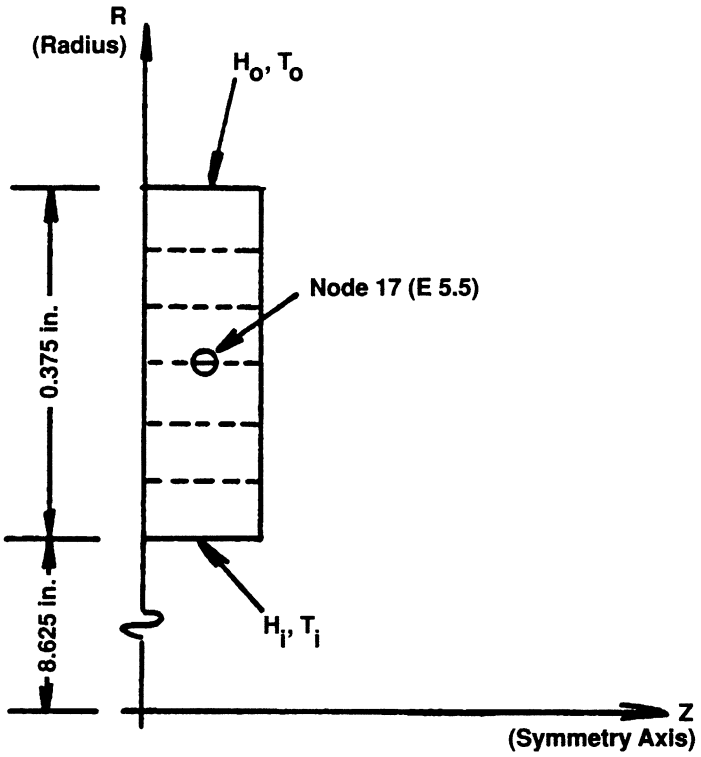

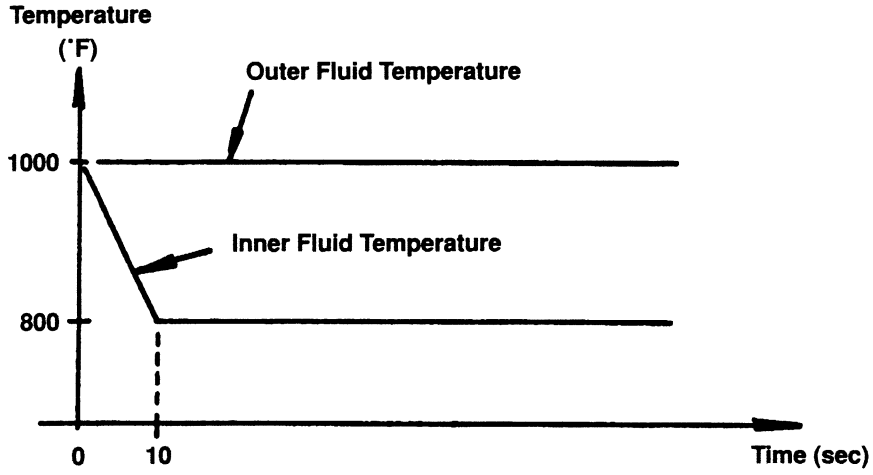

Figure E 5.13-1 Cylinder Model and Fluid Temperature History

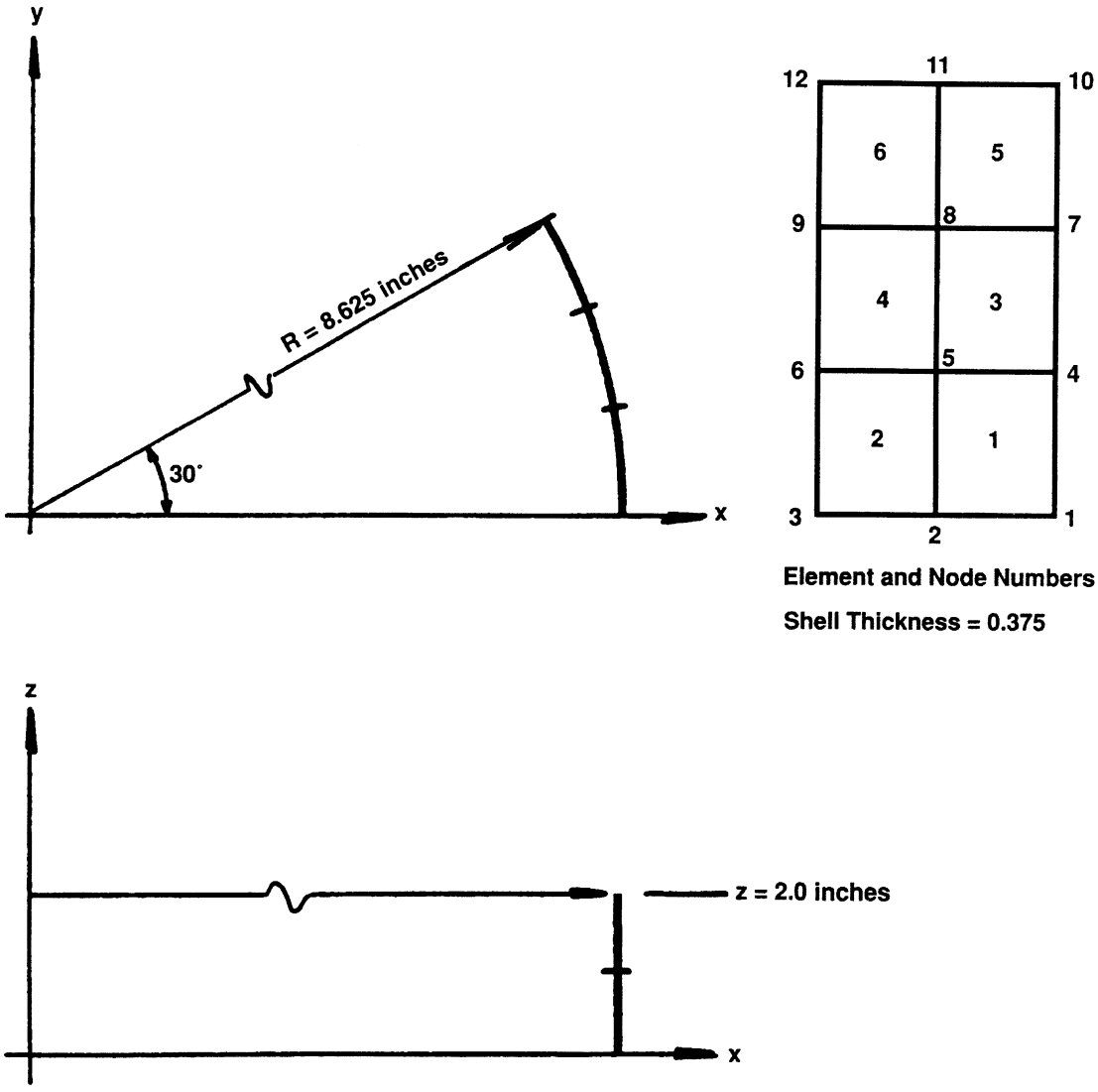

Figure E 5.13-2 Finite Element Model (Model A - Element 85)

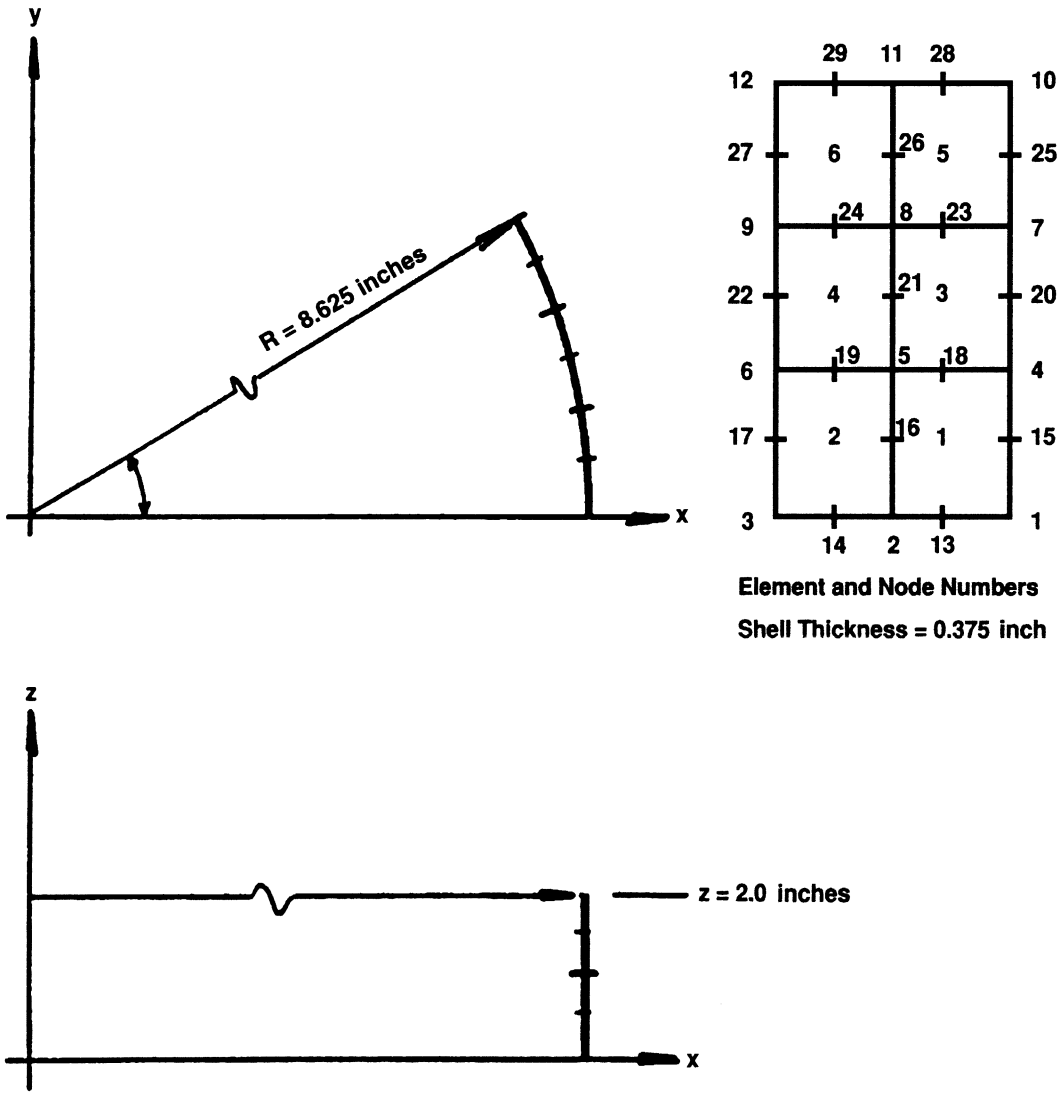

Figure E 5.13-3 Finite Element Model (Model B - Element 86)

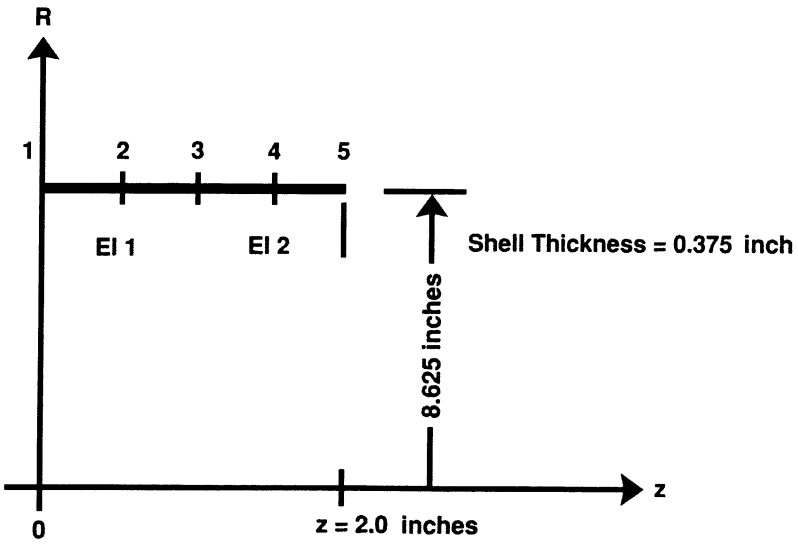

Figure E 5.13-4 Finite Element Model (Model C - Element 87)

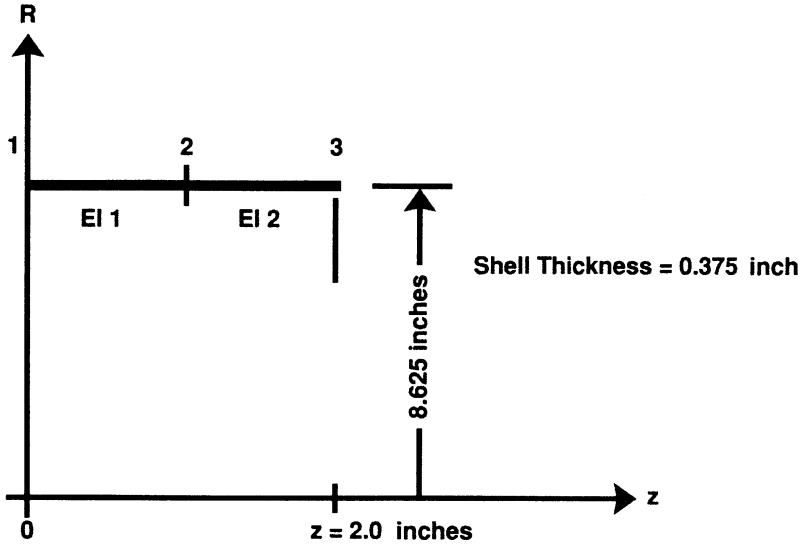

Figure E 5.13-5 Finite Element Model (Model D - Element 88)

E 5.14 Steady-State Temperature Distribution Of A Generic Fuel Nozzle

A steady-state heat transfer analysis is performed on a simplified two-dimensional model of a generic fuel nozzle for a turbine engine. The nozzle has both fluid heat-up and radiation across gaps which are simulated by fluid channel and thermal contact gap elements in the program. Model definition blocks CHANNEL and CONRAD GAP are used for fluid channel and radiation gaps, respectively. A 4-node-planar quad is chosen for modeling the entire nozzle.

Element (Ref. B39.1)

Library element type 39 is a 4-node planar isoparametric quadrilateral heat transfer element. Each nodal point is defined by two global coordinates (x,y) and has temperature as the nodal degrees-of-freedom. See Volume B for further details.

Model

As shown in Figure E 5.14-1, the simplified nozzle model is a two-dimensional structure, made of steel, containing two radiational gaps and a fluid channel. The nozzle is heated up from room temperature by a 200°F fluid flow in the channel as well as convective heat transfers from the external boundaries with ambient temperatures at 400°F and 1600°F, respectively. Thermal properties of steel and fluid are assumed to be dependent on temperatures.

Figure E 5.14-2 shows a finite element mesh for the MARC heat transfer analysis. The mesh contains 103 4-node quad elements and 142 nodes. A fluid channel consisting of elements 1, 30 through 37, 24 through 29, and two thermal contact gaps (GAP1: elements 38 through 45; GAP2: elements 82 through 89), are also depicted in Figure E 5.14-2.

Define (Element Set)

In the MARC input, set names are used to represent various regions in the model. The set WHOLE contains all the elements in the model. The fluid channel and two thermal gaps are represented by set names CHANL, GAP1, and GAP2, respectively. A set operation, WHOLE EXCEPT GAP1 EXCEPT GAP2 EXCEPT CHANL, defines the steel elements.

Material Properties

Thermal properties for steel are: $K = 1.85 \times 10^{-4}$ BTU/sec-in-°F, $C = 0.1$ BTU/lb-°F and $\rho = 0.285$ lb/in^3. The specific heat of the fluid is assumed to be 0.4625 BTU/lb-°F. Both the thermal conductivity (k) and the specific heat (C) are dependent on temperature. Slopes and break point data are entered through the TEMPERATURE EFFECTS model definition block. Material identifications 1, 2 and 3 are assigned to STEEL, CHANL (fluid), GAP1 and GAP2 (thermal gaps), respectively. Both the thermal conductivity and mass density of fluid, as well as the thermal properties of thermal gap elements, are set to zero.

Initial Temp

A constant initial temperature of 70°F is assumed for the entire model.

Geometry

The model thickness of 1.0 inch is entered through the GEOMETRY block.

Input for Thermal Contact Gap

In problems involving thermal contact gaps, the model definition block CONRAD GAP is used for the input of all gap properties. The data needed for each gap are: face identification, emissivity, Stefan-Boltzmann constant, absolute temperature conversion factor, film coefficient, gap closure temperature and a list of elements in the gap. Discussions on the gap face identification can be found in Volume B.

Since the thermal gap element serves as a radiation/convection link or, as tying constraints, thermal properties are not required for the element. Consequently, all the entries (conductivity, specific heat, density) in the ISOTROPIC block must be set to zero for all thermal contact elements.

In addition, because thermal contact and solid elements have same topology, the CONNECTIVITY data format of thermal contact element is same as that of a solid element. As a result, mesh generators such as MESH2D or MENTAT can be used for the generation of thermal contact gaps. All the thermal contact elements in one gap must be numbered in the same order.

CONRAD GAP

The CONRAD GAP Model Definition option is used for entering thermal contact gap information. In the model, the number of thermal gaps is 2; and in each gap: the Stenfan-Boltzmann constant is 0.3306E-14 BTU/sec - in^2 - $^\circ R^4$; the absolute temperature conversion factor from Fahrenheit to Rankine is 459.7; and the gap-closure temperature is assumed to be 2000°F (thermal gaps remain open throughout the analysis). The thermal gap elements are defined in sets GAP1 and GAP2, respectively.

Input for Fluid Channel

The data associated with fluids channels can be entered using the model definition block CHANNEL. The data needed for each channel are: channel face identification, lead element number, inlet temperature, mass flow rate, film coefficient and a list of fluid elements in the channel. Discussions on the channel face identification can be found in Volume B.

The topology of the fluid channel element is the same as that of solid element. Additional input is not needed for the mesh definition of fluid channels. All the fluid channel elements in one channel must be numbered in the same order.

Since the fluid flow in the channel is assumed to be convective, and based on the mass flow rate, in the ISOTROPIC block only the specific heat of the fluid is required. Both the conductivity and density of the fluid must be set to zero. The model definition block TEMPERATURE EFFECTS can be used for temperature dependent specific heat of the fluid.

For planar elements, the GEOMETRY block is needed for the input of channel thickness.

CHANNEL

The CHANNEL Model Definition block is used for the input of fluid channel data. In the current model, the number of channels is 1; the channel face identification is 2; the lead element number is 1; the inlet temperature is 200°F; the mass flow rate is 0.02778 lb/sec (or 100 lb/hr);

and the film coefficients in the channel are entered using user subroutine FLOW (set to 0. in the input deck). A list of the subroutine FLOW is shown on a latter page. Finally, the fluid elements is contained in the set CHANL.

FILMS

Finally, 16 sets of film data are used for the input of convective thermal boundary conditions in the model. The user subroutine FILM is used for entering film coefficient and sink temperature of each film boundary (H = 1.0, T_{inf} = 1.0 in the input). Both the film index and the fluid temp index are used for film boundary condition input.

Transient

Steady state temperatures in the generic fuel nozzle with temperature dependent thermal properties can be obtained from a MARC heat transfer analysis using: (1) several transient time-steps with large time increments or, (2) one time-step with a number of iterations within the time-step. Both approaches converge to the same steady-state solution.

Results

Both the channel and solid temperatures are depicted in Figure E 5.14-3. Comparisons between finite element and finite difference results are favorable.

Summary of Options Used

Listed below are the options used in example e5x14.dat:

Parameter Options

ELEMENT
END
HEAT
PRINT
SIZING
TITLE

Model Definition Options

CHANNEL
CONNECTIVITY
CONRAD GAP
CONTROL
COORDINATE
DEFINE
END OPTION
FILMS
GEOMETRY
INITIAL TEMPERATURE
ISOTROPIC
TEMPERATURE EFFECTS

Load Incrementation Options

TRANSIENT
CONTINUE

Listed below is the user subroutine found in u5x14.f:

FILM
FLOW

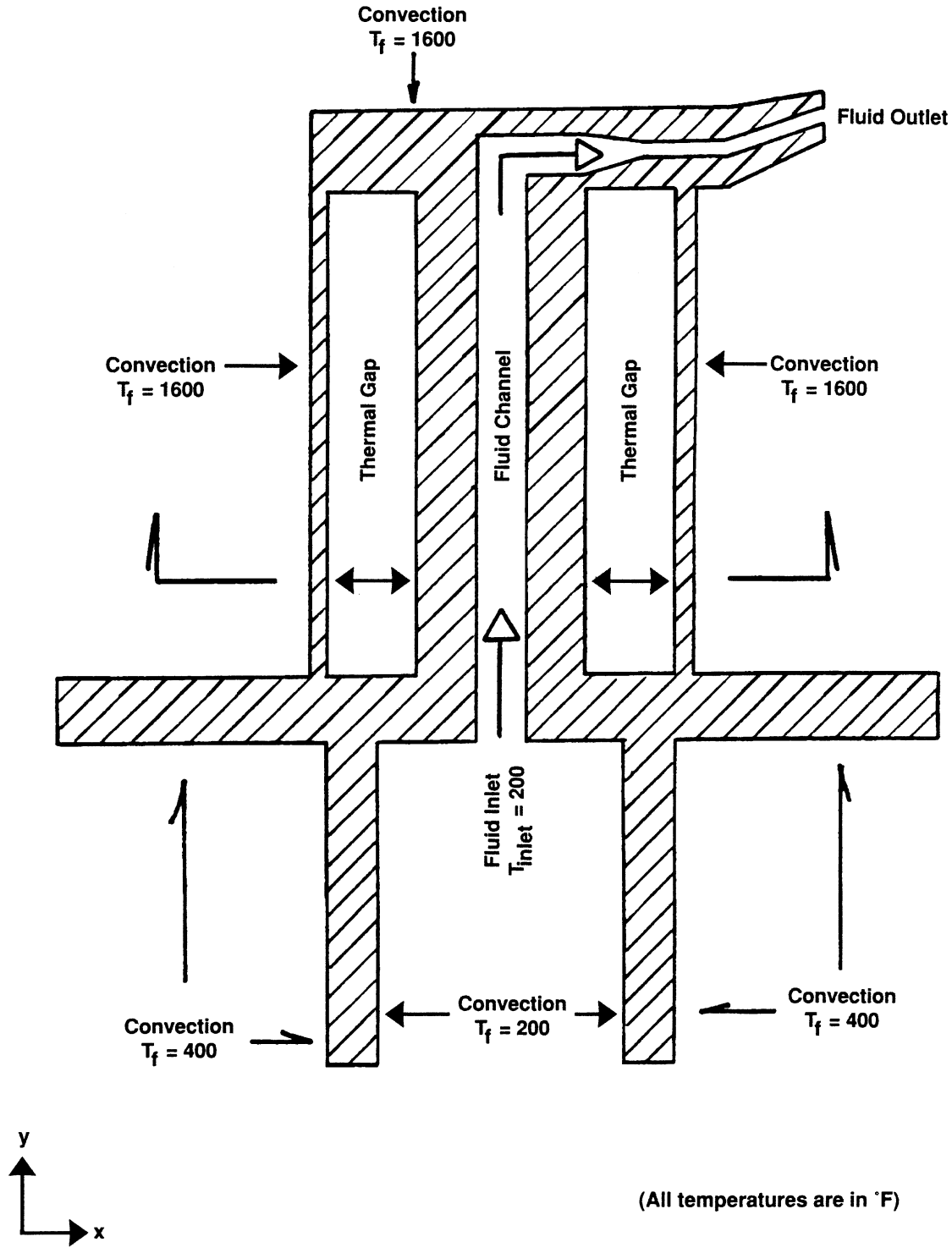

Figure E 5.14-1 Simplified Nozzle

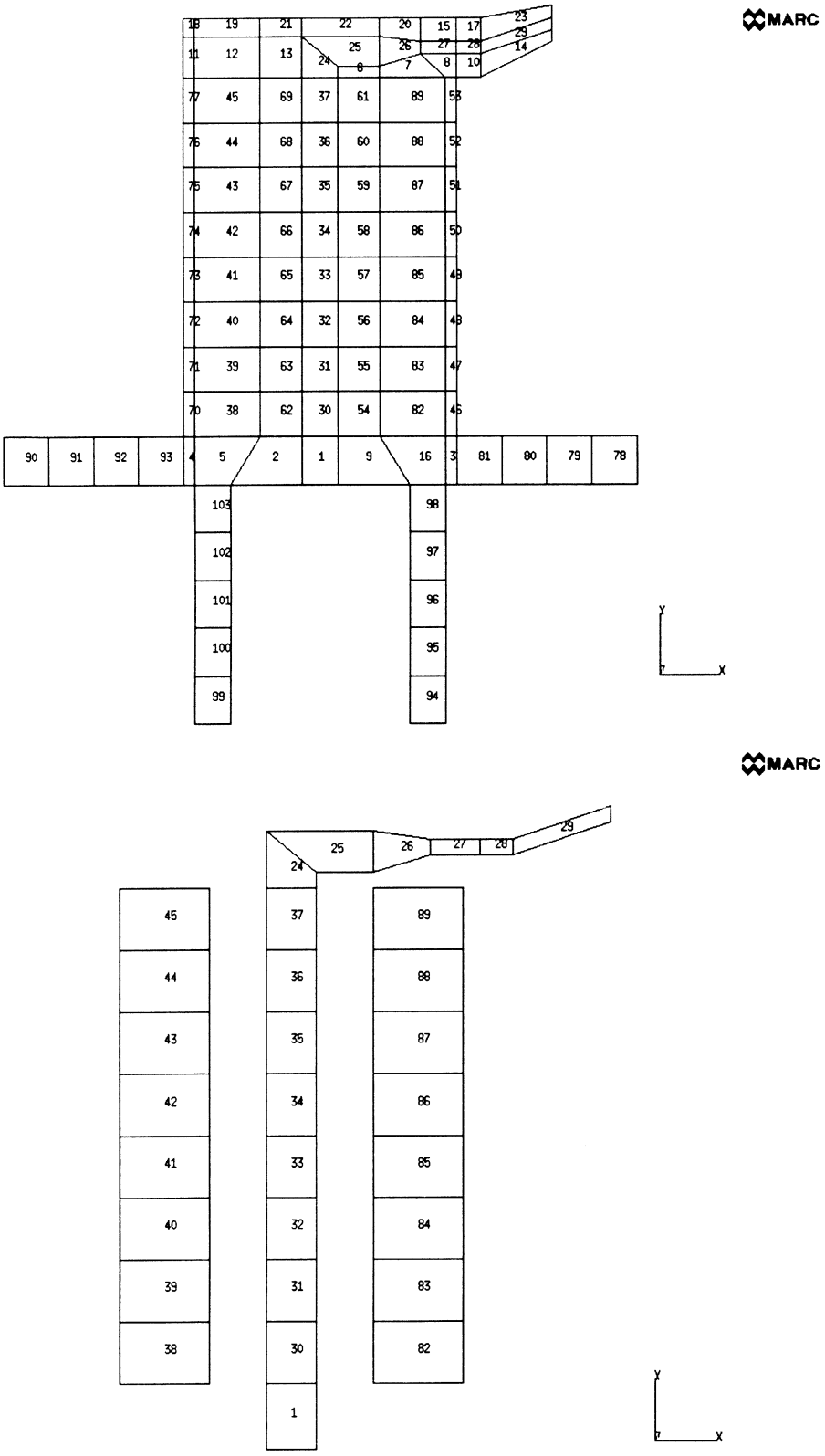

Figure E 5.14-2 Simplified Nozzle (Finite Element Mesh)

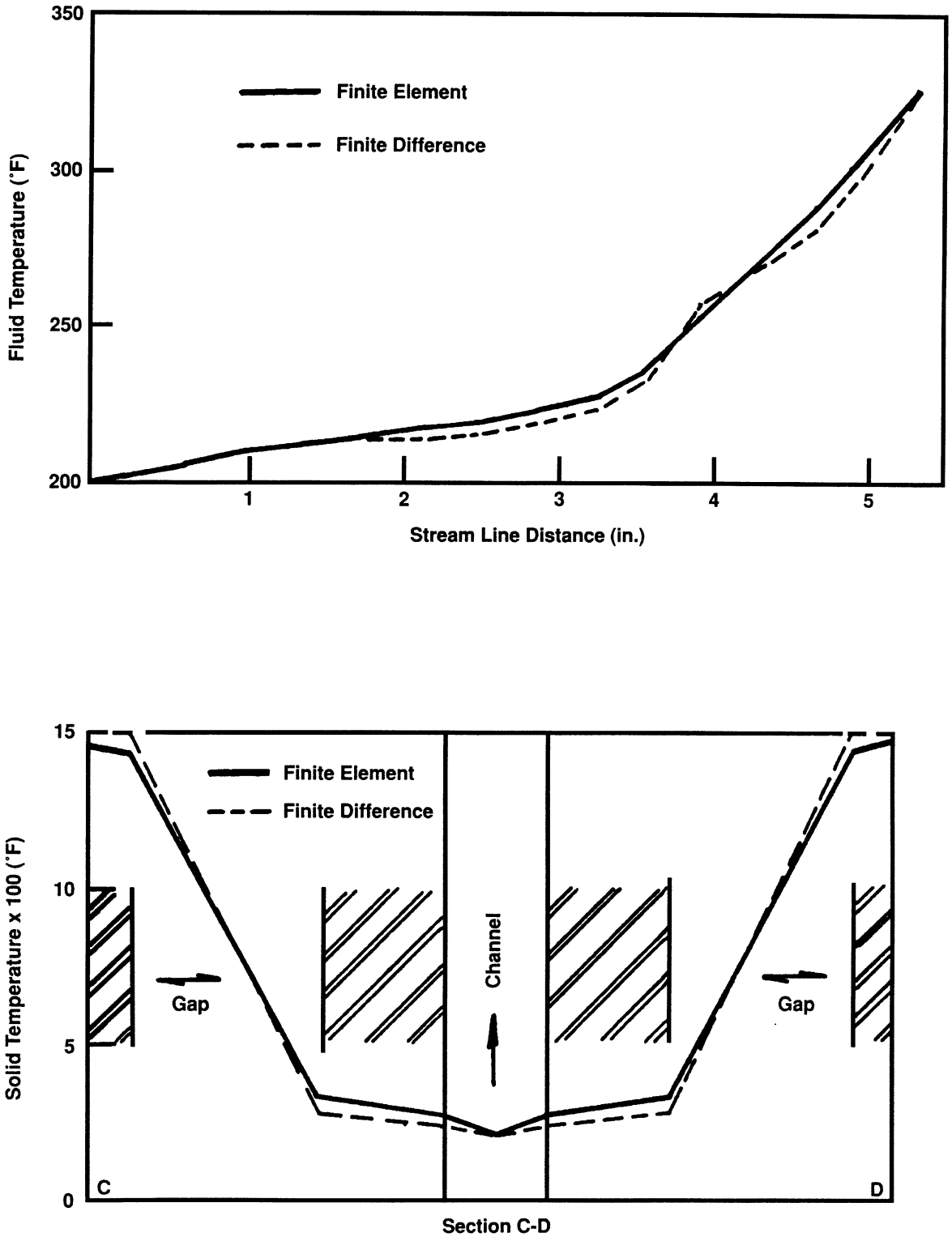

Figure E 5.14-3 Simplified Nozzle Solid and Fluid Temperatures)

E 5.15 Radiation Between Concentric Spheres

A typical radiation heat-exchange problem between gray bodies is solved here in order to show the capabilities of the MARC program in dealing with the radiations boundary conditions in heat conduction problems. The radiation heat exchange is based on the computation of the "view factors" depending purely upon the geometrical shape of the radiating boundaries. The computed steady-state temperature distribution is shown and is compared with an analytical solution.

The geometry of the model is shown in Figure E 5.15-1; two concentric spherical bodies and four spherical surfaces can be identified: surfaces no. 1 and no. 2 define the first body and surfaces nos. 3 and 4 define the second spherical gray body. Temperatures on surfaces 1 and 4 are known; radiative heat transfer takes place between surfaces 2 and 3.

Element

Element type 42, a second order distorted axisymmetric quadrilateral element for heat-transfer analysis, is used. There are eight nodes per element and one degree of freedom (temperature) per node. (See Volume B42.1 for further details.)

Model

The axisymmetric section and the finite element model shown in Figure E 5.15-2; 24 elements, with two elements in the radial direction, describe each body for a total of 48 elements and 202 nodes.

Radiation

The RADIATION parameter option is used to activate the heat transfer analysis with radiative heat exchange and to specify the view-factors calculation (or for reading them from a tape). In addition the units are specified for length and for temperature.

Radiating Cavity

One radiating cavity is defined in this option: the cavity is bounded by the spherical surfaces nos. 2 and 3 in Figure E 5.15-1. The anti-clockwise list of nodes defining the outline of the cavity is assigned.

Thermal Properties

One set of thermal properties is specified in the ISOTROPIC block: the isotropic thermal conductivity value of 1.E-4 W/mm °C is assigned in the first field and the temperature-dependent value of the emissivity is specified in the fourth field. (Special input for radiation problems.)

Thermal Boundary Conditions

The temperature value of the internal and external spherical surfaces in imposed in the FIXED TEMP block as follows:

```
Surface no. 1   T1 = 332.561 °C   Surface no. 4   T4 = 532.114 °C
```

See Figure E 5.15-1 for cross reference.

Control for Thermal Analysis

The maximum error in temperature estimate used for property evaluation is set to 0.1 °C. This control provides a recycling capability to improve accuracy in this highly non-linear heat transfer problem. See Volume C, Model Definition option CONTROL, for further details.

Thermal History

A steady-state thermal analysis is specified via STEADY STATE History Definition option.

Results

The computed distribution of the temperature at the steady-state condition is compared with the analytical solution and it is summarized below.

Surface Temperature	Analytic (°C)	MARC (°C)
T1	332.561	332.561
T2	400.00	399.880
T3	500.00	500.110
T4	532.114	532.114

Reference

Frank Kreith, *Principles of Heat Transfer*, Donnelly Publishing Corp., N.Y.

Summary of Options Used

Listed below are the options used in example e5x15.dat:

Parameter Options

ELEMENT
END
HEAT
RADIATION
SIZING
TITLE

Model Definition Options

BOUNDARY CONDITIONS
CONNECTIVITY
CONTROL
COORDINATE
END OPTION
ISOTROPIC
RADIATING
TEMPERATURE EFFECTS

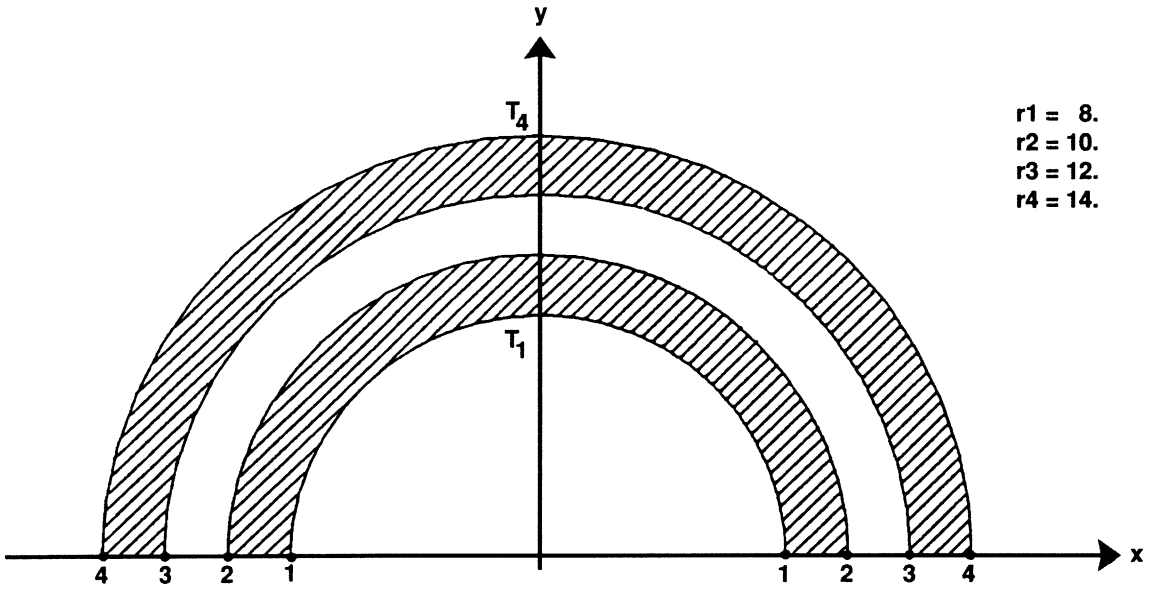

Figure E 5.15-1 Radiating Concentric Spheres

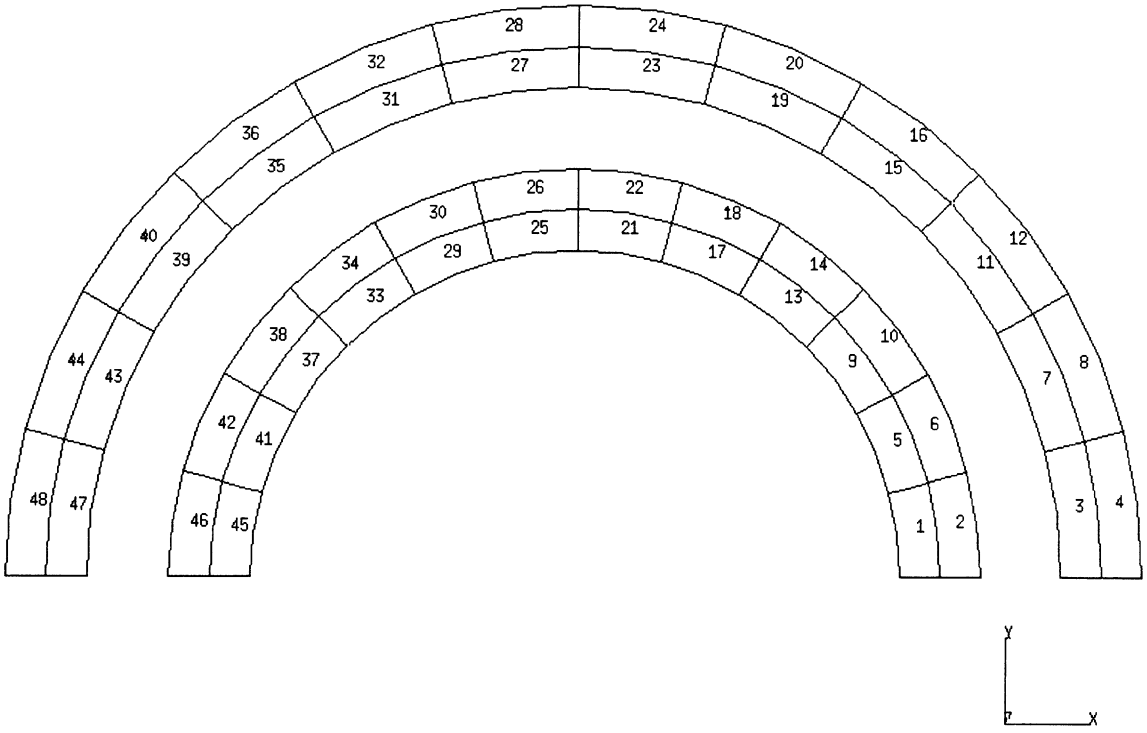

Figure E 5.15-2 Mesh With Element Numbers

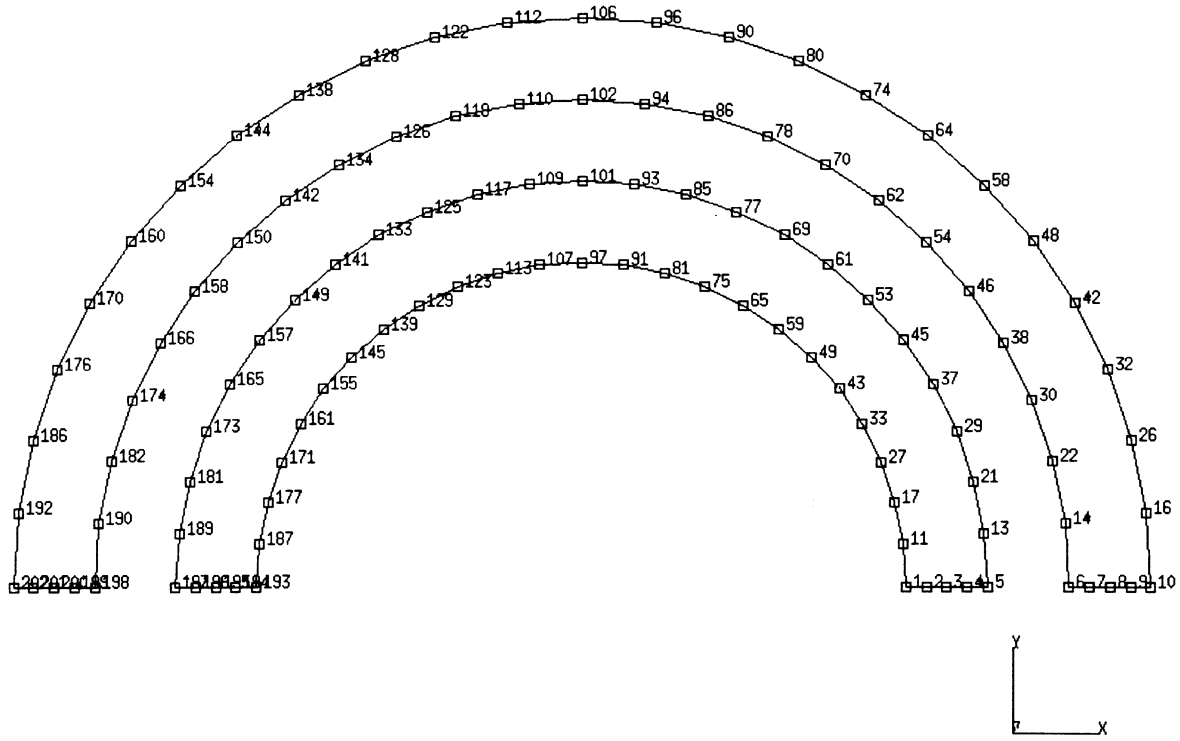

Figure E 5.15-3 Mesh With Node Numbers

E 5.16 Three Dimensional Thermal Shock

The bar of a rectangular cross section is initially at rest. At time t = 0, one end of the bar is held at a fixed temperature of 1000°F, and a transient conduction problem is solved.

Element (Ref B44.1, B123.1 and B133.1)

Element types 44 and 133 are second-order isoparametric three dimensional heat conduction elements. There are twenty nodes for brick element type 44 and 10 nodes for the tetrahedral element type 133. Element type 123 is an 8 node brick with reduced integration and hourglass control.

Model

The bar cross section is square with a thickness of one inch and a length of 2 inches. This transient conduction problem is performed for three meshes comprised of element types 44, 123 and 133.

Thermal Properties

The isotropic thermal conductivity value of 0.42117E-5 Btu/sec.-in.-°F. The specific heat is 0.3523E-3 Btu/lb°F. The mass density is 0.7254E-3 lb/cu.in.

Thermal Boundary Conditions

The initial temperature distribution is that all nodes have a temperature of 0.0°F. A time t = 0, the nodal temperatures of one end of the bar are fixed at 1000°F, and a transient conduction problem is solved to its completion at steady state, where all nodes will have a final temperature of 1000°F.

Control for Thermal Analysis

The maximum number of time points are fixed at 100. The maximum change in nodal temperature will be 100°F.

Thermal History

A transient thermal analysis is specified via the TRANSIENT option, with the automatic time stepping feature turned on. The initial time increment is 1.0E-2 seconds, with a final time period of 1 second.

Results

From the temperature history shown in Figure E 5.16-1, Figure E 5.16-3 and Figure E 5.16-5 for element types 44, 123 and 133, respectively, the automatic time stepping feature shows ever increasing time steps as the solution approaches steady state. The temperature of the free end goes slightly negative by about a tenth of a degree for elemene types 123 and 133. This effect has been minimized by the inclusion of the LUMP parameter option which instructs MARC to lump the capacitance matrix, instead of using the consistent capacitance matrix which is the default. There is virtually no difference in the thermal history of the free end between different element types. Figure E 5.16-2, Figure E 5.16-4 and Figure E 5.16-6 are iso-thermal surfaces

at a time when the free end starts to heat up significantly. These iso-thermal surfaces should be flat and perpendicular to the axis of the bar. The iso-thermal surfaces become flatter as the bar becomes hotter. Also, the iso-thermal surfaces are more irregular for the tetrahedron mesh than the brick mesh, because the brick element faces are either perpendicular or parallel to the head flow. This effect is minimized if more tetrahedron elements are used.

Summary of Options Used

Listed below are the options used in example e5x16a.dat:

Parameter Options

ELEMENT
END
HEAT
LUMP
SIZING
TITLE

Model Definition Options

CONNECTIVITY
CONTROL
COORDINATE
END OPTION
FIXED TEMPERATURE
INITIAL TEMPERATURE
ISOTROPIC
NO PRINT
POST

Load Incrementation Options

CONTINUE
TRANSIENT

Listed below are the options used in example e5x16b.dat:

Parameter Options

ALIAS
ELEMENT
END
HEAT
LUMP
SIZING
TITLE

Model Definition Options

CONNECTIVITY
CONTROL
COORDINATE
END OPTION
FIXED TEMPERATURE
INITIAL TEMPERATURE
ISOTROPIC
POST

Load Incrementation Options

CONTINUE
TRANSIENT

Time	Temperature (˚F)	Time	Temperature (˚F)
0.0	0.0		
1.82307E-04	7.62101E-02	8.46059E-02	4.34587E+02
3.64615E-04	2.46594E-01	1.00722E-01	5.12089E+02
5.92499E-04	5.48778E-01	1.20868E-01	5.93519E+02
8.77355E-04	9.32763E-01	1.41014E-01	6.61590E+02
1.30464E-03	1.32789E+00	1.66196E-01	7.29694E+02
1.83874E-03	1.53547E+00	1.97673E-01	7.94479E+02
2.63990E-03	1.53524E+00	2.44890E-01	8.60475E+02
3.84163E-03	1.49460E+00	3.03910E-01	9.12322E+02
5.64423E-03	2.05263E+00	3.92441E-01	9.53537E+02
7.89748E-03	4.10911E+00	5.25236E-01	9.80063E+02
1.07140E-02	9.03647E+00	7.24430E-01	9.93345E+02
1.42348E-02	1.88757E+01	1.02322E+00	9.98334E+02
1.86356E-02	3.63171E+01	1.47141E+00	9.99697E+02
2.41367E-02	6.43750E+01	2.14369E+00	9.99961E+02
3.23884E-02	1.14785E+02	3.15211E+00	9.99996E+02
4.27029E-02	1.82812E+02	4.66473E+00	1.00000E+03
5.55962E-02	2.67022E+02	6.93368E+00	1.00000E+03
6.84894E-02	3.46206E+02	1.00003E+01	1.00000E+03

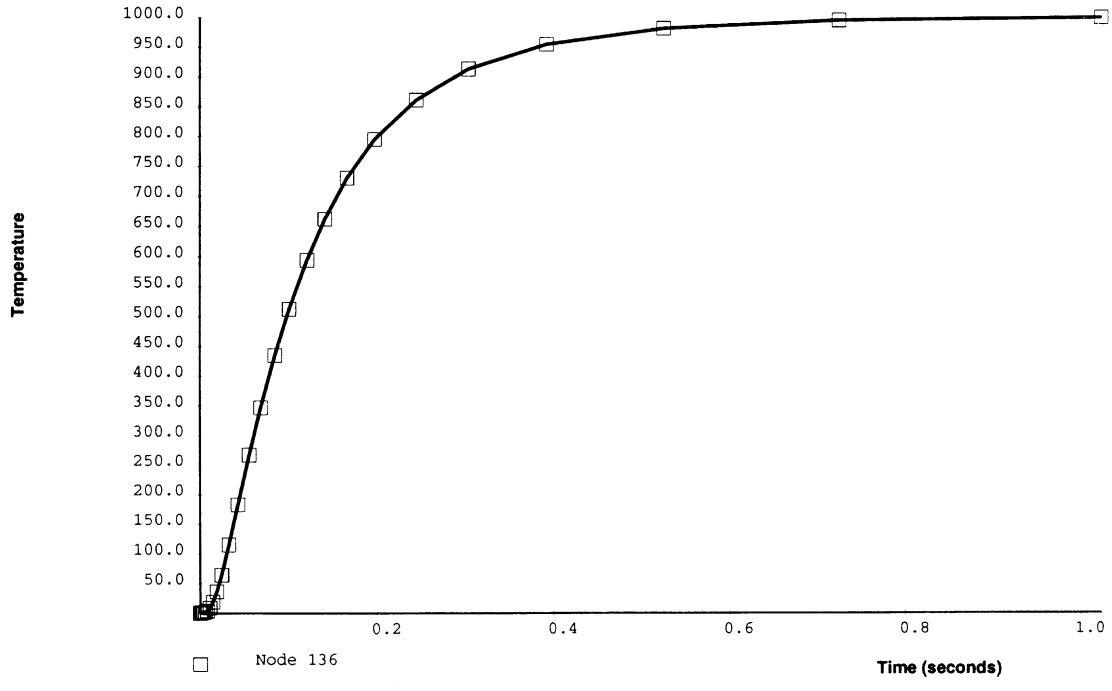

Temperature History (Element Type 44)

Figure E 5.16-1 Temperature History for Free End Node 136 Element Type 44

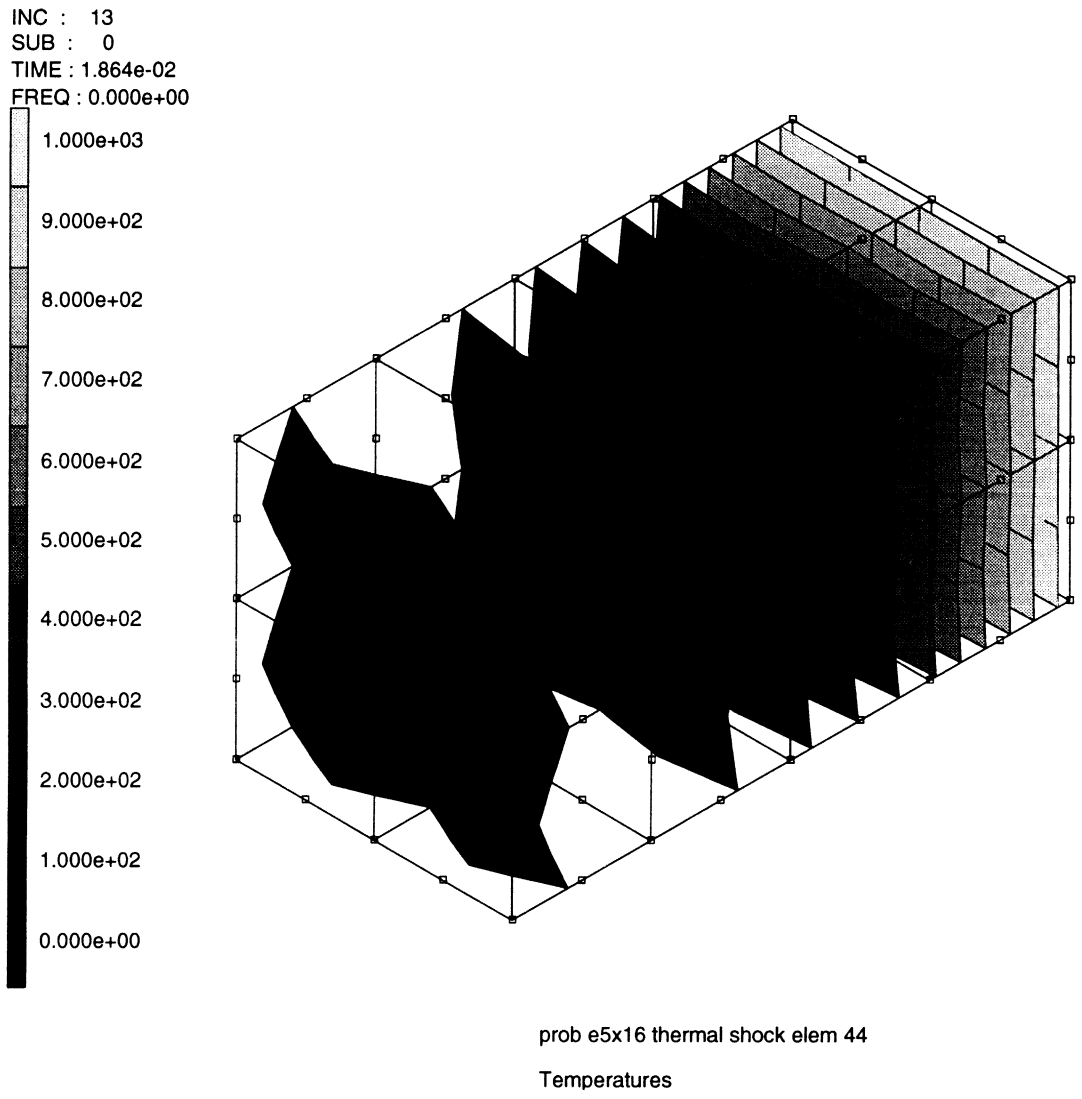

Figure E 5.16-2 Iso-thermal Surfaces at t = 0.0186 seconds (Element Type 44)

Time	Temperature (°F)	Time	Temperature (°F)
0.0	0.0		
1.99113E-04	-3.03712E-03	1.04521E-01	4.03045E+02
3.98226E-04	1.81682E-04	1.24798E-01	4.74083E+02
6.47118E-04	8.32631E-03	1.50145E-01	5.50460E+02
1.02045E-03	3.44541E-02	1.81829E-01	6.29444E+02
1.58046E-03	1.14610E-01	2.13513E-01	6.94672E+02
2.42047E-03	3.42895E-01	2.53118E-01	7.59006E+02
3.68048E-03	9.54424E-01	3.02624E-01	8.19336E+02
5.57050E-03	2.52048E+00	3.76883E-01	8.79604E+02
7.93302E-03	5.50497E+00	4.88272E-01	9.31265E+02
1.08862E-02	1.08245E+01	6.55355E-01	9.67696E+02
1.45776E-02	1.97886E+01	9.05980E-01	9.88009E+02
1.91919E-02	3.40969E+01	1.28192E+00	9.96615E+02
2.61134E-02	6.06809E+01	1.84582E+00	9.99298E+02
3.47652E-02	9.86775E+01	2.69168E+00	9.99896E+02
4.77429E-02	1.59734E+02	3.96047E+00	9.99989E+02
6.39651E-02	2.35397E+02	5.86365E+00	9.99999E+02
8.42428E-02	3.23410E+02	8.71842E+00	1.00000E+03
		1.00001E+01	1.00000E+03

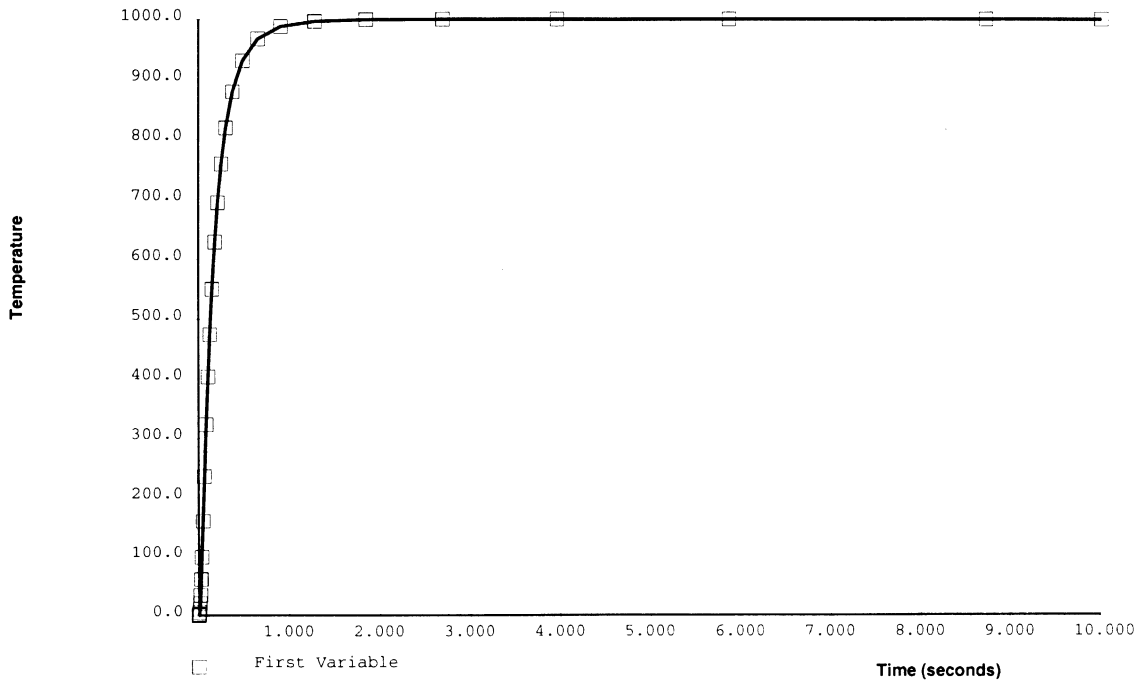

Figure E 5.16-3 Temperature History for Free End Node 126 (Element Type 123)

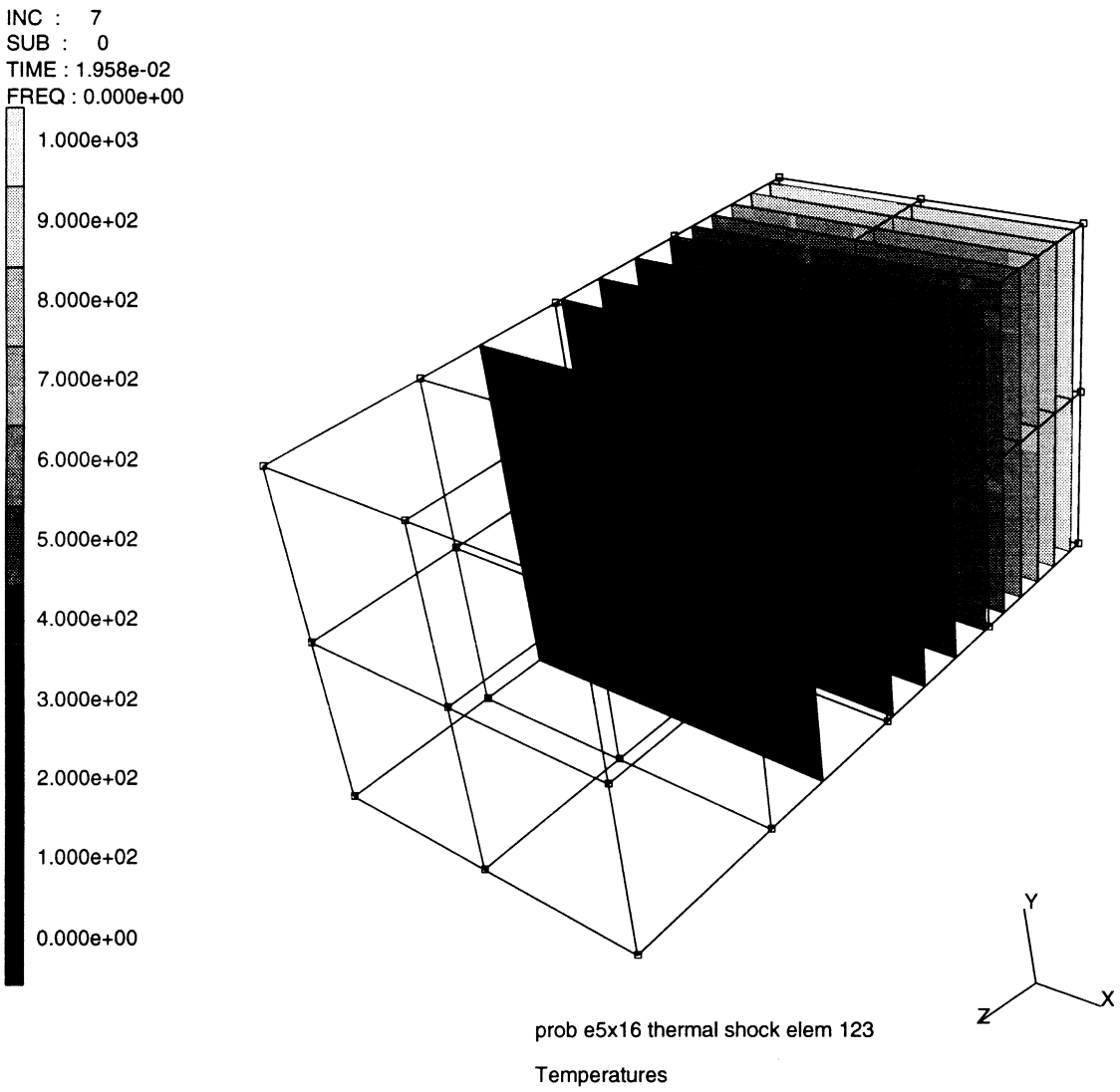

Figure E 5.16-4 Iso-thermal Surfaces at t = 0.0196 seconds (Element Type 123)

Time	Temperature (°F)	Time	Temperature (°F)
0.0	0.0		
7.10402E-04	-1.63117E-01	1.14734E-01	5.64931E+02
1.42080E-03	-3.29948E-01	1.33342E-01	6.33486E+02
2.30881E-03	-4.95783E-01	1.56602E-01	7.03065E+02
3.64081E-03	-6.80945E-01	1.85677E-01	7.70386E+02
5.30582E-03	-7.92613E-01	2.22020E-01	8.31985E+02
7.38707E-03	-4.82283E-01	2.76536E-01	8.91606E+02
1.05090E-02	2.03853E+00	3.58309E-01	9.40608E+02
1.44113E-02	9.60317E+00	4.80968E-01	9.73458E+02
1.92893E-02	2.61956E+01	6.64957E-01	9.90708E+02
2.53867E-02	5.59788E+01	9.40940E-01	9.97545E+02
3.30085E-02	1.02089E+02	1.35492E+00	9.99526E+02
4.25357E-02	1.65698E+02	1.97588E+00	9.99935E+02
5.44447E-02	2.45701E+02	2.90732E+00	9.99994E+02
6.63538E-02	3.21802E+02	4.30449E+00	1.00000E+03
8.12401E-02	4.07738E+02	6.40024E+00	1.00000E+03
9.61264E-02	4.83906E+02	9.54387E+00	1.00000E+03
		1.0000E+01	1.00000E+03

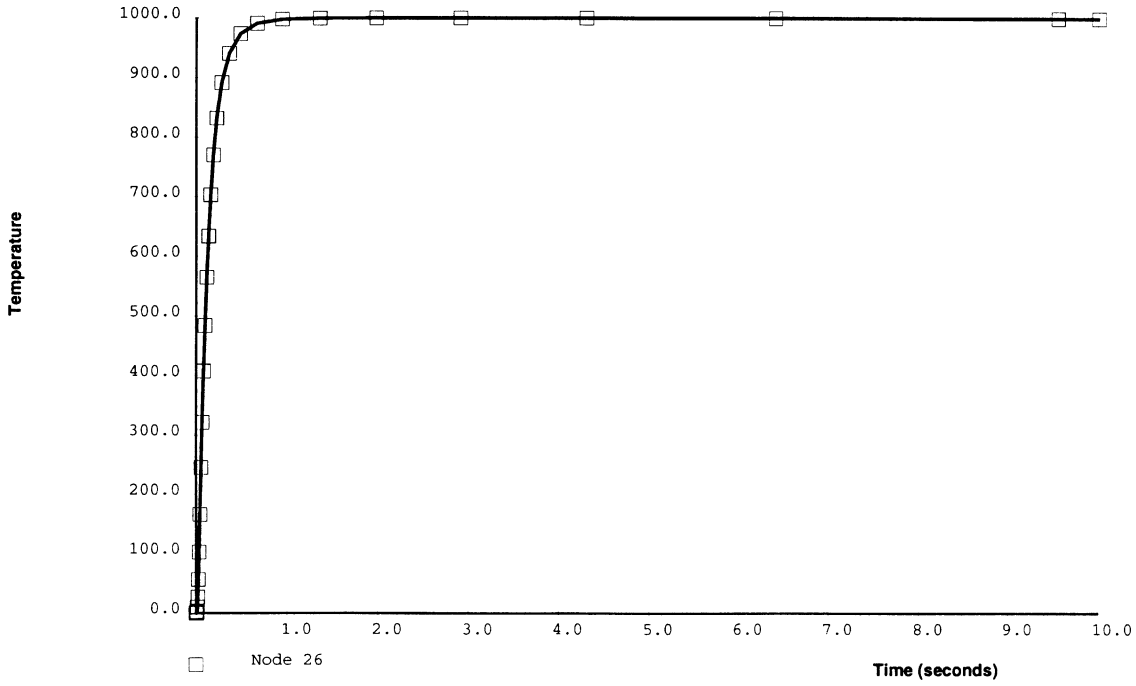

Temperature History (Element Type 133)

Figure E 5.16-5 Temperature History for Free End Node 26 (Element Type 133)

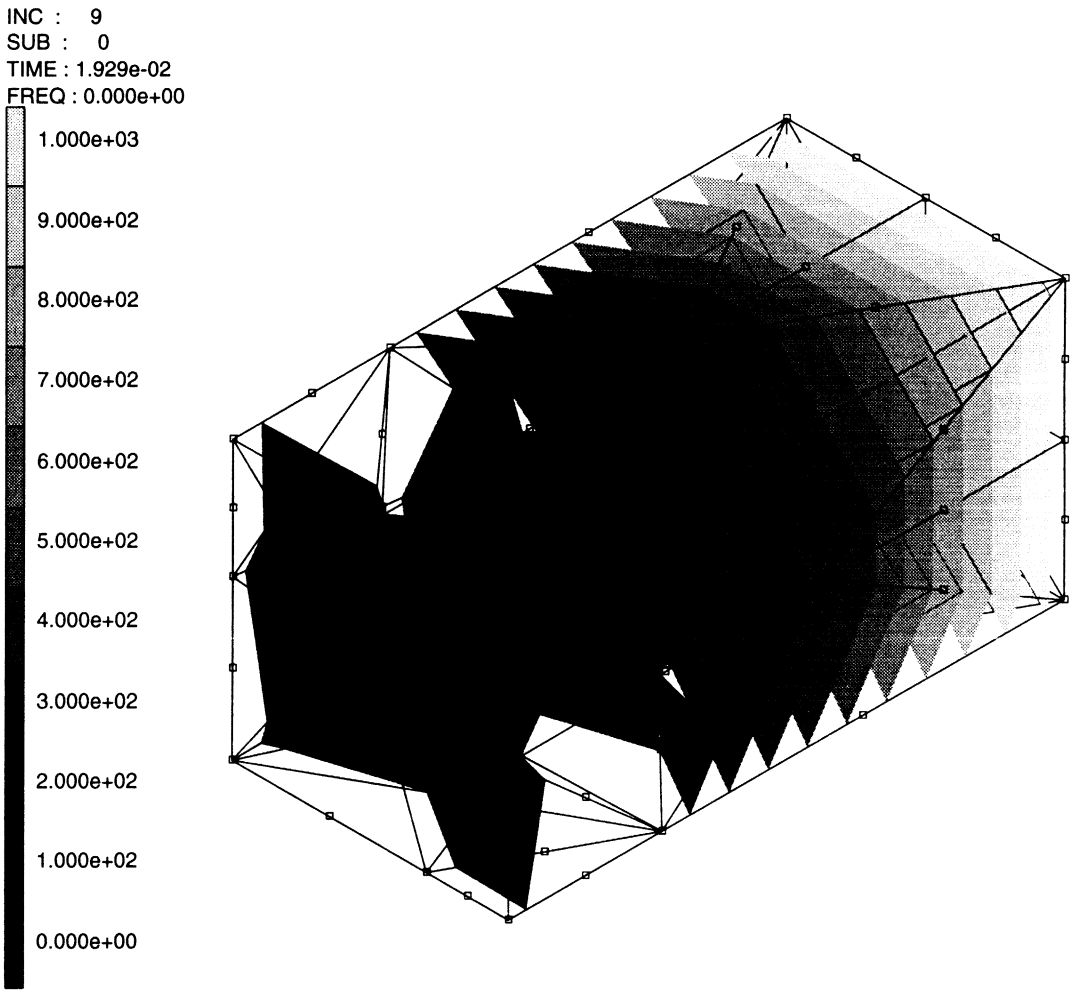

Figure E 5.16-6 Iso-thermal Surfaces at t = 0.0193 seconds (Element Type 133)

VOLUME E
DEMONSTRATION PROBLEMS

Chapter 6
Dynamics

Contents Chapter 6 Dynamics

Chapter 6 Dynamics

MARC K.5 contains both the modal superposition and direct integration capabilities for the analysis of dynamic problems. A discussion on the use of these capabilities can be found in Volume A and a summary of the feature is given below.

Modal Analysis (inverse power sweep or Lanczos)

Direct Integration

- Newmark-beta operator
- Houbolt operator
- Central difference operator
- Modal superposition

Consistent and lumped mass matrices

Damping

- Modal damping
- Stiffness and/or mass damping
- Numerical damping

Initial conditions

- Nodal displacement
- Nodal velocity

Boundary conditions

- Nodal displacement history
- Nodal velocity history
- Nodal acceleration history

Nonlinear effects

- Material nonlinearity (i.e., plasticity)
- Geometric nonlinearity (i.e., large displacement)
- Boundary nonlinearity (i.e., gap-friction)

Variable time steps

- Newmark-beta operator

Compiled in this chapter are a number of solved problems. These problems illustrate the use of dynamic analysis options in the MARC program. Table E 6.0-1 shows MARC elements and options used in these demonstration problems.

Table E 6.0-1 Dynamic Analysis Demonstration Problems

Problem Number (E)	Element Type	Parameter Options	Model Definition	Load Incrementation	User Subroutines	Problem Description
6.1	5 45	DYNAMIC	CONTROL PRINT CHOICE	DYNAMIC CHANGE DIST LOADS	—	Dynamic response of a simply supported beam subjected to a uniformly distributed load.
6.2	45	DYNAMIC	—	MODAL SHAPE RECOVER	—	Frequencies and modal shapes of a Timoshenko beam.
6.3	4 8	DYNAMIC	CONTROL UFXORD FXORD INITIAL CONDITIONS	MODAL SHAPE DYNAMIC CHANGE DIST LOADS	UFXORD	Dynamic analysis of a cantilever plate using the modal procedure. Both inverse power sweep and Lanczos method.
6.4	10	DYNAMIC LARGE DISP FOLLOW FOR	ROTATION A CONTROL	MODAL SHAPE DIST LOADS	—	Frequencies of a rotating disk (centrifugal loading effect).
6.5	27 41	DYNAMIC FLU LOAD	FLUID SOLID	MODAL SHAPE	—	Frequencies of fluid-solid coupled (dam/water) system.
6.6	9	LARGE DISP DYNAMIC RESPONSE	RESPONSE SPECTRUM	MODAL SHAPE SPECTRUM	—	Evaluate eigenvalues for a space frame and perform spectrum response calculation.
6.7	28 33	LARGE DISP HARMONIC	TYING PHI-COEFI MOONEY	HARMONIC DISP CHANGE	—	Evaluate the response of a rubber mount subjected to several frequencies.
6.8	35	LARGE DISP HARMONIC	PHI-COEFI MOONEY	HARMONIC DISP CHANGE	—	Evaluate the response of a rubber block subjected to several frequencies at different amounts of deformation.

Table E 6.0-1 Dynamic Analysis Demonstration Problems (Continued)

Problem Number (E)	Element Type	Parameter Options	Model Definition	Load Incrementation	User Subroutines	Problem Description
6.9	9	PRINT DAMPING LUMP DYNAMIC	POST INITIAL VEL DAMPING MASSES GAP DATA	DYNAMIC CHANGE	—	Elastic impact of a bar.
6.10	52	DYNAMIC	POST TYING MASSES	MODAL SHAPE RECOVER	—	Frequencies of an alternator mount.
6.11	30	DYNAMIC LINEAR	POINT LOADS	MODAL SHAPE	—	Modal analysis of a wing caisson.
6.12	9	DYNAMIC UPDATE LARGE DISP	POINT LOADS	PROPORTIONAL MODAL SHAPE	—	Vibration of a cable.
6.13	16	DYNAMIC LARGE DISP	INITIAL VELOCITY RESTART	AUTO TIME	—	Elastic-perfectly plastic beam explosively loaded.
6.14	27	DYNAMIC	DEFINE LORENZI	DYNAMIC CHANGE DIST LOADS	—	Impact loading of a center cracked rectangular plate. DeLorenzi method used to evaluate K.
6.15	7	LUMP DYNAMIC PRINT, 3	FIXED DISP	MODAL SHAPE RECOVER	—	Modal shape calculations using assumed strain element.
6.16	7	PRINT, 5 LARGE DISP DYNAMIC LUMP	INITIAL VELOCITY FIXED DISP DAMPING CONTACT	DYNAMIC CHANGE	—	Dynamic impact between deformable body and a rigid surface.
6.17	7	PRINT, 5 DYNAMIC LUMP LARGE DISP	DAMPING FIXED DISP INITIAL VELOCITY CONTACT	DYNAMIC CHANGE	—	Dynamic contact between two deformable bodies.

E 6.1 Dynamic Analysis Of A Beam With Small Displacement Response

The dynamic response of a simply supported rectangular beam is analyzed. The beam is subjected to a uniformly distributed load over its length. Three different methods of analysis are employed and their results are compared. These methods are the Newmark-beta and the Houbolt method of direct integration and the method of modal extraction and superposition.

Element (Ref. B5.1)

Element type 5 is a simple, two-dimensional, rectangular section beam-column. It has three degrees of freedom per node: u, v, and right-handed rotation.

Model

The intent of the example is to illustrate the comparable accuracies of different dynamic operators. Therefore, a very simple model is used. Only half the beam is modeled and only the symmetrical response is sought. It is modeled with three type 5 elements. Because this example involves the small displacement and pure bending of a beam, this type of element is adequate. It should be noted that any beam type element in MARC could be chosen for this problem and would produce the same results.

Geometry

The beam is as shown in Figure E 6.1-1 with height 23.13 in. (EGEOM1), cross-sectional area of 14.70 sq.in. and length of 144.0 in.

Material Properties

The material properties input are Young's modulus of 30 x 10^6 psi, Poisson's ratio of 0.3, and mass density of 7.6754 x 10^{-4} lb-sec^2/in^4.

Loading

The beam is loaded with the ramp pressure forcing function shown in Figure E 6.1-2. The pressure load is ramped in the first increment to -655.65 psi and then brought down with constant slope to zero at time of .01 sec. It remains at zero from then on as the beam's displacement oscillates around zero. Two different time steps are used for comparison with the implicit integration schemes, .001 sec. and .00025 sec. For comparison, the natural frequencies are shown below:

Mode	Frequency (cycles per sec)
1	.100 x 10^3
2	.904 x 10^3
3	.257 x 10^4
4	.540 x 10^4
5	.100 x 10^5

Boundary Conditions

The boundary conditions specify that all four nodes are constrained from movement in the u direction, the cantilevered end (node 1) is also fixed in the v direction and the midpoint (node 4) is constrained from any right-hand rotation.

Dynamic

The options are chosen on the DYNAMIC parameter by IDYN = 1 for modal extraction, IDYN = 2 for Newmark-beta, IDYN = 3 for Houbolt direct integration, and IDYN = 4 for the central difference operator. For the modal extraction scheme, the MODAL SHAPE option must be used. Although the beam response has six modes, only the first five modes are extracted in the solution. The assumption is made that the highest mode makes little contribution to the total response.

Results

The results are summarized in the two plots (see Figure E 6.1-3 and Figure E 6.1-4) of the beam's midpoint (node 4) displacement, v, versus time for time steps of .001 and .0025 secs. We know that for any sine, cosine or constant ramping with time forcing function, the modal solution gives an exact integration independent of time step size based on the modes extracted [1]. Since we have assumed that the highest mode made no significant contribution to the response, we can also assume that our modal solution defines an exact solution for the beam's response.

The plot of the larger time step = .001 second (Figure E 6.1-3) illustrates the inherent errors introduced by the implicit integration schemes. The Newmark operator introduces some periodicity error and so its response is slightly out of phase with the exact modal solution. The Houbolt operator shows larger differences both in the amplitude and the period of the response. This larger phase error is due to the artificial damping introduced by the Houbolt operator. Although this damping causes inaccuracies for this large time step, small displacement problem, it is sometimes a useful feature in large nonlinear dynamic analyses. There it serves to damp out any high-frequency responses which may cause instabilities in the solution [2].

The plot of the small time step = .00025 second (Figure E 6.1-4) shows good agreement between the Newmark-beta and the Houbolt direct integration operator solutions and the exact or modal solution.

The central difference operator proves to be unsuitable for this problem. The stability limit for the time increment of this explicit integration operator is $.172 \times 10^{-4}$, which is far too small to show enough of the beam's response in a reasonable number of increments.

When the problem was run with beam element type 45, the curved Timoshenko beam in a plane, the comparative results between the methods were the same. Again, the Newmark operator introduced some error in both the period and amplitude of the response as shown by the exact modal solution (see Figure E 6.1-5).

The Timoshenko beam element is a 3-node planar beam element which allows transverse shear. It has three nodes per element with three degrees of freedom per node. As shown in Figure E6.1-5, the greater flexibility of the Timoshenko beam model gives its displacement function a greater amplitude and a slightly longer period than the response of the type 5 element model.

References

1. Dunham, R. S., Nickell, R. E., Stickler, D. S., "Integration Operators for Transient Structural Response", *Computers and Structures*, Vol. 2, pp. 1-15 (Pergamon Press, 1972).
2. Marcal, P. V., McNamara, J., "Incremental Stiffness Method for Finite Element Analysis of Nonlinear Dynamic Problem," *Numerical & Computer Methods in Structural Mechanics*, Symposium, Urbana, Illinois, September, 1971.

Summary of Options Used

Listed below are the options used in example e6x1a.dat:

Parameter Options

DIST LOADS
DYNAMIC
ELEMENT
END
SIZING
TITLE

Model Definition Options

CONNECTIVITY
CONTROL
COORDINATE
END OPTION
FIXED DISP
GEOMETRY
ISOTROPIC
POST
PRINT CHOICE

Load Incrementation Options

CONTINUE
DIST LOADS
DYNAMIC CHANGE

Listed below are the options used in example e6x1b.dat:

Parameter Options

DIST LOADS
DYNAMIC
ELEMENT
END
SIZING
TITLE

Model Definition Options

CONNECTIVITY
CONTROL
COORDINATE
END OPTION

FIXED DISP
GEOMETRY
ISOTROPIC
PRINT CHOICE

Load Incrementation Options

CONTINUE
DIST LOADS
DYNAMIC CHANGE

Listed below are the options used in example e6x1c.dat:

Parameter Options

DIST LOADS
DYNAMIC
ELEMENT
END
SIZING
TITLE

Model Definition Options

CONNECTIVITY
CONTROL
COORDINATE
END OPTION
FIXED DISP
GEOMETRY
ISOTROPIC
PRINT CHOICE

Load Incrementation Options

AUTO TIME
CONTINUE
DIST LOADS
DYNAMIC CHANGE
PROPORTIONAL INCREME

MARC

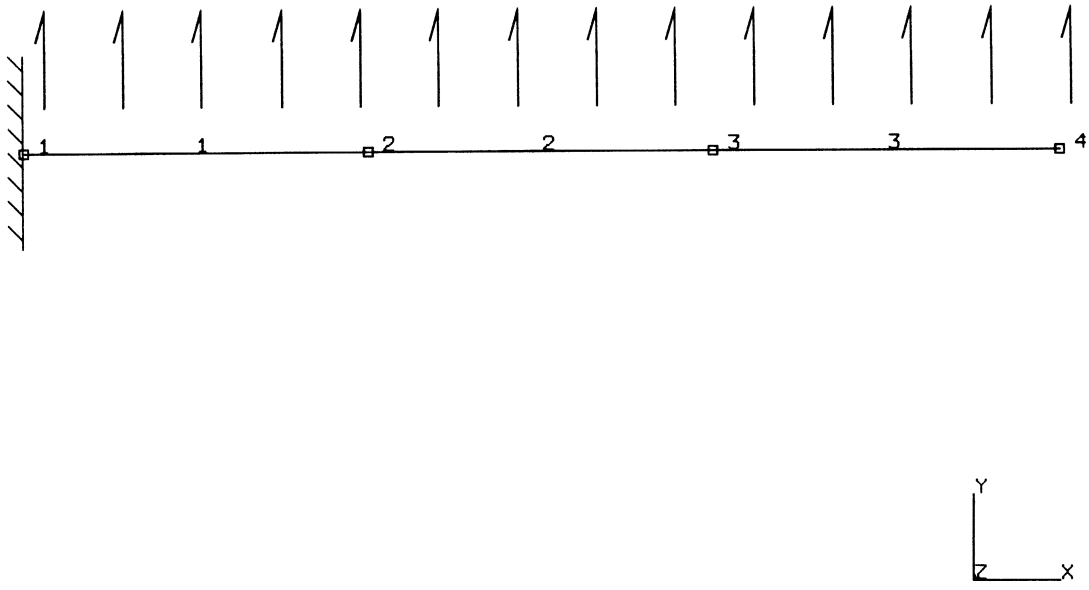

Figure E 6.1-1 Element Type 5 Beam-Column Model

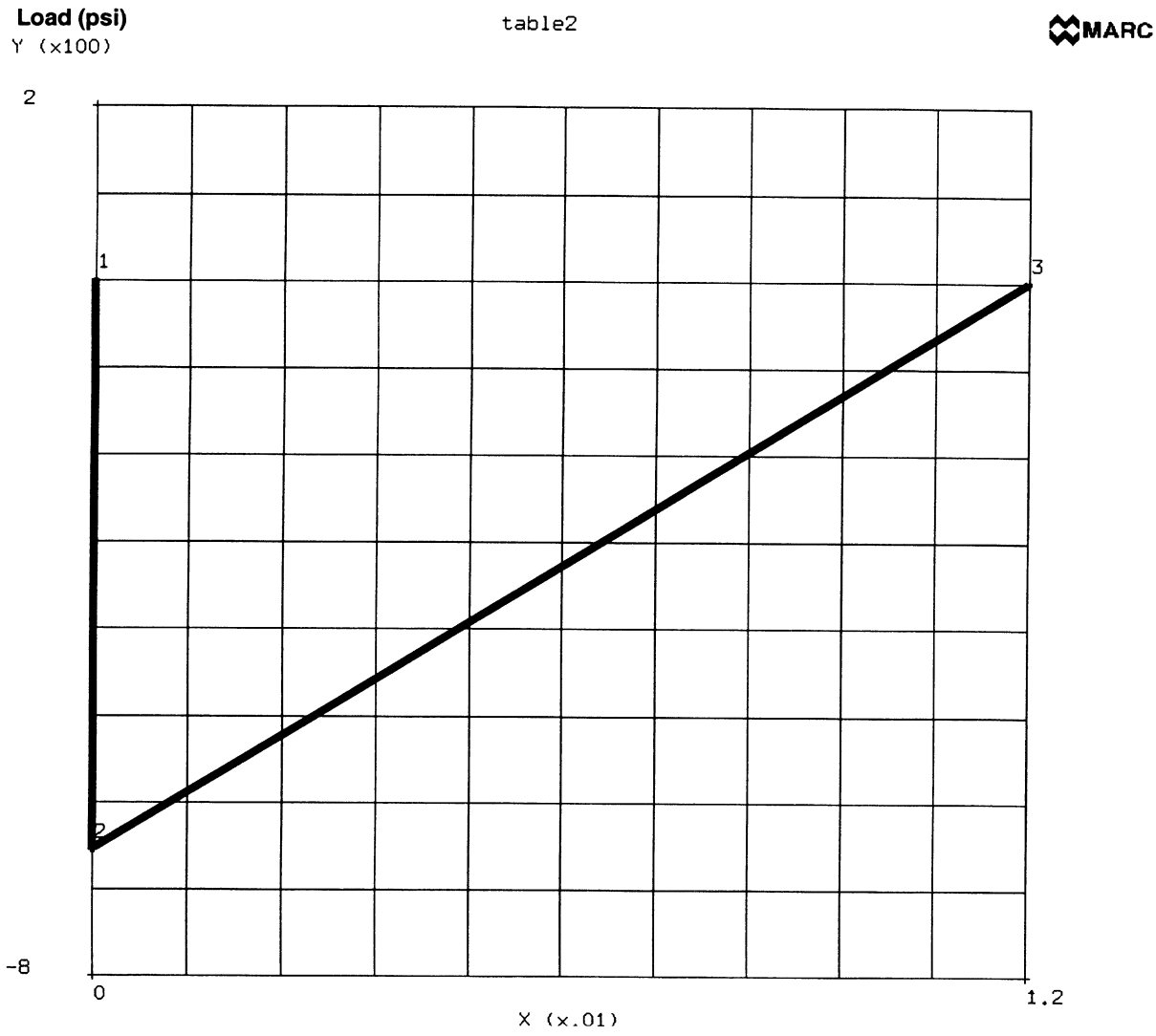

Figure E 6.1-2 Ramp Pressure Forcing Function

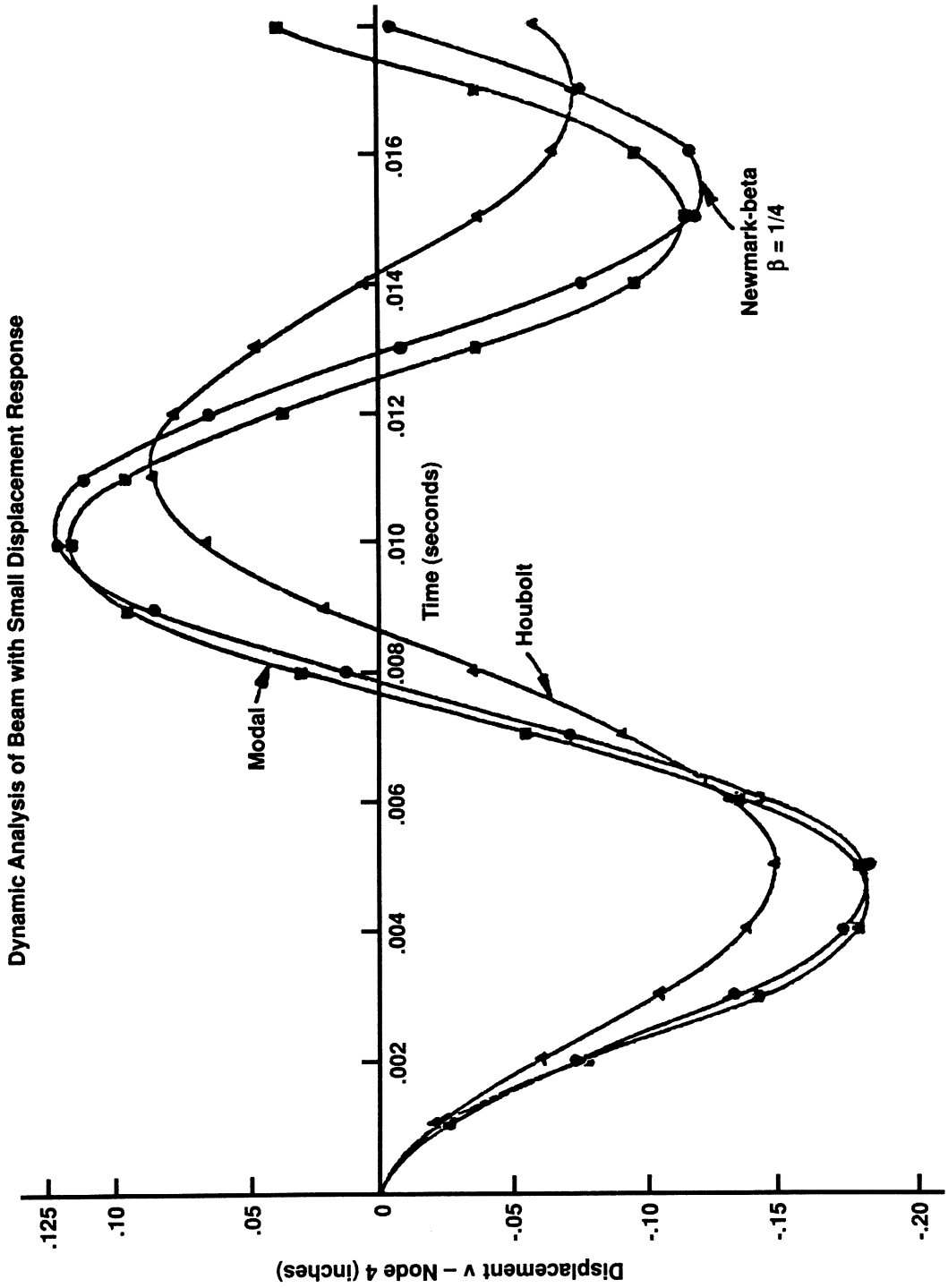

Figure E 6.1-3 Time Step = .001 Sec.

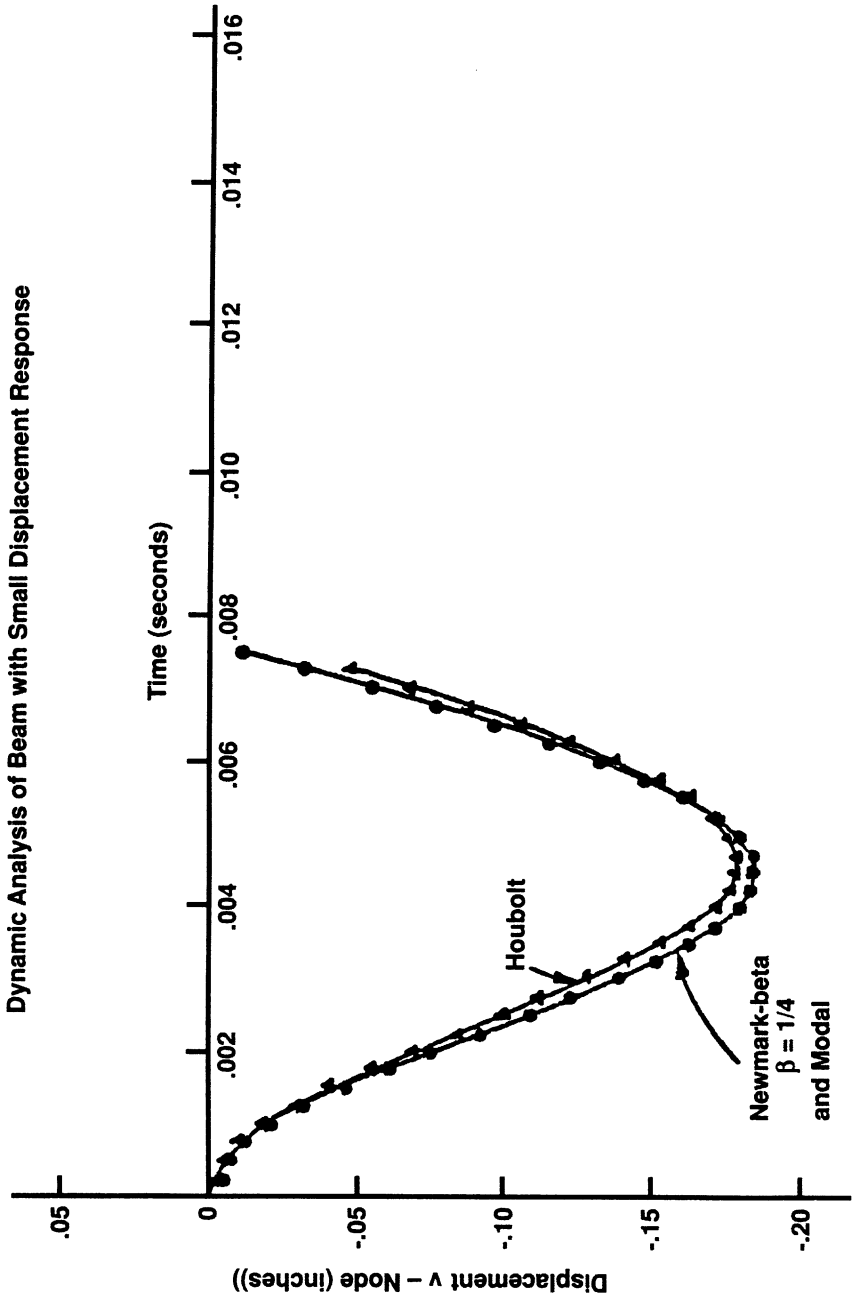

Figure E 6.1-4 Time Step = .00025 Sec.

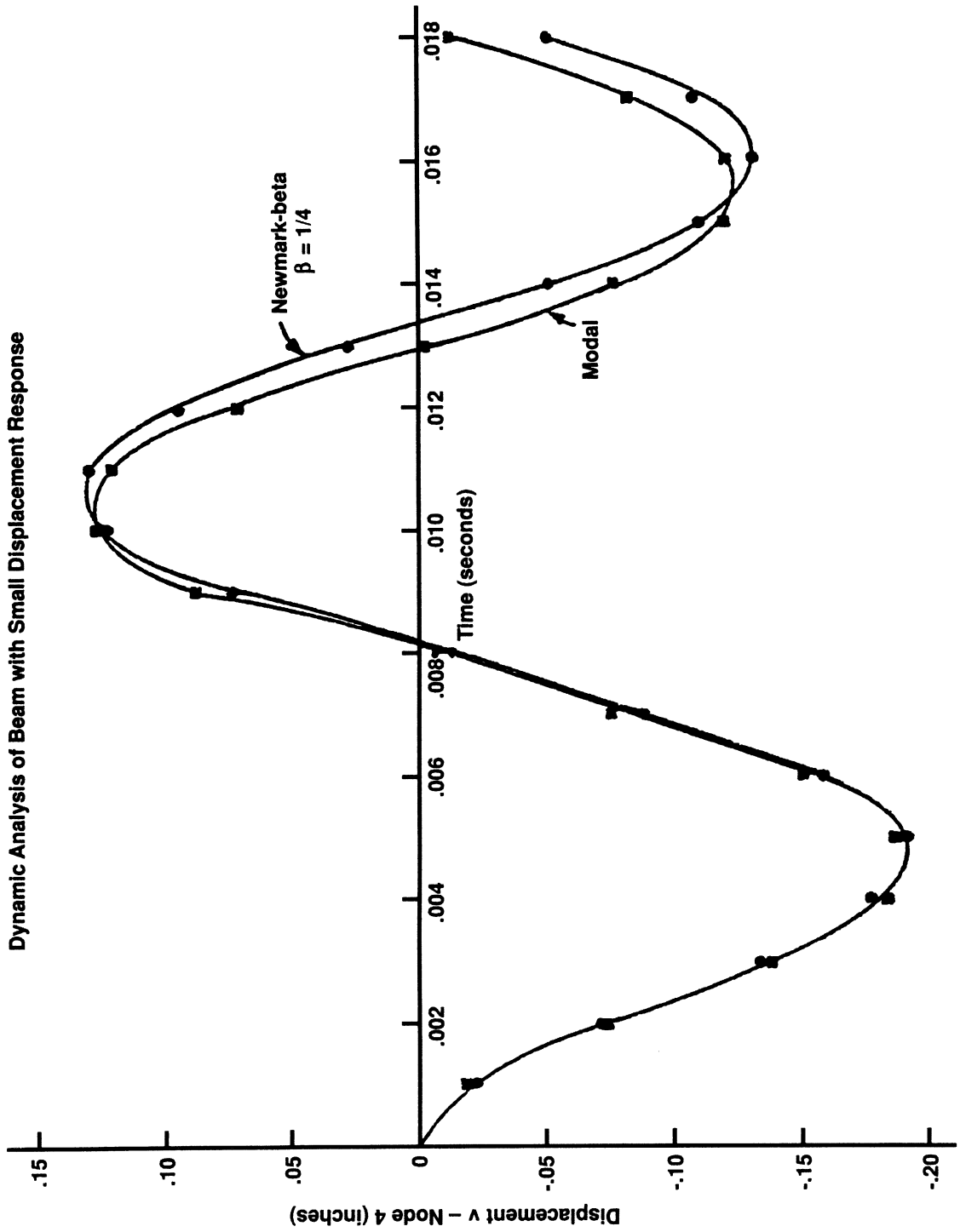

Figure E 6.1-5 Timoshenko Beam, Time Step = .001 Sec.

E 6.2 Beam Modes And Frequencies

This problem is an illustration of the use of the Timoshenko beam element. The first three modes of a square-section, cantilever beam are extracted.

Element (Ref. B45.1)

Element type 45 is a two-dimensional Timoshenko beam with three nodes. Each node has two displacements and one rotational degree of freedom. The element uses a three-point Gaussian integration for mass and a two-point integration for stiffness. This is a consistently derived Timoshenko beam element.

Such elements are most commonly used in dynamic problems, because of the importance of shear and rotatory inertia effects in high-frequency beam response. The particular example is chosen because an exact Timoshenko beam solution is available.

Model

The geometry and dimensions are shown in Figure E 6.2-1.

Material Properties

The program only allows input of Poisson's ratio and Young's modulus as elastic material properties. The shear modulus is calculated from these. The Young's modulus is 30×10^6 psi and the Poisson's ratio is 1/3. The density is 7.25257×10^{-4} lb-sec^2/in^4.

Loading

No load is imposed, since only modes and frequencies are calculated.

Boundary Conditions

One end of the beam is built-in. All displacements and rotations are fixed. Thus, $u = v = \phi_a = 0$ for the built-in end node.

Results

The results in Table E 6.2-1 are obtained for the first three modes. This mesh has 16 active degrees of freedom; a more refined mesh would show the calculated values converging on the exact values.

The first three mode shapes are shown in Figure E 6.2-2.

Table E 6.2-1 Beam Frequencies (cps)

Node	Exact*	Calculated
1	995.2	992.3
2	6065.0	6098.0
3	16469.0	16594.0

*Huang, T. C., "The Effect of Rotary Inertia and Shear Deformation on the Frequency and Normal Modes of Uniform Beams with Simple End Conditions," *J. Applied Mechanics.*, Vol. 28, pp. 279-584 (December 1961).

Summary of Options Used

Listed below are the options used in example e6x2.dat:

Parameter Options

DYNAMIC
ELEMENT
END
SIZING
TITLE

Model Definition Options

CONNECTIVITY
COORDINATE
END OPTION
FIXED DISP
GEOMETRY
ISOTROPIC

Load Incrementation Options

CONTINUE
MODAL SHAPE

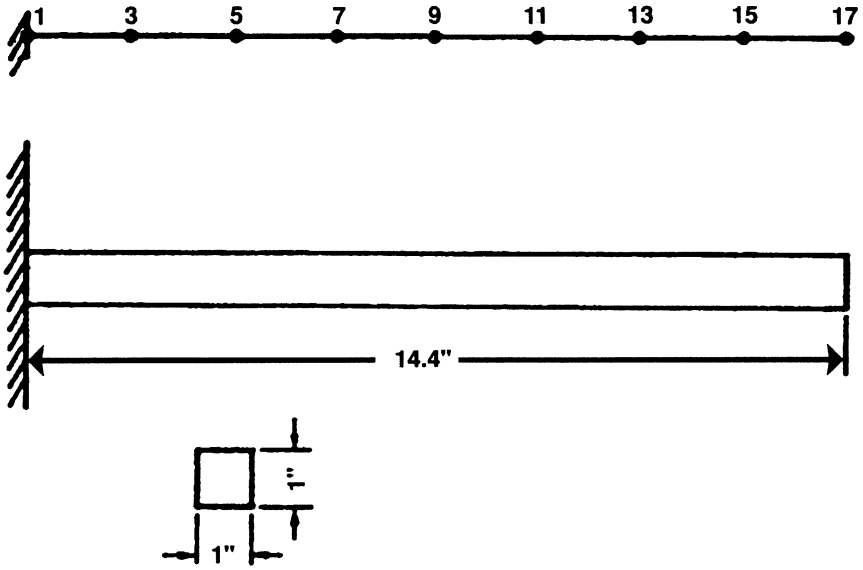

Figure E 6.2-1 Timoshenko Beam

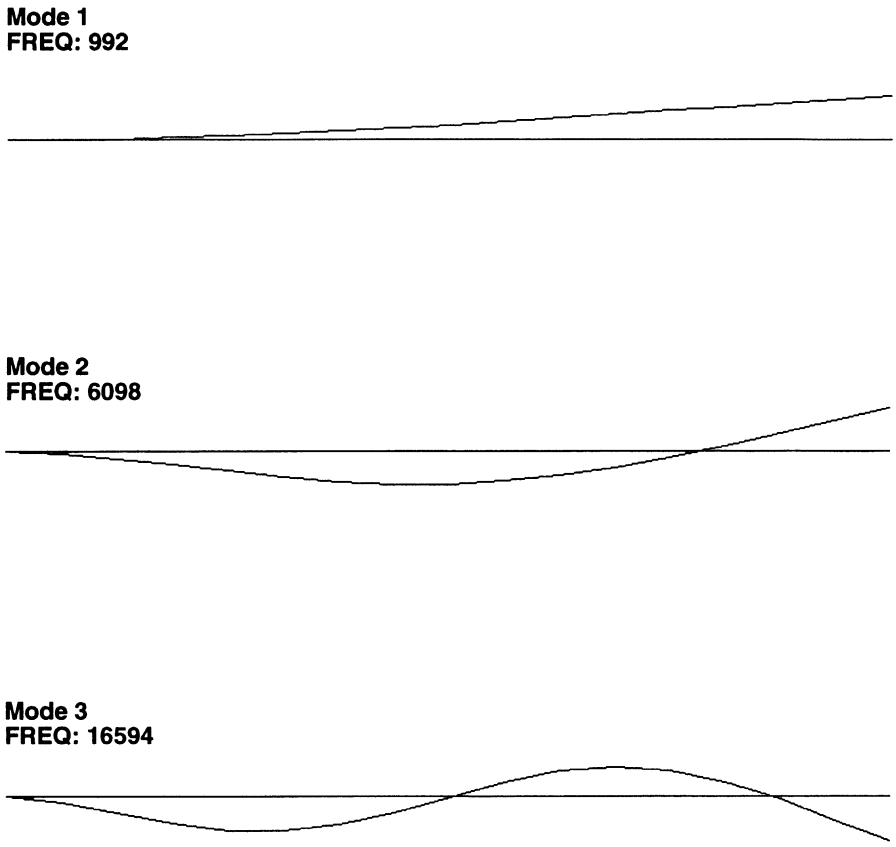

Figure E 6.2-2 Calculated Mode Shapes and Frequencies for a Timoshenko Cantilever Beam

E 6.3 Dynamic Analysis Of A Plate With The Modal Procedure

The vibration analysis of a cantilevered plate is considered here. The use of the modal analysis procedure available in the program is demonstrated. The normal modes are subsequently used for a transient analysis of the same plate subjected to a suddenly applied pressure. This analysis is repeated four times for comparison of different techniques. The plate is modeled using element type 4 and element type 8. Each finite element model is analyzed once using the power sweep method (four modes are extracted), and again utilizing the Lanczos technique (20 modes are calculated).

Element (Ref. B4.1, B8.1)

This problem illustrates the use of both element 4 and element 8, the doubly-curved quadrilateral and triangular shell elements.

Model

The mesh for the element 4 model is shown in Figure E 6.3-1. It consists of 2 elements and 6 nodes with 66 degrees of freedom. The element 8 model is given in Figure E 6.3-2 and consists of 4 elements, 6 nodes and 54 degrees of freedom.

For the element 4 model, use was made of the internal FXORD option for generation of the required 14 coordinates per node. The flat plate (type 5) option requires only the specification of two coordinates (global x and y) in this case.

The element 8 model makes use of the user subroutine UFXORD option and illustrates the ease with which various complex coordinate systems may be programmed by the user. This routine provides the 11 nodal coordinates required for element 8 at each of the nodes specified in the UFXORD option. The subroutine is written to allow for inclusion of various twist angles such as would be evident in a turbine blade for example.

Geometry

For both models the plate is assumed to have a uniform thickness of 0.1 in. and is specified as EGEOM1.

Material Properties

The following material data was assumed for both models: Young's modulus (E) is 30.0×10^6 psi, Poisson's ratio (ν) is 0.3, weight density (w) is 0.283 lb/in^3, and mass density (ρ) is 7.324×10^{-4} lb-sec^2/in^4. The use of the default value for yield stress precludes any material nonlinear effects.

Boundary Conditions

In both cases, a clamped end condition is specified for nodes 1 and 2.

Dynamics

The modal method is selected by setting IDYN as 1 in the DYNAMIC parameter; the number of modes to be extracted (4 in this case) is also specified.

For input to E6.3A and E6.3B, the four designated modes and eigenvalues are extracted with the inverse power sweep method. This is accomplished by use of the MODAL SHAPE option immediately following the END OPTION card. A tolerance of 0.00001 was specified in this option as well as a limit on the number of sweeps of 40. The program will iterate until the change in eigenvalue is below the specified tolerance or the maximum number of iterations is reached.

Twenty modes are requested in E6.3C and E6.3D; and the user requests that the Lanczos technique of eigenvalue extraction be used.

Loading

The calculated modes and corresponding eigenvectors are then used to generate the transient solution induced by a suddenly applied uniform pressure transverse to the plate. The pressure time history is shown in Figure E 6.3-3.

This loading is accomplished by use of a DYNAMIC CHANGE and DIST LOADS option. As may be seen in the input, the pressure (100 psi) is applied over a short time interval (0.00002 sec.) by the first of these options and removed by a second set with the same time interval but a reversed pressure loading. The final set of these options continues the transient analysis with the pressure held at zero for a total time of 0.001 seconds.

Control

The number of increments has been limited to six in the input decks; more complete output can be obtained by increasing the total number of increments allowed.

Output

The output provides first the increment zero results, which serve only to show the resulting initial accelerations. The output then provides four modal eigenvalues and eigenvectors as requested. This is followed by the transient analysis results.

Results

Referring to Table E 6.3-1, the frequencies obtained for the first three modes compare quite well with the results found in Zienkiewicz, O. C., T*he Finite Element Method in Engineering Science*, McGraw-Hill, 1971.

The element type 4 results show agreement in this case, although results at the higher modes do not agree with those found in Zienkiewicz for element type 8. The fifth mode calculated by MARC agrees with the fourth mode of the reference; therefore, it is presumed that the Zienkiewicz solution omitted the fourth mode.

The modes and eigenvalues are used to follow the transient solution for a suddenly applied pressure on the top face of the beam. Figure E 6.3-4 shows the variation with time of the displacement of two nodes at the end of the cantilever. A maximum of 0.145 in. was reached

during the first excursion. This displacement may be compared with the static displacement of 0.08 in. for the same beam and loading. The dominance of the first mode is indicated as the maximum displacement was reached at about half the longest period.

Table E 6.3-1 Comparison of Frequencies in Cycles/Seconds

	Element 4		Element 8		
Modes	**Inverse Power Sweep**	**Lanczos**	**Inverse Power Sweep**	**Lanczos**	**Zienkiewicz**
1	845	845	858	858	846
2	3,651	3,651	4,190	4,190	3,638
3	5,280	5,280	6,348	6,348	5,266
4	7,137	7,137	7,371	7,371	11,870
5		12,100		15,130	
6		17,830		19,370	
7		25,630		25,750	
8		26,000		29,190	
9		27,060		30,890	
10		28,150		35,200	
11		34,930		42,770	
12		49,980		64,360	
13		55,160		65,150	
14		60,540		75,480	
15		60,720		78,280	
16		74,830		81,830	
17		76,060		96,710	
18		90,760		107,000	
19		92,070		111,600	
20		97,170		119,500	

Summary of Options Used

Listed below are the options used in examples e6x3a.dat, e6x3b.dat, e6x3c.dat, and e6x3d.dat:

Parameter Options

DIST LOADS
DYNAMIC
ELMENT
END
SIZING
TITLE

Model Definition Options

CONNECTIVITY
CONTROL
COORDINATES
END OPTION
FIXED DISP
GEOMETRY
ISOTROPIC
POST

Load Incrementation Options

DIST LOADS
DYNAMIC CHANGE
CONTINUE
MODAL SHAPE

Listed below is the user subroutine found in u6x3b.f and u6x3d.f:

UFXORD

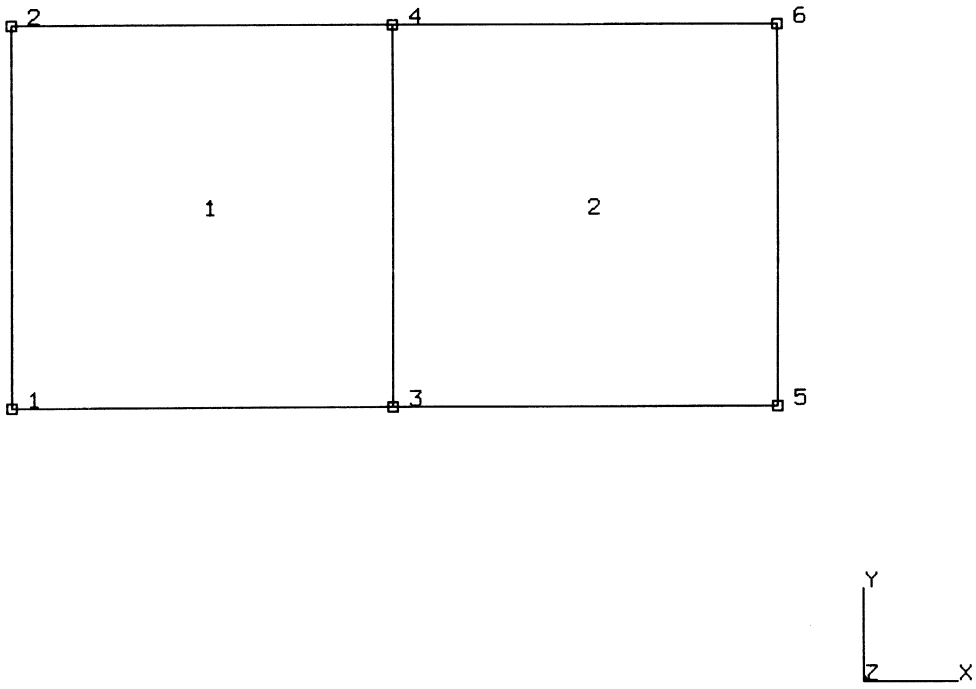

Figure E 6.3-1 Element 4 Plate Model

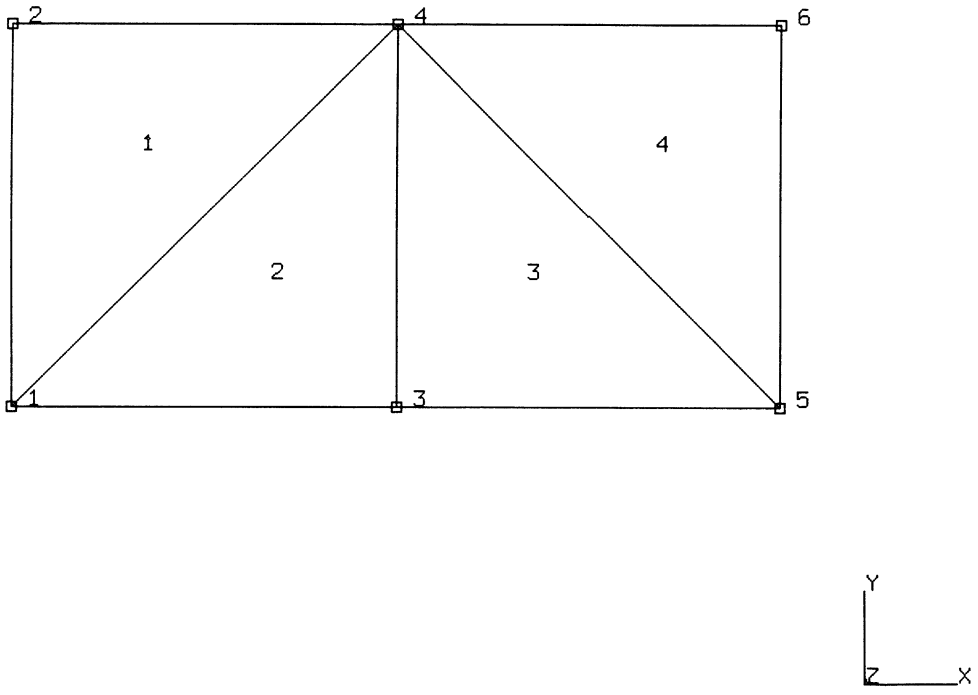

Figure E 6.3-2 Element 8 Plate Model

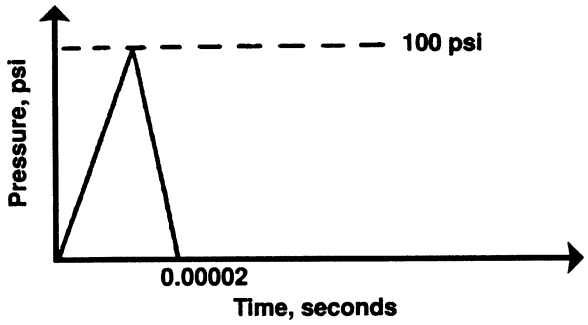

Figure E 6.3-3 Applied Pressure History

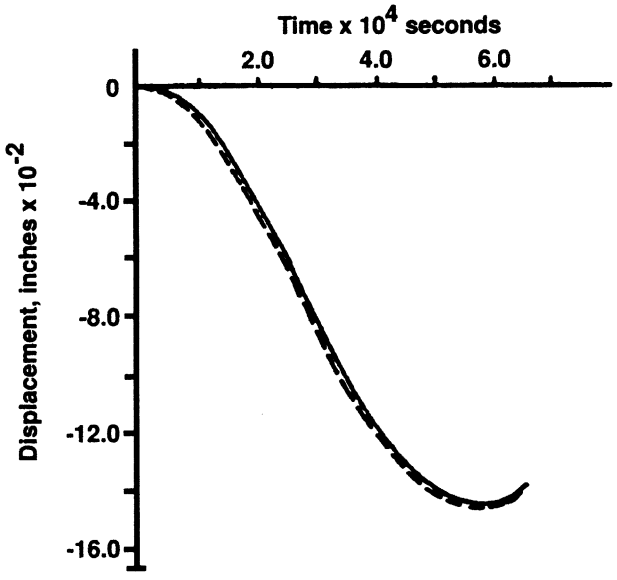

Figure E 6.3-4 Displacements at Tip

E 6.4 Frequencies Of A Rotating Disk

This problem illustrates the use of the Large Displacement and Centrifugal Loading options for the study of natural frequencies of a rotating disk.

Model

Element type 10 is used in this analysis. There are five elements and a total of 12 nodes. Disk dimensions and a finite element mesh are shown in Figure E 6.4-1.

Material Properties

The material properties of the disk are: Young's modulus is 30 x 10^6 psi, and Poisson's ratio is 0.3. Mass density is 7.338 x 10^{-4} lb-sec/in^4.

Boundary Conditions

The z-displacements are constrained at the disk faces (z = 0 and z = 0.5). The radial-displacements are constrained at the line of symmetry (r = 0).

Centrifugal Loading

The input data for centrifugal loading is supplied by using the Model Definition block, ROTATION A, the direction of the axis of rotation and a point on that axis. The actual load is then invoked in the DIST LOADS option by specifying an IBODY load type = 100 and entering the quantity square of rotation speed in radians per time (ω^2), for the magnitude of the distributed load.

In the current problem the angular speed is:

ω = 1000 rad/sec = 500/π cycles/sec

and the axis of rotation is the symmetry axis.

LARGE DISPLACEMENT Option

The load stiffness matrix is a large displacement effect; therefore, it is only formed after increment 0. To obtain the modes and frequencies including all the large displacement terms, the user inputs the centrifugal load in the DIST LOADS block in increment 0. Following increment 0, use one or two steps of zero increments of load. This will update the stiffness matrix so that the user can then invoke the MODAL SHAPE option in the next increment. The FOLLOW FOR option should also be invoked since centrifugal loading is a follower force effect.

Results

Natural frequencies of the disk with and without rotation are shown in Table E 6.4-1. The effect of centrifugal force on natural frequencies of the disk is evident. A body which is in tension will have its natural frequencies increased due to the initial stress stiffness effects; the opposite will be true for a body in compression.

Table E 6.4-1 Frequencies of the Disk (cps)

No Rotation: $\omega^2 = 0$ (Small Displacement)	$\omega^2 = 1.E8$ (Large Displacement)	% Increase
$\omega_1 = 1.593 \times 10^4$	1.620×10^4	1.6
$\omega_2 = 4.172 \times 10^4$	4.236×10^4	1.4
$\omega_3 = 6.978 \times 10^4$	7.118×10^4	1.4
$\omega_4 = 1.008 \times 10^5$	1.040×10^5	1.5

Summary of Options Used

Listed below are the options used in example e6x4.dat:

Parameter Options

DYNAMIC
ELEMENT
END
FOLLOW FORCE
LARGE DISP
SIZING
TITLE

Model Definition Options

CONNECTIVITY
CONTROL
COORDINATE
DIST LOADS
END OPTION
FIXED DISP
ISOTROPIC
ROTATION AXIS

Load Incrementation Options

CONTINUE
DIST LOADS
MODAL SHAPE

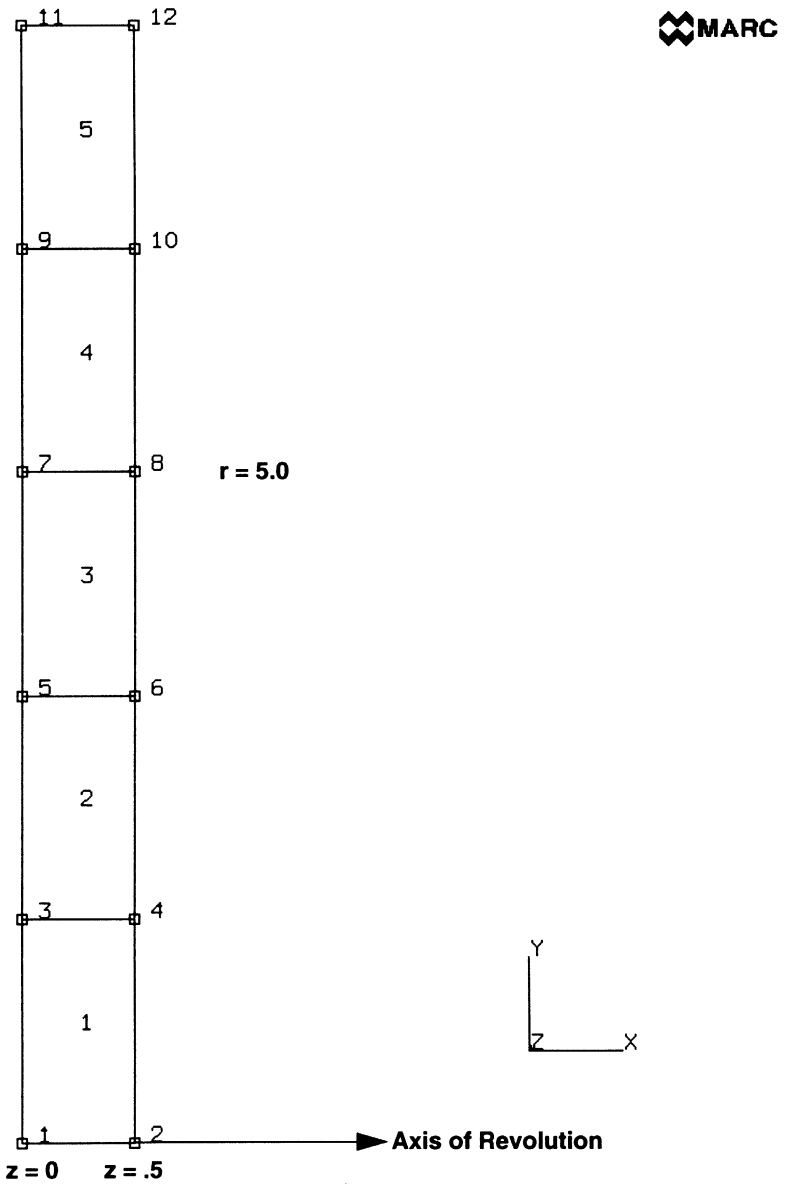

Figure E 6.4-1 Disk and Mesh

E 6.5 Frequencies Of Fluid-Solid Coupled System

Utilizing the low viscosity and incompressibility of water, a fluid-solid interaction model has been developed and included in the MARC program. This capability allows the study of natural frequencies of structures immersed in, or containing a fluid which is assumed to be inviscid and incompressible. The fluid model allows infinitesimal vibrations only, so that a pressure potential description of the fluid is assumed. The model allows for the effect of pressure waves in the fluid. It is only relevant to dynamic analysis, since the only effect of the fluid is to augment the mass matrix of the structure.

The fluid is modeled with heat transfer elements (potential theory) and the structure modeled with normal stress-displacement elements. The element choice should ensure the interface between the structural and fluid models has compatible interpolation; i.e., first order solid and fluid elements, or both second order. If necessary, the tying option may be used to achieve compatibility.

A dam vibration problem was solved using the solid/fluid interaction option. As shown in Figure E 6.5-1, the problem consists of a concrete dam section with water on one side, all on a rigid foundation. The model and input data of the problem are:

Model

Number of elements = 6 (water: four element 41's; concrete: two element 27's)
Number of nodes = 31
Dimensions of the model and a finite element mesh are shown in Figure E6.5-1.

Material Properties

For concrete elements:

$E = 288 \times 10^6$ psf
$\nu = 0$
$\rho = 4.66$ lb-sec/ft^4

For fluid (water) elements:

$\rho = 1.94$ lb-sec/ft^4

Boundary Conditions

u = 0 at nodes 1, 6, 9, 14, 17
u = v = 0 at nodes 23, 26, 31

Fluid-Solid Interaction

The inputs for this option are:

On the parameter cards the FLU LOAD and the number of solid/fluid interface element surfaces (2) must be entered.

Using the Model Definition FLUID SOLID option and the element number and element face number for solid and fluid elements must be entered. The element numbers and face numbers are, respectively:

Solid Element Number	Solid Element Face Number	Fluid Element Number	Fluid Element Face Number
5	1	3	10
6	1	4	10

Geometry

The thickness of the dam/water system is 1.0 ft.

Modal Shape

Default control values are used for the eigenvalue extraction.

Results

Frequencies of the dam/water system are given in Table E 6.5-1. As anticipated, the inclusion of the water increases the effective mass and reduces the natural frequency of the dam.

Table E 6.5-1 Natural Frequencies of Dam/Water System (f = cps)

Mode	Dam Without Water	Dam With Water
1	4.74	2.46
2	13.6	9.09

Summary of Options Used

Listed below are the options used in example e6x5.dat:

Parameter Options

DYNAMIC
ELEMENT
END
FLU LOAD
SIZING
TITLE

Model Definition Options

CONNECTIVITY
COORDINATE
END OPTION
FIXED DISP
FLUID SOLID
GEOMETRY

ISOTROPIC
POST
UDUMP

Load Incrementation Options

CONTINUE
MODAL SHAPE
RECOVER

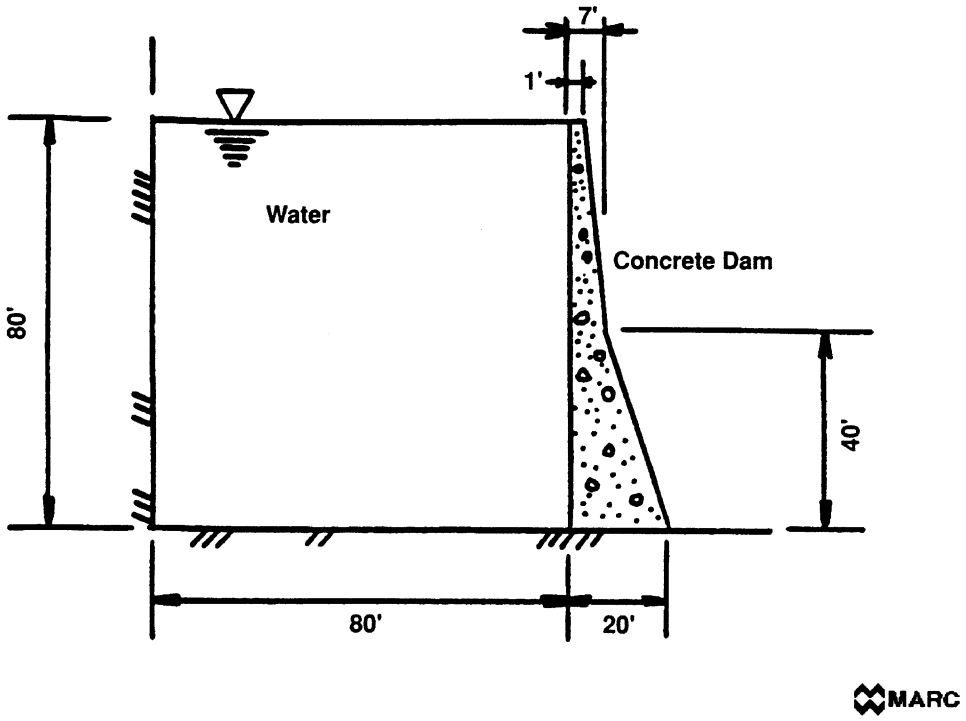

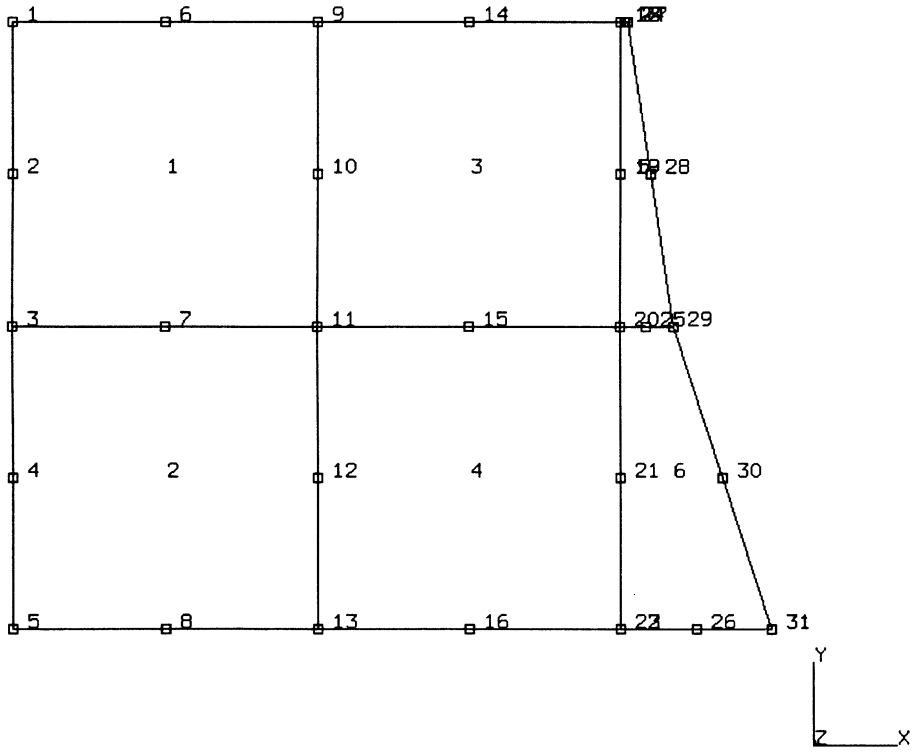

Figure E 6.5-1 Dam/Water System and Mesh

E 6.6 Spectrum Response Of A Space Frame

This problem illustrates the spectrum response capabilities of the program to determine the behavior of a three-dimensional frame. In addition, the influence of a compressive load on the eigenvalues of the system will be demonstrated. This in turn affects the spectrum response analysis.

Model

The model is identical to that used in problem E 2.24, consisting of 20 truss elements (type 9) and 9 nodes. The dimensions of the frame structure and a finite element model are shown in Figure E 6.6-1.

Material Properties

The Young's modulus is 10×10^6 psi. The mass density is 0.1 lb-sec^2/in^4.

Geometry

The primary members (elements 1-12) have a cross-sectional area of 1 sq.in. The secondary members (elements 13-20) have a cross-sectional area of 0.25 sq.in.

Loads

A concentrated load at the apex (node 1) of 200,000 lb. is applied in the negative z-direction. This load is used to apply a compressive stress in the frame, as would be produced by guy wires.

Boundary Conditions

The base (nodes 3, 5, 7, and 9) is assumed to be fixed in space.

Displacement Spectral Density

A typical displacement spectral density function is entered. This could have optionally been specified through user subroutine USSD. The frequency is given in cycles per time unit (second). This function is shown in Figure E 6.6-2.

Eigenvalue Response

This problem was run twice to observe the eigenvalue with and without the influence of the applied load. In the first case, the MODAL shape was placed immediately after the END OPTION; the stiffness matrix used includes only the elastic stiffness. In the second case, the MODAL shape was placed following a zero load step; the stiffness matrix also includes the initial stress stiffness contribution. In both problems, ten modes were extracted using the inverse power sweep method. The program performs a shift after the fifth mode. Table E 6.6-1 gives the eigenvalues for the two cases. The "double modes" are clearly due to the symmetry with respect to the x,y axes.

As anticipated, the inclusion of the initial compressive stress resulted in a reduction in the magnitude of the eigenvalues. The mode shapes for the first, second, and third modes are shown in Figure E 6.6-3 through Figure E 6.6-5. It is important to ensure the body is in equilibrium before extracting mode if the initial stress stiffness is included.

Spectrum Response

After the eigenmodes were extracted, a spectrum response calculation was performed. This response was calculated using only the lowest eight modes. This was done in an arbitrary manner. It is also possible to give a range of frequencies for which the response is based. The program computes the root mean square of the displacement (RMS), velocity, and acceleration. Table E 6.6-2 gives the response at node 2 of the structure.

Table E 6.6-1 Eigenvalues (cps)

	No Initial Stress	With Initial Stress
1	13.205*	12.520*
2	14.999	13.442
3	16.386	14.944
4	13.204*	18.867*
5	25.172*	12.520*
6	25.172*	18.745*
7	60.196	59.840
8	121.12*	120.29*
9	123.11	122.42
10	121.11*	120.29*

*Indicate "double mode" pairs (closely-spaced modes).

Table E 6.6-2 Spectrum Response at Node 2

	No Initial Stress	With Initial Stress
RMS – Displacement	0.405 in	0.47 in
RMS – Velocity	33.600 in/sec	37.00 in/sec
RMS – Acceleration	2793.000 in/sec^2	2923.00 n/sec^2

Summary of Options Used

Listed below are the options used in example e6x6a.dat:

Parameter Options

DYNAMIC
ELEMENT
END
LARGE DISP
MESH PLOT
RESPONSE SPECTRUM
SIZING
TITLE

Model Definition Options

CONNECTIVITY
COORDINATE
END OPTION
FIXED DISP
GEOMETRY
ISOTROPIC
POINT LOAD
RESPONSE SPECTRUM
RESTART

Load Incrementation Options

CONTINUE
MODAL SHAPE
PROPORTIONAL INCREME
SPECTRUM

Listed below are the options used in example e6x6b.dat:

Parameter Options

DYNAMIC
ELEMENT
END
MESH PLOT
RESPONSE SPECTRUM
SIZING
TITLE

Model Definition Options

CONNECTIVITY
COORDINATE
END OPTION
FIXED DISP
GEOMETRY
ISOTROPIC
POINT LOAD
RESPONSE SPECTRUM
RESTART

Load Incrementation Options

CONTINUE
MODAL SHAPE
SPECTRUM

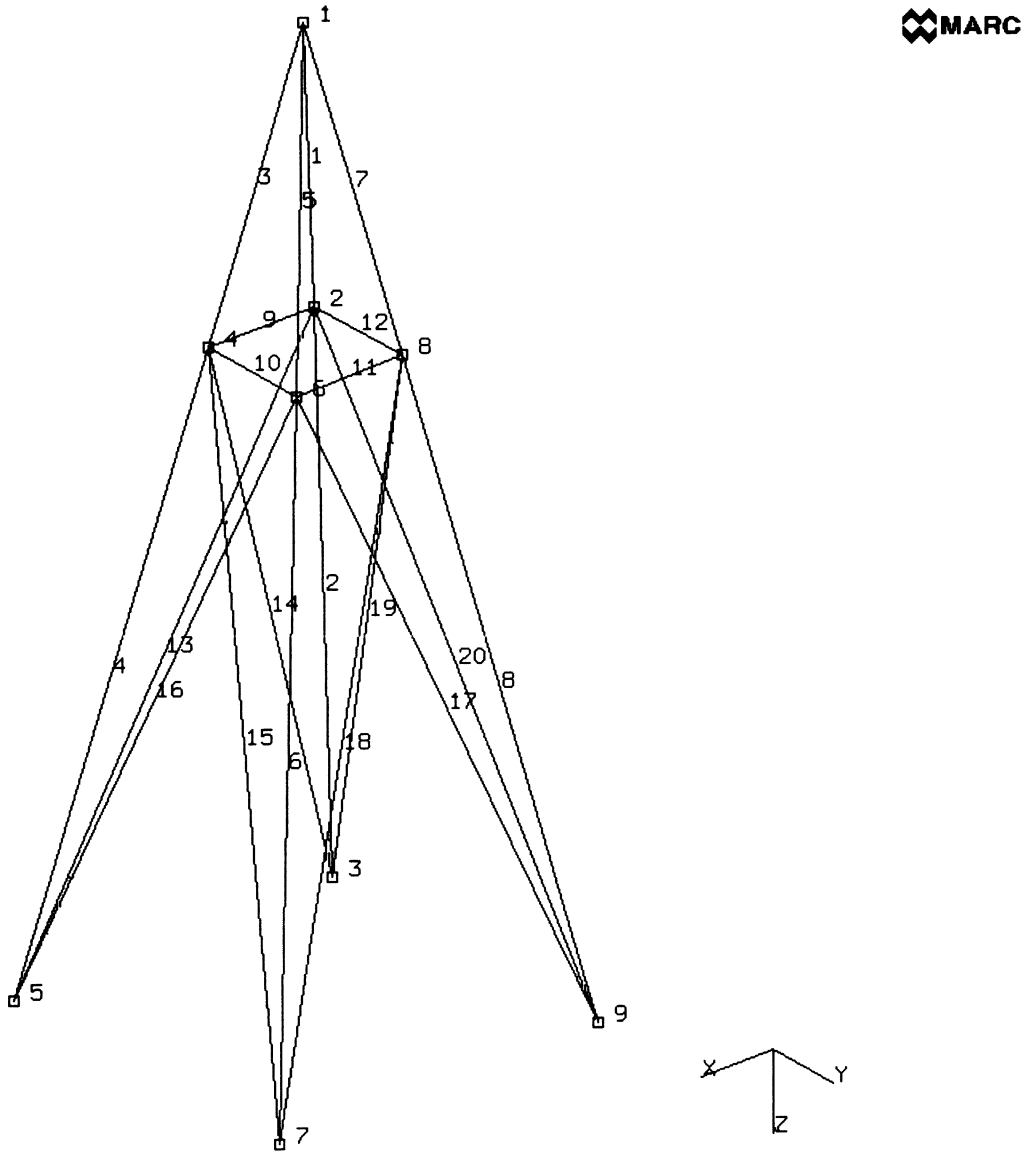

Figure E 6.6-1 Three-Dimensional Frame and Model

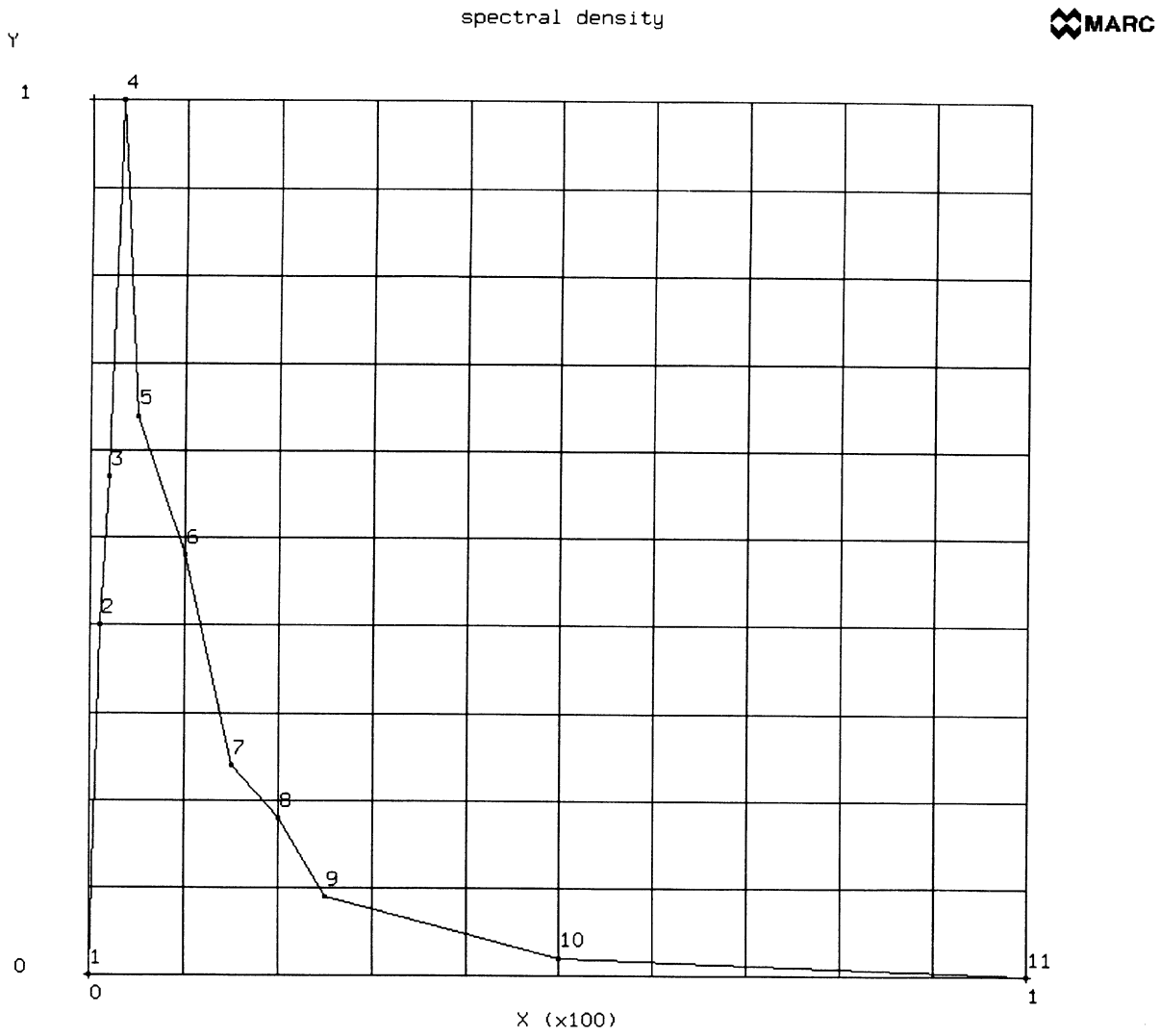

Figure E 6.6-2 Spectral Density Function

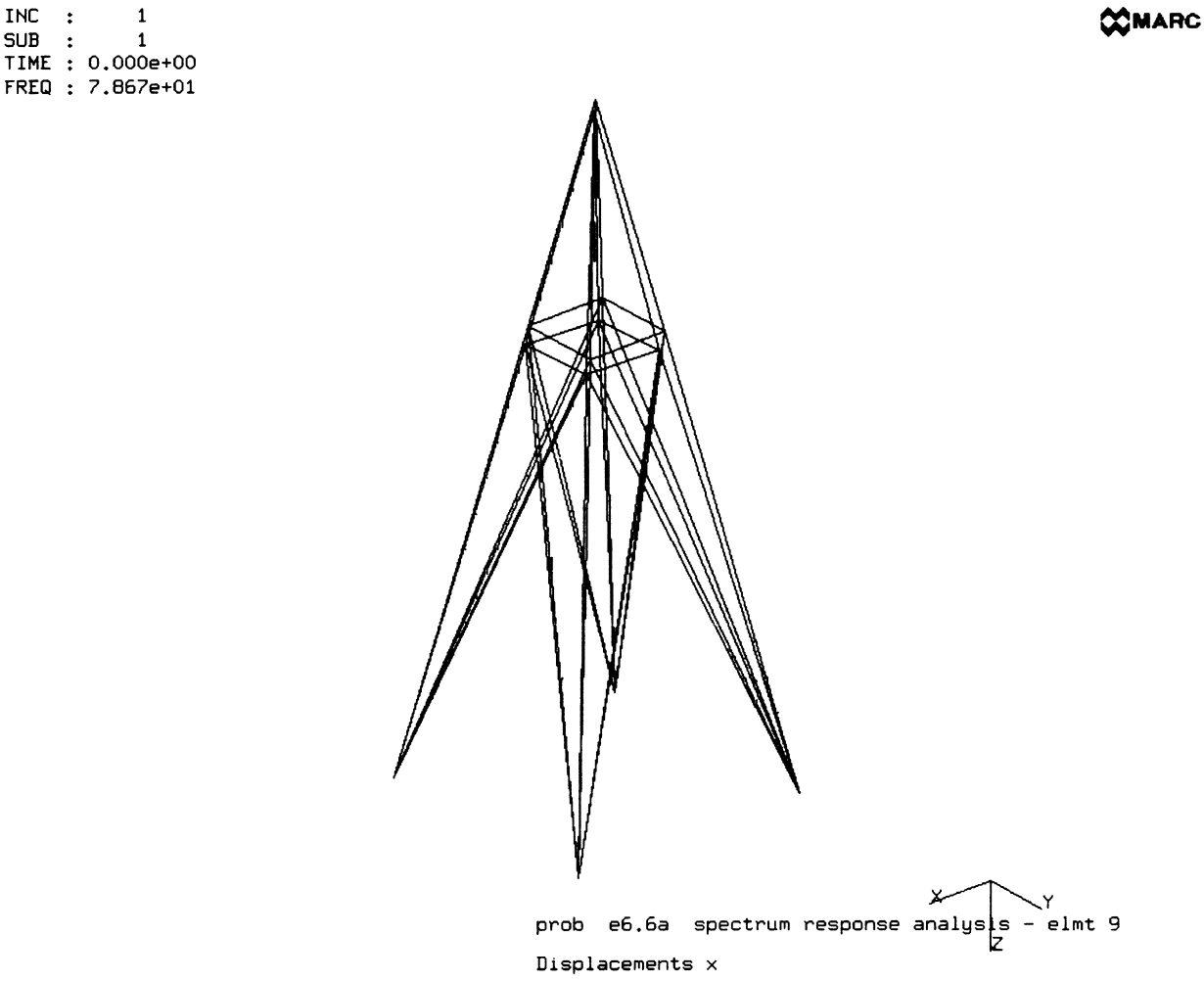

Figure E 6.6-3 Three-Dimensional Frame – Mode 1 (Extensional)

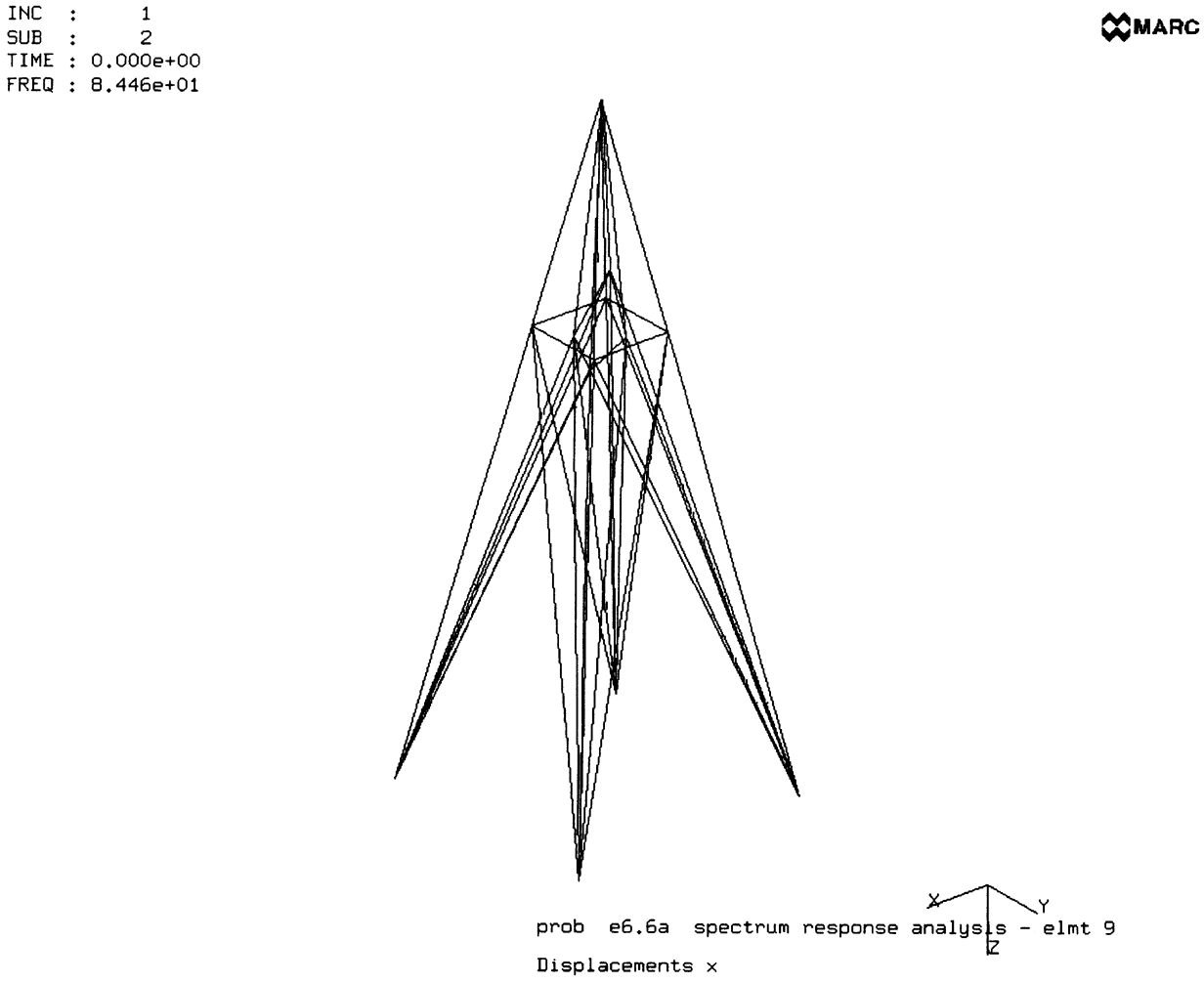

Figure E 6.6-4 Three-Dimensional Frame – Mode 2 (Bending)

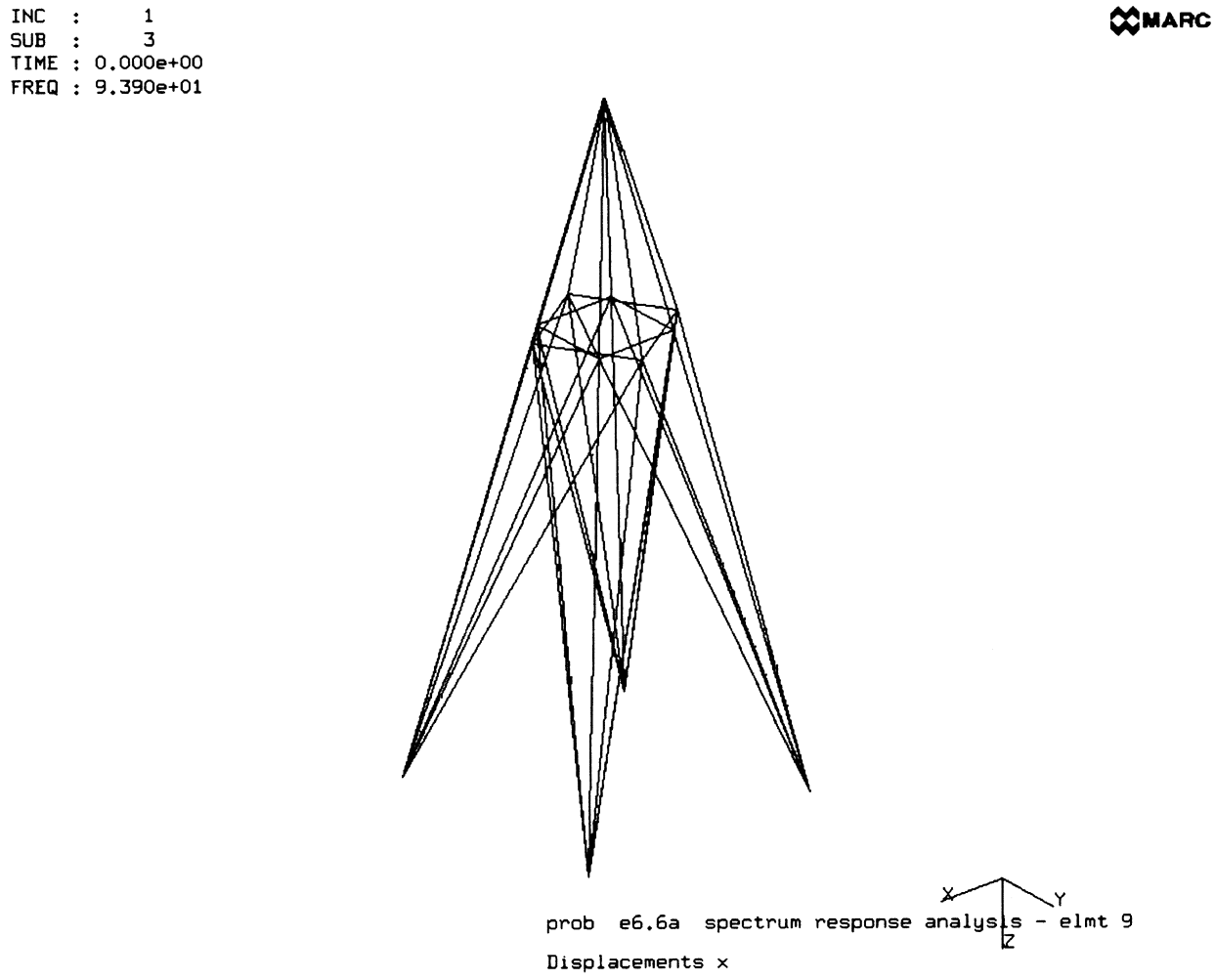

Figure E 6.6-5 Three-Dimensional Frame – Mode 3 (Torsional)

Optimize

The Cuthill-McKee bandwidth optimization algorithm is requested. This reduces the half-bandwidth for this problem to 27 from 68 in 19 iterations resulting in improved efficiency.

Restart

The RESTART option is included such that the analysis may be continued at some later time. This may be used to perform either additional quasi-static deformation, perform a harmonic response calculation at an additional frequency, or for postprocessing.

Harmonic

The HARMONIC History Definition option defines an excitation frequency of 0.05 cycles/sec for the first analysis, and 0.5 cycles/sec during the second.

Tying

In this option, the cap/rubber interface is defined by tying the first two degrees of freedom of nodes representing the rubber material to corresponding metal cap model nodes. The third degree of freedom of corner nodes in this first layer of elements (4, 8, 12, 16) are tied. Here, the reduction of Herrmann variables in the intefacing elements improves the solution quality.

Proportional Increment

A proportional increment of 0.0. enforces equilibrium after the initial deformation. This was necessary because the total displacement was applied in the zeroth increment, where linear behavior is assumed. Thus, the subsequent harmonic analysis is performed on an equilibrated configuration of the mount model.

Results

The displacement after the initial displacement is shown in Figure E 6.7-2. The von Mises stresses for this configuration are plotted in Figure E 6.7-3. The real and imaginary stress components are plotted for excitation frequencies 0.05 cycles/sec and 0.5 cycles/sec in Figure E 6.7-4 through Figure E 6.7-7.

Summary of Options Used

Listed below are the options used in example e6x7.dat:

Parameter Options

END
HARMONICS
LARGE DISP
SIZING
TITLE

Model Definition Options

CONNECTIVITY
CONTROL
COORDINATE
END OPTION

FIXED DISP
ISOTROPIC
MOONEY
PRINT CHOICE
TYING

Load Incrementation Options

CONTINUE
DISP CHANGE
HARMONIC
PROPORTIONAL INCREMENT

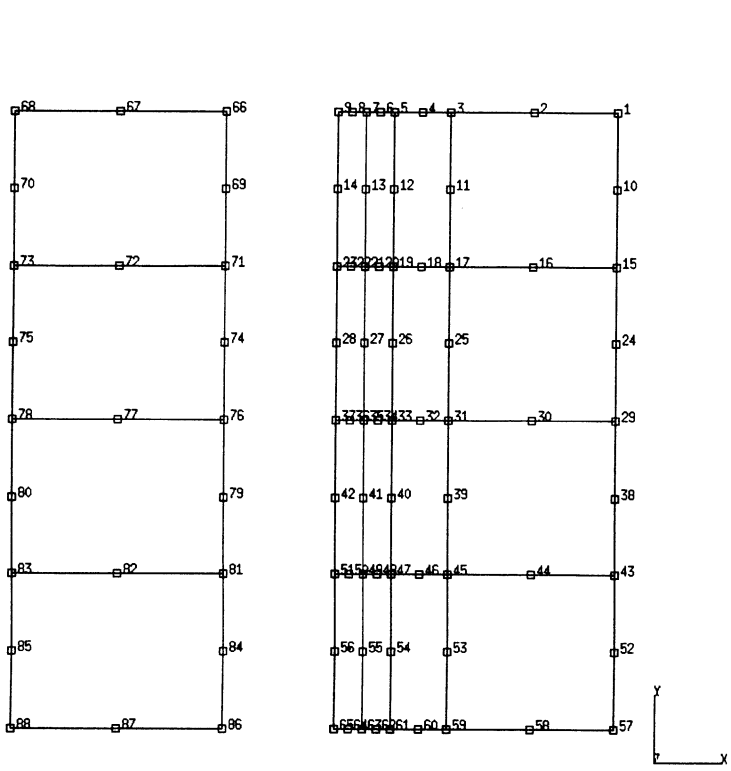

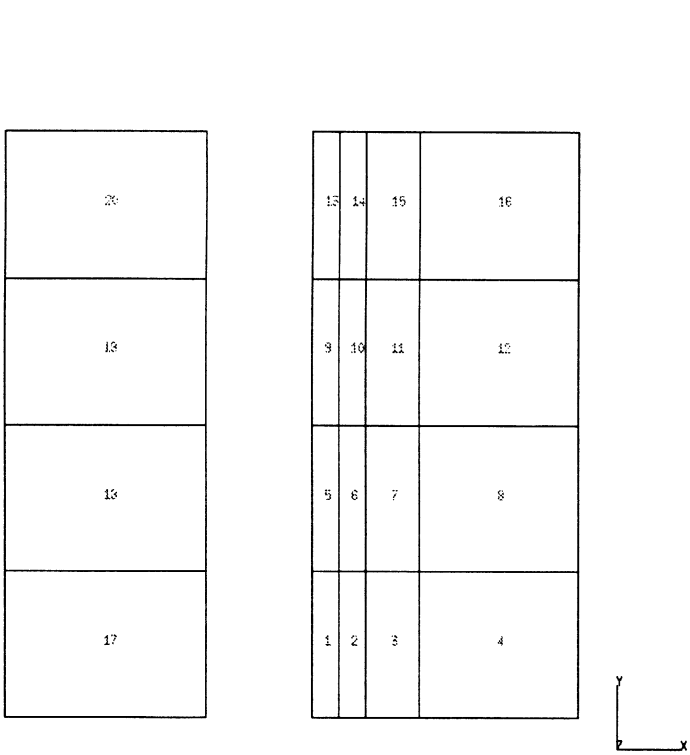

Figure E 6.7-1 Capped Rubber Mount

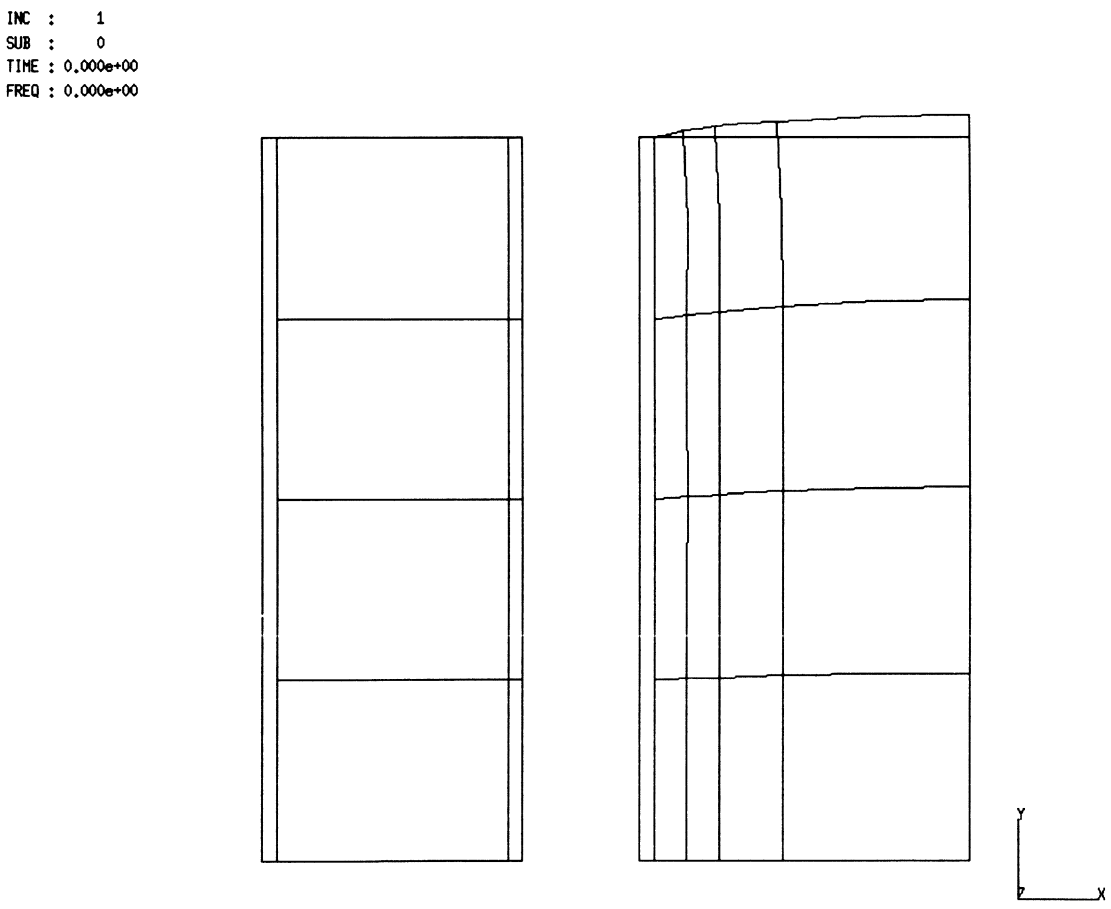

Figure E 6.7-2 Displaced Mesh, Increment 1

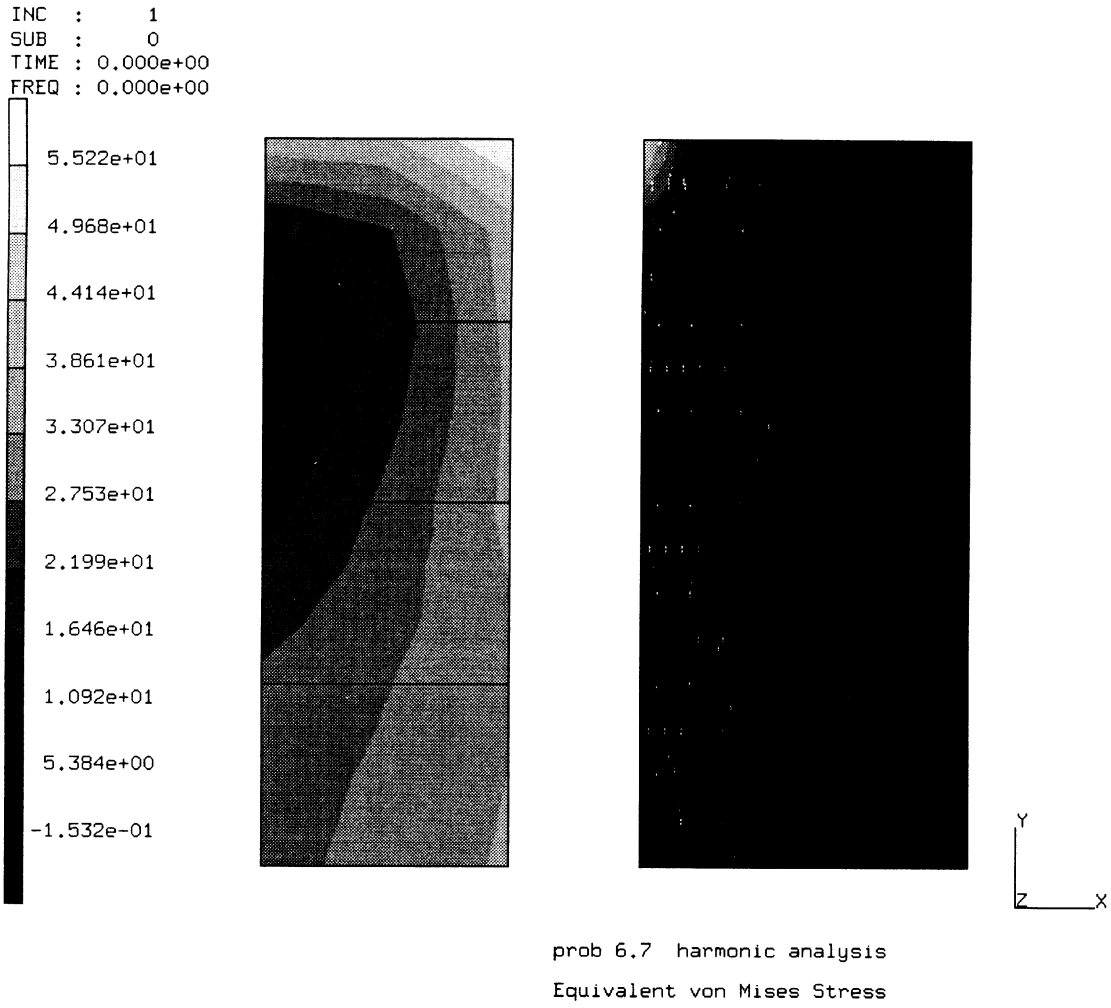

Figure E 6.7-3 von Mises Stress Distribution, Increment 1

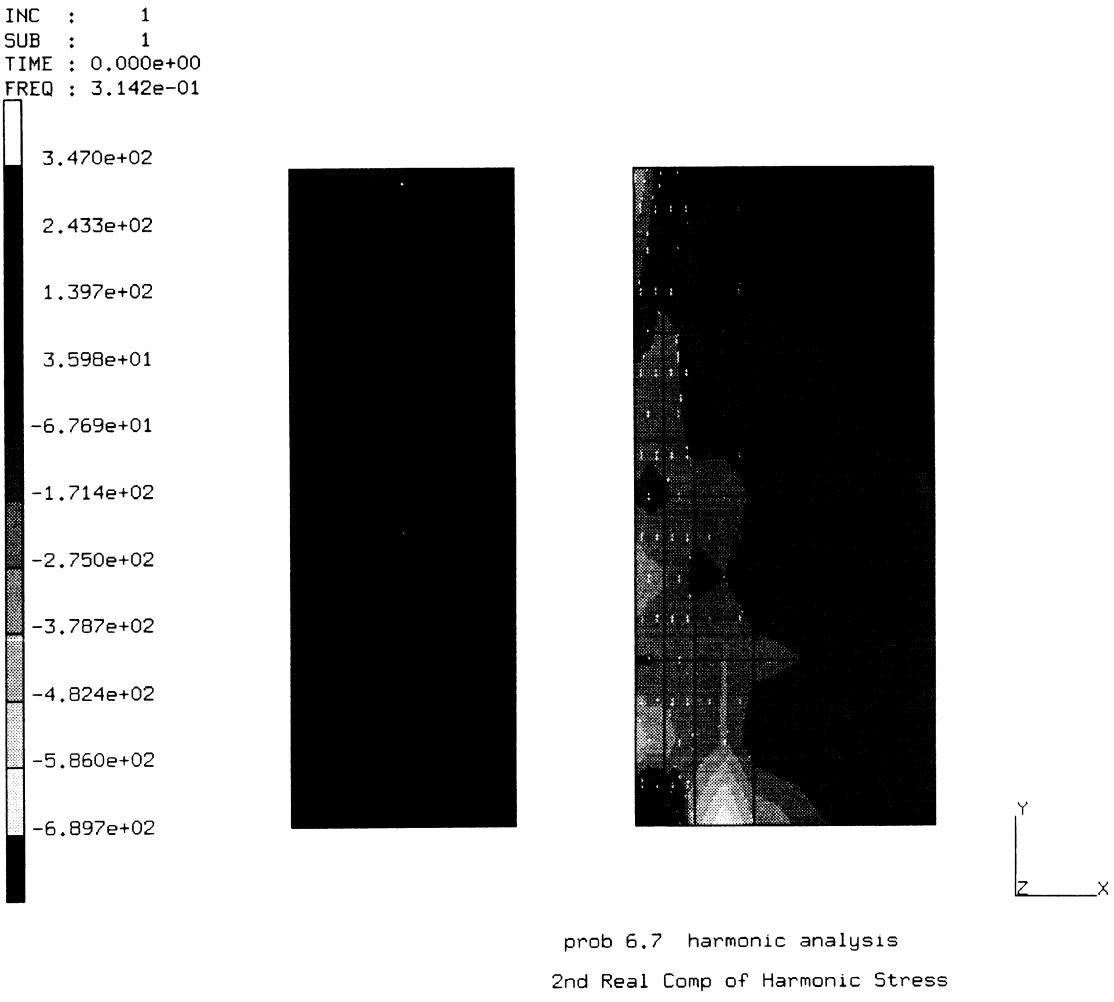

Figure E 6.7-4 Real Radial Stress 0.05 Cycle/Sec.

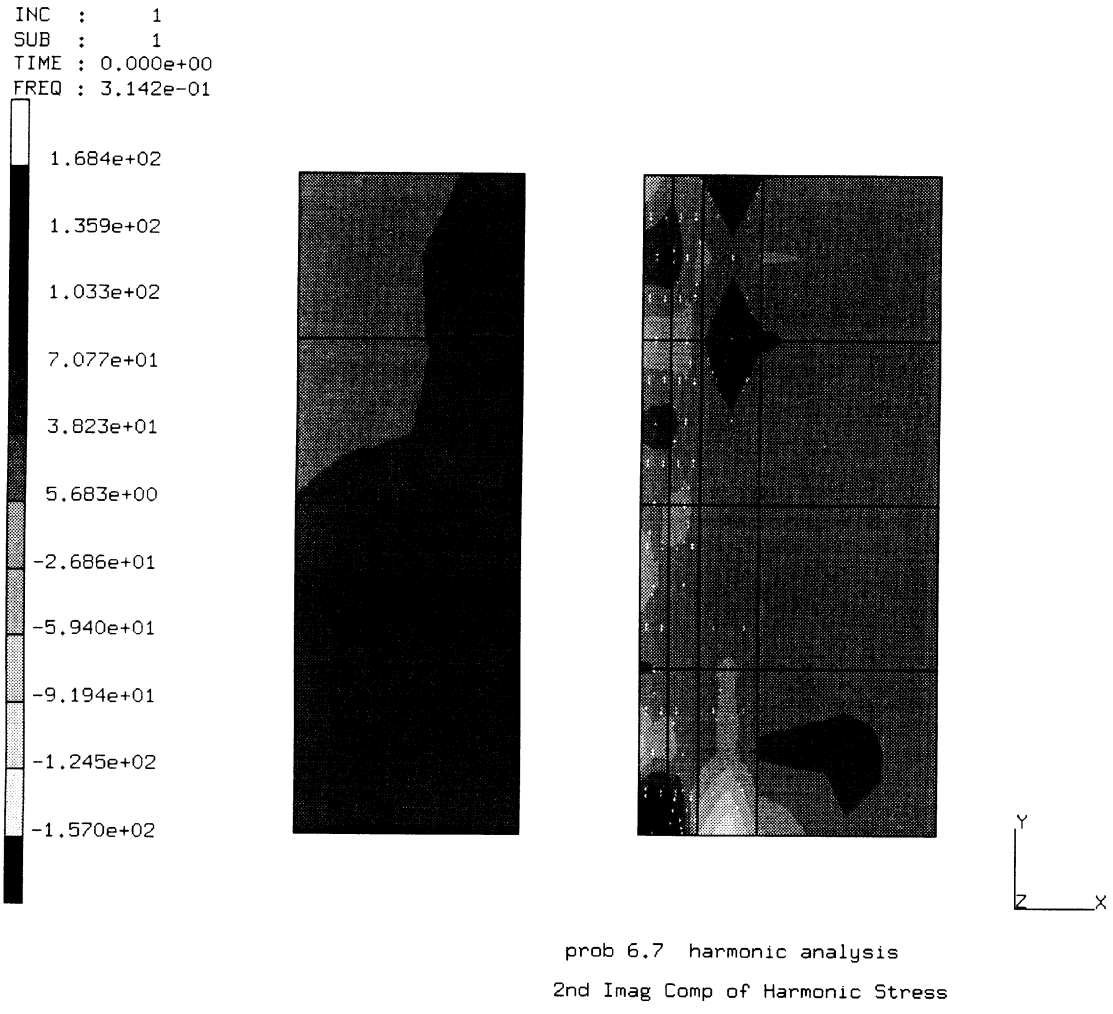

Figure E 6.7-5 Imaginary Radial Stress 0.05 Cycle/Sec.

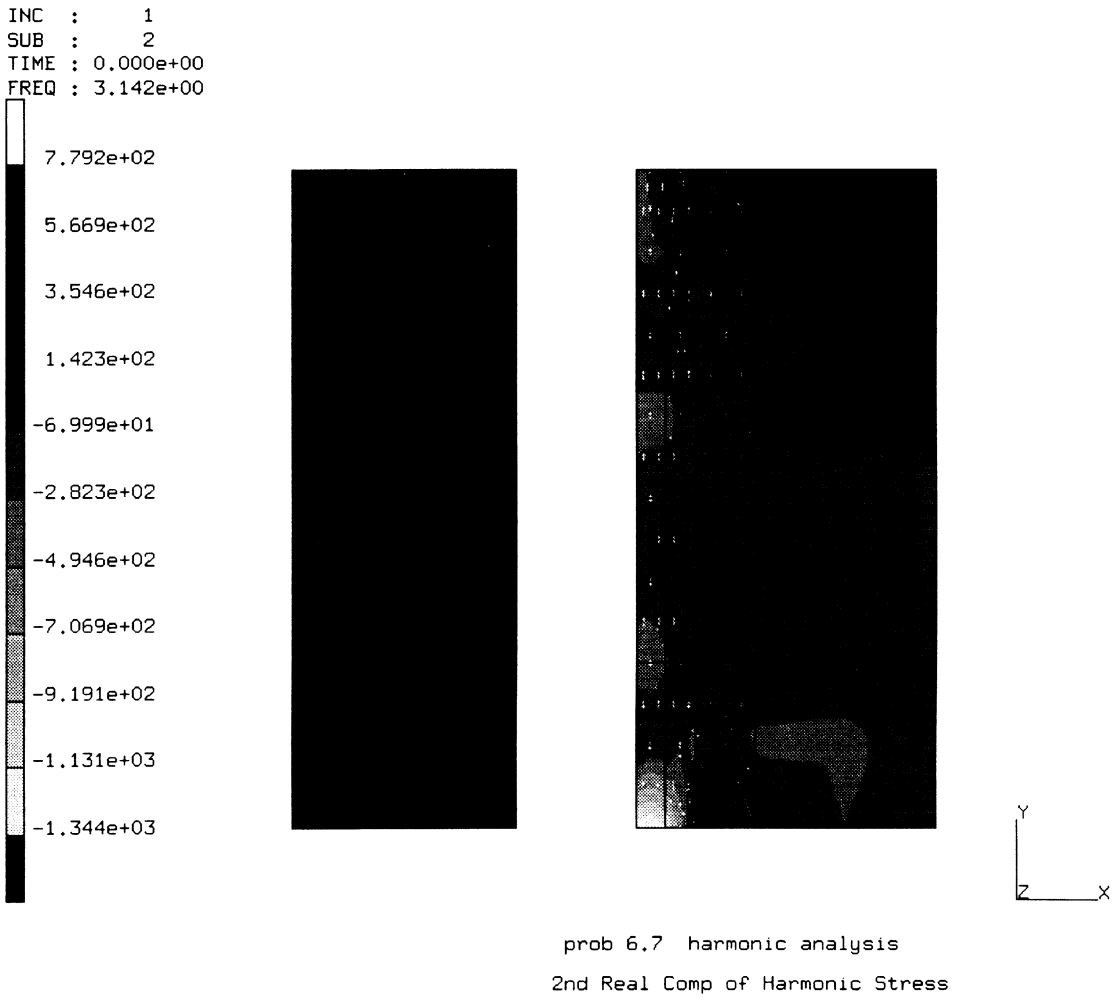

Figure E 6.7-6 Real Radial Stress 0.5 Cycle/Sec.

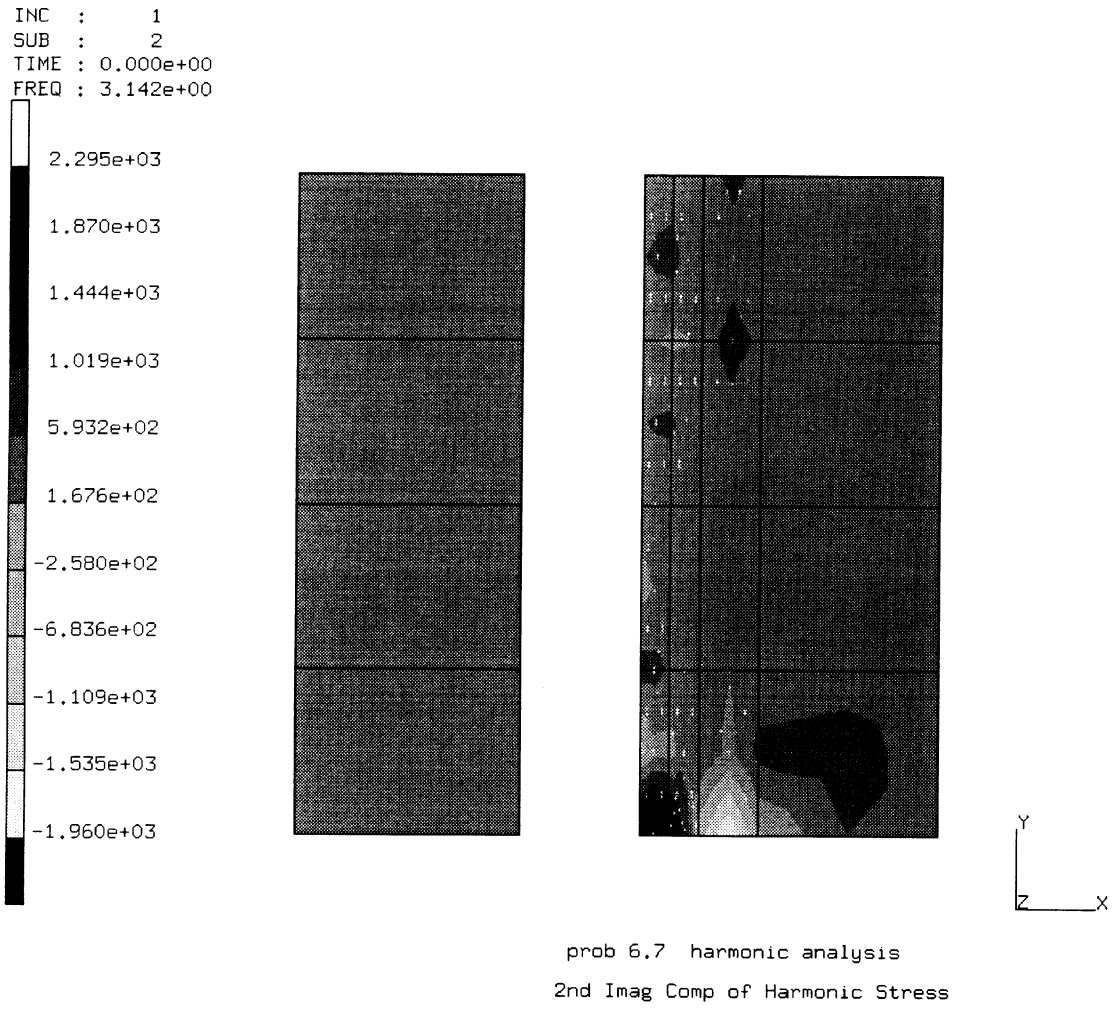

Figure E 6.7-7 Imaginary Radial Stress 0.5 Cycle/Sec.

E 6.8 Harmonic Response Of A Rubber Block

Using the HARMONIC option, the response of a solid block of elastometric material is calculated. The block is stretched in a quasi-static manner. The harmonic response of the block at three distinct frequencies are evaluated for three stretch ratios.

Element

Element type 35 is used to model the block.This is a 20-node isoparametric brick element using the Herrmann formulation for Mooney or Ogden material models.

Model

The finite element model of the block is shown in Figure E 6.8-1. Only one element is used to model the block. Applying symmetry boundary conditions allows this single element to represent the whole block. The block dimensions are 50.8 x 9.754 x 9.754 inches.

Geometry

No geometry is specified.

Mooney

The material constants for the third order invariant form C_{10}, C_{01}, C_{11}, C_{20}, and C_{30} are specified as 36.012, 6.061, 1.443, -1.504, and 1.690 psi, respectively. The mass density is given as 9.53 x 10^{-5} lbm/in^3.

Boundary Conditions

The base of the block is constrained axially. The x = 0 and y = 0 faces have symmetry conditions applied. Initially, the block is stretched 2.54 in. or 10% of the block height. Subsequently, the DISP CHANGE option increases the stretch to 4.791 inches, and then to 7.086 inches.

The DISP CHANGE option with a flag 1 in the second field of card 2 is used to specify the harmonic excitation magnitude of 1 in.

PHI-COEFF

The relaxation function coefficients are specified as a function of frequency in this option.

Harmonic

Excitation frequencies of 0.1, 1.0 and 5.0 cycles/seconds are specified for each deformed configuration.

Results

A summary of the harmonic displacements at node 19 for three stretch ratios are given in Table E 6.8-1.

Table E 6.8-1 Summary of Results: Real and Imaginary Displacements of Node 19

Frequency (cycles/sec)		Stretch Ratios		
		1.2	1.338	1.558
0.1	U_R	.4966	.4773	.4872
0.1	U_I	.00028	.00040	.00339
1.0	U_R	.4966	.4764	.4792
1.0	U_I	.00022	.00025	.00145
5.0	U_R	.4949	.4721	.4876
5.0	U_I	.00015	.00012	.0004

Summary of Options Used

Listed below are the options used in example e6x8.dat:

Parameter Options

END
HARMONICS
LARGE DISP
SIZING
TITLE

Model Definition Options

CONNECTIVITY
CONTROL
COORDINATE
END OPTION
FIXED DISP
MOONEY
PRINT CHOICE
RESTART

Load Incrementation Options

CONTINUE
DISP CHANGE
HARMONIC
PROPORTIONAL INCREMENT

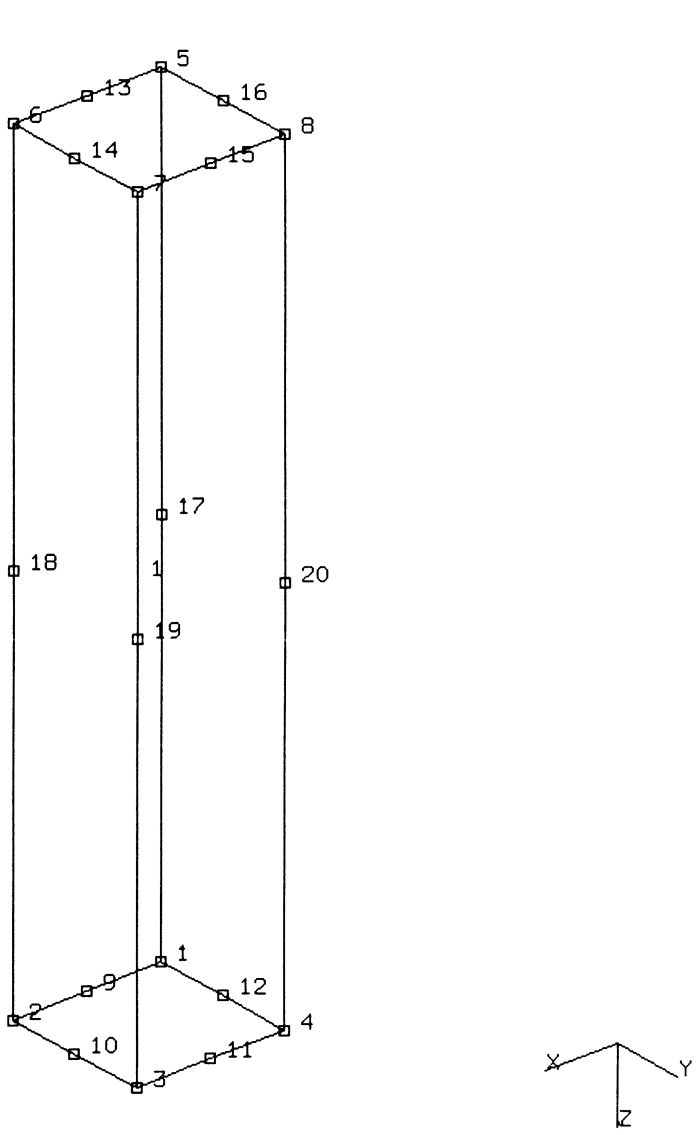

Figure E 6.8-1 Tensile Harmonic Analysis Mesh

E 6.9 Elastic Impact Of A Bar

The dynamic impact of a bar hitting against a rigid wall has been computed using the Newmark-beta direct integration algorithm. The contact has been represented by a gap element. The material is assumed to remain elastic.

Element

Element type 9, a simple linear straight truss with constant cross-section, has been used to represent the bar. It has three coordinates per node in the global x, y, z directions and uniaxial stress and strain. A gap element type 12 has been used to impose the contact condition.

Model

A simple model is assumed to represent the problem of a bar hitting against a wall. The mesh consists of 15 elements of type 9 and 1 gap element – a total of 19 nodes. The mesh is more refined where the contact will occur.

Geometry

The bar is shown in Figure E 6.9-1. It is 100 mm long and has a uniform cross-section of 314.15 mm^2.

Material Properties

The material properties of the bar are:

Young's modulus is E = 1.96E+5 N/mm^2,
Poisson's ratio is $\nu = 3$,
mass density is ρ = 7.85E-6Kg/mm^3, and
yield point is $\sigma_y = 235.2\ N/mm^2$.

Boundary Conditions

Only the axial displacements are free. The end node of the gap element associated with the wall has every degree of freedom constrained.

Dynamics

The body has an initial velocity of 50 m/sec.

The case has been studied for 200 seconds using 200 time-steps of 1 sec in the DYNAMIC CHANGE option.

Results

The displacement of the last node is shown in Figure E 6.9-2. The velocity is shown in Figure E 6.9-3. The elastic wave is moving with a velocity:

$$c = \left[\frac{E}{\rho}\right]^{1/2} = 5 \times 10^3 \text{m/sec.}$$

The bar rebounds after a time:

$$t = \frac{21}{c} = 40 \times 10^{-6} \text{sec.}$$

In Figure E 6.9-4, the reaction in the gap is equal to zero in the 4th increment, implying that separation has occurred.

Summary of Options Used

Listed below are the options used in example e6x9.dat:

Parameter Options

DAMPING
DYNAMIC
END
LUMP
SIZING
TITLE

Model Definition Options

CONNECTIVITY
CONTROL
COORDINATE
DAMPING
END OPTION
FIXED DISP
GAP DATA
GEOMETRY
INITIAL VELOCITY
ISOTROPIC
MASSES
POST
PRINT CHOICE

Load Incrementation Options

CONTINUE
DYNAMIC CHANGE

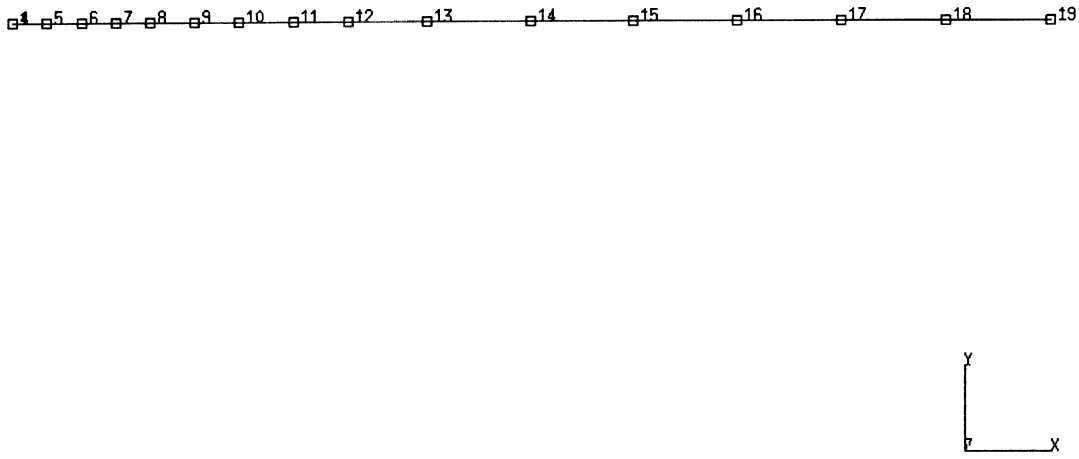

Figure E 6.9-1 Mesh of the Bar

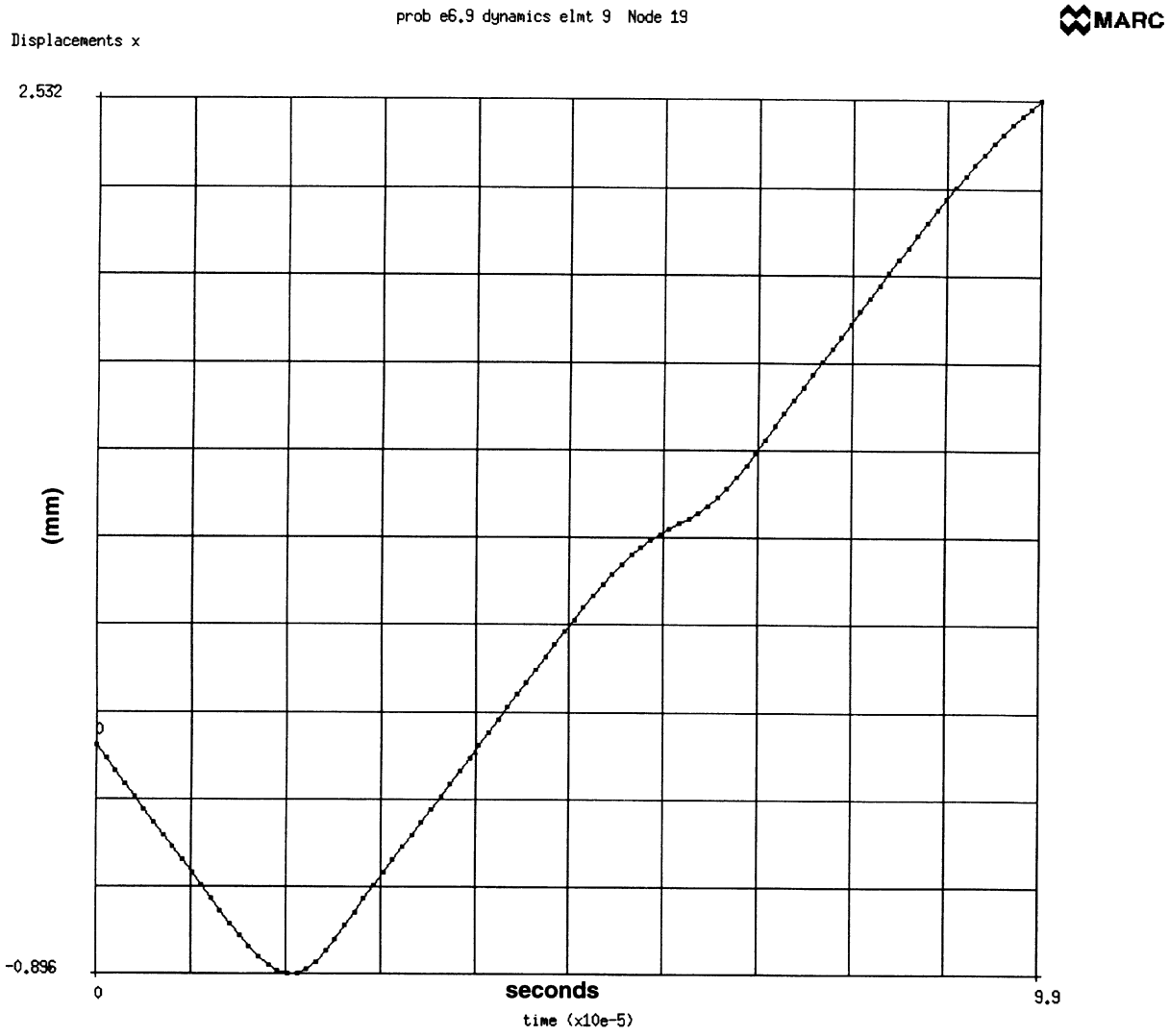

Figure E 6.9-2 Time History of Displacements

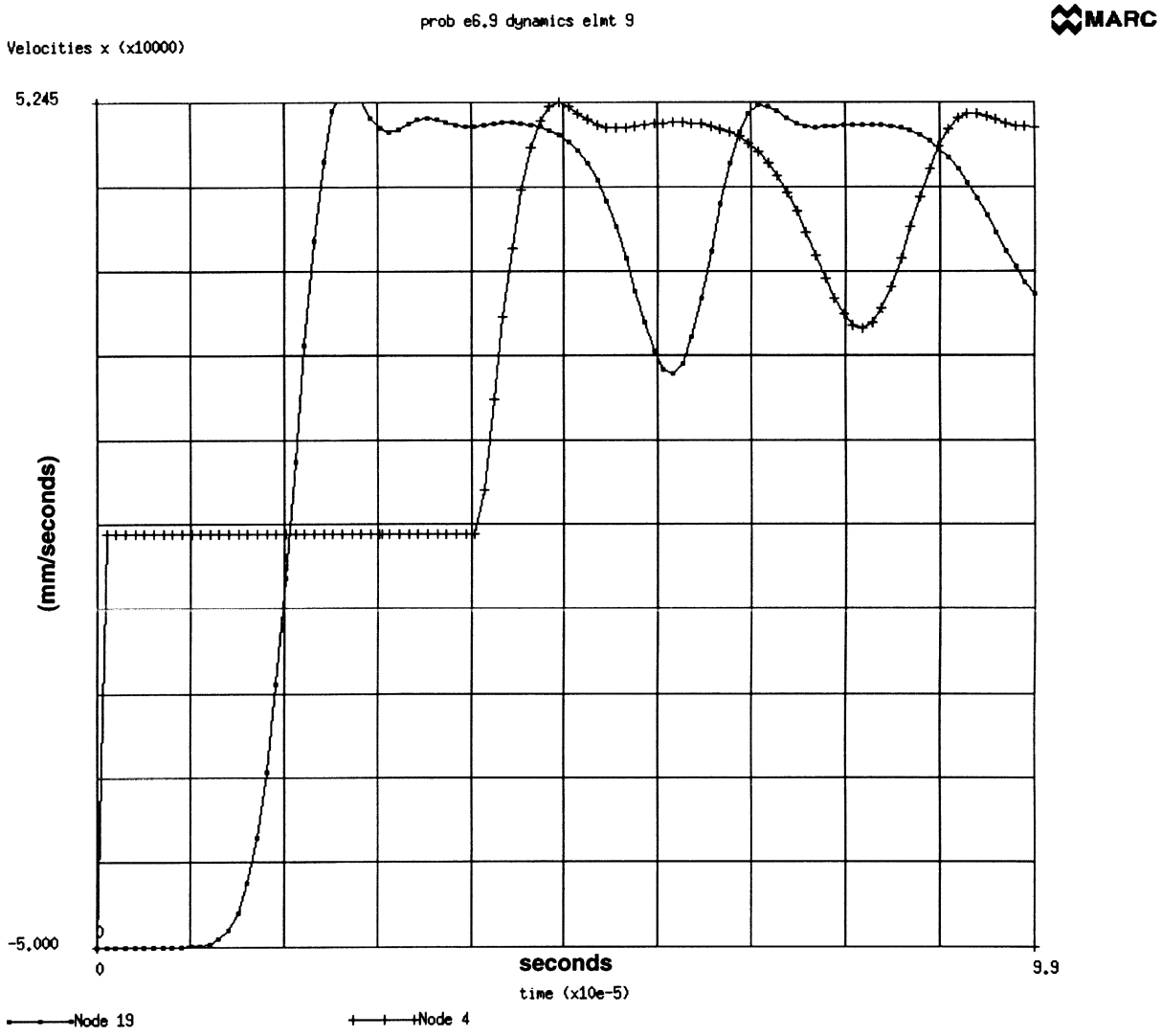

Figure E 6.9-3 Time History of Velocity

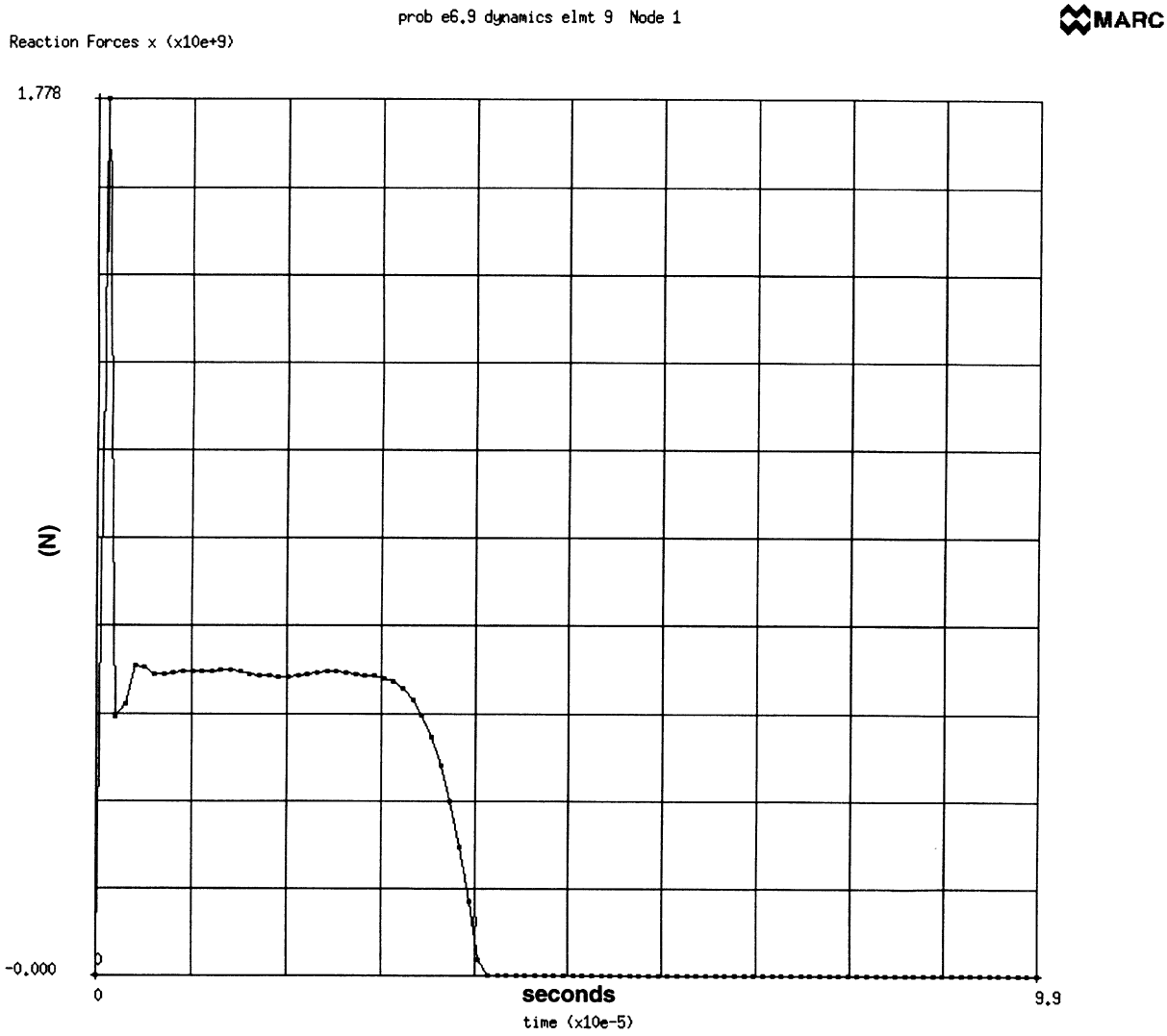

Figure E 6.9-4 Time History of the Reaction

E 6.10 Frequencies Of An Alternator Mount

The first six modal frequencies are computed for a spatial frame representing the support of an alternator. Two masses are lumped in the middle of two horizontal beams, at nodes 14 and 18 (Figure E 6.10-1). The use of Load Incrementation option RECOVER for modal stress calculations is also demonstrated in this problem.

Element

Element 52, a straight Euler-Bernoulli beam in space with linear elastic response, has been used. It has six coordinates per node: the first three are (x,y,z) global coordinates of the system, the other three are the global coordinates of a point in space which locates the local x-axis of the cross section.

Model

The spatial frame has been modeled using 16 elements and 20 nodes. The columns are clamped at the base.

Geometry

The columns are 250 cm. high; the beams in the x-direction are 192.5 cm. long and 157.5 cm in the z-direction. The geometric properties of the sections are given in Table E 3.10-1.

The torsional stiffness for the rectangular section is as follows:

$$K_t = \frac{E}{2(1+\nu)} I_t$$

$$I_t = hb^3\left[\frac{1}{3} - \frac{3.35}{16}\frac{b}{h}\left(1 - \frac{b^4}{12h^4}\right)\right]$$

Element 52 computes the torsional stiffness of the section as:

$$K_t = \frac{E}{2(1+\nu)} (I_{xx} + I_{yy})$$

Then, in order to use the correct stiffness, an artificial Poisson's ratio ν^* is chosen so that:

$$\frac{E}{2(1+\nu)} I_t = \frac{E}{2(1+\nu^*)} (I_{xx} + I_{yy})$$

$$\nu^* = \frac{(I_{xx} + I_{yy}) \cdot (1+\nu)}{K_t} - 1$$

Material Properties

The frame is made of reinforced concrete. Young's modulus is $E = 2.5 \times 10^8 kg/cm.sec^2$ and the density is $\rho = 2.55\ 10^{-3}\ kg/cm^3$. Poisson's ratio is 0.3. The lumped masses are M = 19000 kg.

Analytical Solution

An approximate analytical solution is used to compare analytic results with MARC output. The volume of concrete, the total mass and the moment of inertia are as follows:

$V = 30.923 \times 10^6\ cm^3$
$M = 1.09 \times 10^5\ kg$
$I = 5.4 \times 10^9\ kg.\ cm^2$

Let us write the following:

$$K_x \approx \frac{12\ E\ \Sigma\ (J_y)\,col}{h^3} = 5.86 \times 10^8 kg/sec^2$$

$$K_y \approx \frac{12\ E\ \Sigma\ (J_x)\,col}{h^3} = 1.03 \times 19^9 kg/sec^2$$

The first three modal frequencies are as follows

$$T_x = \frac{1}{2\pi} \qquad \frac{K_x}{M} = 11.7\ Hz$$

$$T_z = \frac{1}{2\pi} \qquad \frac{K_z}{M} = 15.5\ Hz$$

$$T_\theta = \frac{1}{2\pi} \qquad \frac{K_\theta}{I} = 21.7\ Hz$$

Recover

The RECOVER option is used to first place the six eigenvectors on the POST tape.

The load incrementation option RECOVER is then used for the modal stress calculations for the first and second modes. The modal stresses are computed from the modal displacement vector ϕ (eigenvector without normalization), and the nodal reactions are calculated from $F = K\phi - \omega^2 M\phi$.

Results

The comparison between the approximate analytical solution and the numerical results is shown below:

Eigenvalue	MARC Solution	Approximate Solution	Difference
1	10.3 Hz	11.7 Hz	12%
2	14.0 Hz	15.5 Hz	10%
3	19. 2 Hz	21.7 Hz	10%

It can be seen that the MARC solution is different from the analytical one by no more than 12%; the analytical solution is approximate. The three different modes are shown in Figure E 6.10-2.

Summary of Options Used

Listed below are the options used in example e6x10.dat:

Parameter Options

DYNAMIC
ELEMENT
END
SIZING
TITLE

Model Definition Options

CONNECTIVITY
COORDINATE
END OPTION
FIXED DISP
GEOMETRY
ISOTROPIC
MASSES
POST
TYING

Load Incrementation Options

CONTINUE
MODAL SHAPE
RECOVER

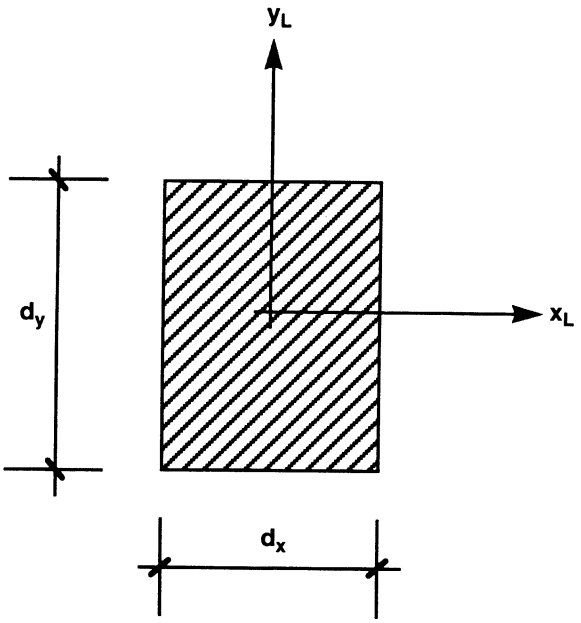

Table E 6.10-1 Geometric Properties of Beams Sections

Set n	Elements n	d_x [cm]	d_y [cm]	A [cm]	J_x [cm^4]	J_y [cm^4]
1	1, 2, 7, 8	75	115	8,625	9,500,000	4,000,000
2	3, 4, 5, 6	85	115	10,925	12,000,000	8,200,000
3	9, 10, 13, 14	196	74	4,810	2,194,000	1,693,000
4	1, 12	196	74	14,504	6,618,000	46,430,000
5	15 16	133	74	9,842	4,491,000	14,500,000

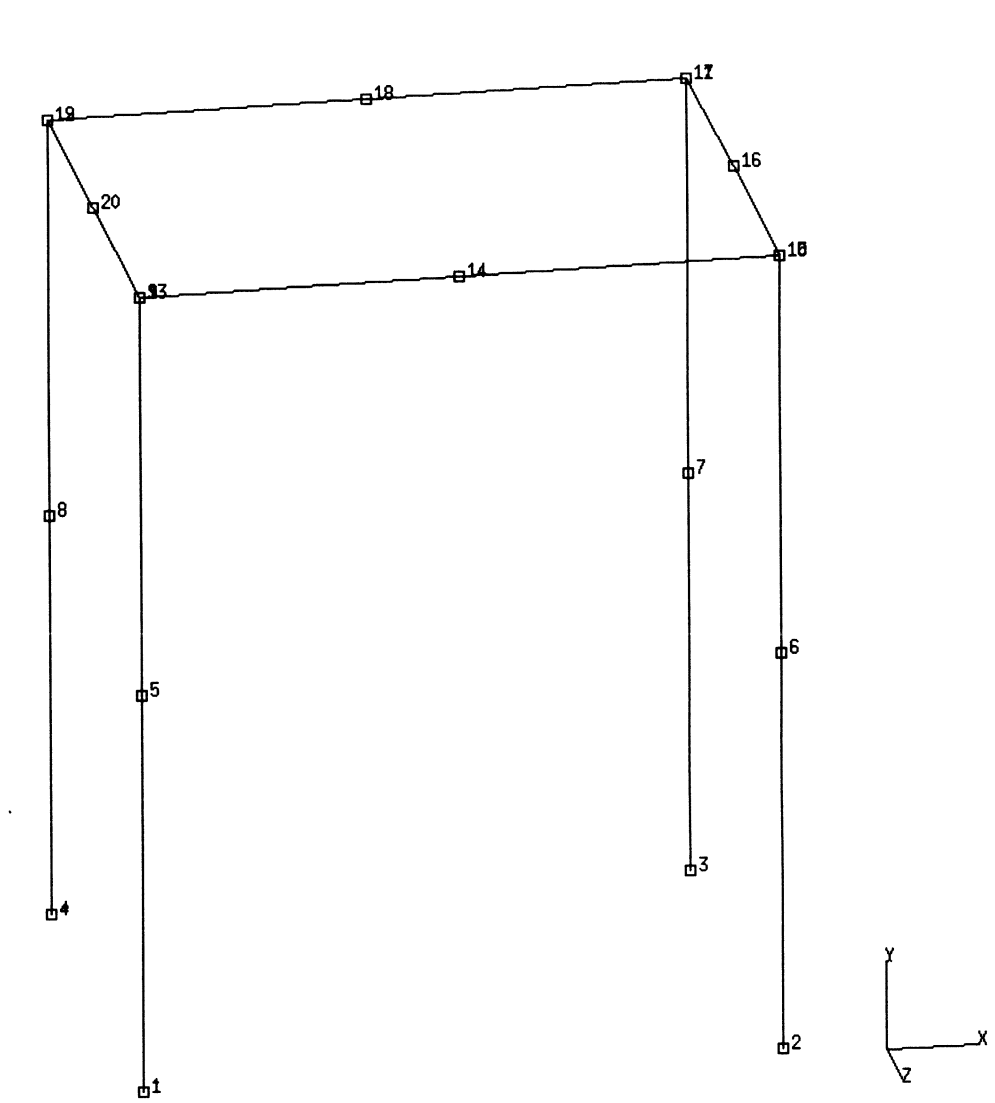

Figure E 6.10-1 Alternator Mount Model

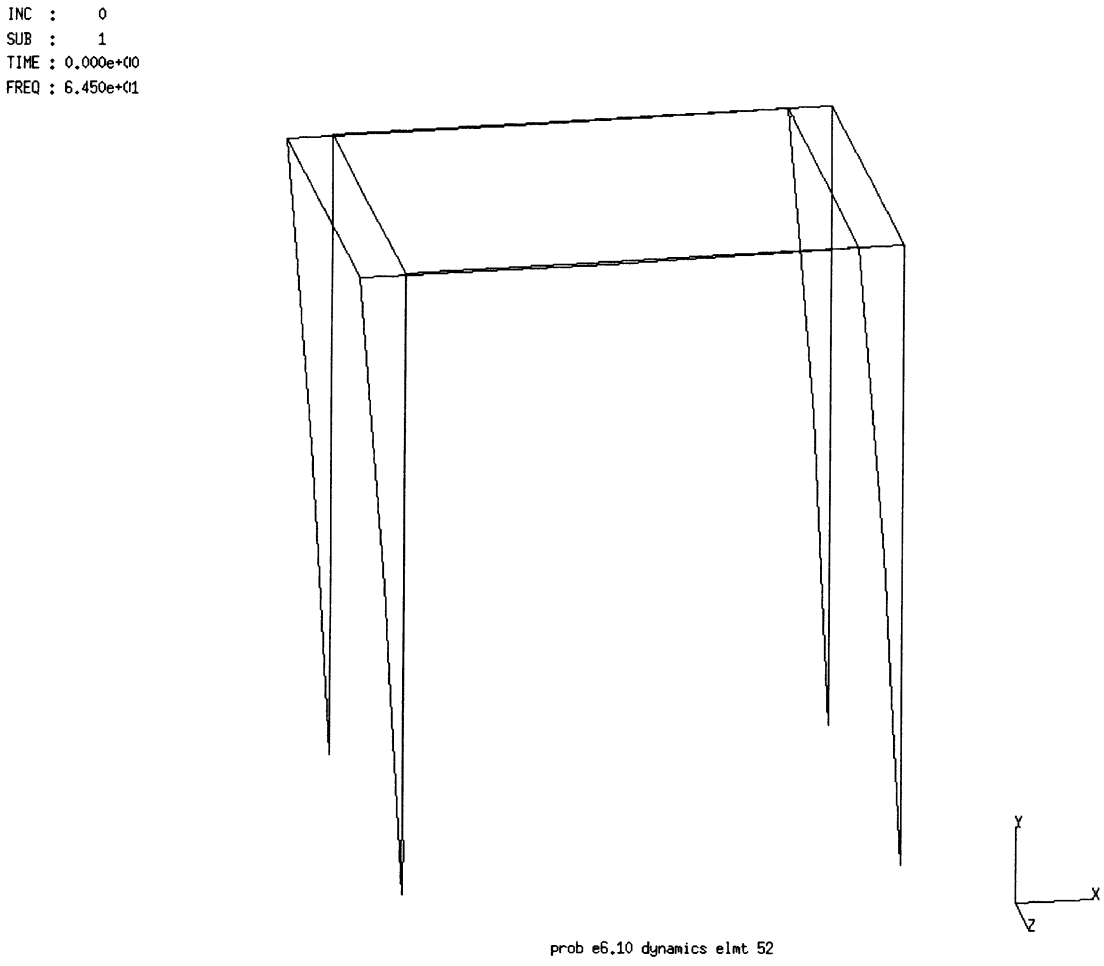

Figure E 6.10-2 First Mode

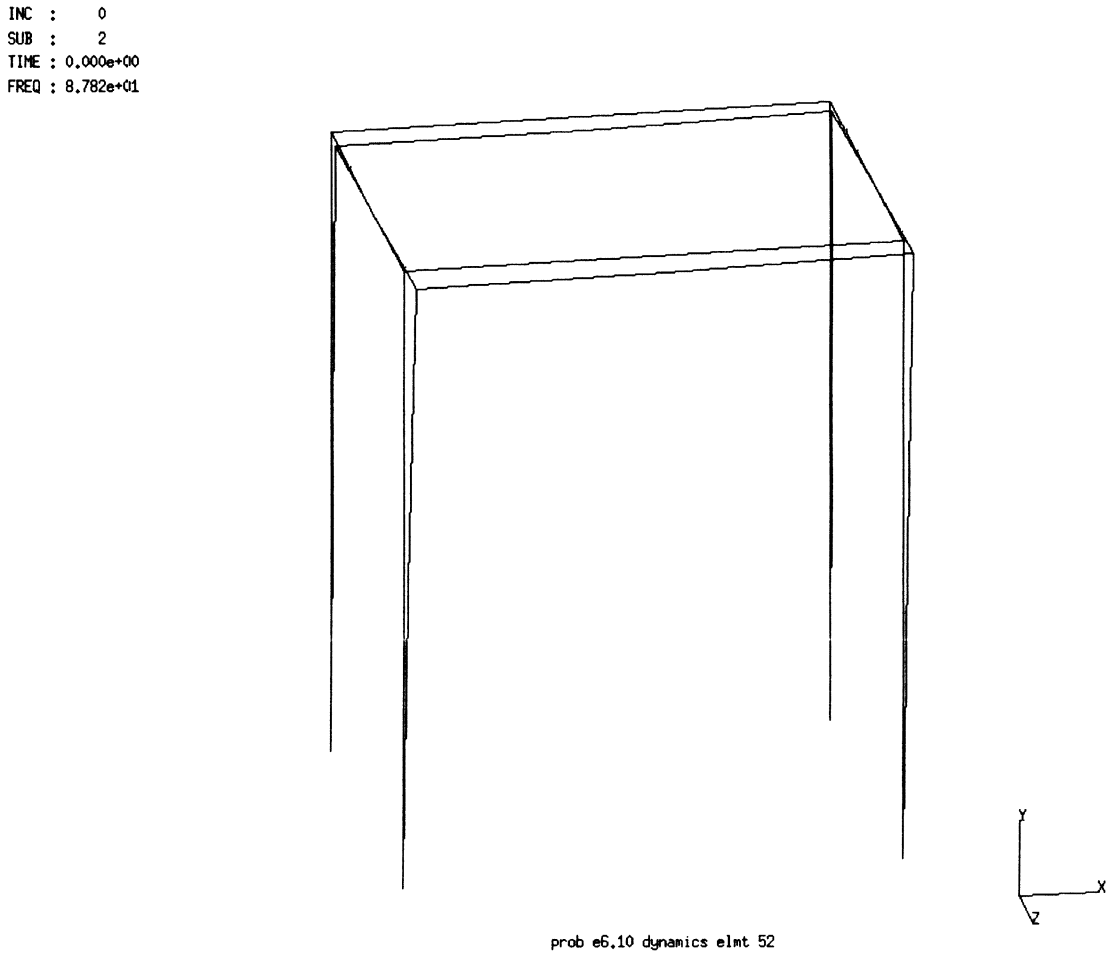

Figure E 6.10-3 Second Mode

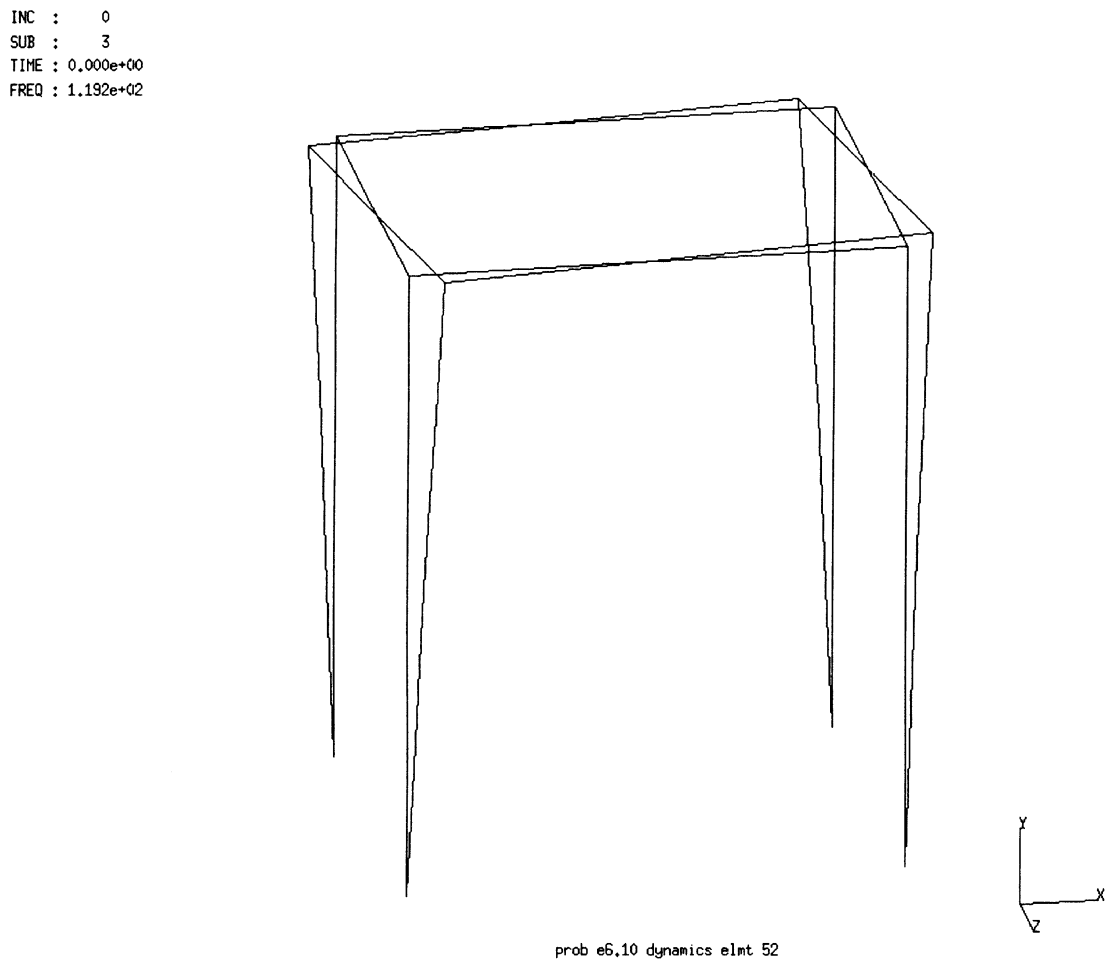

Figure E 6.10-4 Third Mode

E 6.11 Modal Analysis Of A Wing Caisson

The modal analysis is performed of a thin-walled caisson in a wing structure. The problem is simplified by assuming the cross section of the wing to remain constant.

In this case, the MARC results will be compared with approximate analytical results.

Element

Elements type 30 are used in the mesh. They are 8-node, second order isoparametric membrane elements, and have three global coordinates (x,y,z) at each node. The stress state of element 30 is that of a flat membrane.

Model

The generated mesh is shown in Figure E 6.11-1. It has 174 elements and 353 coordinates.

Geometry

The caisson in 6000 mm long and the section is 1200 mm x 200 mm. The following geometric properties of the structure are computed, to be used in the analytical solution:

bending moment of inertia $I_x = 2.6984 \times 10^7$ mm^4
bending moment of inertia $I_y = 4.6764 \times 10^8$ mm^4
polar moment of inertia $I_\rho = 4.9473 \times 10^8$ mm^4

Material Properties

The element properties are uniform; the material is elastic. Values for Young's modulus and Poisson's ratio are respectively E = 7750 kg/mm^2 and $\nu = 0.3$; density is $\rho = 2.75$ kg/mm^3.

Boundary Conditions

The model is clamped in the first 22 nodes, along the edge at y = 0.

Approximate Analytic Solution

The structure has been analyzed as a thin-walled closed section beam. The first two bending modes are:

$$\omega_n = K_n^2 \frac{\pi^2}{1^2} \sqrt{\frac{EI}{M}}$$

where $K_1 = 0.597$ and $K_2 = 1.49$. Thus,

$\omega_1 =$ 46.3 rad/sec
$\omega_2 =$ 169.2 rad/sec

The torsional frequency is:

$$\omega_4 = n \frac{\pi}{21} \sqrt{\frac{GJ}{I_o}} = 353.29 \text{ rad/sec}$$

Results

The approximate solutions provided by beam theory are compared with the results from MARC as shown below. The largest difference among the first three modes is 6%.

Eigenvalue	MARC Output	Approximate Solution	Difference
1	43.3	46.3	6%
2	172.1	169.2	2%
3	342.3	353.3	3%

Summary of Options Used

Listed below are the options used in example e6x11.dat:

Parameter Options

DYNAMIC
END
LINEAR
SIZING
TITLE

Model Definition Options

CONNECTIVITY
COORDINATE
END OPTION
FIXED DISP
ISOTROPIC
POINT LOAD
POST

Load Incrementation Options

CONTINUE
MODAL SHAPE

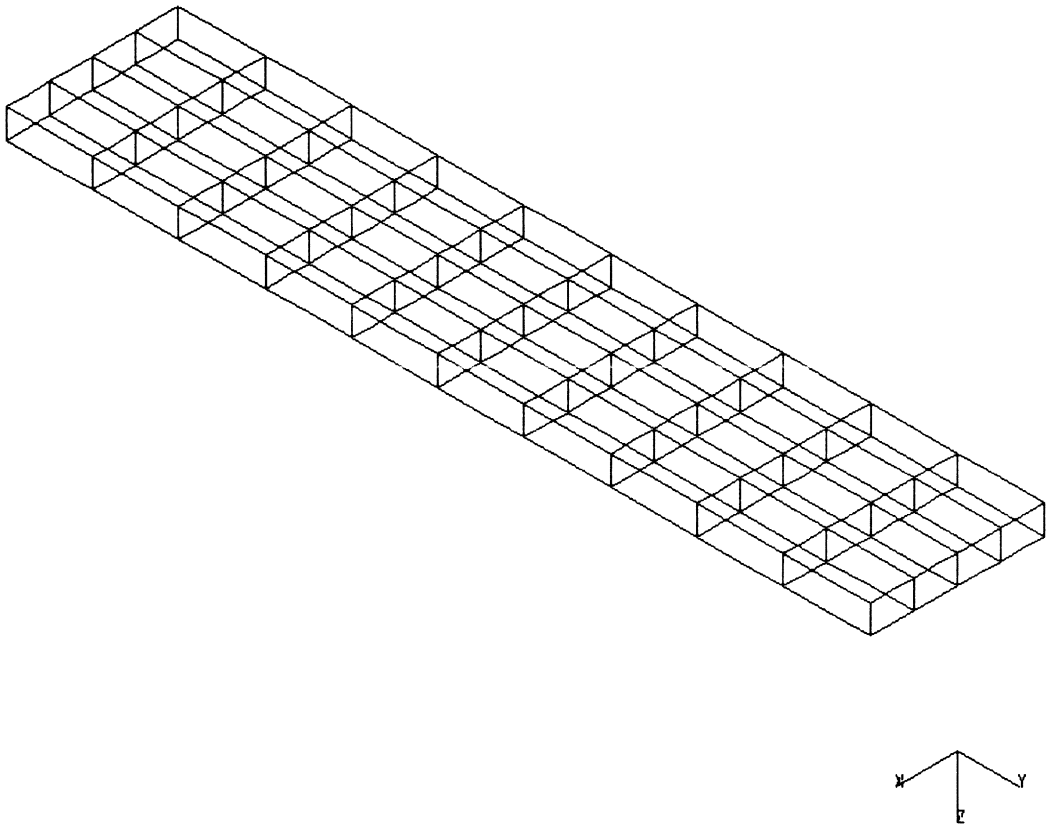

Figure E 6.11-1 Mesh of a Wing Structure

E 6.12 Vibrations Of A Cable

The first two modal frequencies are computed for a straight flexible cable. The MARC results are checked against the analytical solution.

Element

Element type 9, a three-dimensional two-node straight truss, is used. It has three coordinates per node in the global x, y and z directions and an uniaxial state of stress.

Model

The mesh is generated using the CONN GENER card. It has 11 elements and 12 nodes. One end is fixed; the other is free.

Material Properties

The density is uniform throughout the cable and it is $\rho = 84.969$ t/m^3. The Young's modulus varies along the length of the cable:

$0 < L < 4.31$ m	$E = 1.4715 \times 10^8$ kN/m^2
$4.31 < L < 96.5$ m	$E = 6.658 \times 10^6$ kN/m^2

Geometry

The cable has length $L = 96.5$ m and $A = 2.54 \times 10^{-4}$ m^2.

Loading

A normal force is applied at the free end and its value is $p = 49.05$ kN.

Analytical Solution

The analytical formula for the modal frequencies of a prestressed cable is:

$$f_n = \frac{n}{2}\sqrt{\frac{p}{\rho A L^2}}$$

In this case, we obtain $f_1 = 0.247$ Hz and $f_2 = 0.494$ Hz.

Results

The structure is not statically stable. Thus it has been necessary to use a nonlinear step of PROPORTIONAL INCREMENT, to apply the load before asking for the modes. This MARC option forces the assembly of the incremental stiffness matrix.

The results are as follows:

Eigenvalue	MARC Output	Analytical Solution
1	0.2477 Hz	0.247 Hz
2	0.5010 Hz	0.494 Hz

It can be seen that the MARC results are very close to the analytical results. In fact, the larger difference is only 1.3%.

Summary of Options Used

Listed below are the options used in example e6x12.dat:

Parameter Options

DYNAMIC
END
LARGE DISP
SIZING
TITLE
UPDATE

Model Definition Options

CONNECTIVITY
COORDINATE
END OPTION
FIXED DISP
GEOMETRY
ISOTROPIC
POINT LOAD
POST

Load Incrementation Options

CONTINUE
MODAL SHAPE
PROPORTIONAL INCREMENT

E 6.13 Perfectly Plastic Beam Explosively Loaded

This demonstration problem illustrates the use of the adaptive time-stepping procedure for the analysis of a beam subjected to an impulsive load. The beam is elastic, perfectly plastic. The analysis is performed twice, first with no geometric nonlinearities included, and then doing a finite strain plasticity, updated Lagrange analysis.

A simple beam with built-in ends is modeled using element type 16. Only one half of the beam is used because of symmetry. The model consists of five elements with six nodes. The beam is five inches long.

Geometry

The beam has a height of 0.125 inches and a depth of 1.2 inches.

Material Properties

Young's modulus is 10.4×10^6 psi, and Poisson's ratio is 0.3. The mass density is 2.5×10^{-4} lb/in^3. The yield stress is 41,400 psi and there is no work hardening in the material.

Boundary Conditions

The first node is given the boundary conditions of built in $u = v = \frac{\partial v}{\partial s} = 0.$

The last node is given the symmetry boundary conditions $u = \frac{\partial v}{\partial s} = 0.$

Loading

The problem is driven by the initial conditions, which are a large initial velocity at the center of the beam. An initial condition of 5020 in/s is applied at nodes 5 and 6.

Control

The AUTO TIME option is used to control the time step size. The procedure is such that if the residuals are large compared to the reactions, the time step is reduced. If the convergence is well satisfied, the time step is increased in the next increment. The initial time step is chosen as 5×10^{-6} s. This time step was chosen such that $[\Delta t \cdot V_0]$ was small compared to the other geometric dimensions. The total time to be modeled is 1.5×10^{-3}s. A maximum of 100 steps will be allowed.

Results

Figure E 6.13-2 through Figure E 6.13-4 show the displacements, velocities and accelerations for the small displacement analysis. Figure E 6.13-5 through Figure E 6.13-7 show the results for the large displacement analysis. Each mark on the graph indicates when a new increment, hence one can observe the change in the time step. In the problem including geometric

nonlinearities, many more time steps are used to remain in equilibrium. One can observe that there is a large acceleration initially, which reverses the sign for the center node and then begins to approach zero.

Summary of Options Used

Listed below are the options used in example e6x13.dat:

Parameter Options

DYNAMIC
ELEMENT
END
SIZING
TITLE

Model Definition Options

CONNECTIVITY
CONTROL
COORDINATE
END OPTION
FIXED DISP
GEOMETRY
INITIAL VELOCITY
ISOTROPIC
POST
PRINT CHOICE
RESTART

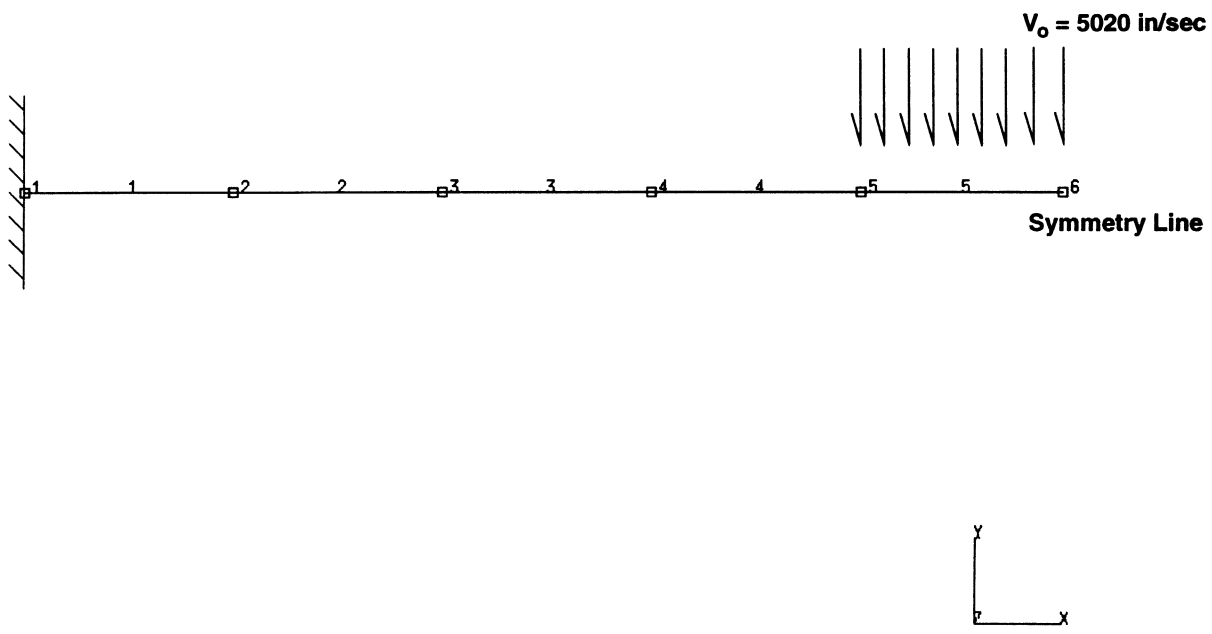

Figure E 6.13-1 Mesh with Initial Velocity

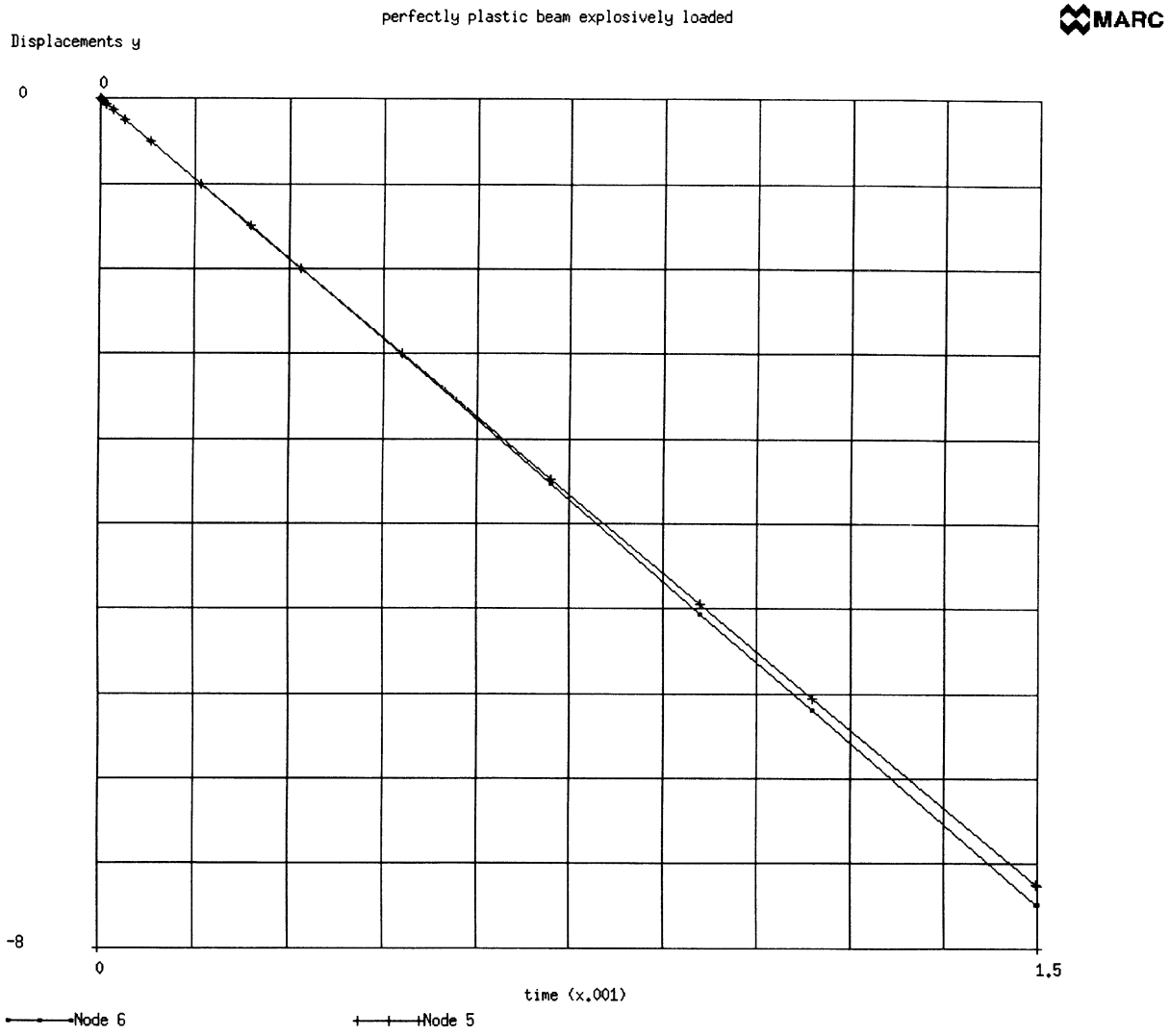

Figure E 6.13-2 Small Displacement Analysis

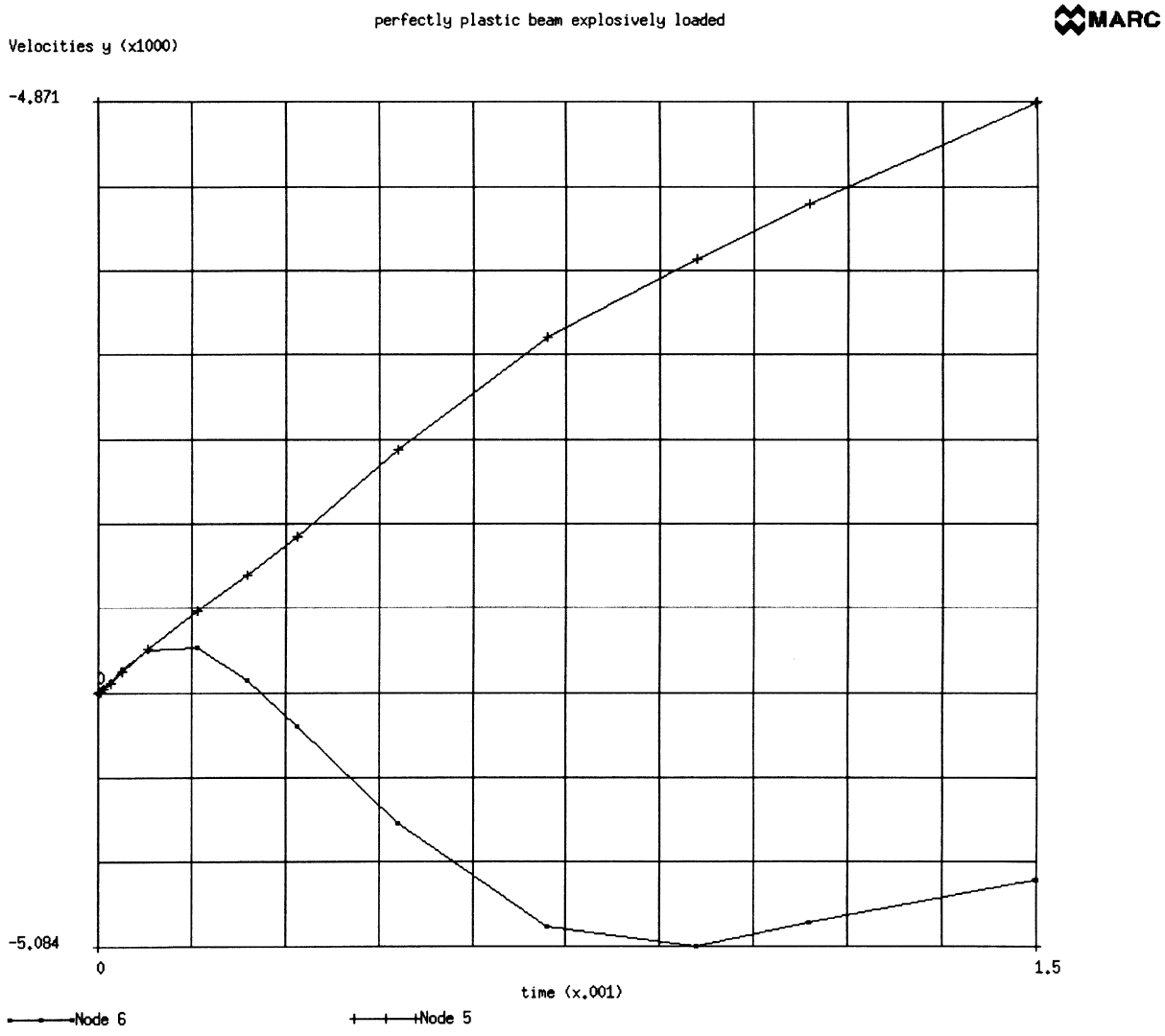

Figure E 6.13-3 Small Displacement Analysis

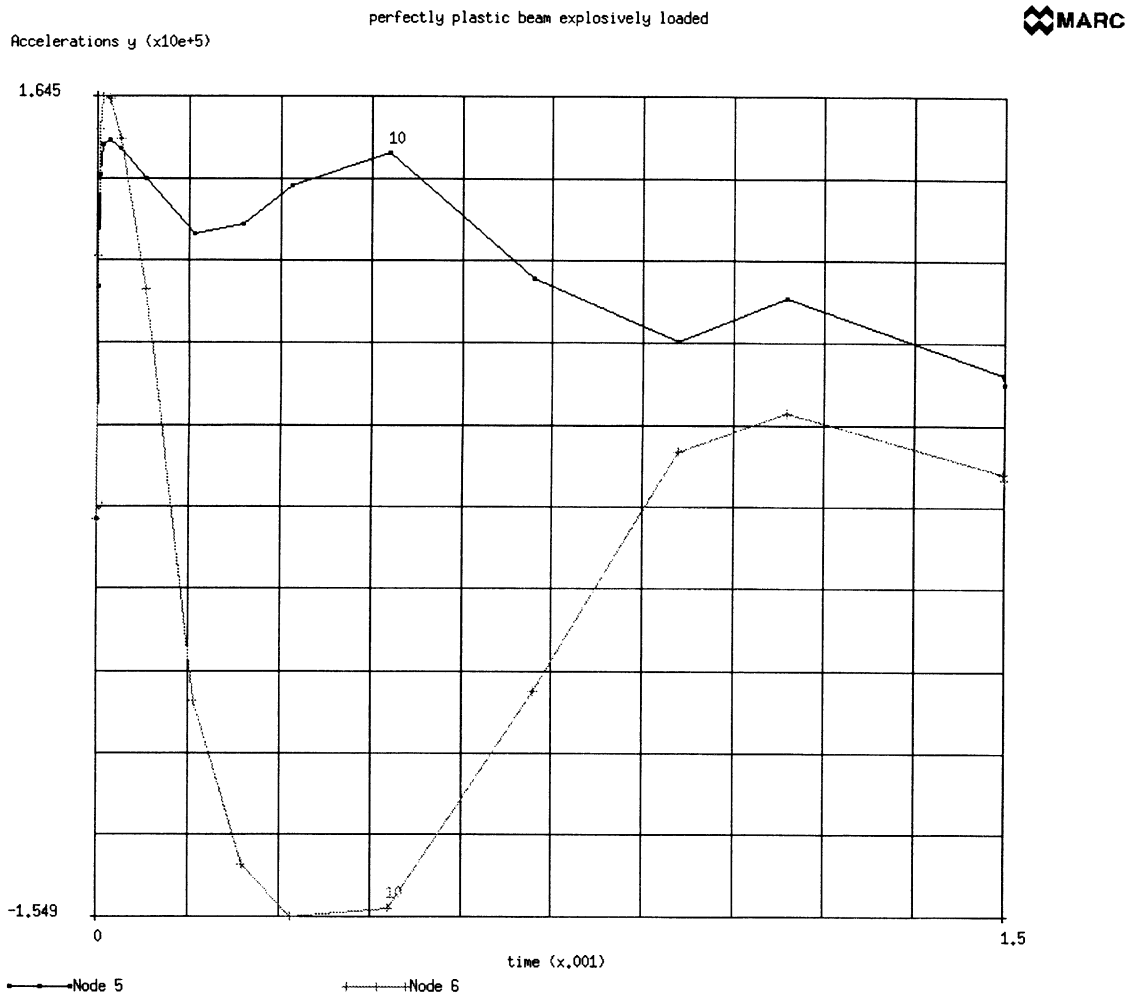

Figure E 6.13-4 Small Displacement Analysis

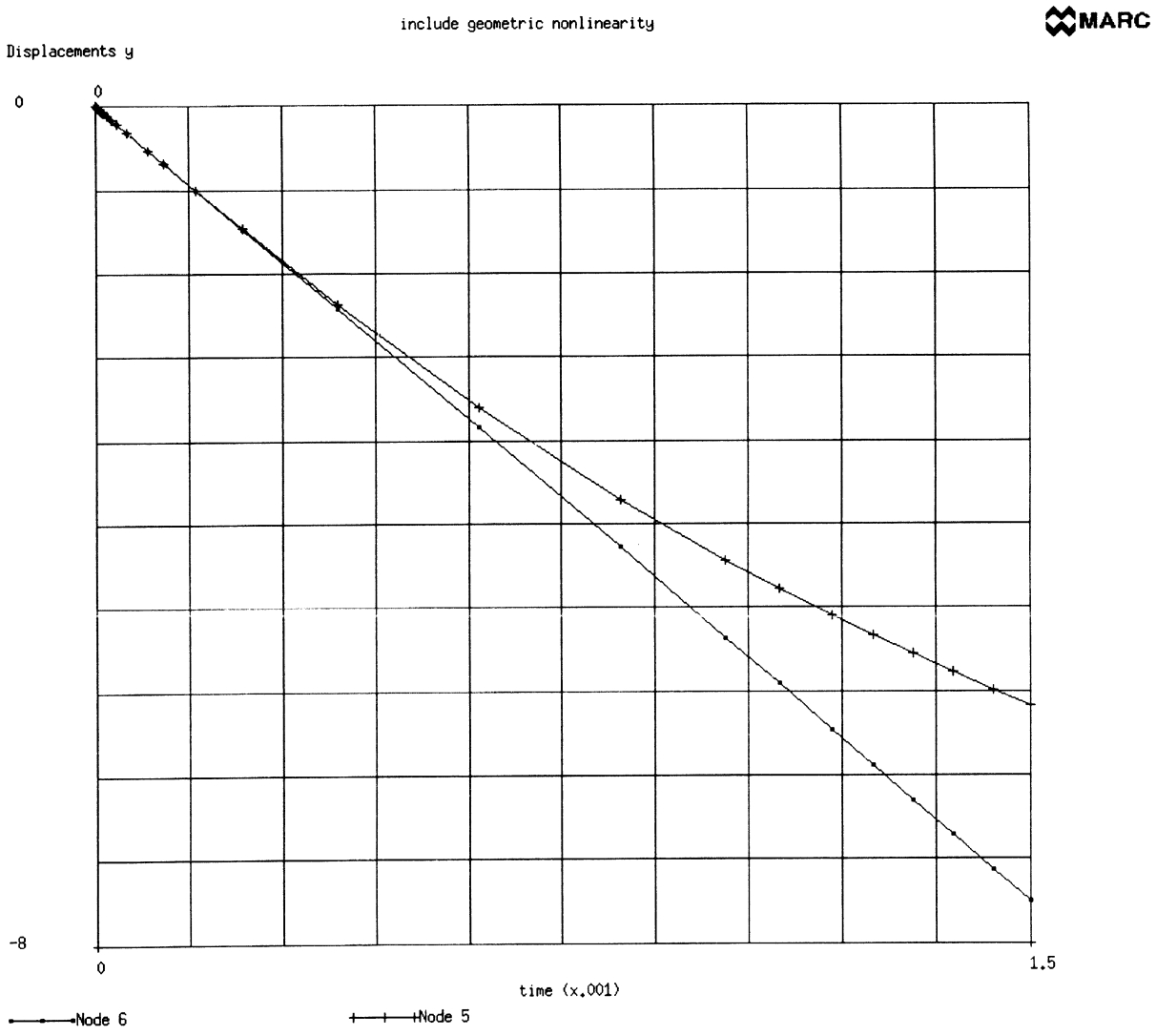

Figure E 6.13-5 Includes Geometric Nonlinearity

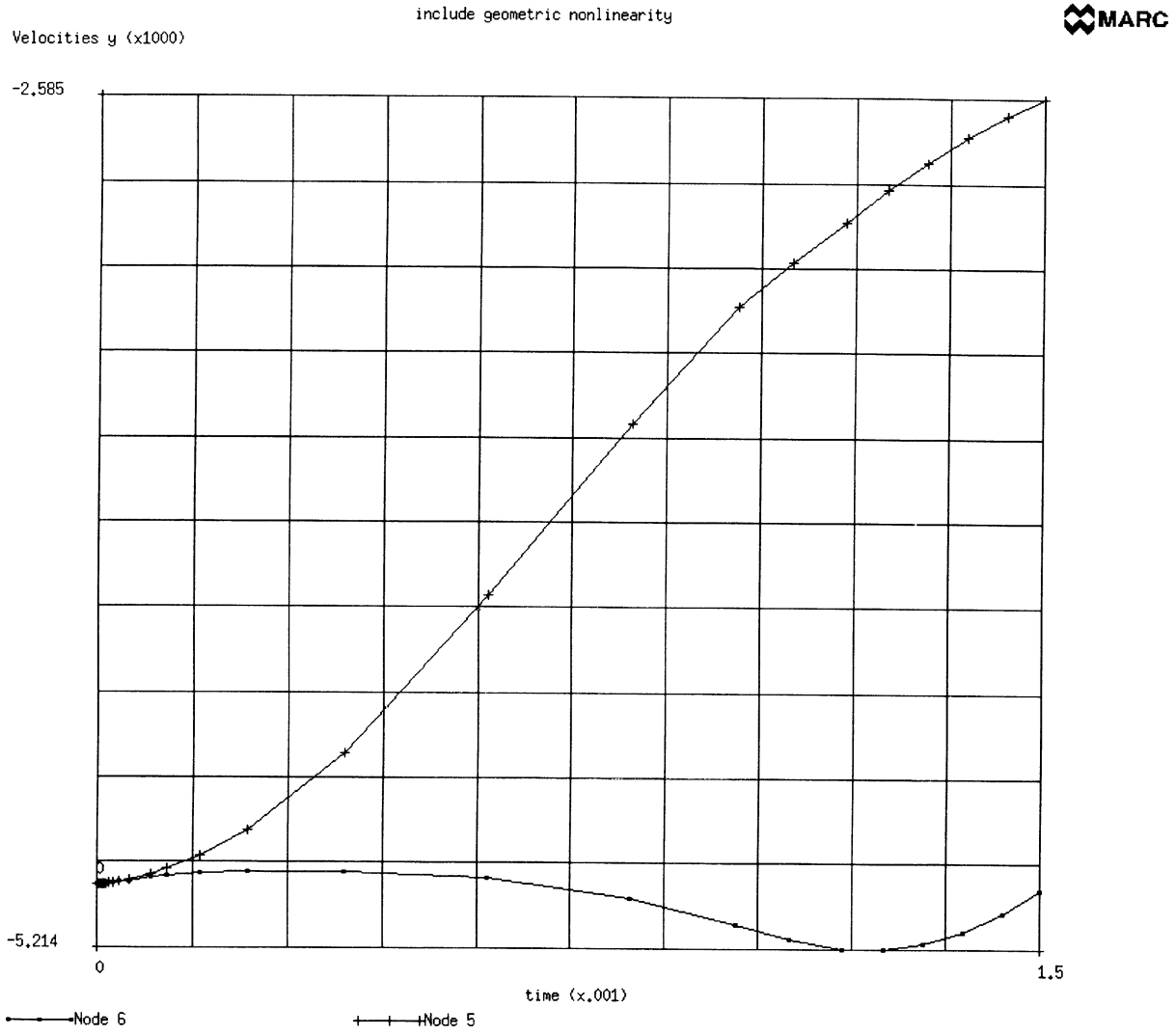

Figure E 6.13-6 Includes Geometric Nonlinearity

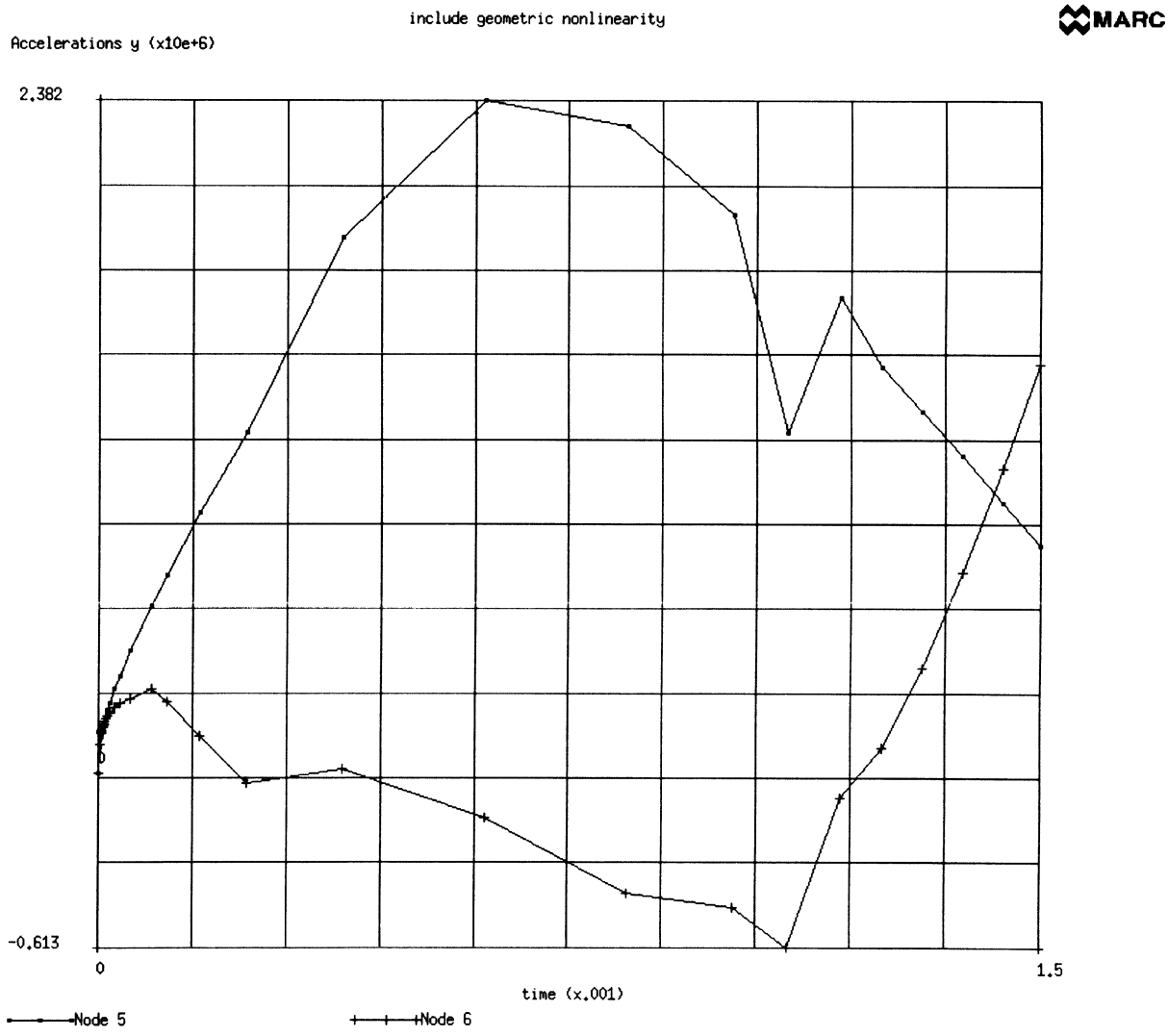

Figure E 6.13-7 Includes Geometric Nonlinearity

E 6.14 Dynamic Fracture Mechanics

This example illustrates the use of the DeLorenzi method [1] to evaluate J-integral values in MARC for dynamically responding structures. The problem consists of a center-cracked plate which is initially at rest, and which is subjected to a uniform tensile load that is suddenly applied and then maintained for $t > 0$. This problem was originally analyzed by Chen [2] who used a finite difference method. Over the past years it has become more or less a benchmark problem for demonstrating the applicability of various alternative procedures to calculate dynamic stress intensity factors. See Brickstad [3] and Jung [4].

Details on the dimensions, material properties and loading conditions are given in Figure E 6.14-1.

Element

Element type 27, an 8-noded plane strain quadrilateral, is used.

Model

Because of symmetry only one quarter of the plate is modeled. A graded mesh subdivision is chosen, identical to the mesh used in [4]. No quarter-point elements are used. Figure E 6.14-2 shows the finite element model.

Geometry

No geometry is specified and thus a unit thickness is assumed by the program.

Material Properties

The Young's modulus is set to 2000 N/cm^2 and Poisson's ratio is 0.3. The mass density amounts to 5 g/cm^3. In order to obtain consistent units, a value of 5.0×10^{-5} has to be entered in the mass density field of the PROPERTY block.

Boundary Conditions

Because of symmetry conditions all nodal DOF's in the first coordinate direction are suppressed along $x = 0$. All nodal DOF's in the second coordinate direction are suppressed along the uncracked part of $y = 0$.

Loading

The step function in the tensile load is specified as follows:

increment zero : $\sigma = 0$
increment one : $\Delta\sigma = 40000\ N/cm^2$
increment > 1 : $\Delta\sigma = 0$

The full tensile load is applied in a single short time step of 1 x 10^{-4} μsec. The implicit Newmark-beta method with a constant time step of 0.15 μsec. is employed for the direct time integration up to a time of 12 μsec. The time step is chosen such that the longitudinal wave will reach the crack-plane in approximately 10 increments. Because of the linear nature of the problem the control value for residual checking has been set to a large value (i.e., 10).

LORENZI

A unit crack extension of 1 cm. has been specified for three different paths. The first J-value is based on a unit movement of the crack tip only. Elements 3 and 4 will be the only deforming elements. The second J-value is based on a rigid movement of the first ring of elements (3 and 4). The third J-value is based on a rigid movement of the first and second ring of elements. In order to incorporate all inertia effects, all movements of the nodes in the regions with "rigid" movements must be specified. Figure E 6.14-3 shows the relevant element and node numbers in the crack-tip region.

Results

The program provides for the output of the strain energy changes per crack movement for each increment. These values have to be normalized by the crack opening area to obtain the J-values. Because of symmetry the actual strain energy that can be released at every crack tip will be twice the value that is printed out. In addition, the J-values may be converted to K_I values using the relation:

$$K_I = \sqrt{\frac{E}{1-\nu^2}\ J}$$

Table E 6.14-1 summarizes the J-values that are obtained for the first path as well as the normalized K_I values $\left(\text{i.e. } K_I/\sigma\sqrt{\pi a}\right)$ for every 10th increment. More details about the results and a comparison with other numerical solutions can be found in [5]. Figure E 6.14-4 shows the dynamic stress intensity factors normalized with respect to a static stress intensity factor of an infinite plate as a function of time for the complete analysis.

Table E 6.14-1 Normalized Dynamic Stress Intensity Factors

Increment Number	Time (μsec)	J/2	$K_{dynamic}/\sigma\sqrt{\pi a}$
11	1.5	0.103E-4	0.0061
21	3.0	29.92	1.0442
31	4.5	82.26	1.7313
41	6.0	171.50	2.4998
51	7.5	146.62	2.3114
61	9.0	45.58	1.2887
71	10.5	11.91	0.6588

References

1. DeLorenzi, H.G., "On the Energy Release Rate and the J-integral for 3D Crack Configurations", *Inst. J. Fracture*, Vol. 19, 1982, pp. 183-193.
2. Chen, Y.M, "Numerical Computation of Dynamic Stress Intensity Factors" by a Lagrangian Finite Difference Method (the HEMP Code)", *Eng. Fract. Mech.*, Vol. 7, 1975, pp. 653-660.
3. Brickstad, B., "A FEM Analysis of Crack Arrest Experiments", *Int. J. Fract.*, Vol. 21, 1983, pp. 177-194.
4. Jung, J., Ahmad, J., Kanninen, M.F. and Popelar, C.H., "Finite Element Analysis of Dynamic Crack Propagation", presented at the 1981 ASEM Failure Prevention and Reliability Conference, September 23-26, 1981, Hartford, Conn., U.S.A.
5. Peeters, F.J.H. and Koers, R.W.J., "Numerical Simulation of Dynamic Crack Propagation Phenomena by Means of the Finite Element Method", *Proceedings of the 6th European Conference on Fracture*, ECF6, Amsterdam, The Netherlands, June 15-20, 1986.

Summary of Options Used

Listed below are the options used in example e6x14.dat:

Parameter Options

DYNAMIC
ELEMENT
END
SIZING
TITLE

Model Definition Options

CONNECTIVITY
CONTROL
COORDINATE
DIST LOADS
END OPTION
FIXED DISP
ISOTROPIC
LORENZI
NO PRINT

Load Incrementation Options

CONTINUE
DIST LOADS
DYNAMIC CHANGE

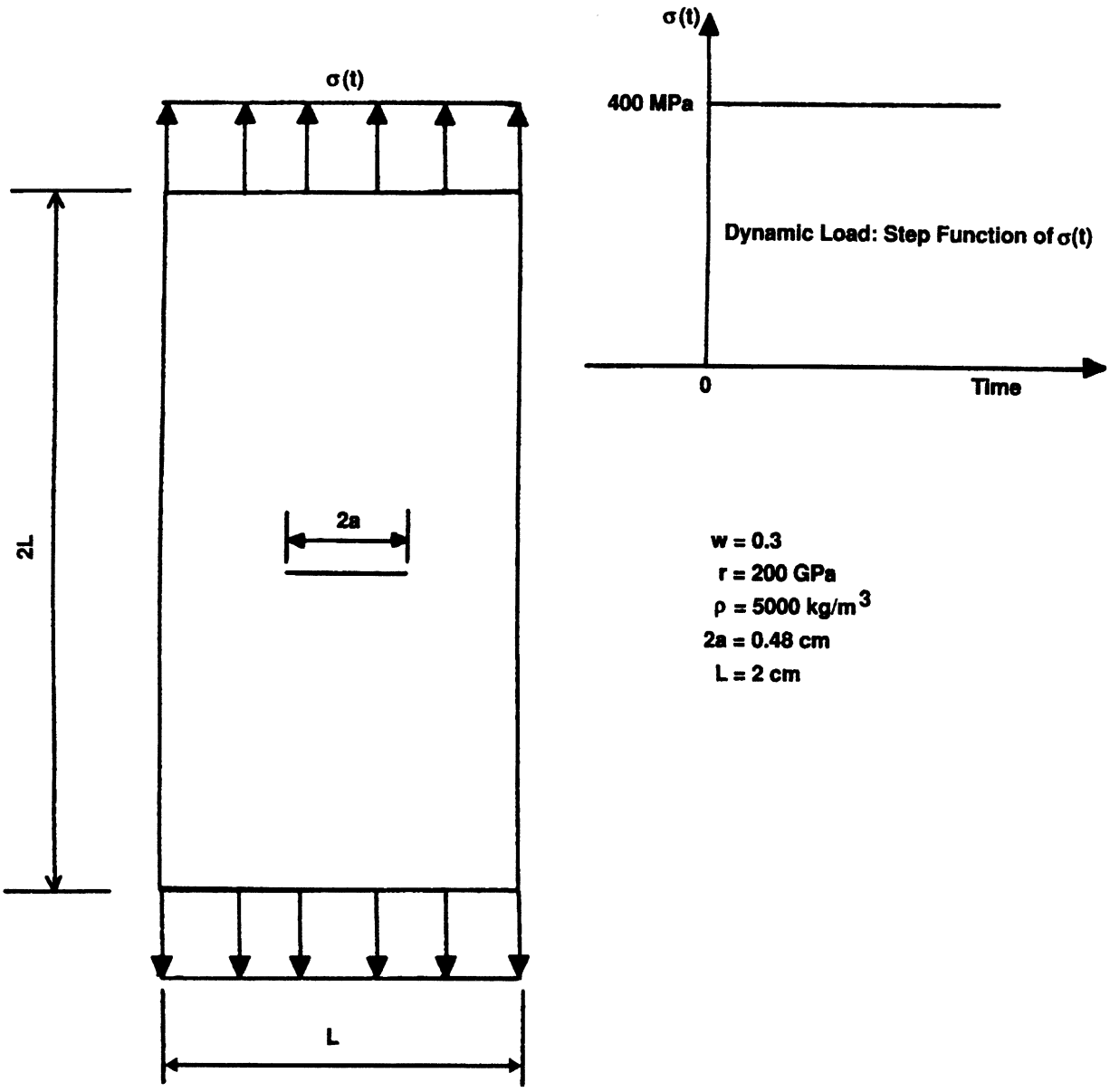

Figure E 6.14-1 Dynamically Loaded Center-Cracked Rectangular Plate Problem

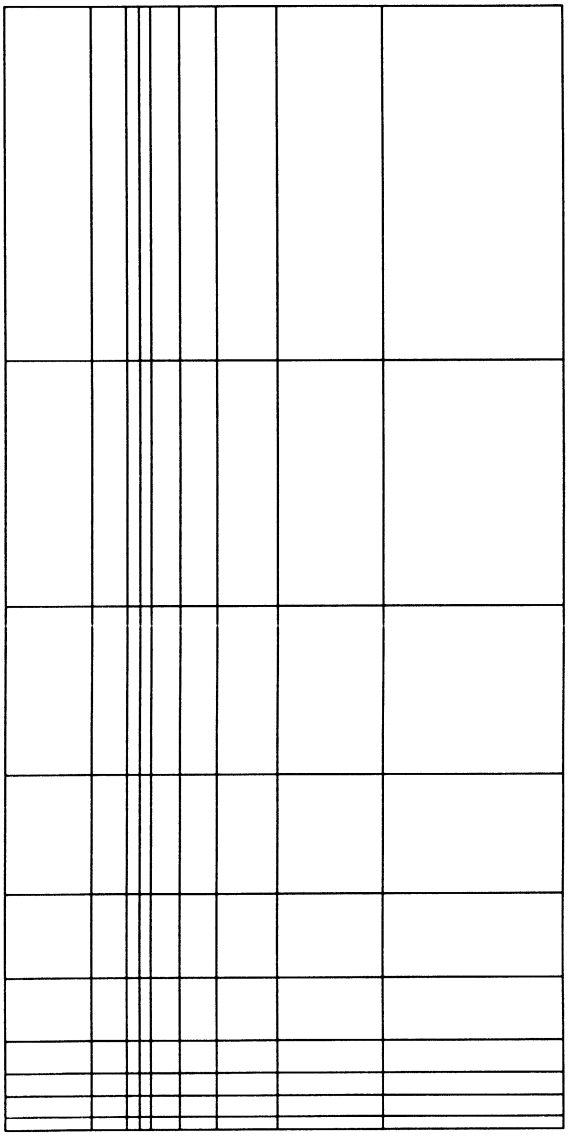

Figure E 6.14-2 Dynamic Crack Problem Mesh

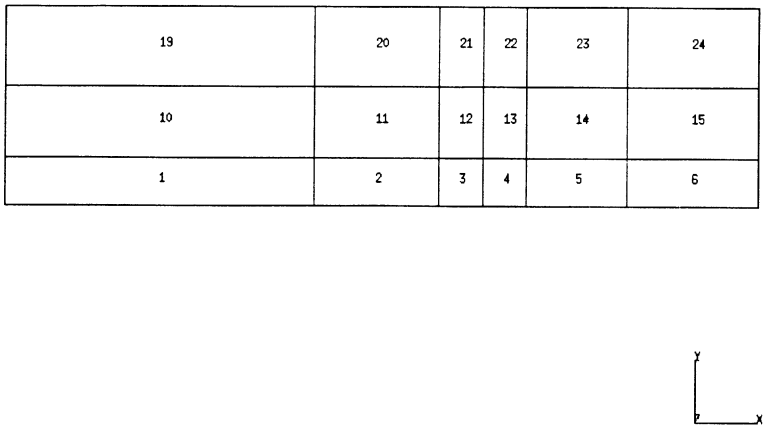

Element Numbers

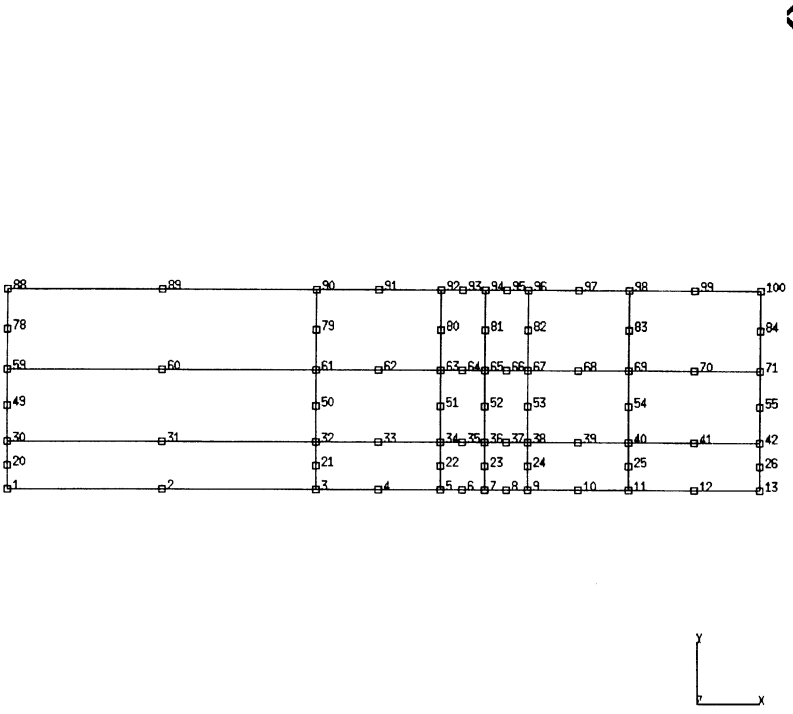

Node Numbers

Figure E 6.14-3 Crack Tip Region

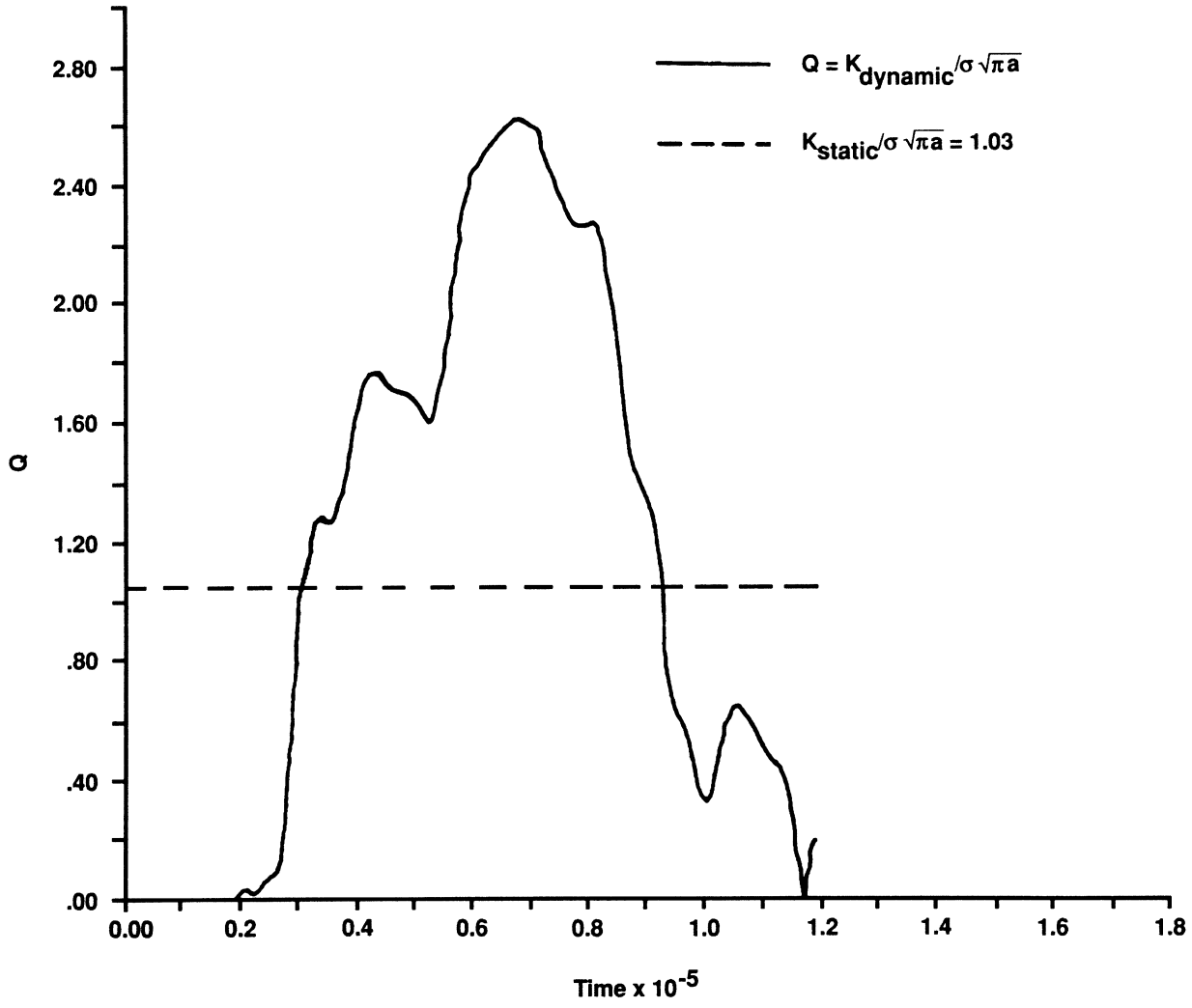

Figure E 6.14-4 Normalized Dynamic Stress Intensity Factors

E 6.15 Eigenmodes Of A Plate

In this problem, the eigenvalues will be calculated for a cantilevered, rectangular plate, using element type 7. In the first case, the assumed strain formulation will be used. In the second case, the conventional isoparametric element will be used. This eigenproblem illustrates the superiority of the assumed strain element over the conventioanl isoparametric element in the plate or shell analyses.

Model

The plate is of length 0.6 inch and width 0.25 inch and thickness of 0.003 inch. It is modeled using a 28x14 mesh of element type 7, eight-node brick as shown in Figure E 6.15-1. Four eigenvalues will be extracted using the inverse power sweep method. The lumped mass matrix will be formed.

Geometry

In the first case, a "1" is placed in the third field to indicate that the assumed strain formulation is to be used.

Material Properties

The material has a Young's modulus of 26 x 10^6 psi, and a Poisson's ratio of 0.32. The mass density is 0.000755 lb/in^3.

Boundary Conditions

The one end is completely constrained to represent the cantilevered boundary conditions. The other end is simply supported at its midpoint.

Results

The frequencies calculated are summarized in Table E 6.15-1. For comparison, the results using element 75 are also included.

Table E 6.15-1 Frequencies in Hertz

Mode	Assumed Strain Element	Conventional Isoparametric Element	Element 75
1	1140	1929	1140
2	1323	5024	1324
3	3551	8469	3553
4	4235	14713	4239

One observes that using the conventional elements, the frequencies are significantly higher and incorrect. This is because the element is too stiff in bending. The agreement between the assumed strain element and the shell element is very good.

Figure E 6.15-2 and Figure E 6.15-3 show the first and third mode shapes.

Summary of Options Used

Listed below are the options used in example e6x15.dat:

Parameter Options

DYNAMIC
ELEMENT
END
LUMP
PRINT
SIZING
TITLE

Model Definition Options

CONNECTIVITY
COORDINATE
END OPTION
FIXED DISP
GEOMETRY
ISOTROPIC

Load Incrementation Options

CONTINUE
MODAL SHAPE

Listed below are the options used in example e6x15b.dat:

Parameter Options

DYNAMIC
ELEMENT
END
LUMP
SIZING
TITLE

Model Definition Options

CONNECTIVITY
COORDINATE
END OPTION
FIXED DISP
GEOMETRY
ISOTROPIC

Load Incrementation Options

CONTINUE
MODAL SHAPE

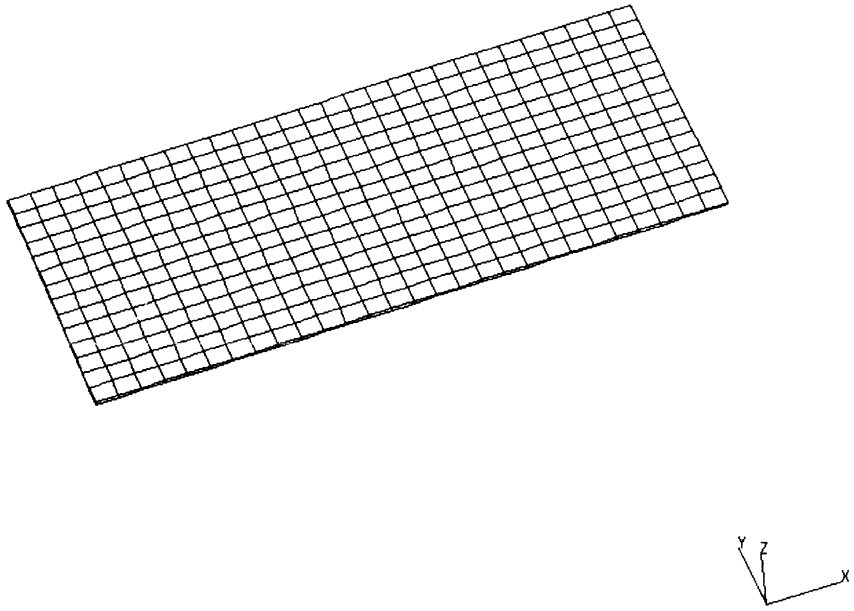

Figure E 6.15-1 Mesh

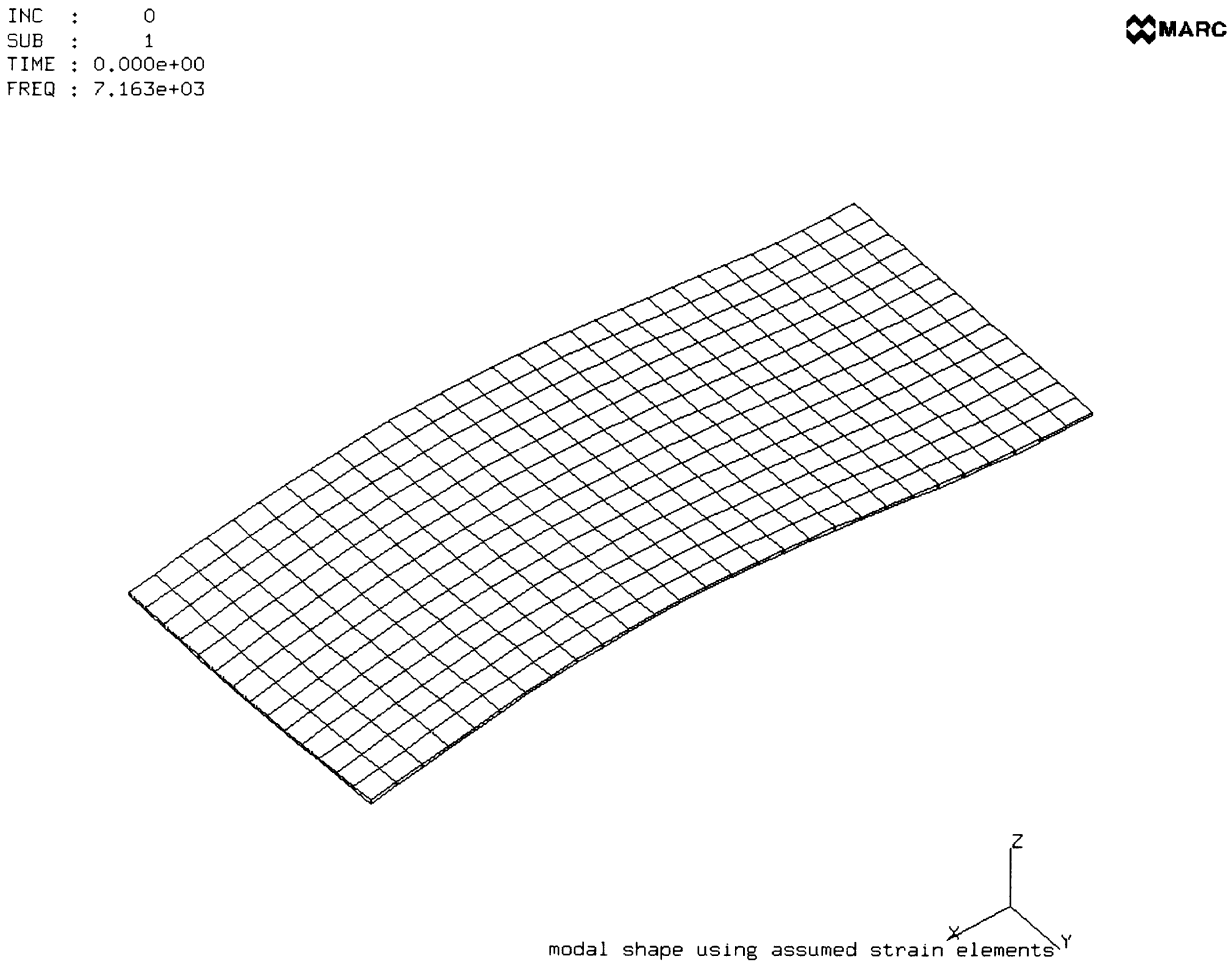

Figure E 6.15-2 First Mode Shape of Cantilevered Plate

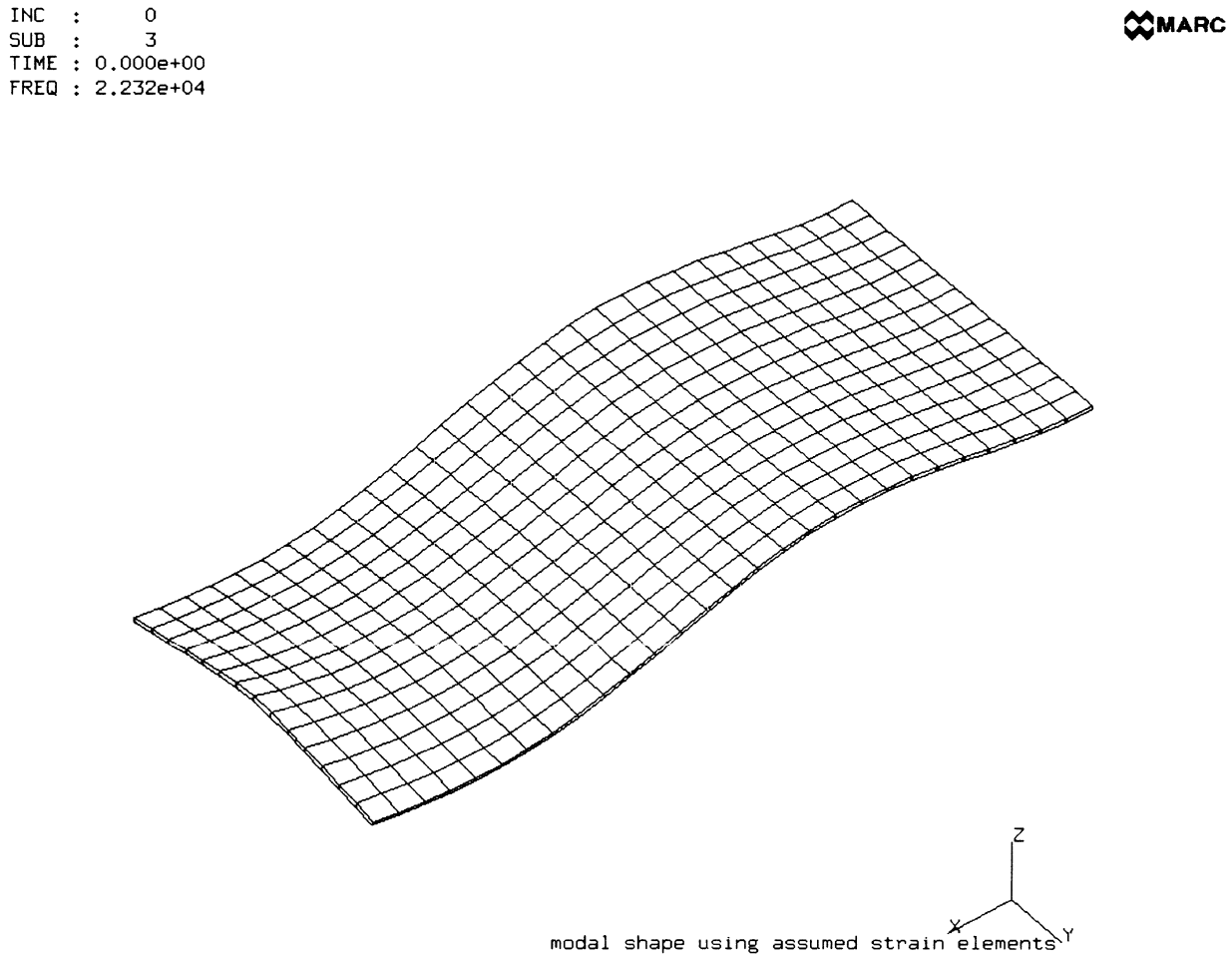

Figure E 6.15-3 Third Mode Shape of Cantilevered Plate

E 6.16 Dynamic Contact Between A Projectile And A Rigid Barrier

This problem demonstrates the dynamic impact between a deformable body and a rigid surface. The problem is executed using both an implicit Newmark-beta operator and the explicit central difference operator.

Model

A deformable projectile consists of nine element type 7, eight-node bricks as shown in Figure E 6.16-1. As an alternative, the analysis is also performed with element type 120 which is the reduced integration formulation. The projectile is initially 0.1 units away from the rigid surface. The DYNAMIC parameter card specifies which operator is to be chosen: a "2" indicates Newmark-beta and a "4" indicates central difference. The projectile may undergo large deformations, so a LARGE DISP parameter is included. The projectile is considered elastic and a total Lagrange analysis will be performed.

Material Properties

An artificial material was created, such that the stability limit for central difference was a large number. The Young's modulus is 10,000 psi and the mass density is 0.1 lb/in^3. A lumped mass matrix will be created based upon the LUMP parameter card. The projectile is given a numerical damping of 0.4. Numerical dampening is preferred over stiffness damping, because the time step can change in contact analyses, resulting in stiffness damping overdamping the system.

Given the material parameters, the elastic wave speed is $c = \sqrt{E/\rho} = 316$ in./s.

Boundary Conditions

The nodes on the xz-plane have been constrained in the y-direction. The nodes on the xy-plane have been constrained in the z-direction. The projectile has an initial velocity of -100 in/sec in the x-direction.

Controls

The maximum number of increments will be 100 with the maximum number of iterations being 3. Relative displacement error control will be used with a tolerance value of 10%. Note that when using the explicit dynamic method, iteration will not occur. A formatted post tape will be written which will contain only nodal information. The restart tape is written at every increment.

Contact

There are two bodies in this analysis. The first is the deformable projectile. The second is the rigid barrier. There is no friction between these two surfaces.

The other parameters on the second card are upper bounds to the number of surface entities and surface nodes.

The contact tolerance is 0.03 inch which is small compared to an element dimension. A very large separation force is given which effectively ensures that the projectile will stick to the barrier.

The first body is the deformable one consisting of nine elements. The second body consists of one patch. The order of the numbering ensures the correct normal direction is associated with the rigid surface.

Time Step

The time step chosen is 0.0005 second which is below the stability limit of 0.002 second. In this period, the elastic wave will travel 0.158 inch which is smaller than a typical element dimension. The total period is 0.01 second, so 20 increments will be performed.

Results

Figure E 6.16-3 and Figure E 6.16-4 show the projectile at increment two after contact first occurs, and at increment 20 at the end of the analysis. Figure E 6.16-5, Figure E 6.16-6, and Figure E 6.16-7 show the displacement, velocity, and reaction forces at selected nodes for the Newmark-beta analysis and central difference analysis. One can observe that the results are almost indistinguishable. Node 26 first comes into contact at increment 2, the displacement is .1 and remains fixed for the remainder of the analysis; velocity is zero. Node 25 comes into contact during increment 10 and remains fixed the remainder of the analysis. Nodes 31 and 32 simply decelerate during the analysis. The reactions show that spikes occur at the increments where contact occurs. The results using the reduced integration element are not substantially different.

The implicit Newmark-beta ran three times longer. This is an anomaly due to the fact that an artificial material was created such that the time steps in the two procedures were allowed to be the same.

Summary of Options Used

Listed below are the options used in example e6x16a.dat:

Parameter Options

DYNAMIC
ELEMENT
END
LARGE DISP
LUMP
PRINT
SIZING
TITLE

Model Definition Options

CONNECTIVITY
CONTACT
CONTROL
COORDINATE
END OPTION
FIXED DISP
INITIAL VELOCITY
ISOTROPIC
POST
PRINT ELEM
RESTART

Load Incrementation Options

CONTINUE
DYNAMIC CHANGE

Listed below are the options used in example e6x16b.dat:

Parameter Options

DYNAMIC
ELEMENT
END
LARGE DISP
LUMP
PRINT
SIZING
TITLE

Model Definition Options

CONNECTIVITY
CONTACT
CONTROL
COORDINATE
END OPTION
FIXED DISP
INITIAL VELOCITY
ISOTROPIC
POST
PRINT ELEM
RESTART

Load Incrementation Options

CONTINUE
DYNAMIC CHANGE

Listed below are the options used in example e6x16c.dat:

Parameter Options

ALIAS
DYNAMIC
ELEMENT
END
LARGE DISP
LUMP
PRINT
SIZING
TITLE

Model Definition Options

CONNECTIVITY
CONTACT
CONTROL
COORDINATE
END OPTION
FIXED DISP

INITIAL VELOCITY
ISOTROPIC
POST
RESTART

Load Incrementation Options

CONTINUE
DYNAMIC CHANGE

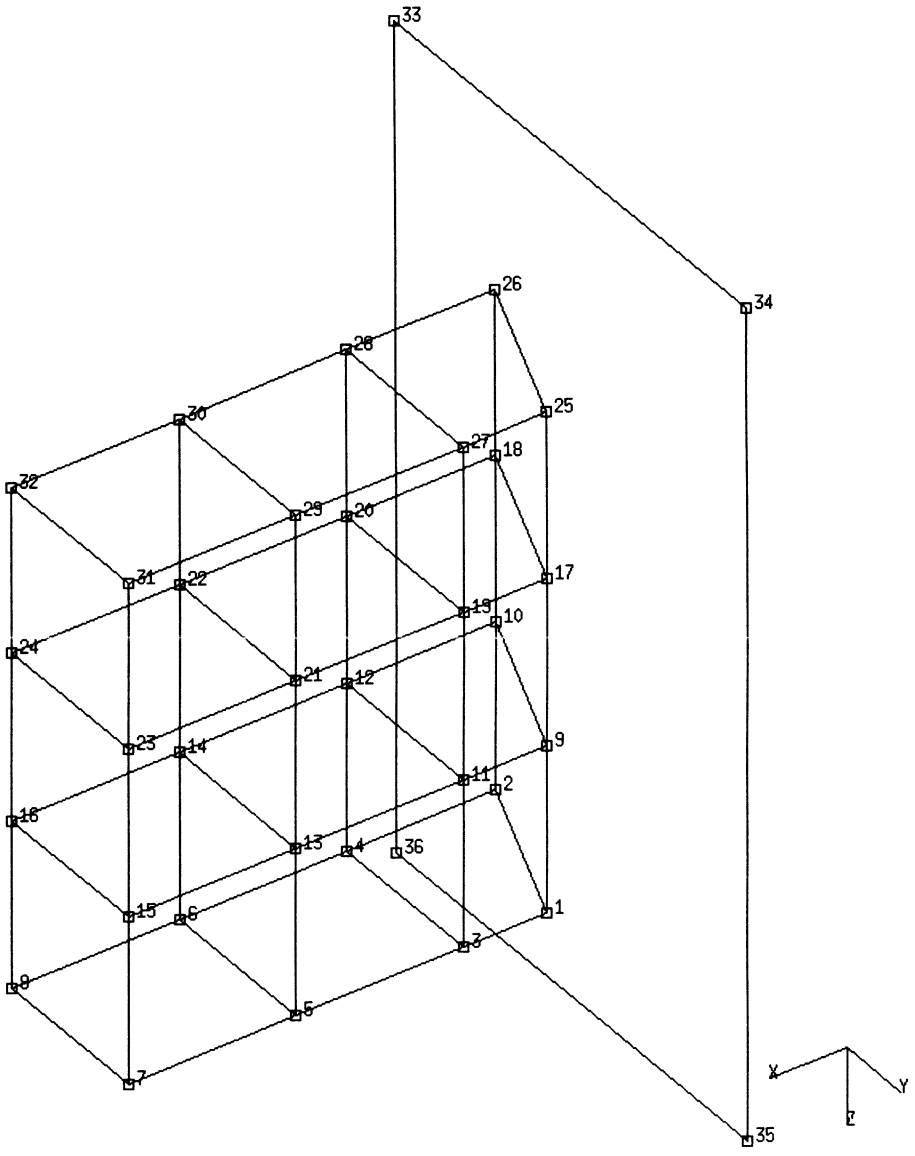

Figure E 6.16-1 Impactor and Rigid Wall

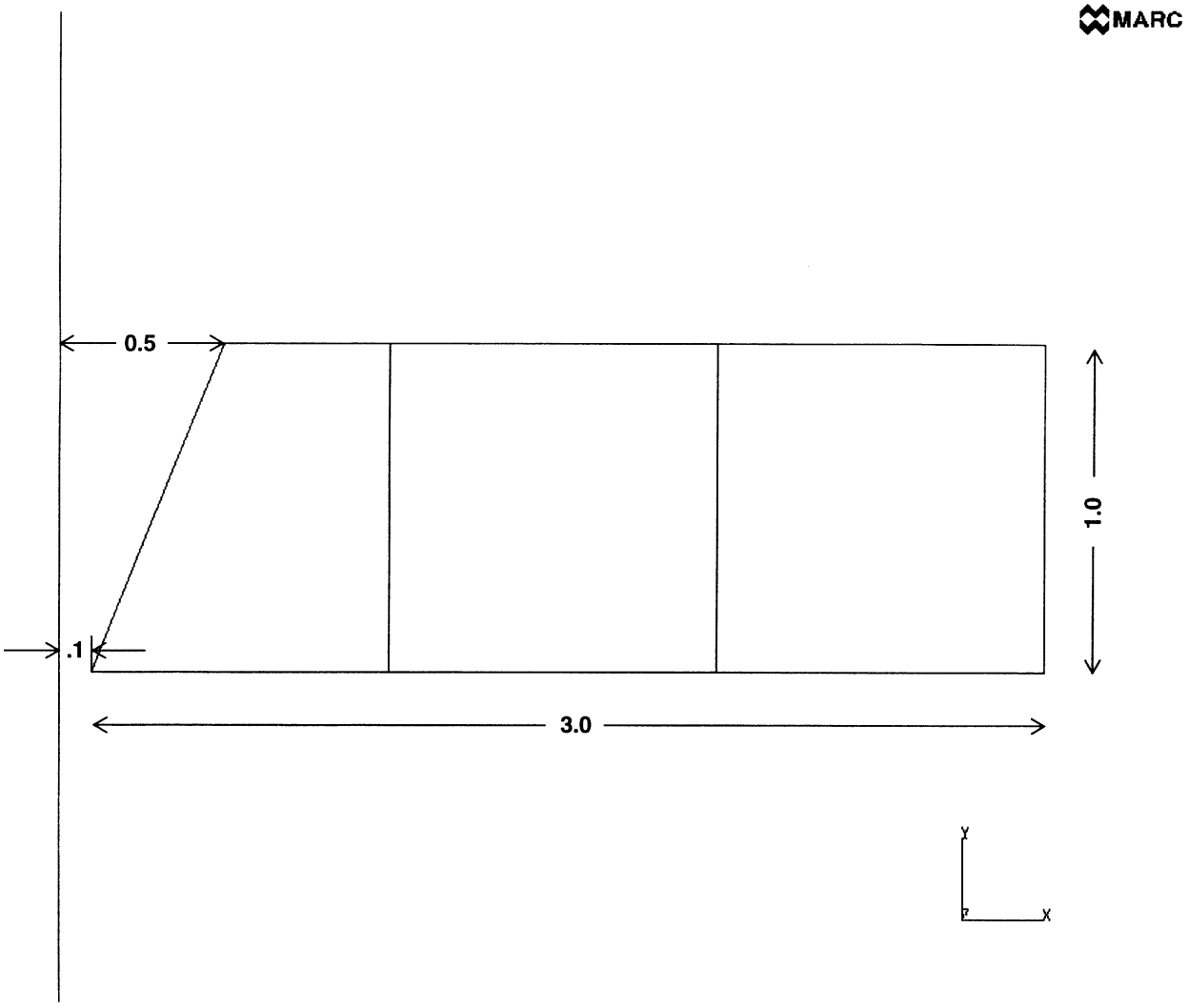

Figure E 6.16-2 Impactor Geometry

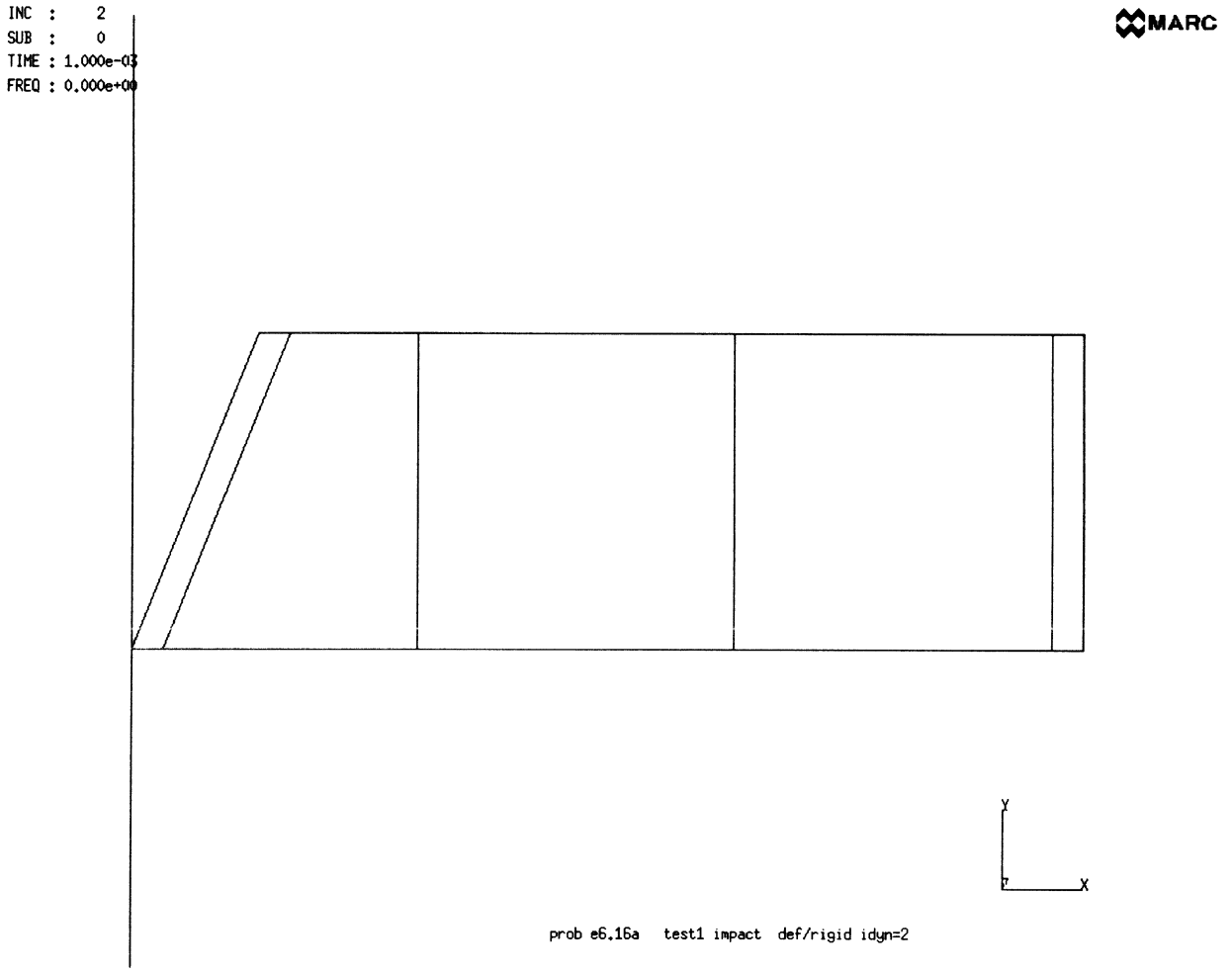

Figure E 6.16-3 Deformation at Initial Contact

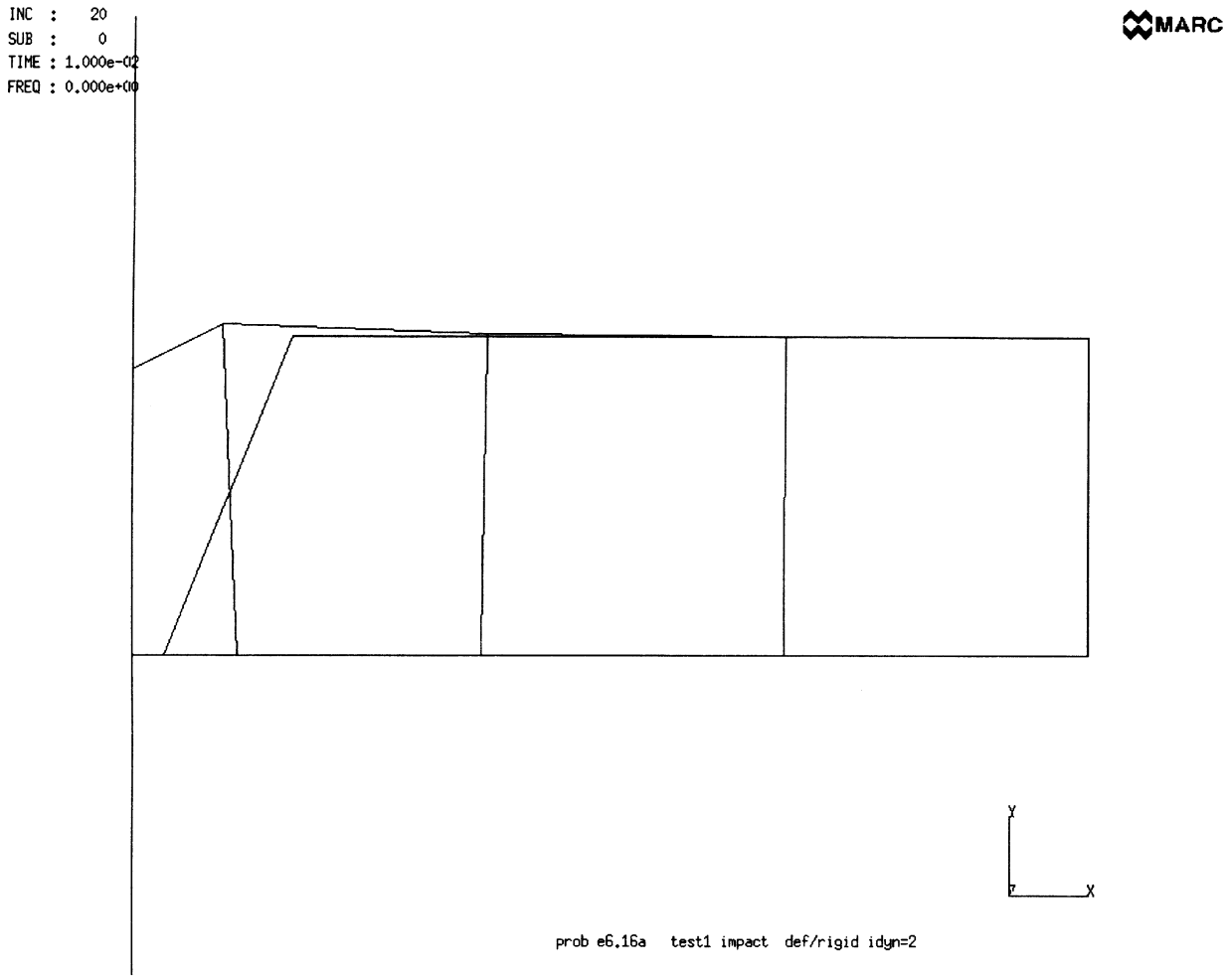

Figure E 6.16-4 Final Deformation

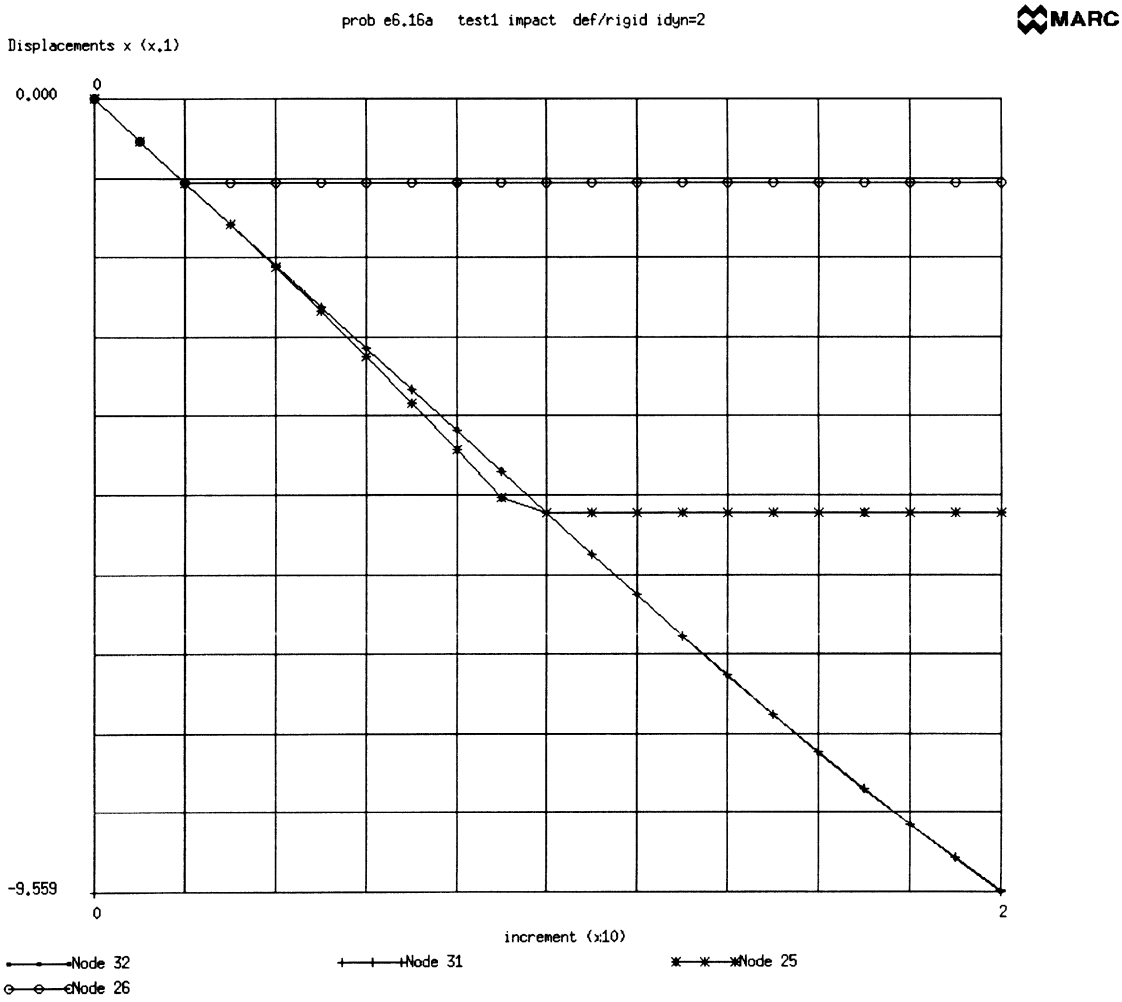

Figure E 6.16-5 (A) Displacement History (Newmark-Beta Method)

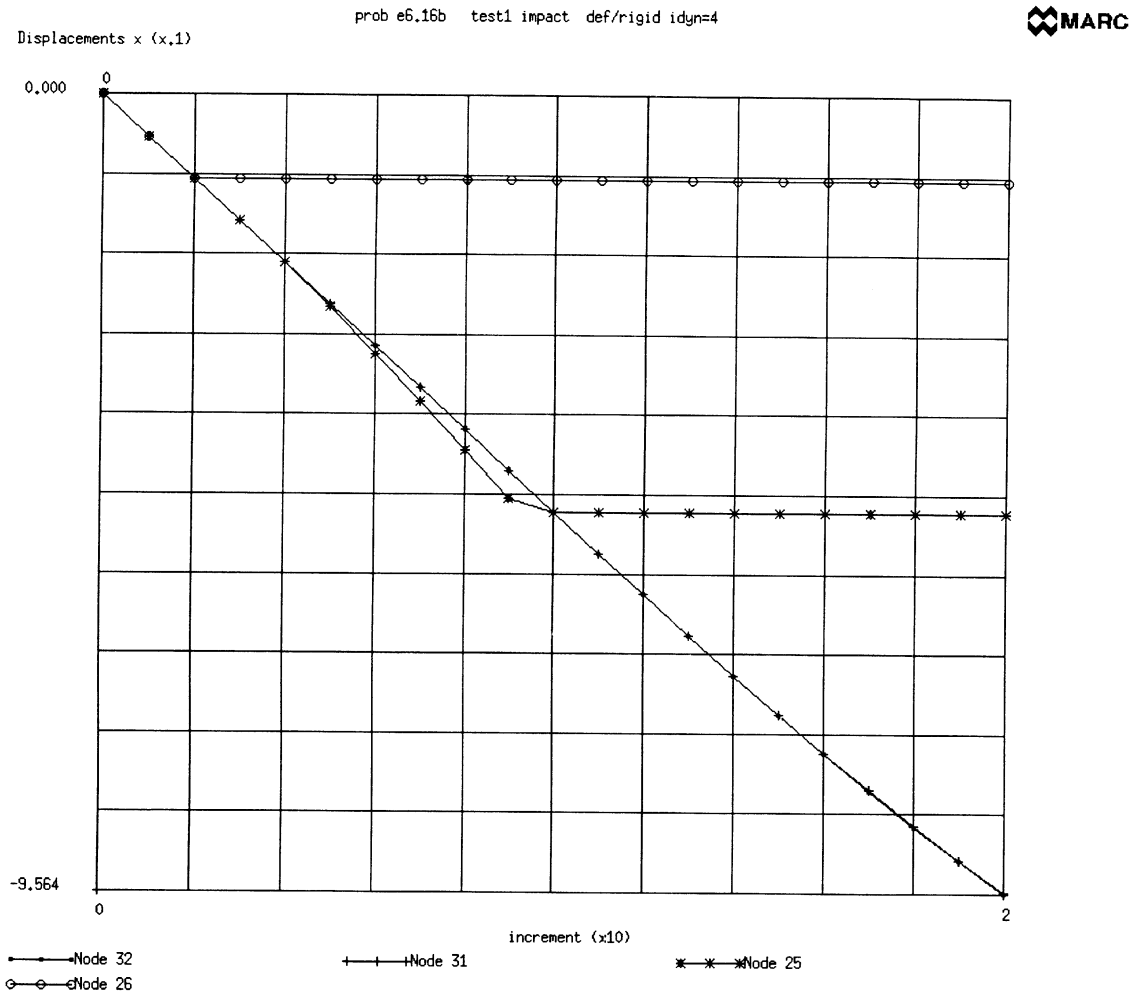

Figure E 6.16-5 (B) Displacement History (Central Difference Method)

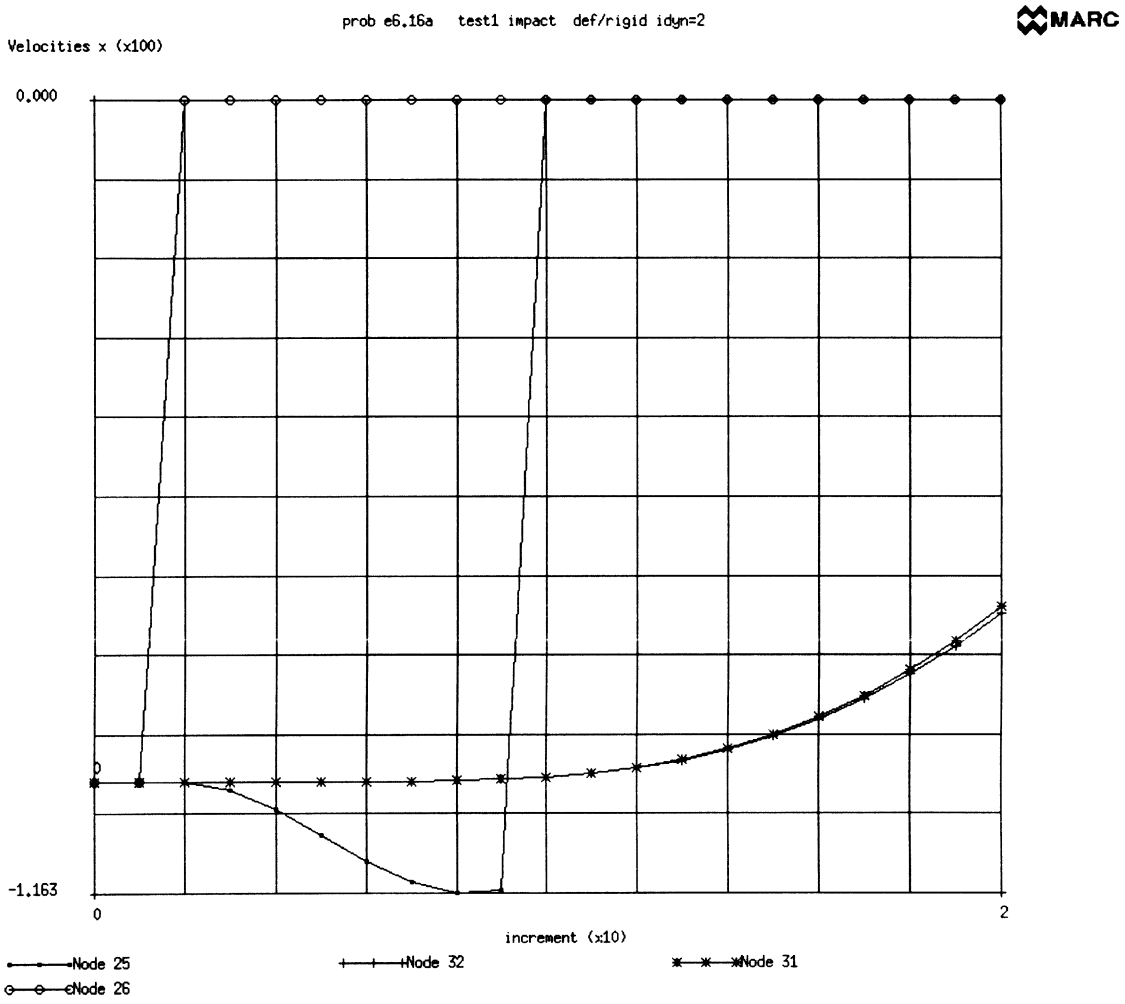

Figure E 6.16-6 (A) Velocity History (Newmark-Beta Method)

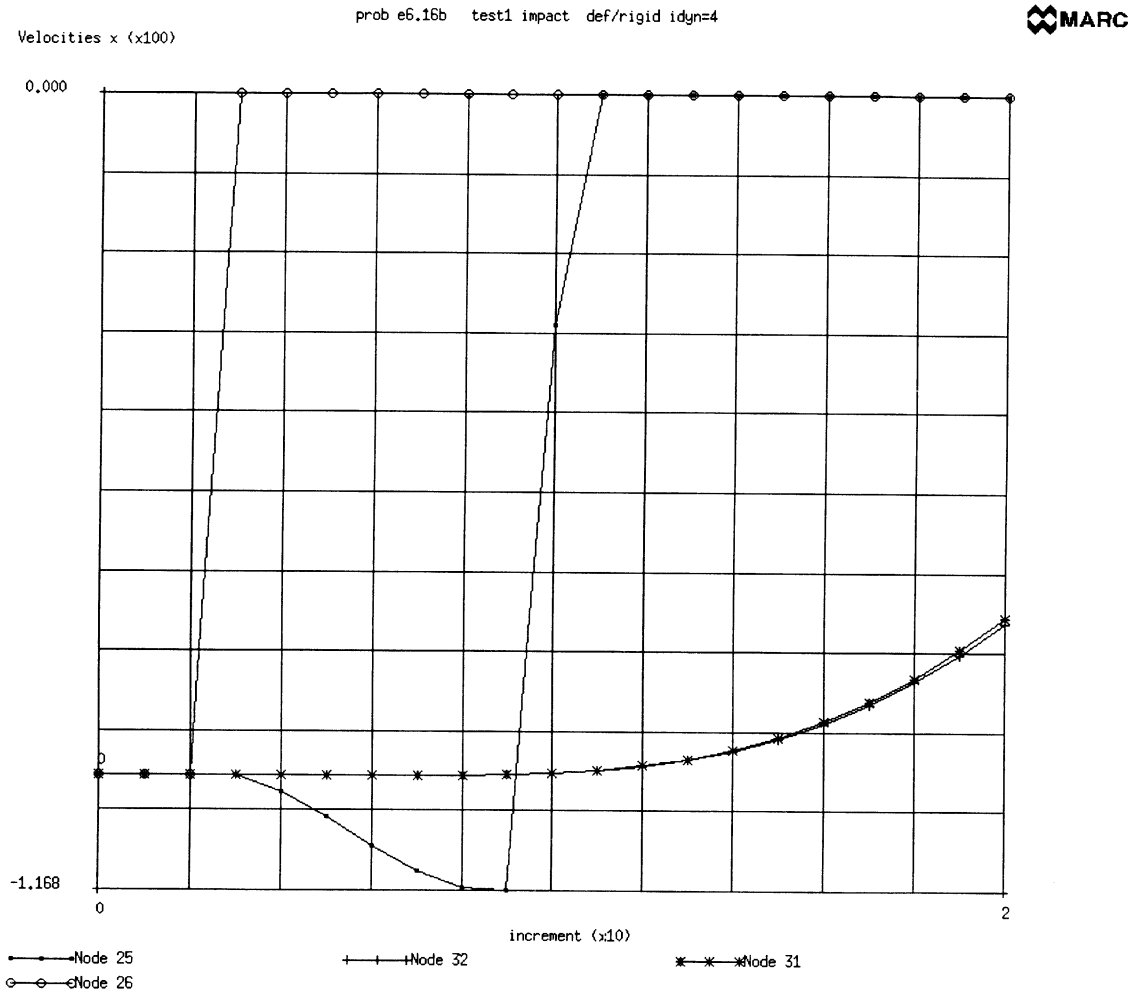

Figure E 6.16-6 (B) Velocity History (Central Difference Method)

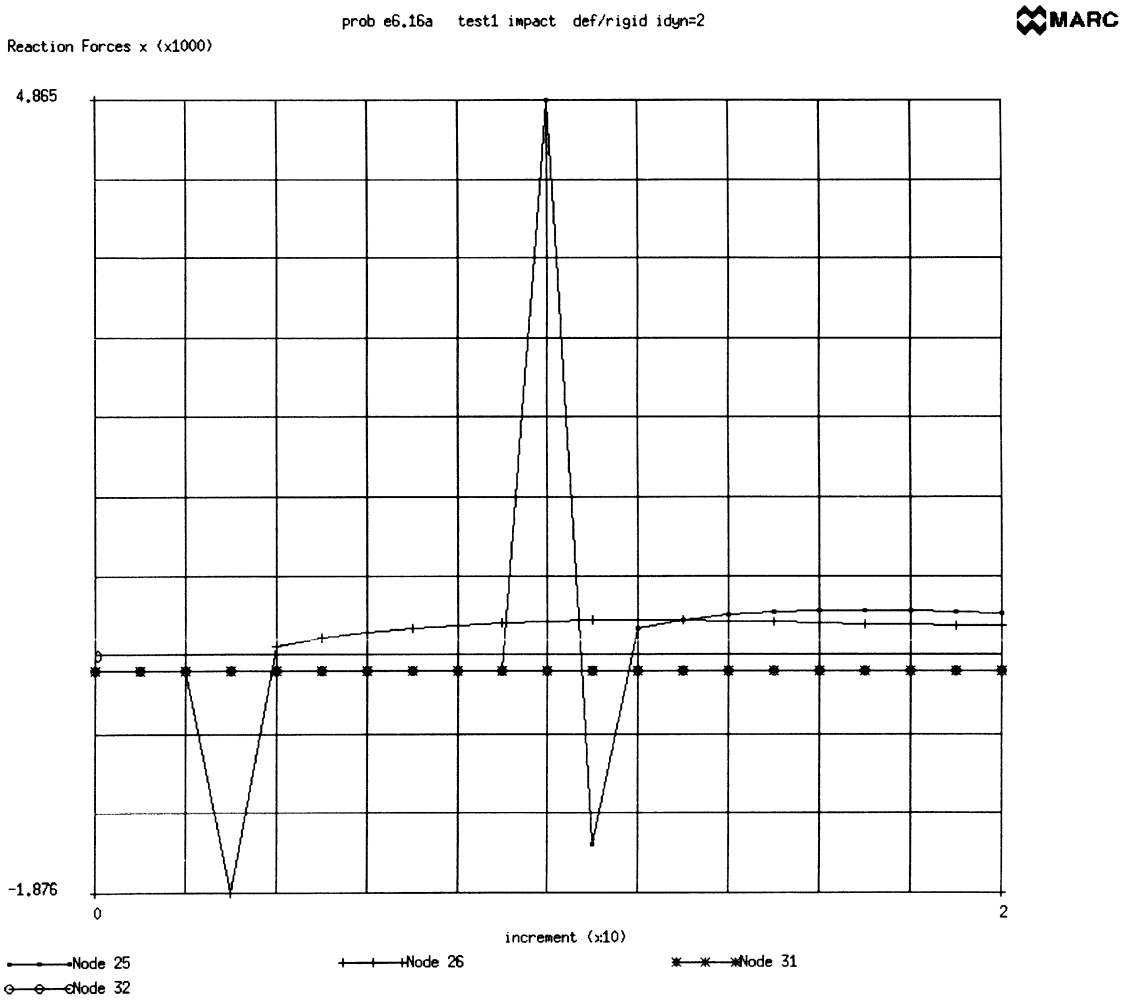

Figure E 6.16-7 (A) Reaction/Impact Force History (Newmark-Beta Method)

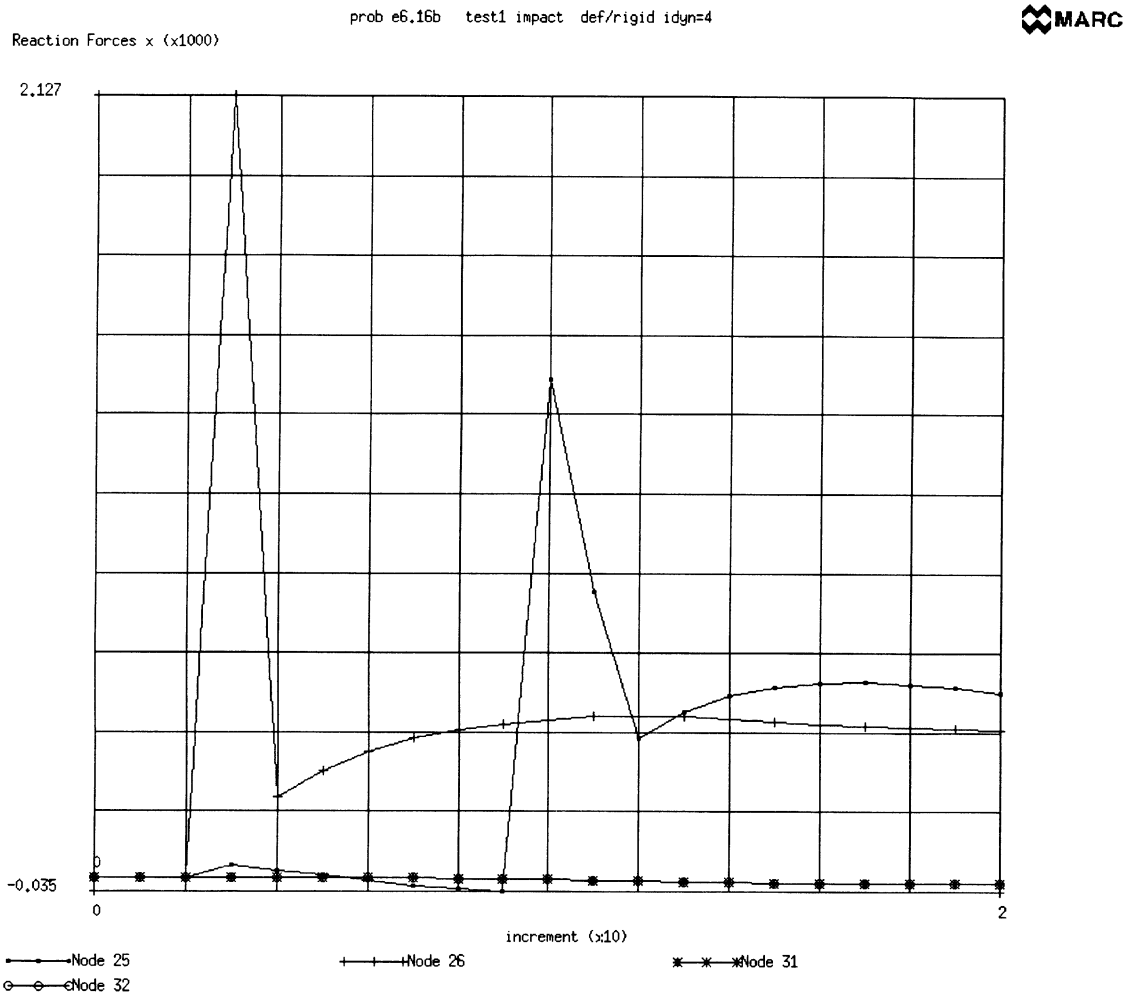

Figure E 6.16-7 (B) Reaction/Impact Force History (Central Difference Method)

E 6.17 Dynamic Contact Between Two Deformable Bodies

This problem demonstrates the dynamic impact between two deformable bodies. It is very similar to problem E 6.16, except the rigid barrier has been replaced by a deformable, yet stiff, body. Both the implicit Newmark-beta and explicit central difference procedures are demonstrated.

Model

The model is shown in Figure E 6.17-1 and Figure E 6.17-2. The project is made up of nine brick elements type 7, where the barrier is composed of 40 brick elements. The DYNAMIC parameter card specifies which operator is to be chosen: a "2" indicates Newmark-beta and a "4" indicates central difference. The projectile may undergo elastic deformation, so the LARGE DISP parameter option is included.

Material Properties

An artificial material was created, such that the stability limit for central difference was a large number. For the projectile (elements 1 – 9), the Young's modulus is 10,000 psi and the mass density is 0.1 lb/in^3. The barrier is ten times stiffer with a Young's modulus of 100,000 psi. A lumped mass matrix will be created based upon the LUMP parameter card. The model is given a numerical damping of 0.4. Given the material parameters, the elastic wave speed in the projectile is $c = \sqrt{E/p} = 316$ in/sec . In the barrier, it is 1000 in/sec.

Boundary Conditions

The nodes on the xz-plane have been constrained in the y-direction. The nodes on the xy-plane have been constrained in the z-direction for the projectile. The projectile has an initial velocity of -100 in/sec in the x-direction.

Controls

The maximum number of increments will be 100 with the maximum number of iterations as 25. Relative displacement error control will be used with a tolerance value of 10%. A formatted post tape will be written which will contain only nodal information. Both the restart and post tape are written every increment.

Contact

There are two bodies in this analysis. The first is the deformable projectile. The second is the deformable barrier. There is no friction between these two surfaces.

The other parameters on the second card are upper bounds to the number of surface entities and surface nodes.

The contact tolerance is 0.032 inch which is small compared to an element dimension. A very large separation force is given which effectively ensures that the projectile will stick to the barrier.

Time Step

The time step chosen is 0.0005 second which is below the stability limit of 0.0012 second. The stability limit is smaller in this problem than in E 6.16 because of the stiff barrier. The total period is 0.01 second, so 20 increments will be performed.

Results

Figure E 6.17-3 shows the deformation at increment 20. The barrier is significantly stiffer and undergoes very little deformation. The projectile is originally 0.2 inches from the barrier. One can observe in Figure E 6.17-4 that node 26 contacts the barrier in increment 3 using the implicit procedure, and increment 4 in the explicit procedure. This is due to the nature of these two different methods. There is more deformation of the barrier using the implicit procedure. Figure E 6.17-5 shows the velocity histories using the new methods. The basic correlation is good. The Newmark-beta method shows some oscillations at later increments. This could be eliminated by using more damping or decreasing the time step.

Summary of Options Used

Listed below are the options used in example e6x17a.dat:

Parameter Options

DYNAMIC
ELEMENT
END
LARGE DISP
LUMP
PRINT
SIZING
TITLE

Model Definition Options

CONNECTIVITY
CONTACT
CONTROL
COORDINATE
END OPTION
FIXED DISP
INITIAL VELOCITY
ISOTROPIC
POST
PRINT ELEM
RESTART

Load Incrementation Options

CONTINUE
DYNAMIC CHANGE

Listed below are the options used in example e6x17b.dat:

Parameter Options

DYNAMIC
ELEMENT
END
LARGE DISP
LUMP
PRINT
SIZING
TITLE

Model Definition Options

CONNECTIVITY
CONTACT
CONTROL
COORDINATE
END OPTION
FIXED DISP
INITIAL VELOCITY
ISOTROPIC
POST
PRINT ELEM
RESTART

Load Incrementation Options

CONTINUE
DYNAMIC CHANGE

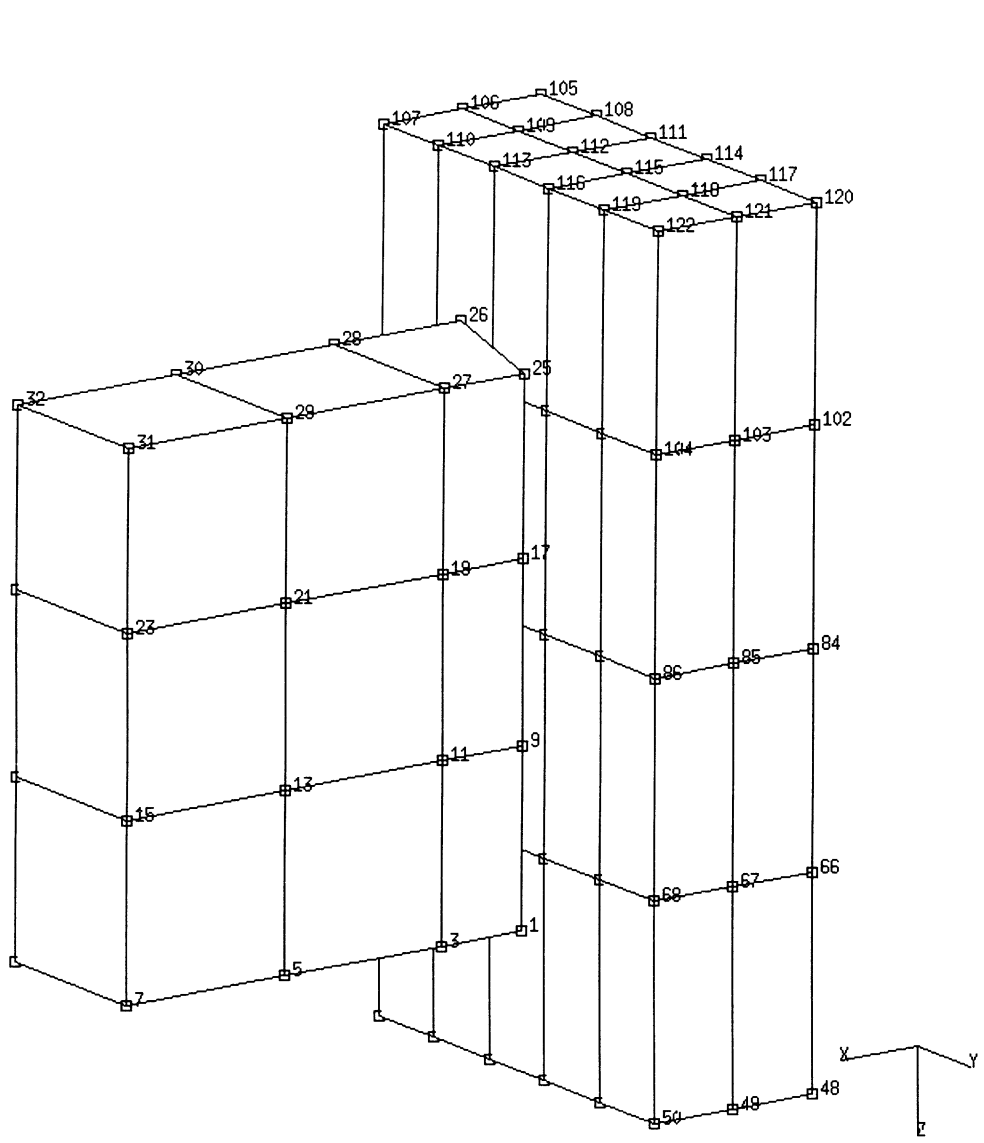

Figure E 6.17-1 Impactor and Deformable Barrier

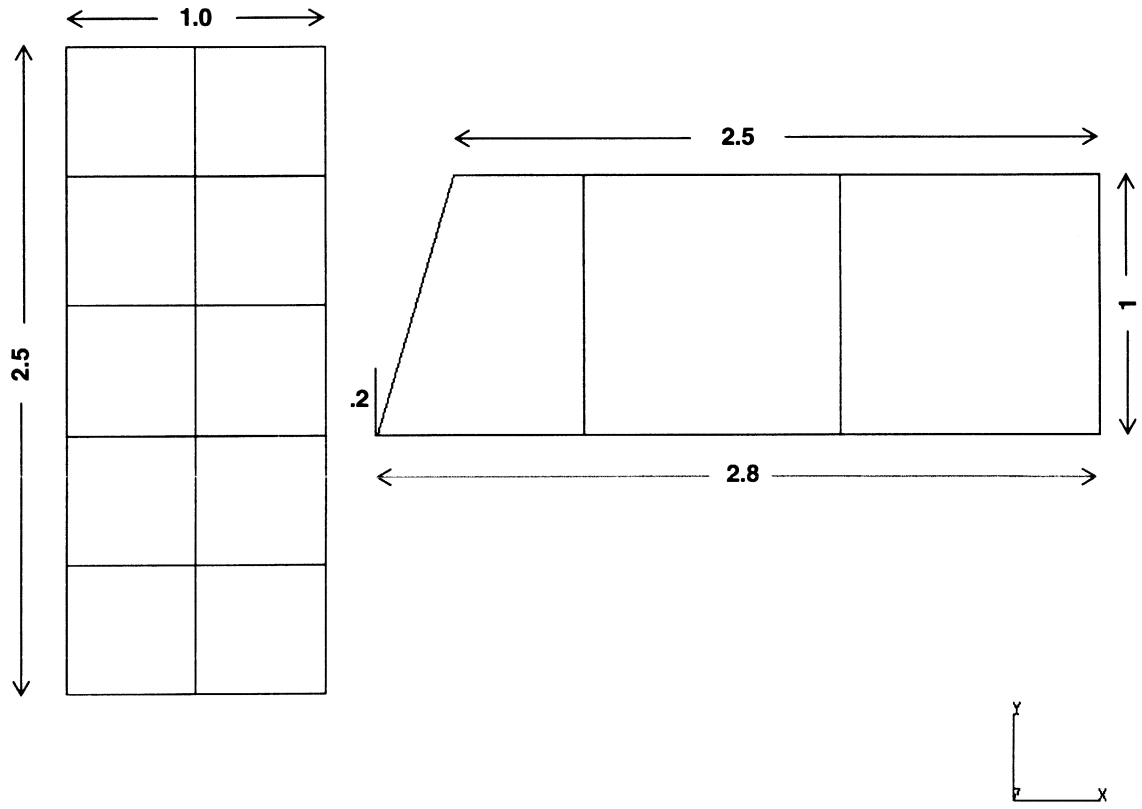

Figure E 6.17-2 Geometries

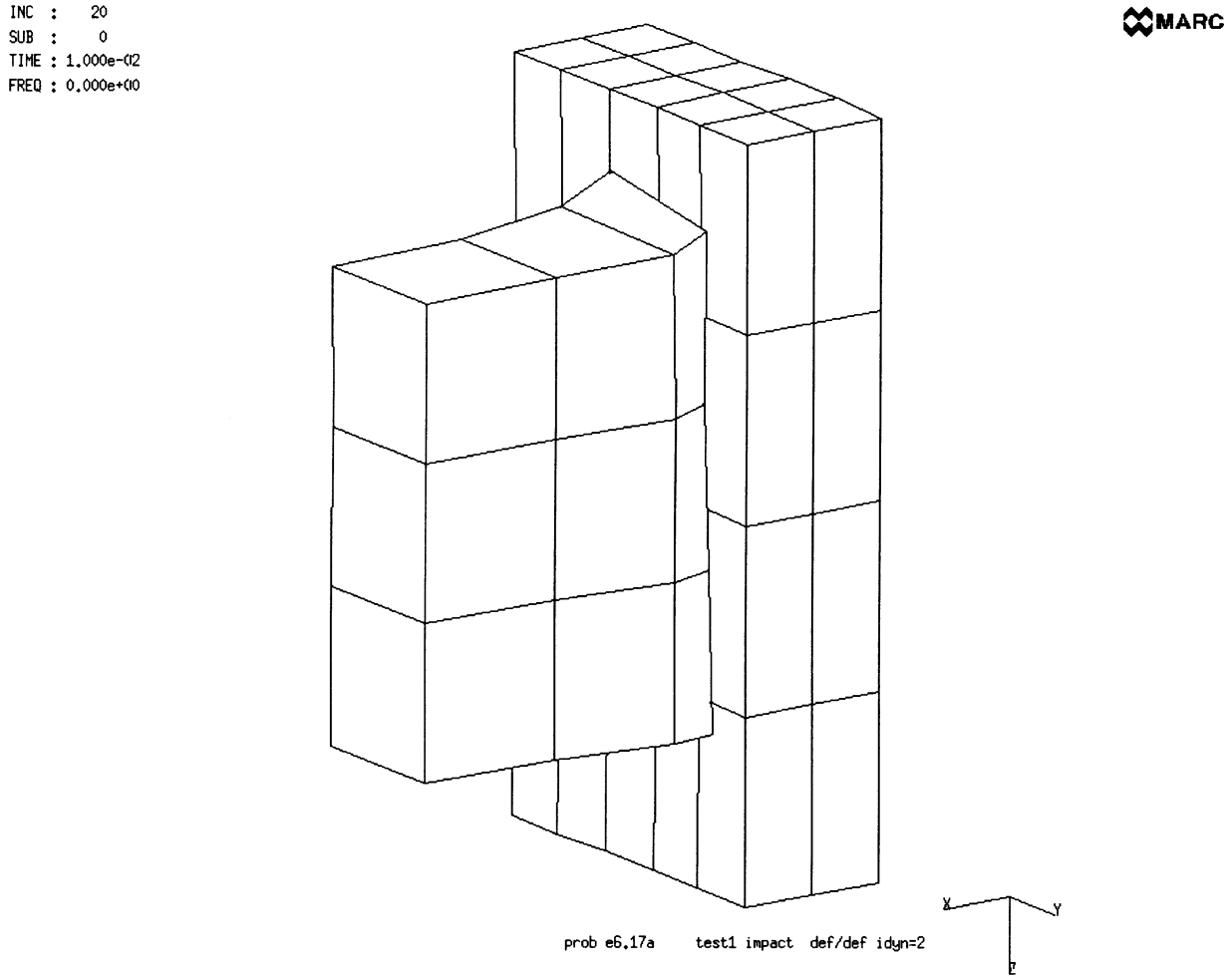

Figure E 6.17-3 Final Deformation

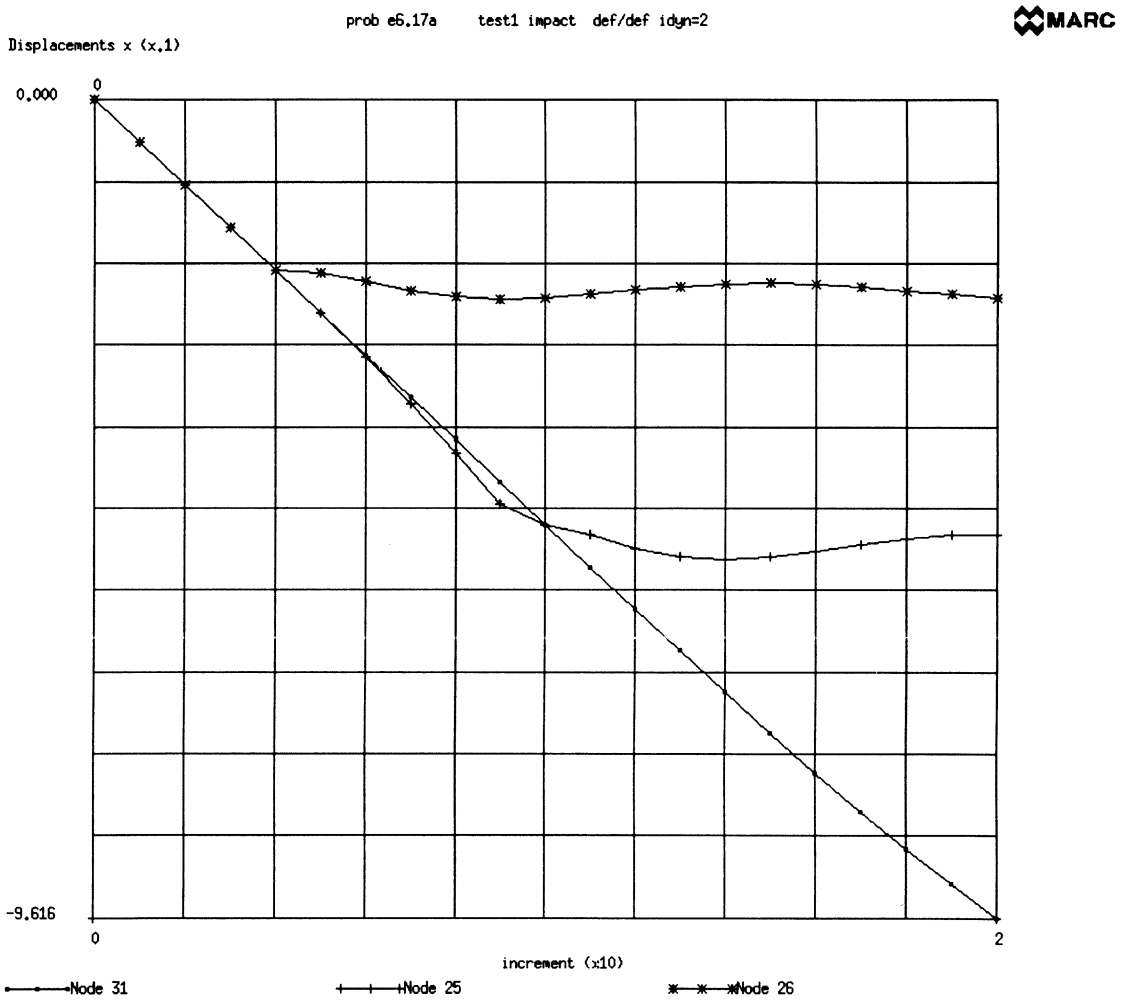

Figure E 6.17-4 (A) Displacement Histories (Newmark-beta Method)

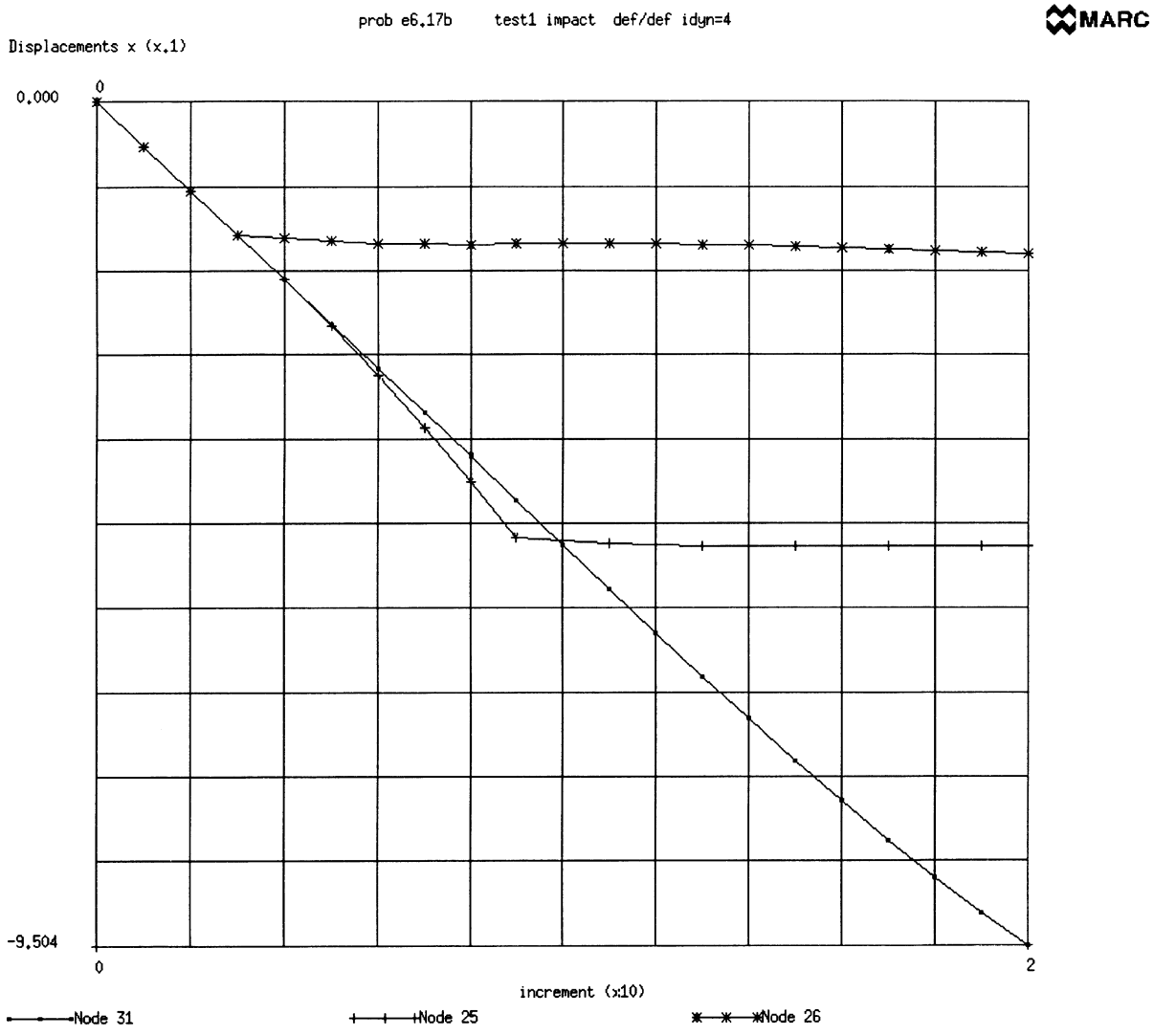

Figure E 6.17-4 (B) Displacement History (Central Difference Method)

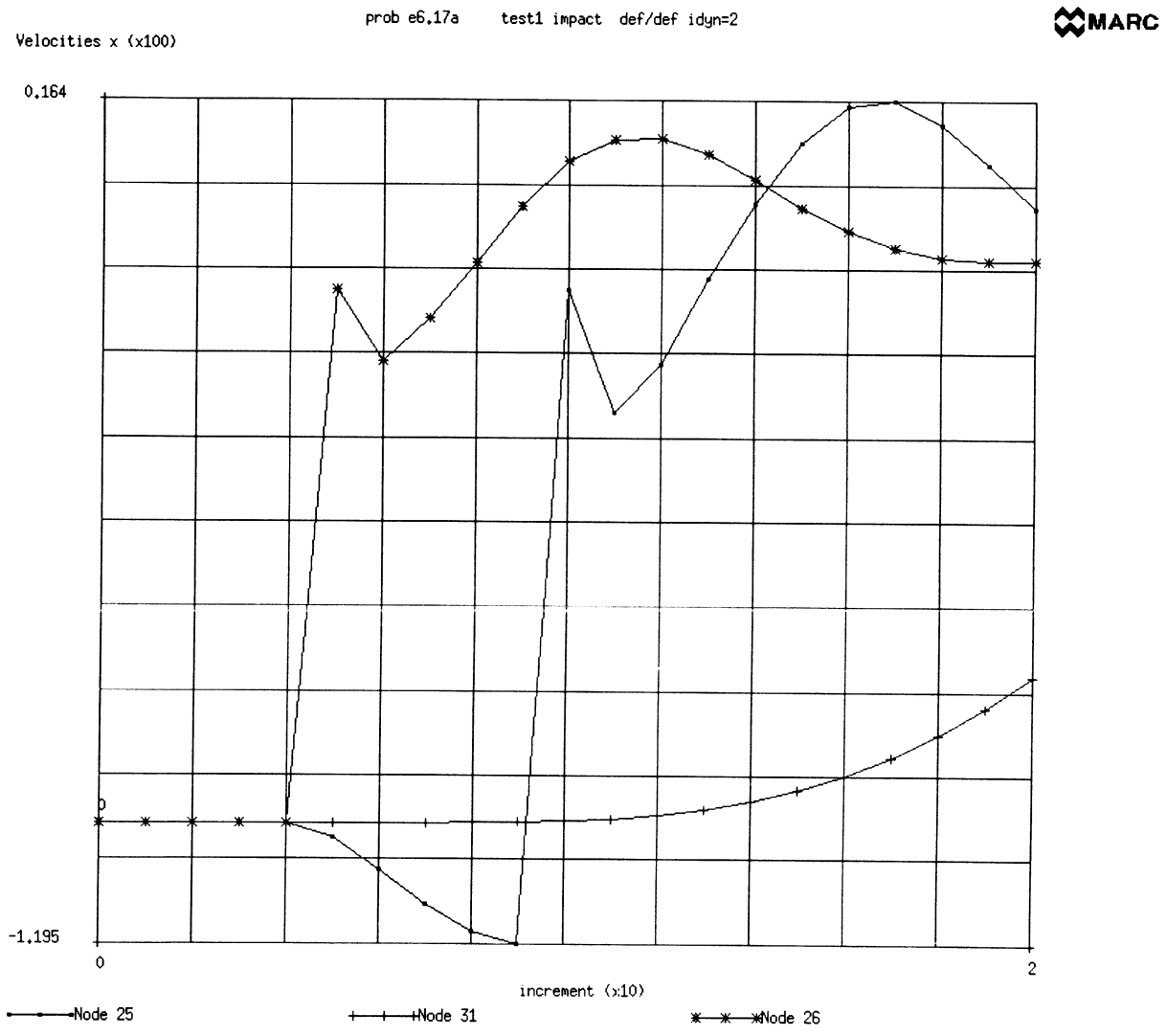

Figure E 6.17-5 (A) Velocity History (Newmark-beta Method)

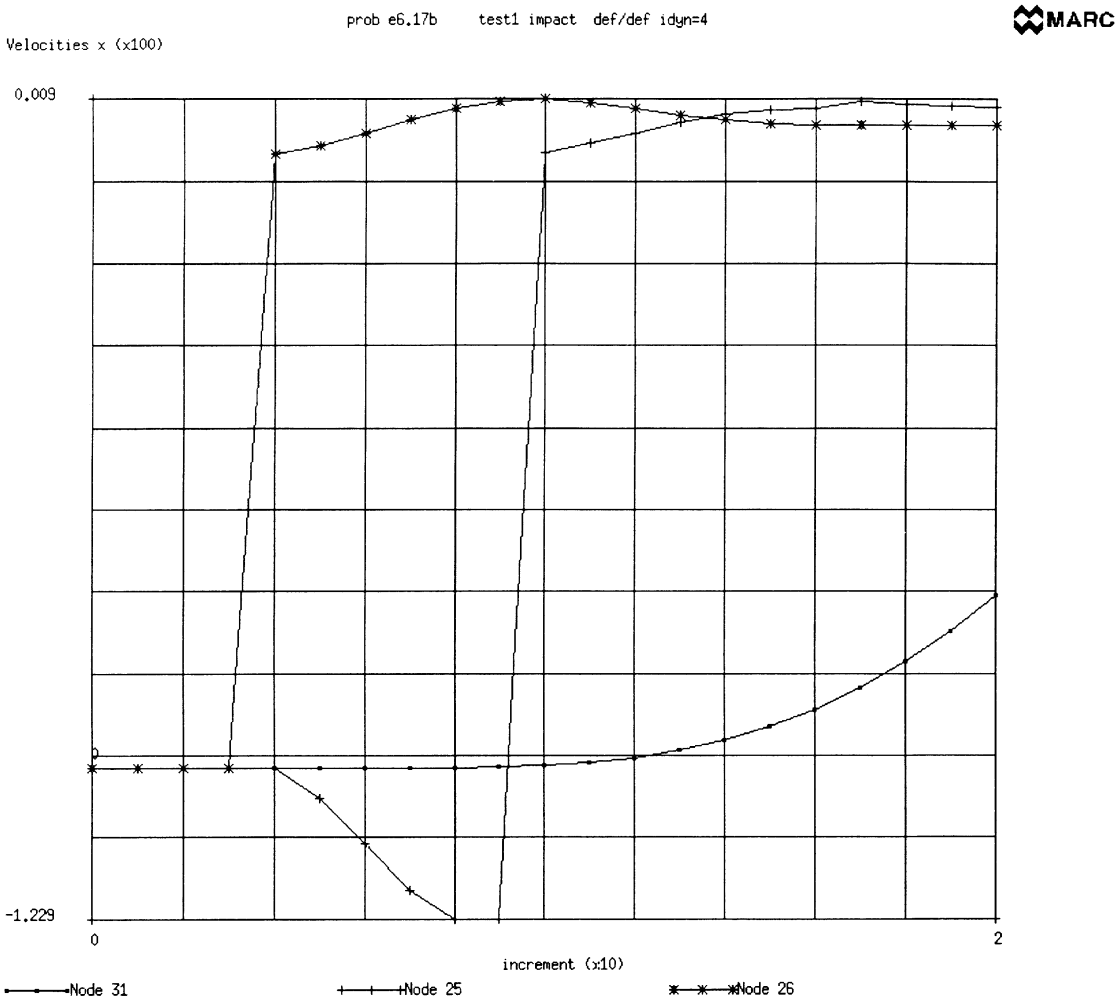

Figure E 6.17-5 (B) Velocity History (Central Difference Method)